Microplastics' Journey into the Gut

Human exposure to microplastics
and associated chemicals

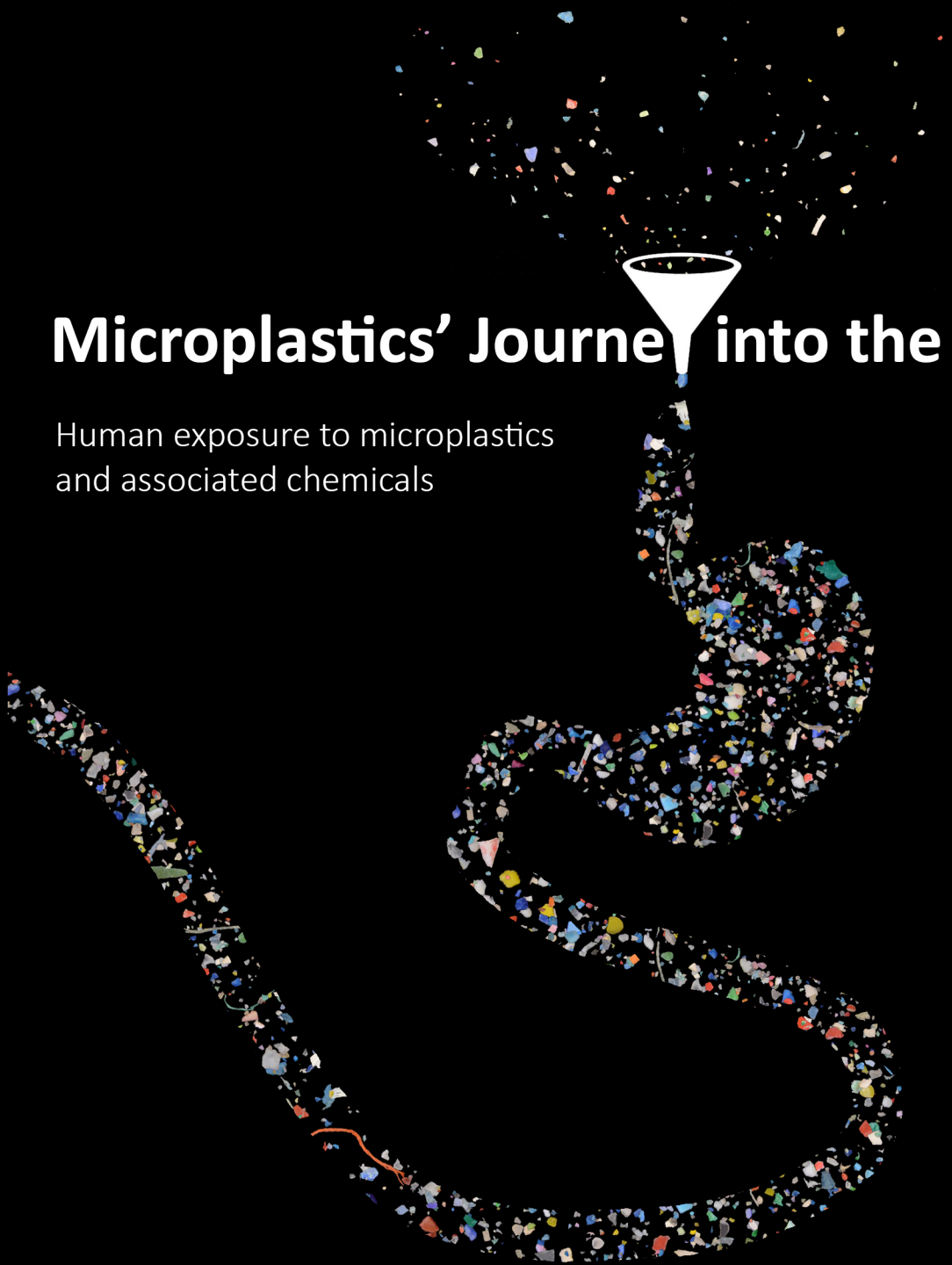

Nur Hazimah Bte Mohamed Nor

Propositions

1. In order to study the full impact of microplastics on the ecosystem, their full spectrum of characteristics needs to be considered.
   (this thesis)

2. Quantifying uncertainties is one way of overcoming challenges in microplastic research.
   (this thesis)

3. Experimental data should be coupled with appropriate models for application of data in other contexts.

4. Translation of scientific information in news coverage on popular scientific topics such as plastic pollution is inaccurate.

5. Social media platforms are a good media channel for science communication and tool for research discussion and collaboration.

6. Aggressive language among reviewers discourages early career scientists and is ineffective in providing constructive feedback.

7. Scientific integrity is affected by hypercompetition for funding and quantitative metrics such as journal impact factors.

8. Propositions should be banned in a PhD thesis.

Propositions belonging to the thesis, entitled

Microplastics' journey into the gut – Human exposure to microplastics and associated chemicals
Nur Hazimah Bte Mohamed Nor
Wageningen, 2 March 2022

Microplastics' Journey into the Gut

Human exposure to microplastics and associated chemicals

Nur Hazimah Bte Mohamed Nor

Thesis committee

Promotor
Prof. Dr A. A. Koelmans
Professor of Aquatic Ecology and Water Quality Management
Wageningen University & Research

Other members
Prof. Dr A. J. Tinka Murk, Wageningen University & Research
Prof. Dr A. D. Vethaak, Vrije Universiteit Amsterdam
Dr Ana Catarino, Flanders Marine Institute, Ostend, Belgium
Dr Andrew Booth, Stiftelsen for industriell og teknisk forskning (SINTEF), Trondheim, Norway

This research was conducted under the auspices of the Graduate School for Social-Economic and Natural Sciences of the Environment (SENSE)

Microplastics' Journey into the Gut

Human exposure to microplastics and associated chemicals

Nur Hazimah Bte Mohamed Nor

Thesis

submitted in fulfilment of the requirements for the degree of doctor
at Wageningen University
by the authority of the Rector Magnificus,
Prof. Dr A.P.J. Mol,
in the presence of the
Thesis Committee appointed by the Academic Board
to be defended in public
on Wednesday 2 March 2022
at 1.30 p.m. in the Aula.

Nur Hazimah Bte Mohamed Nor

Microplastics' Journey into the Gut – Human exposure to microplastics and associated chemicals

182 pages

PhD thesis, Wageningen University, Wageningen, The Netherlands (2022)
With references, with summary in English.

ISBN: 978-94-6395-901-8
DOI: https://doi.org/10.18174/550353

Table of contents

Chapter 1	Introduction	7
Chapter 2	Transfer of PCBs from microplastics under simulated gut fluid conditions is biphasic and reversible	19
Chapter 3	How digestive processes can affect the bioavailability of PCBs associated with microplastics. A modelling study supported by empirical data	53
Chapter 4	Lifetime accumulation of microplastic in children and adults	83
Chapter 5	Synthesis	135
References		150
Summary		172
Acknowledgments		175
About the author		177
Scientific publications		178
SENSE diploma		180

Chapter 1

Introduction

1.1. Microplastic pollution

The word “microplastic” is commonly seen and heard in the news in the past decade. Concerns about this pollutant have been increasing since it was first identified by a team of researchers along the coastlines around Plymouth, United Kingdom.[1] As the word suggests, “microplastics” are plastic particles that are micro-sized. A commonly accepted size range definition for these particles is still lacking. In this thesis, microplastic is defined as plastic particles with size ranging between 1 and 5000 µm to align with the size definition used by most recent major expert group reports and reviews.[2–4] These small plastic particles are ubiquitous in the environment and can be found in every compartment, from air to groundwater to human food products.[2] Microplastic particles either originate from industrial sources in the form of pellets (Figure 1.1) or microbeads or form by the fragmentation and weathering of bigger plastic items in the environment.[2,5]

Figure 1.1. Black microplastic pellets found on the Scheveningen beach in the Netherlands

Due to its formation from an array of sources, this pollutant is unique in its characteristics from other presently known environmental contaminants, such as persistent organic pollutants and nanoparticles. Microplastics comprise a heterogenous mixture of particles with different sizes, shapes, and polymer types. To further add on to this complexity, they also contain different mixtures of chemicals, which are either due to adsorption from the environment or native to the material. The huge diversity of microplastic particles has made the pollutant a complex one to study. Pioneering microplastic studies typically categorized the identified microplastics into discrete classes of sizes, shapes and polymer types. However, such categorization techniques are not sufficient to fully understand the characteristics of microplastics in ecosystems and its associated risks.[6]

As these microplastic particles are omnipresent, there is a high likelihood for a large range of species to ingest them, including humans. To date, there have been many studies focusing on the occurrence of microplastics in the marine organisms since it was first identified in the marine environment.[7] Until more recently, interest of its occurrence has shifted towards freshwater[8] and terrestrial[9] biota. In addition, there has been an increasing concern about microplastic exposure and effects in humans, since the pollutant was found in several seafood species,[10] drinking water[11] and is also airborne.[12] The first evidence proving that microplastics are indeed involuntarily ingested by humans was the detection of microplastics in human stool samples of eight adult volunteers from Europe and Asia.[13] Besides the empirical evidence, several preliminary exposure assessments have been performed to estimate the level of exposure of microplastics in humans from presently known sources.[14,15] These studies have reported estimates of microplastic exposure reaching up to 10,000,000 particles per person per year.[15] However, the reported particle numbers do not reflect the full spectrum of microplastics that we are actually exposed to. Furthermore, the implications of these particles for human health are still unknown as there is very little information on the effects of these particles and its associated chemicals.

Two main potential effects of microplastics have been identified for biota: particle and chemical toxicity. In addition, these small particles can reduce feeding efficiency when they accumulate or block the digestive tracts of the organisms. The particle effects of microplastics have been mainly investigated in aquatic organisms in the laboratory[16] and have yet to be explored in larger species such as humans. Knowledge on its speculated toxic effects for human health mostly come from adjacent disciplines such as nanoparticle and airborne particulate matter.[17] On the other hand, the chemical toxicity of microplastics (also commonly referred to as the chemical vector effect) has been highly debated in the scientific community.[18] Few studies have interpreted their outcomes on the chemical vector effect in light of environmentally relevant conditions. Additionally, the extent of the chemical vector effect is especially unknown for humans. This is because information such as the realistic human intake of microplastics and amount of chemicals released from ingested microplastics

are still unknown. These knowledge gaps are of primary interest in the society and scientific community and hence, initiated the necessity of this thesis.

1.2. The chemical vector effect controversy

Microplastics are vectors for a mixture of chemicals, which may either be intentionally or unintentionally added. Additives such as plasticizers, stabilizers, and flame retardants are intentionally added to plastics during the manufacturing process to achieve the appropriate structure for the designated application.[2] The most common plastic additives include bisphenol A (BPA), nonylphenols, and polybrominated diphenyl ethers (PBDEs).[19] Other chemicals may also be unintentionally added to plastics by sorption onto the surface of the plastic during its entire lifecycle, such as hydrophobic organic compounds (HOCs).

HOCs are widely discussed as one of the major chemical class of concern with regards to microplastics risks. Due to the hydrophobic nature of most polymer types, microplastics have a high sorption capacity for HOCs. Some of the HOCs that have been detected on environmental microplastics include polychlorinated biphenyls (PCBs), polycyclic aromatic hydrocarbons (PAHs), organochlorine pesticides, BPA, nonylphenols and PBDEs.[19–24] The ingestion of microplastics with these sorbed chemicals may contribute to the bioaccumulation of HOCs in biota ("carrier") (Figure 1.2).[25,26] However, it has been debated that the relevance of these microplastics to chemical bioaccumulation compared to other chemical intake media such as food and water is small or even negligible under natural conditions.[27] For example, aquatic organisms take up these chemicals also through other pathways such as dermal uptake and absorption from food. Therefore, the ingested microplastics may be relatively cleaner than the organisms' body burden. The microplastics would then absorb chemicals from the organism's tissues or gut as it passes through the gut, decreasing bioavailability and bioaccumulation of chemicals ("cleaning") following subsequent egestion of the microplastics (Figure 1.2).[25] Whether these microplastics will act as a source or sink of HOCs to organisms when ingested depend on several factors, which is the focus of this thesis.

1.3. Chemical dynamics of microplastics in biota

Chemical dynamics of microplastics in the biota mainly depends on sorption and desorption processes. These processes are largely governed by physico-chemical characteristics, which can be categorized into three main factors (Figure 1.3): (1) plastic properties, (2) chemical characteristics, and (3) gut characteristics.

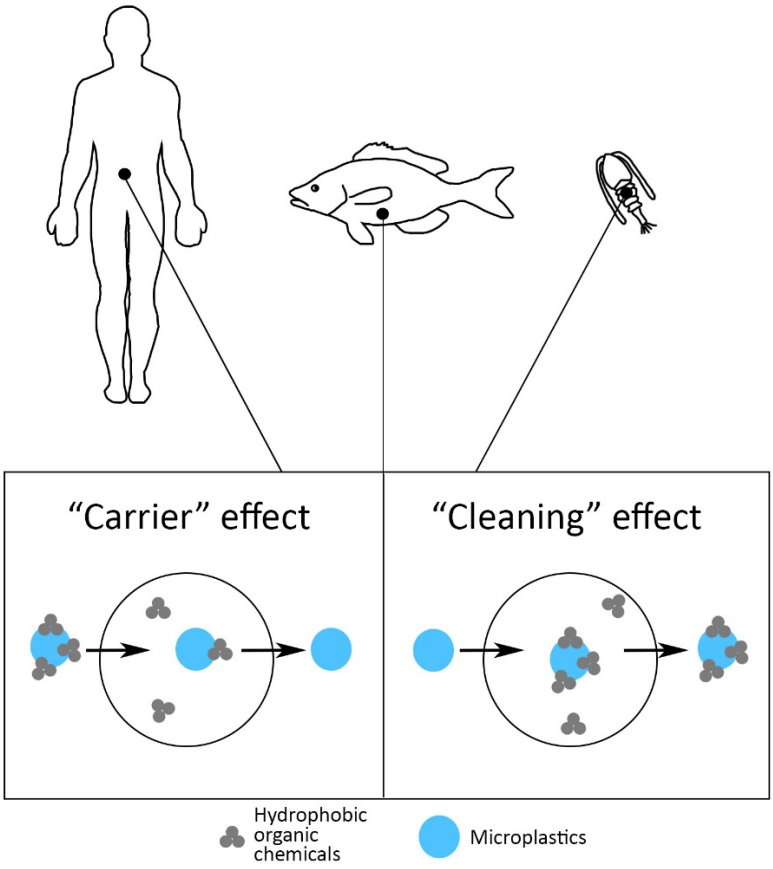

Figure 1.2. Schematic diagram illustrating the "carrier" and "cleaning" effect of microplastics. In the "carrier" effect, ingested microplastics releases its associated chemicals in the gut and increases the chemical body burden of the organism. In the "cleaning" effect, ingested microplastics absorbs chemicals from the gut and decreases the chemical body burden of the organism.

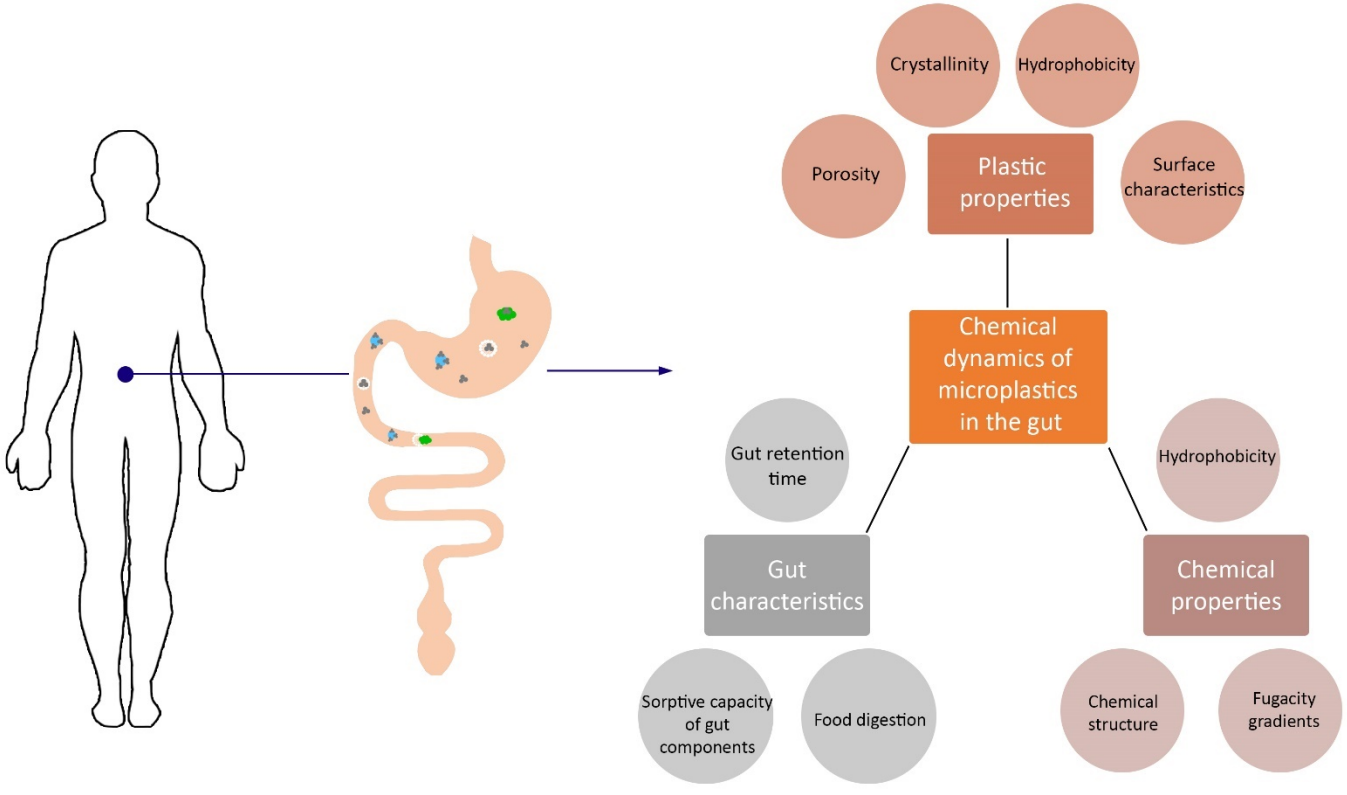

Figure 1.3. Overview of factors involved in the chemical dynamics of microplastics in the gut of biota

Besides the hydrophobicity of a polymer, other plastic properties such as the polymer matrix structure and surface characteristics due to weathering and biofilm formation, also influence the chemical dynamics on microplastics.[28–30] Transport of the HOCs within the polymer matrix structure depends on several factors such as the porosity within the polymer and the segmental mobility of the polymer chains, defined by the glass transition temperature (T_g). T_g of a polymer determines if it is in a rubbery or glassy state. The state of the polymer depends on the crystalline (ordered) and amorphous (random) regions. For any polymer type, the degree of crystallinity can vary considerably since it highly depends on the polymer production process. The sorption of chemicals typically occurs in the amorphous regions of the polymer, which are more capable of segmental chain movements. On the other hand, sorption on the surface of the plastic, depends on factors such as, surface area and oxygen groups.[28] When microplastics are subject to weathering, micro-cracks would develop on the surface, increasing surface roughness and area to allow more sorption of chemicals.[31] Additionally, natural weathering also increases the abundance of oxygen containing groups that will result in a reduction in the hydrophobicity of the polymer.[29,31]

Chemical dynamics of microplastics depend on the characteristics of the chemicals in the biota, which include, among many others, chemical structure, hydrophobicity and fugacity gradients. While chemical structures and hydrophobicity of the chemicals are commonly discussed in the microplastic scientific community, there is a lack of focus on the chemical fugacity gradients between microplastics and biota. When microplastics enter the biota via ingestion or inhalation, the microplastic-associated chemicals interact with chemicals in the other components of the biota. The net direction of transfer of the chemicals on the microplastics are partly governed by fugacity gradients between microplastics and other components of the biota.

Finally, as the focus of this thesis is on microplastics that are ingested and pass through the gut, the gut characteristics of the biota also plays an important role in the chemical dynamics on the ingested microplastics. Gut retention times vary considerably across species, ranging from hours to days. If microplastics are retained in the gut for a longer period of time, the associated chemicals have more time to transfer in and out of the microplastics. Other gut characteristics such as the sorptive capacities of the micelles and food, and food digestion are also important factors which may influence the chemical dynamics and also the relative chemical contribution of microplastics compared to other intake media.

1.4. Knowledge gaps

The level of microplastic exposure and the extent of the role of microplastic as a vector for chemical bioaccumulation is especially unknown for humans around the world. The

uncertainty on the microplastic vector effect stems from the lack of clarity on the chemical exchange dynamics of HOCs on microplastics under realistic gut conditions in biota.

Gap 1: Most chemical vector studies on microplastics have investigated the vector effect by only considering the desorption of chemicals from microplastics. They demonstrated that microplastics can enhance chemical bioavailability in the gut. However, reversibility of the sorption process has been largely neglected. This may reduce the chemical bioavailability and bioaccumulation in the organism.

Gap 2: Previous studies did not fully mimic environmentally realistic conditions in which chemicals are also present in the water, food, or in the organism. But in reality, chemical fluxes from these pathways need to be considered.

Gap 3: Another unanswered aspect of the chemical vector effect is if it is influenced by digestion kinetics. So far, only inert food compartment has been considered in previous studies whereas in fact, food is constantly being broken down in the gut and would logically release sorbed chemicals. Whether microplastics can act as a sorbent to clean the released chemicals is unexplored.

Gap 4: The lack of standard approaches in microplastics research has led to data incomparability in the microplastic concentration reported for food items and beverages consumed by humans and also in the air. This non-alignment of data has limited the ability of present human exposure assessments to provide a more accurate estimate of the full microplastic continuum.

Gap 5: Presently, singular estimates for human microplastic intake do not provide a comprehensive overview of the distribution of microplastic intake and exposure around the world. A more realistic exposure assessment framework that describes the variability of the magnitude of exposure to the full continuum of microplastics, along with the variability of the populations exposed, is lacking. Furthermore, it is unclear to what extent ingested microplastics are actually absorbed and accumulated in the human body over a lifetime.

Gap 6: The chemical vector effect of microplastics for humans has been evaluated by several expert group reviews based on the worst case scenario. Their assessments have preliminarily concluded that at present microplastic intake concentrations and maximum chemical leaching levels, the role of microplastics in chemical bioaccumulation is negligible and will not exceed unsafe levels. However, a comprehensive model framework and toolset that can provide a more accurate and realistic assessment, including uncertainties, of the chemical vector effect of microplastic in humans under natural conditions is lacking.

1.5. Understanding the problem: A mechanistic approach

There is an urgent need for more sophisticated experimental methods, chemical exchange models, and modeling toolsets, which can be applied to understand microplastic exposure in humans and the extent of the vector effect of different chemicals associated with the heterogenous mixture of microplastic particles. Such approaches are common in adjacent disciplines such as environmental chemistry and, sediment and soil science. However, these existing approaches have not been adequately assimilated in the field of microplastic research. It is necessary to recognize that to move the microplastic research forward, methods and theories from adjacent disciplines can be borrowed.

To set the stage in understanding the role of microplastics as a vector for chemical bioaccumulation in humans and other biota, the sorption behavior and rate kinetics of microplastic particles in the gut environment needs to be elucidated first. Different scenarios should be assessed since microplastics are not equally contaminated with chemicals and there are other chemical uptake routes such as absorption from food. An in vitro simulated gut fluid method would allow the understanding of the aforementioned scenarios in a step-wise manner to include different configurations of possibilities (i.e., different hydrophobicities of chemicals, polymer types, sizes). Furthermore, it helps to reduce the complexity of the chemical processes in the gut when microplastics are ingested and focus specifically on the sorption mechanisms in the microplastics. Such an approach allows the determination of more accurate sorption parameters than in whole organism studies, which can be applied to compare the chemical bioavailabilities from microplastics in different biota. These chemical kinetic parameters and dynamic models can then be integrated in larger modeling frameworks, such as food web models[32] and physiologically based pharmacokinetic (PBPK) models for ecological and human risk assessments.[33]

To address the knowledge gaps 4 to 6, a large modeling framework needs to be developed that can address the current limitations in microplastics research to provide probabilistic estimates of the microplastic intake and exposure in humans around the world. Such probabilistic exposure assessments are typically performed for chemicals. However, the application of the approach is not very straightforward for microplastics due to its heterogeneity. Therefore, new correction tools need to be developed to account for the diversity of microplastics.

1.6. Aims of this thesis

This thesis aims to address the aforementioned knowledge gaps on the human exposure of microplastics and its role as a vector for chemical bioaccumulation:

- How do the chemicals interact with the microplastic particles (glassy/rubbery) in the gut environment of biota under different feeding scenarios – equilibrium and kinetics?
- What are the sorption affinities of the chemicals for gut components such as micelles and food lipids, information that is required to fully understand chemical dynamics in the gut?
- How does food digestion influence chemical transfer kinetics in microplastics and affect the overall chemical bioavailability to biota?
- What are the variabilities of microplastic concentrations in food types, beverages and air; intake media relevant for humans?
- How much microplastics from known sources are people exposed to throughout their lives?
- To what extent do microplastics contribute to the overall chemical bioaccumulation in humans?

1.7. Thesis outline

This thesis comprises 3 main chapters **(Chapter 2 – 4)** which addresses the aforementioned knowledge gaps in 3 separate studies. These studies grow in sophistication to understand the sorption behavior and the underlying mechanisms for a range of chemicals with different hydrophobicities. The final main chapter comprises of **three subchapters** that delves into the lifetime exposure of microplastics in humans, and the chemical vector effect of microplastics using the developed chemical exchange models in **Chapters 2 and 3**, in the human gut. In the final chapter **(Chapter 5)**, the weight of evidence for the microplastic chemical vector effect is discussed based on **Chapters 2 – 4** and also other microplastic vector studies, specifically, in vitro gut fluid studies.

Chapter 2 addresses the sorption behavior and dynamics of HOCs with microplastics in a simulated gut environment. This is done in conjunction with the development of a dynamic multicompartment model describing the chemical exchange kinetics on microplastics. Three scenarios are investigated. In the first scenario, an organism ingests contaminated microplastics only. The second scenario; an organism ingests contaminated microplastics and contaminated food (prey). The third scenario; an organism ingests clean microplastics and contaminated food. Additionally, the chemical dynamics are investigated for two polymer types to compare a rubbery (low density polyethylene (LDPE)) and glassy (polyvinyl chloride

(PVC)) polymer. Kinetic parameters fitted to empirical data can be used to further compare across different biota with varying gut retention times.

Chapter 3 expounds on the sorption behavior and dynamics of HOCs with microplastics by including food digestion, which adds another new aspect of environmental realism. In this chapter, the gut fluid conditions of humans and physiologically similar biota were simulated. Olive oil is used as a proxy for food lipids (triglycerides) and LDPE plastics were used to represent ingested microplastic particles. Both food and plastics are pre-equilibrated with the gut fluid. Food digestion is initiated with the lipase enzyme which breaks down the olive oil triglycerides. The earlier dynamic multicompartment model developed in **Chapter 2** is expanded to include the food digestion process. The effect of food digestion kinetics on the chemical dynamics with microplastics is then elucidated.

Chapter 4 uses the insights from **Chapter 2 and 3** to understand the contribution of microplastics to chemical bioaccumulation in humans. The chapter comprises three major components (subchapters): (a) characterizing microplastics in food, beverages, and air using novel quality assurance and quality criteria standards and probabilistic alignment methods, (b) first probabilistic human exposure modeling for microplastics, (c) first probabilistic assessment of the role of microplastic as vectors for chemical bioaccumulation in humans. A model framework for estimating the microplastics exposure from different food types and air is developed. This framework accounts for non-alignment of methods used to assess microplastic occurrence data, and also the full microplastic continuum (1–5000 µm). A lifetime microplastic exposure model for children and adults, here implemented for intake via eight food types and inhalation, intestinal absorption and biliary excretion, is developed. This can estimate the microplastics accumulated in the body tissue, gut and excreted in the stools. The amount of chemical bioavailable from microplastics under realistic feeding conditions is then calculated using the dynamic biphasic model developed in **Chapter 2** and microplastic exposure amounts in the gut from the probabilistic microplastic exposure modeling.

Finally, in **Chapter 5**, the weight of evidence for the microplastic chemical vector effect is evaluated based on the products from **Chapters 2–4**, and evidences from other in vitro gut fluid studies are also reviewed. Some recommendations are made to ensure quality assurance for such studies to be relevant with respect to understanding the chemical vector effect of microplastics. The usefulness of the multicompartment dynamic models developed in this thesis are compared to other sorption models that have been widely used in other studies to describe chemical sorption dynamics on microplastics. Finally, an outlook on further improvements on the exposure and risk assessment for microplastic and its associated chemicals, is provided.

Chapter 2

Transfer of PCBs from microplastics under simulated gut fluid conditions is biphasic and reversible

Nur Hazimah Mohamed Nor, Albert A. Koelmans

This chapter is published as: Mohamed Nor, N.H. and Koelmans, A.A., 2019. Transfer of PCBs from microplastics under simulated gut fluid conditions is biphasic and reversible. *Environmental Science & Technology*, 53(4), pp.1874-1883.

Abstract

The role of plastic as a vector for bioaccumulation of toxic chemicals is central to the risk assessment of microplastic for human health and the environment. However, transfer kinetics of sorbed contaminants from ingested microplastics are poorly understood. We develop and parameterize a chemical exchange model on microplastics in a gut fluid mimic of aquatic biota, and also included food to provide a better representation of contaminant dynamics when plastic and food are ingested, as would occur in nature. The transfer kinetics of 14 polychlorinated biphenyls (PCBs) were measured in gut fluid mimic systems under three environmentally relevant exposure scenarios of plastic ingestion by organisms, for low-density polyethylene (LDPE) and polyvinyl chloride (PVC), and were evaluated with the model. Chemical transfer was demonstrated to be biphasic and fully reversible, with fast exchange within hours followed by a slow transfer lasting for weeks to months. In *clean* gut systems, the bioavailability of plastic-associated PCBs for lugworms and cod ranged from 14–42% and 45–83% respectively. However, in *contaminated* gut systems, clean microplastic was capable of rapidly extracting ("cleaning") PCBs from food inside the gut, thus demonstrating that the effect of microplastic is context dependent. Therefore, chemical contamination and cleaning are likely to occur simultaneously due to the ingestion of microplastic.

2.1. Introduction

Plastics found in the environment have been reported to contain hydrophobic organic chemicals (HOCs), such as polychlorinated biphenyls (PCBs), polycyclic aromatic hydrocarbons (PAHs), bisphenol-A and nonylphenol at ppb concentrations.[24,34–38] This has led to the hypothesis that ingested microplastics (particles smaller than 5 mm) could act as a carrier, i.e., a "vector" of HOCs to organisms, increasing their exposure to HOCs and thereby increasing chemical risks.[24,26,38–41] The vector effect is one of the major concerns in the field of plastic pollution, and is heavily debated in the research community.[26,42–44] Transfer of HOCs from ingested plastics to biota has been investigated either with models accounting for a variety of exposure conditions using scenario analysis,[25–27,32,45–47] in feeding experiments[38,41,48–51] or in in vitro studies,[52–54] which mimic the organism's gastrointestinal (GI) system.

While data from in vivo feeding experiments better represent the ultimate reality of nature and are essential for effects assessment, in vitro experiments provide significant advantages when determining chemical exchange rates between microplastics and gut fluid mimic. By using in vitro set-ups as a proxy for the gut, the level of control and accuracy can be higher than when using whole organisms studies. Pioneering in vitro studies have demonstrated that the desorption of plastic associated chemicals was rapid and enhanced under gut conditions compared to desorption to water only.[52–54] However, these previous studies have interpreted data on the desorption of chemicals in the gut fluid as a one-compartment unidirectional process.[52–54] In contrast, the reversibility of chemical sorption is acknowledged and taken into account for many sorbents of environmental interest, e.g., for soils and sediments[55] and for the widely used passive samplers, composed of polymers like polyethylene (PE)[56], polyoxymethylene (POM)[57] or polydimethylsiloxane (PDMS).[58] In the field of microplastic research however, quantifying the resorption of chemicals from the gut fluid content to plastic has been largely neglected thus far. Accounting for the reversibility of sorption would lead to different values for the chemical desorption rate parameters than those derived in the aforementioned literature on in vitro experiments.[52,53] It would also demonstrate and quantify the potential of ingested microplastics to decrease the chemical bioaccumulation in organisms once the particles are egested.[25,32,45,46] This depuration effect whereby bioaccumulation decreases with the ingestion of clean plastic, has not been addressed in these experimental studies. To date, only modeling studies have accounted for reversibility of the chemical transfer.[25,26,32,45,46,59] However, parameterization was largely based on first principles, that is, polymer diffusivities found in other studies, leaving considerable uncertainty with respect to the actual values. Hence, uncertainties still surround the extent to which plastics affect bioaccumulation of HOCs. Furthermore, the previous in

vitro as well as several in vivo studies did not fully mimic environmentally realistic exposure conditions in which chemicals would be present in the water or in food, outside the organism and/or in the gut fluid.[26] Contaminant fluxes via the common natural pathways, for example, contaminated food, besides via plastic ingestion alone, need to be considered for a realistic assessment of the bioavailability of contaminants from ingested plastics in gut fluids under gut conditions.[26,60] To date, rate kinetics and time scales of chemical transfer to/from plastics in the gut are not known. Knowledge of such kinetic parameters would allow for more rigorous risk assessments of plastics associated chemicals using food web bioaccumulation models.[32] Finally, earlier studies assumed microplastic to behave as one homogeneous compartment with respect to its chemical kinetics,[25,46,52,53] an assumption that needs to be verified.

The aim of this study is to verify and quantify the reversibility and kinetic rates of chemical transfer from microplastics under simulated gut fluid condition of aquatic biota, and to assess the homogeneity of the sorption domains in the polymer. To this end, a dynamic multi-compartment model is developed that describes the chemical exchange kinetics on plastics. The rate constants for chemical transfer of polychlorinated biphenyls (PCBs) spanning a wide range of hydrophobicities, to and from low-density polyethylene (LDPE) and polyvinyl chloride (PVC), and the characteristic time scales are determined with the model. We examine the effect of simultaneously ingested contaminated food on the chemical exchange between plastic and gut fluid. To address the implications of the above for environmentally realistic settings, gut fluid studies were carried out for three scenarios. The first scenario; an aquatic organism ingests contaminated plastics, is included for comparison purposes with previous studies, represents cases where for instance additives still leach from ingested plastics, and was designed to result in the most accurate determination of parameters as it has a large gradient between plastic and gut fluid chemical concentrations. The second scenario; an aquatic organism ingests contaminated plastics and contaminated food (prey), is considered relevant for cases where chemicals have reached (near-)equilibrium in the environment. The third scenario; an organism ingests clean plastics and contaminated food (prey), represents the case where relatively freshly emitted microplastics would not have equilibrated yet so that they are “cleaner” than natural prey that has already bioaccumulated the chemicals from the ambient water. Following earlier studies,[52–54] sodium taurocholate, a vertebrate bile salt,[61–63] was used to simulate the micelles produced in the gut as a result of bile salts and fatty acids. These micelles act as fourth medium for the HOCs, besides plastic, water and organic matter (representative of natural food).

2.2. Materials and methods

2.2.1. Materials

Materials used were 14 PCB congeners (log K_{ow}: 5.24 to 7.42), LDPE and PVC strips of thickness 30 and 250 µm respectively to allow for similar intrapolymer diffusion path lengths as those in 30–250 µm spherical or irregularly shaped environmentally relevant microplastics, and dried *Gammarus* used as natural food representation. Details are provided in the Supporting Information (SI).

2.2.2. Experimental design

Three different set-ups were used to simulate three environmentally relevant scenarios of microplastic ingestion by organisms: (S1) Contaminated plastic strips; (S2) Contaminated plastic strips and contaminated *Gammarus*; (S3) Clean plastic strips and contaminated *Gammarus*.

The plastic strips and *Gammarus* were preloaded with PCBs by spiking 100 µL of PCB mixture stock (SI Table S2.1) per 350 mL MQ-water and shaken on a horizontal shaker at 100 rpm in the dark at room temperature (20°C) over 28 days. A longer loading time assures chemicals are more deeply absorbed by the polymeric phase, which can be considered as more environmentally relevant than the short equilibration times (24–48 h) used previously.[52,53] Subsequently, the plastic strips were removed with a sieve and air-dried in the chemical fume hood overnight. *Gammarus* was sieved then freeze-dried overnight and grinded to powder prior to use in the gut fluid experiments. The gut fluid mixture consisted of 10 mM of sodium taurocholate and 5.0 g/L of bovine serum albumin (BSA), constituted in 35 ppt artificial seawater.[52–54,62] To limit biodegradation of the food component, sodium azide (NaN_3) was added as a biocide to a final concentration of 25 mg/L. The pH was adjusted by drop-wise addition of 1 M HCl to pH 4.04 to mimic the acidic environment of the gut. The final measured salinity of the gut fluid was 34.1 ppt.

In S1, 14 contaminated plastic strips were transferred to 70 mL gut fluid in a 100 mL amber jar. For S2, 14 contaminated plastic strips were added to gut fluid containing ~0.9 g dry weight contaminated *Gammarus* (note that the plastic and *Gammarus* do not necessarily need to be at equilibrium). Conversely, in the S3 setup, 14 precleaned plastic strips were added to gut fluid containing ~0.9 g dry weight contaminated *Gammarus*. The solid-to-gut fluid ratio achieved in setup S1 is 0.005 g dry wt/mL, 3.8 times lower than the ratio in setups S2 and S3 (0.019 g dry wt/mL). This was to ensure that there was an adequate volume of fluid in S1 for the plastic strips to mix in. The initial plastic to food ratio in S2 and S3 was ~0.33 to represent systems where organic matter dominates over microplastic, which is most likely to

occur in nature.[26,49] All three setups were applied to LDPE and PVC and conducted in triplicate. The gut fluid kinetics experiment was carried out over 28 days with continuous shaking on a horizontal platform shaker incubator at 100 rpm at 26.9±0.6 °C, to obtain kinetics for the average temperature of cold- and warm-blooded organisms. Two plastic strips were removed after 672, 674, 680, 696, 840, 1008 and 1344 h (exposure to gut fluid starts from t = 672h) with tweezers, and subsequently sprayed with MQ water and wiped with a tissue to ensure there are no particles on the surface. The strips were kept in precleaned aluminum foils and stored at -20°C until chemical extraction. The method for chemical analysis of the plastic strips is provided as SI.

2.2.3. Model design, description and implementation

To describe sorption to soils, sediments or polymer particles, two schools of modeling exist, one using diffusion models and the other using first-order multiple compartment models.[64,65] Whereas diffusion models are better equipped to relate parameters to actual physical properties of sorbents and adsorbates, including microplastics,[66] first order models have remained popular as they are much easier to apply in larger modeling frameworks, such as fate models or plastic-inclusive bioaccumulation models.[25,26,32,46] Furthermore, biphasic or triphasic multiple component first order models have a long history in understanding and describing HOC sorption to sediments and soils.[67–70] We used a model simulating the exchange of chemicals between plastics, water, micelles and food components, dependent on initial conditions and kinetic rate parameters, while fully accounting for sorption reversibility and possible biphasic sorption behavior. A schematic overview of the model is provided in SI Figure S2.1. Contaminants enter our gut fluid mimic, either sorbed onto microplastics (S1 and S2) or to organic matter (S2 and S3) and subsequently partition into the different gut compartments. Due to the chemical mass conservation, the sum of the concentrations residing in water, micelles, organic matter and plastic remains equal to the initial concentration at all times:

$$C_{total} = C_W + C_M + C_{OM} + C_P{}^*[P] \quad (2.1)$$

where C_{total} (µg/L) is the initial concentration of contaminants sorbed either on microplastics (S1 and S2) and/or organic matter (S2 and S3). C_W, C_M, C_{OM} are concentrations normalized to water volume (µg/L) in water, micelles (i.e. aggregates of sodium taurocholate) and organic matter, respectively. $C_P{}^*$ (µg/kg) is the concentration of contaminants in the microplastics and $[P]$ (kg/L) is the mass concentration of microplastics in the gut fluid. PCB concentration in BSA is assumed to be negligible due to its hydrophilic properties.[71] Intraparticle diffusivities are much higher in amorphous organic matter and in the fluidic micelles than in the plastics, as the ground organic matter particles and nanometer-sized

micelles[72] are much smaller than the plastics used. Therefore, based on earlier studies,[55,73] the exchange kinetics of contaminants to the bulk solid polymer was assumed to be rate limiting, such that the chemical partitioning to micelles and organic matter could be assumed to be fast and at (pseudo)equilibrium. These equilibria were parameterized using $\log K_d$–$\log K_{OW}$ relationships from the aforementioned studies (equations are provided in SI Table S2.2).[55,73]

To represent the possibly biphasic transfer kinetics of the contaminants to/from microplastics, two sorption domains are defined (SI Figure S2.1). The outer domain is the fast-sorbing compartment which uptakes and releases contaminants from the water component and the interior mass of the polymer. The interior domain represents the slow-sorbing compartment which uptakes and releases contaminants from the outer domain, dependent on intrapolymer transport kinetics. The exchange of contaminants between the fast and slow reservoir is modeled as

$$\frac{dC_1{}^*}{dt} = \frac{k_1}{f_1[P]} C_W - k_2 C_1{}^* - k_3 C_1{}^* + k_3 C_2{}^* \quad (2.2)$$

$$\frac{dC_2{}^*}{dt} = k_3 C_1{}^* - k_3 C_2{}^* \quad (2.3)$$

where $C_1{}^*$ and $C_2{}^*$ are concentrations of contaminants in the fast and slow reservoirs of the polymer (µg/kg) respectively, f_1 is the fast reservoir fraction of the total bound mass of chemical (dimensionless), k_1 is the sorption rate constant (d^{-1}), k_2 is the desorption rate constant (d^{-1}) and k_3 is the intrapolymer rate constant (d^{-1}).

The total concentration of contaminants on the microplastic, $C_P{}^*$, is then computed from $C_1{}^*$ and $C_2{}^*$ according to the following equation:

$$C_P{}^* = f_1 C_1{}^* + (1 - f_1) C_2{}^* \quad (2.4)$$

For all scenarios, the boundary condition for C_W when plastics were added to the gut fluid mimic (t=672 h) was calculated by assuming a fast pseudoequilibrium redistribution of the PCBs bound to food organic matter, micelles and water. This is based on the same arguments of polymer diffusion being rate limiting as mentioned above. Hence, these effectively represent systems with contaminated food entering equally contaminated gut systems as would occur for sorbing chemicals in nature.[26,44]

The PCB concentration in plastic ($C_P{}^*$) over time was modeled by fitting the aforementioned mass balance and ordinary differential equations, where k_1, k_2, k_3 and f_1 are fitted parameters, using the minpack.lm package[74] and deSolve[75] in R.[76] The Levenberg-Marquardt algorithm was used to estimate the set of parameters based on the least residual sum squares of the modeled versus measured values. We also allowed the model to parameterize the

C_{total} in Scenarios 1 and 3. The information from these scenarios was then used to predict the total PCB concentration in Scenario 2 during the exposure in gut fluid mimic (from t=672 h). Because a fraction of the plastic and its associated PCBs was removed from the systems at each time point, this was accounted for in the modeling.

As the steady state solution of the biphasic differential equations results in equal chemical concentrations in the fast and slow reservoir fractions (${C_1}^* = {C_2}^*$), the equilibrium partition coefficient of the polymer with water was calculated as

$$K_P = \frac{k_1}{k_2 f_1 [P]} \tag{2.5}$$

2.2.4. Statistical analysis

The Shapiro-Wilk test was used to check for normality and Levene's test (found in car[77] R package) for homogeneity of variance before carrying out multiple comparisons of means across groups. Log transformations were performed accordingly when data were not normally distributed. In S2, differences in the total concentration of PCBs on plastic strips over time were evaluated using one-way ANOVA.[76] Tukey's Honest Significance Difference (HSD) was implemented when variance between groups were significantly different (p<0.05). Multcomp package was used to demonstrate the differences between groups.[78] Kruskal-Wallis test was used when data were not normally distributed or homogenous.

2.3. Results and discussion

2.3.1. Scenario 1: Desorption from contaminated plastic in the gut

***Kinetics for PE microplastics*.** This scenario was meant to mimic chemical transfer upon ingestion of contaminated microplastic by organisms. The two compartment model was applied to the sorption as well as the desorption phase in one go, where the concentrations after 672 h were used as boundary condition for the desorption stage from 672 to 1344 h. This implies that any non-equilibrium after 672 h of sorption is accounted for and thus no assumption on sorption equilibrium is required. Fits to the data were excellent and indeed revealed that after 672 h, full equilibrium was not achieved in the polymer phase, especially for PVC, and that (de)sorption was biphasic (Figure 2.1; individual plots for other PCBs are presented in SI Figure S2.2). That desorption was biphasic is formally proven by the fact that the parameters f_1 and k_3 were statistically significant for all (f_1) and part (k_3) of the congeners (SI Table S2.3–2.4), implying a relatively fast release of contaminants from the outer reservoir of the plastic (f_1) followed by a slower release, governed by intrapolymer transport (k_3). Our other hypothesis, that is, that (de)sorption is reversible, was also

confirmed. After all, most values for k_1, which is the rate parameter for backward sorption, were statistically significant especially for the PCBs at the lower end of the hydrophobicity range (SI Table S2.3–2.4). For these less hydrophobic PCB congeners the ratio of desorption (k_2) to sorption (k_1) rates is lower, leading to relatively high C_W, rendering backward sorption more relevant and therefore statistically significant. In any case, this implies that backward sorption cannot just be neglected.

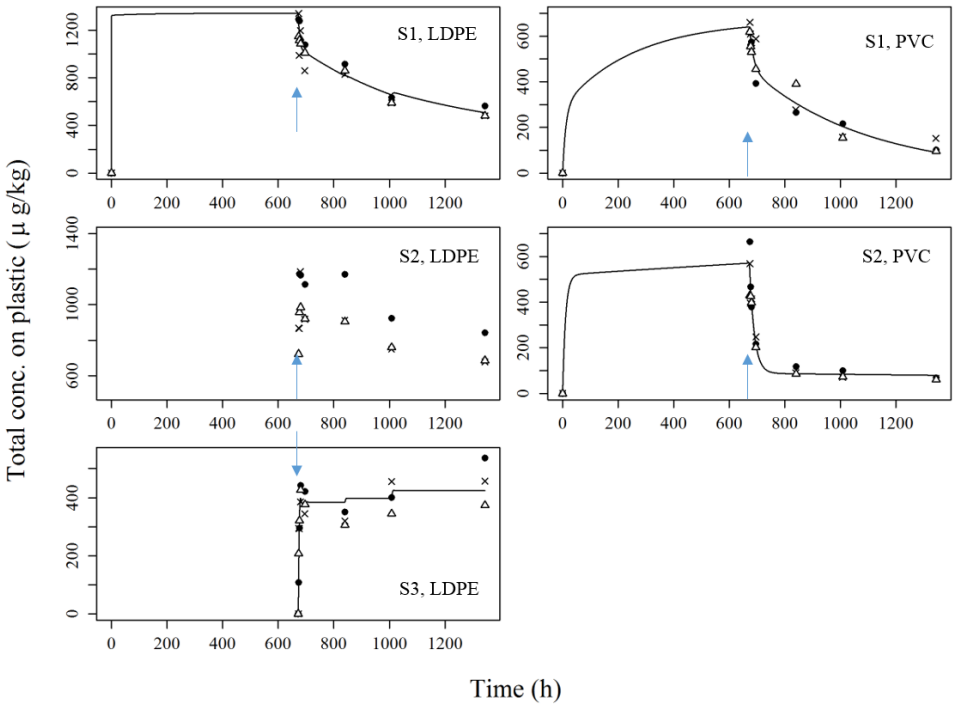

Figure 2.1. Total concentration (µg/kg) of PCB 77 on plastics measured (symbols) and modelled (curves) over time in Scenario 1, 2 and 3 (from top to bottom). Plastics were exposed to contaminants in the aqueous phase from t=0 to 672 h followed by exposure in gut fluids from t=672 to 1344 h. The moment of simulated ingestion is indicated by blue arrows. Each symbol represents a replicate system.

The k_2 values for LDPE ranged from 0.21 to 0.67 h^{-1} (SI Table S2.3), translating into desorption half-lives of 1.03 to 3.36 h. This rate constant k_2 only applies to the fast reservoir fraction of the plastic-bound chemicals. The range of k_2 values for the lower PCBs (5 to 11.89 d^{-1}) is consistent with the desorption rate constants between 1 and 10 d^{-1} provided by Koelmans et al. 2013,[25] which was based on first-principles regarding polymer diffusion. The k_3 values for LDPE ranged from 0.09 to 0.22×10^{-2} h^{-1} (SI Table S2.3), translating into 2 orders of magnitude longer desorption half-lives than k_2; ranging from 13.12 to 31.76 days. This rate constant k_3

applies to only the slow reservoir fraction of the plastic-bound chemicals. Consequently, the outer and inner fractions of the polymer did not reach equilibrium over the experimental period, with the concentration in the outer sorption domain being higher than in the inner domain, when desorption started. As mentioned, our dynamic model however fully accounted for this nonequilibrium. For LDPE, f_1 values ranged from 0.17 to 0.60 (SI Table S2.3), which means that both kinetic domains need to be taken into account when assessing the amount of chemicals solubilized from the plastic into the gut fluid.

Among PCB congeners, the (de)sorption behavior from LDPE differed as a function of their hydrophobicity. As shown in SI Figure S2.3, K_P values derived from the fitted parameters k_1, k_2 and f_1 (eq. 2.5) correlated positively with K_{OW} ($\log K_P = 0.51\ (\pm 0.11) \times logK_{OW} + 1.45\ (\pm 0.70), r^2 = 0.65, n = 14$), complying to previous studies.[56,79] However, the regression had a smaller slope than other studies, which for instance were developed for PE passive samplers. The difference can be attributed to the differences in the plastics used. The partition coefficient of a polymer does not only depend on polymer type but other characteristics such as plasticizers may also influence the ability of the polymer to uptake the compounds.[80,81] The change in K_P with K_{OW} for LDPE is mainly governed by the variation in k_1 which significantly increases with K_{OW} ($logk_1 = 0.86\ (\pm 0.08) \times logK_{OW} - 4.08\ (\pm 0.54), r^2 = 0.90, n = 14$).

Kinetics for PVC microplastics. Like for PE, reversibility and biphasic behavior of chemical exchange between PVC and gut fluid are demonstrated based on the good fits of the observations with the proposed model (Figure 2.1; see also SI Figure S2.2) and significance levels of parameter values (SI Table S2.4). The kinetic rate constants, k_1, k_2 and k_3 ranged from 0.010 to 0.067 h^{-1}, 0.021 to 0.302 h^{-1} and 0.084 to 0.642x10^{-2} h^{-1}, respectively (Figure 2.2, SI Table S2.4). Significant positive correlations (p<0.05) were observed for both k_1 and k_2 with K_{OW} ($logk_1 = 0.17\ (\pm 0.07) \times \log K_{OW} - 2.65\ (\pm 0.47), r^2 = 0.32, n = 14$; $logk_2 = 0.43\ (\pm 0.11) \times logK_{OW} - 3.80\ (\pm 0.69), r^2 = 0.57, n = 14$). The intra-polymer transport, k_3, also positively correlated with K_{OW} ($logk_3 = 0.33\ (\pm 0.09) \times logK_{OW} - 4.79\ (\pm 0.58), r^2 = 0.53, n = 14$). The positive correlations of the fast and slow kinetic parameters with K_{OW} suggest that sorption processes in PVC are somehow influenced by hydrophobicity of the compounds. In addition, the fast fraction reservoir f_1 increased linearly with K_{OW} ($f_1 = 0.08\ (\pm 0.04) \times logK_{OW} - 0.10\ (\pm 0.23), r^2 = 0.30, n = 14$). This increase in the apparent fast fraction might be explained from nonequilibrium when desorption starts. Very slow and incomplete absorption into the slow domain would cause the chemical fraction in the fast domain to be relatively large, leading to larger *apparent* fast fractions for more hydrophobic chemicals. At the same time, the effective diffusion path lengths in the smaller slow fractions are shorter, thus accelerating the transport of the

chemicals from the slow domain to the fast domain during desorption, which explains k_3 to be higher for these more hydrophobic chemicals. The apparent affinity of chemicals with PVC also decreases as K_{OW} increases (SI Figure S2.3), quantified as $logK_P = -0.35\ (\pm 0.06) \times logK_{OW} + 4.49\ (\pm 0.42)(r^2 = 0.71, n = 14)$.

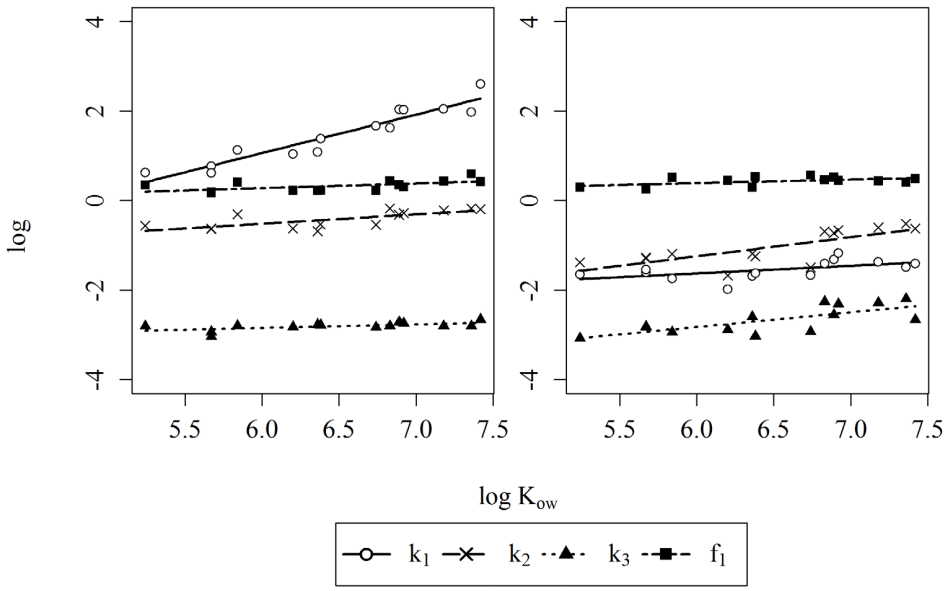

Figure 2.2. Log values of kinetic parameters vs log K_{OW} relationships for LDPE (left) and PVC (right).

The trends observed for PVC are contrasting to those found for LDPE. Overall kinetics was slower for PVC than for PE (Figure 2.1), with desorption rate constants k_2 being about five times lower on average. This difference may be attributed to the polymer characteristics of LDPE and PVC, the latter being classified as more glassy than LDPE.[82] Due to the higher glass transition temperature of PVC than LDPE, the mobility of the segments within the PVC chains is lower. Consequently, it has a more condensed structure and lower free volume. Pascall et al. (2005)[83] observed that larger PCB congeners had a lower partitioning potential in PVC possibly due to this lower free volume. It was suggested that the increasing molar attraction of the molecules would result in an increasing resistance to the diffusion of the molecules through the polymer. Hence, the lower diffusivities of the molecules coupled with the limited free volume may have resulted in lower affinity of the larger congeners in PVC.

Comparison with earlier published data from gut fluid studies. Bakir et al. 2014[53] had previously reported rates ranging from 0.27 to 12.10 d^{-1} for release of sorbed phenanthrene (Phe), 4,4'-DDT and di-2-ethylhexyl phthalate from PE and PVC particles (200–250 µm) under

varying gut conditions. However, desorption rates in their study were determined from the slopes of ln ($C_i/C_{i,0}$) vs. time, thus assuming an irreversible, desorption-only one compartment first order rate kinetics model. Inspection of their release data (SI Fig S10–S15 in Bakir et al. 2014[53]) actually suggests biphasic behavior with fast release in the first 15–30 mins followed by a slower release kinetics, similar to what we observed here. Similarly, an earlier study investigating desorption of Phe in artificial gut fluids reported first order desorption rate constants from 2.29 ± 1.40 to 9.70 ± 2.10 d^{-1} in PE, PP and PVC.[52] Both studies reported desorption rate constants obtained from a first order rate kinetics model that averaged out the fast and slow transport of chemicals from the plastic. The aforementioned model thus is likely to underestimate the initial transport rates of chemicals and hence, exposure when chemicals desorb in the gut. On the other hand, release at longer time scales would be overestimated. To illustrate the differences between the two modeling approaches, we also fitted our data with the desorption-only one compartment first order rate kinetics model. The one-compartment first order desorption rate constants obtained based on our data in the first 4 h ranged from 0.034 to 0.154 h^{-1} for LDPE and 0.016 to 0.108 h^{-1}, which are 2 to 6 times lower than the k_2 values obtained with our present model, implying that previously reported desorption rate constants in the aforementioned studies may have also been underestimated. In addition, we demonstrated slow equilibration times, with more than 50 days required to acquire equilibrium for PCBs at the higher end of the hydrophobicity range. These time scales agree to earlier findings,[84–86] and also illustrate that the short equilibration times in earlier gut fluid studies may have been too short, leading to overestimation of desorption rate constants.

2.3.2. Scenario 2: Mimicking the simultaneous ingestion of contaminated plastic and contaminated food

We investigated the environmentally realistic scenario in which an organism ingests plastic and food (prey) that are both contaminated, at the same time. Since both the plastic and food which an organism ingests come from the same environment, the contaminants that the plastic and food are exposed to would be the same.[26,27,60] The relative amount of contaminant desorbed from plastic in the gut fluid will then also depend on the amount desorbed from the food within the organism's gut. Based on simple principles of chemical partitioning, we hypothesize that food organic matter will compete for the chemicals with the plastic in the gut, and thus when compared to S1, less of the chemicals will be desorbed.[32] For this scenario LDPE was used, which can be assumed to have K_P values of similar magnitude as organic matter and micelles in the gut.[55,73]

Indeed, little or no significant desorption of PCBs occurred from LDPE when introduced into gut fluid at the same time as contaminated natural prey items. We show concentrations of PCB 77 on LDPE strips over time, showing no significant changes (p>0.05; ANOVA; Figure 2.1). The behavior of this compound represents that of most of the PCBs except for the lower congeners (i.e., PCB18, 28, 31 and 52) where we observed a slight decrease at the end of the desorption phase (SI Figure S2.4). For most of the higher PCB congeners, the observations agree with our hypothesis in which the contaminated LDPE competes with food organic matter and micelles for the PCBs in the system. Given the higher relative abundance of food compared to LDPE and micelles, and the fact that the equilibrium partition coefficient of organic matter (K_{OM})[55] was similar to K_P for LDPE (our study), a larger fraction of chemicals resided in the food and thus a lower desorption from LDPE was observed. Due to the lack of concentration change and the higher number of model parameters in this system, a quantitative assessment of model parameters was not possible for this system.

The PVC case was meant as a control to the aforementioned LDPE scenario by using same PCB concentrations, however with a lower K_P for PVC than for LDPE by about 2 orders of magnitude and even lower than K_{OM}. Compared to LDPE, PVC thus has a low apparent affinity for PCBs, leading to more desorption from the plastic. Indeed, we observed a significant decreasing trend in the PCB concentrations on PVC over time (p<0.001; ANOVA, Figure 2.1 and SI S2.5). For PVC, the desorption data could be fitted with the model for PCB 18, 28, 31, 66, 77, 126 and 169 as the chemicals were measurable in the plastic over time (SI Figure S2.6). The fast sorption rate constant (k_1) ranged from 0.04 to 0.08 h^{-1}, desorption rate constant (k_2) ranged from 0.06 to 0.34 h^{-1} and the slow kinetic rate constant (k_3) ranged from 0.002 to 0.141 ($\times 10^{-2}$) h^{-1} (SI Table S2.5). The kinetic rate constants observed here which were significant (p<0.05) falls within the ranges found for PVC in S1.

2.3.3. Scenario 3: Mimicking ingestion of clean plastic with contaminated food

There are two reasons why microplastics could take up chemicals from aquatic organisms rather than the other way round. First, part of the plastics that are recently introduced in the environment will not have equilibrated with environmental contaminants. Hence, for these relatively “clean” plastics, there is a possibility that the concentration of contaminants sorbed would be lower than that of the food (prey). Second, aquatic organisms biomagnify chemicals to higher than equilibrium concentrations, which implies that plastic may uptake chemicals from organisms even if the chemical-bound plastic would be at equilibrium with the ambient water.[26,45,87] The capacity of microplastics to take up chemicals from food in gut fluids has however not been demonstrated, because no earlier studies included this scenario.

Therefore, in S3 we assessed potential transfer from contaminated food to precleaned plastic, under artificial gut fluid conditions. Data show a fast uptake of PCBs by LDPE with a half-life ranging from 0.003 to 0.113 mins, followed by a slower uptake with a half-life ranging from 5.65 h up to 44.9 weeks (Figure 2.1 and SI Figure S2.7; SI Table S2.6). Here, the ingested plastic thus rapidly "cleans" the gut since LDPE has a high sorption capacity and fast uptake kinetics (k_1) for hydrophobic compounds.[56] That chemical transfer is reversible was already demonstrated indirectly in S1, because parameters driving backward sorption were statistically significant. Here, the reversibility of the process is also demonstrated directly: clean microplastic accumulates chemicals from food components under conditions simulating an organism's gut. Like the biphasic desorption observed in S1, uptake is demonstrated to be biphasic. A strong positive correlation between k_1 and K_{OW} is also shown here as is evident from S1 ($\log k_1 = 0.73\ (\pm 0.04) \times logK_{OW} - 1.34\ (\pm 0.25), r^2 = 0.97, n = 14$). The range of k_1 values estimated in S3 is higher by about 2 orders of magnitude than in S1, whereas the rate constant k_2 is lower than the values observed in S1. We assume that these differences are caused by the presence of organic matter in S3, which has been shown to affect sorption and transport kinetics for hydrophobic chemicals, for example, by colloid facilitated transport.[66,88–90] For k_3, only the values for PCB28, 52 and 180 were statistically significant in both scenarios and the values differed by a factor of 2. The very slow sorption to the interior domain implies that concentration changes in the longer term were small, which explains the lower number of significant values for k_3. The fact that we find considerable "cleaning" by plastics (i.e., decreased bioavailability) may be perceived as contradictory to some earlier studies. For instance, Rummel et al. 2016[91] claimed that microplastics did not depurate chemicals in rainbow trout as they did not observe significant differences between the control (without microplastics) and treatment (40% microplastics) groups. However, given the wide confidence intervals in their data, this evidence may not have been sufficient to make the assumption that the cleaning effect was not present. In another study, chemical bioaccumulation was assumed to have occurred in rainbow fish through ingestion of microbeads.[92] This is however contentious as the contaminants bound on the microbeads may have been released into the water and taken up by the fish through uptake from water instead.

In contrast to PE, PVC did not take up measurable quantities of PCBs from the food in 28 days. This is explained from the low partition coefficient for PVC compared to those for the food organic matter and for the micelles. Calculation showed that at equilibrium 0.001 to 0.24 % of the chemical mass would have been taken up by PVC, which is well below the detection limits ($\sim$1 ppb) in our study. The scenario with PVC however illustrates that the microplastic and micelles in this scenario compete for the PCBs originally residing in the organic matter,

and that measurable uptake occurs only if the microplastic has sufficient abundance and affinity for the chemicals.

2.4. General discussion and implications

We demonstrated chemical exchange between microplastics and gut components closely mimicking those in aquatic biota to be biphasic and reversible. Whereas earlier models assumed either irreversible, monophasic[38,53] or reversible, monophasic[25,26,32,59] exchange, the revised and fully parameterized model tool allows for a more accurate and realistic dynamic assessment of bioavailability of plastic-associated contaminants. We assessed differences in behavior among chemicals, polymers, and exposure scenarios, whereas the presence of organic matter also appeared to be relevant. Mechanistic explanations for the latter could not be unambiguously provided and further studies are warranted to address this.

The model parameters from this study can be used to extrapolate the chemical behavior in the gut of animals and humans in general, because the main components of gut fluids of organisms (bile salts and protein) are similar to the gut fluid mimic used, even though they differ to some extent across species, their ages and diets. Here, we use the model parameters from S1 to simulate the percentage bioavailability of PCBs from ingested plastic as a function of gut retention times of different organisms, for the hypothetical case that the organism would be cleaner than the plastic with respect to the chemical in question (SI Figure S2.8). As the gut retention time for most organism ranges between a couple of hours to days, all or most of the fast fraction will be available if a gradient for transfer would exist like in S1. For instance, a small marine organism such as lugworm (*Arenicola marina*), would have a gut retention time between 2.4 and 6h.[25] As shown in the present study, only the fast fraction reservoir in the plastic is relevant as it is the most bioavailable fraction, with desorption half-lives within the first 4 h. Hence, in a lugworm, 14 to 42% of sorbed contaminants on LDPE would be solubilized in the gut fluid, depending on the kinetic parameters of the contaminants with the polymer. On the other hand, the gut retention time of plastic particles in an Atlantic cod ranges from 10 to 20 days.[93] During this time period, it is estimated that 45 to 76% of the sorbed contaminants would solubilize. Since its retention time spans across the slow desorption step, the increment in the amount solubilized is lesser as the rate is limited by intrapolymer transport. For PVC, the percentages may reach up to 41% in lugworms and almost 83% in Atlantic cod due to the aforementioned differences of kinetic parameters between LDPE and PVC. At times, ingested plastic may get lodged in the gut due to its size relative to the GI tract and may reside in the biota for longer periods of time.[94–97] For such particles, the early peak exposure from the outer sorption domain as well as the slower leaching of chemical governed by intrapolymer transport from the slow sorption domain are relevant for bioavailability over such longer timescales. Therefore, over longer time scales of

28 days, the chemical mass in the slow domain also leaches out, increasing the percentage bioavailable to 53–82% for LDPE and 73–89% for PVC. We would like to emphasize though that the bioavailability percentages presented here are only applicable for conditions similar to S1. The percentages may differ when gut characteristics, such as solid to liquid ratios and pH, vary, or when the gut contents are constantly renewed, scenarios which however still could be covered by the model.

On the other hand, it is also possible for ingested MP to clean the gut content of biota, like in the case for S3. Using the model parameters from S3, we simulated the percentage of chemicals remaining in the gut fluicd upon addition of clean microplastic. When the LDPE to food organic matter mass ratio is 0.33, like in our experiment, the decrease in the percentage of PCB remaining in the gut content ranges from 2 (PCB28) to 9% (PCB138), dependent on chemical hydrophobicity (Figure 2.3). However, higher plastic to food ratios may be relevant on hot spot locations or in the future. When performing scenario calculations for slightly higher plastic to food ratios (0.35–0.38), it appears that all of the initially present chemical concentration can be removed from the gut, further indicating the cleaning effect by LDPE (Figure 2.3).

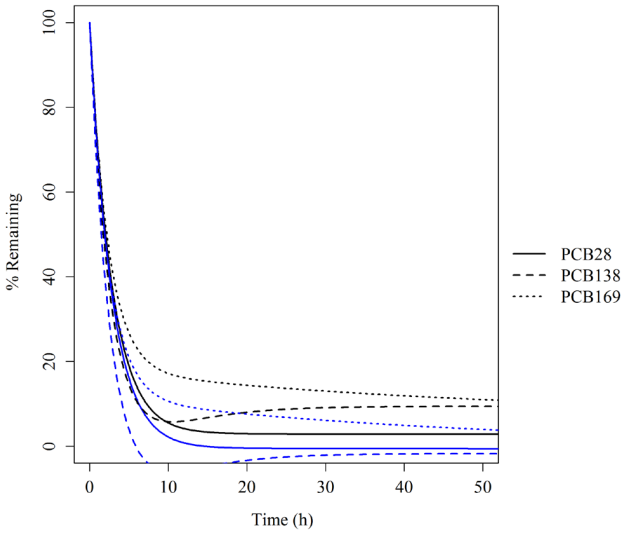

Figure 2.3. Percentage of the initial concentrations of PCB 28, 138 and 169 remaining in the gut fluid over time, due to the presence of clean LDPE. The percentages decrease over time, which thus demonstrates “cleaning” of the gut of a contaminated organism by microplastic ingestion. Black curves are based on experimental conditions (plastic:food = 0.33) and demonstrate cleaning up to 98%. Blue lines are based on higher plastic concentrations with higher plastic:food ratios of 0.35, 0.38 and 0.37 for PCB 28, PCB 138 and PCB 169, respectively, and demonstrate cleaning up to 100% of the initial concentration.

With the model, we can also predict the exposure of humans to chemicals from ingested microplastics in detail. After all, the concentration of sodium taurocholate used in the present study is similar to the recommended concentration for fed-state simulated intestinal fluid in humans.[61] Furthermore, micelles are responsible for most of the solubilization of HOCs[62,63,98,99] and digestive enzymes have shown little effect on bioavailability.[62] Human exposure to microplastics upon ingestion is likely and relevant as microplastics have been detected in mussels,[100–104] seafood,[105,106] beer,[107,108] honey,[109] sea salt[107,110,111] and most importantly drinking water.[107,112] Since absorption takes place mainly in the small intestine for humans (where micelles are present), gut retention times of 3–4 h[113] would be plausible depending on the age, leading to 12–40 % and 6-33% of released individual chemical for LDPE and PVC respectively, if the ingested plastic is the only source of the chemical such that S1 would apply.

There is a common misconception that ingestion of microplastics would always increase the chemical load of an organism and act as a vector of hydrophobic contaminants. Here, we have empirically demonstrated that plastics can make no difference (S2) or can also uptake contaminants from the gut contents of an organism (S3), thus decreasing the bioavailability of chemicals present in the gut. This “cleaning” effect is trivial from an environmental chemistry perspective and therefore has been accounted for in theoretical models.[4,13,16,20] However, the direct evidence presented here reconfirms the principle empirically in the context of microplastic research and allows for refinement of earlier model scenario calculations[32] by implementing biphasic kinetics and congener specific rate constants. The scenarios we presented illustrate that whether ingested plastics act as a source or sink of HOCs depend on the fugacity gradients between the organism’s gut contents and the ingested microplastics and thus is context dependent.[25]

Acknowledgements

We would like to thank Yayasan Mendaki (Singapore) for the Ridzwan Dzafir Distinction Award. The Aquatic Ecology and Water Quality group of Wageningen University and Research is acknowledged for co-funding this project. We would like to thank Frits Gillissen and Urbain Vaes for their assistance and advise in the project.

Supporting Information for Chapter 2

Table S2.1. Details of PCB congeners and respective concentrations in stock mixture used for spiking in experiment setup.

Congener	Chlorine	Molecular formula	Molecular weight	Planarity	Log K_{OW}[a]	Concentration (µg/L)
PCB 18	Tri	$C_{12}H_7Cl_3$	257.538	Non-planar	5.24	22630.21
PCB 28	Tri	$C_{12}H_7Cl_3$	257.538	Non-planar	5.67	24368.48
PCB 31	Tri	$C_{12}H_7Cl_3$	257.538	Non-planar	5.67	28329.43
PCB 52	Tetra	$C_{12}H_6Cl_4$	291.98	Non-planar	5.84	23992.15
PCB 66	Tetra	$C_{12}H_6Cl_4$	291.98	Non-planar	6.2	24333.64
PCB 77	Tetra	$C_{12}H_6Cl_4$	291.98	Planar	6.36	21952.15
PCB 101	Penta	$C_{12}H_5Cl_5$	326.422	Non-planar	6.38	25584.65
PCB 118	Penta	$C_{12}H_5Cl_5$	326.422	Non-planar	6.74	23712.2
PCB 126	Penta	$C_{12}H_5Cl_5$	326.422	Planar	6.89	26402.43
PCB 138	Hexa	$C_{12}H_4Cl_6$	360.864	Non-planar	6.83	24761.73
PCB 153	Hexa	$C_{12}H_4Cl_6$	360.864	Non-planar	6.92	29445.97
PCB 156	Hexa	$C_{12}H_4Cl_6$	360.864	Non-planar	7.18	27176.08
PCB 169	Hexa	$C_{12}H_4Cl_6$	360.864	Planar	7.42	26833.81
PCB 180	Hepta	$C_{12}H_3Cl_7$	395.306	Non-planar	7.36	26037.08

[a] from Hawker et al.[114]

Materials

We used 14 PCB congeners with log K_{OW} values spanning from 5.24 to 7.42. Details of the PCB congeners are listed in Table S2.1. All PCB stock solutions were prepared in acetone (HPLC grade) at ~500 mg/L. To represent environmentally relevant microplastics that would also be manageable, thin polymer strips were used in the gut fluid experiments. LDPE strips were cut from zipper bags found in the supermarket. PVC strips were cut from sheets obtained from Vink Kunststoffen (Article no.: 104702, Didam, Netherlands). The strips were cut to different sizes to achieve a final mass of about 0.0227 and 0.0236 g per strip respectively. They had thickness of 30 and 250 µm respectively to allow for intrapolymer diffusion paths being of similar length as those in 30-250 µm spherical or irregularly shaped microplastic particles occurring in nature. The selection of the sizes of microplastics in this study are relevant to ingestion by fish and marine organisms based on their dietary habits. The polymer strips were cleaned in methanol for 2 h and kept in acetone-rinsed aluminum foils prior to tests. In two of the scenario setups, the gut fluid solubilization tests included a natural food component which was represented by dried *Gammarus* from JBL (Neuhofen, Germany). Gut fluid solution was prepared with sodium taurocholate hydrate (97%, Alfa Aesar) and bovine serum albumin (fraction V, ≥96%, Sigma-Aldrich) in 0.45 µm pre-filtered artificial seawater made with sea salt (Jozo, Netherlands). Sodium azide (99%) was obtained from Aldrich. All solvents and HCl used were of analytical HPLC grades.

Chemical analysis of plastic strips

One of the strips from each time point was transferred into a 7 mL glass centrifuge tube and 100 µL of internal standard, PCB 72 was added on the strip and left to evaporate. Extraction was conducted by sonication for 30 minutes with 5 mL of hexane:acetone, 5:1 by volume. Sonication was repeated twice with a cooling off period of 5 minutes in between. Solvent extracts were then pooled in a clean glass centrifuge tube. Extraction was repeated on the same plastic strip with another 5 mL of the solvent mixture. The pooled extracts from the two extractions were concentrated to ~2 mL by evaporating under a gentle stream of N_2. The concentrate was solvent exchanged with 5 mL of hexane twice to ensure there is little or no acetone left in the extract for PCB quantification. 100 µL of internal standard, PCB 143 was added to the final extract (~0.9 mL) before quantification. PCB 72 and 143 was used to account for method recovery and instrument fluctuations respectively. Extractions were analyzed by gas chromatography with electron capture detection following previously published procedures[48,115] (Agilent 7890B equipped with an Agilent 7693 autosampler with two capillary fused silica columns: CP Sil 5 CB and CP-Sil 8 CB). The temperature at the injection port was 50°C, the column temperature was 50°C and temperature of the detector

was 300°C. The limit of detection (LOD) was set at half of the signal of the lowest concentration of the calibration standards (~1 ppb).

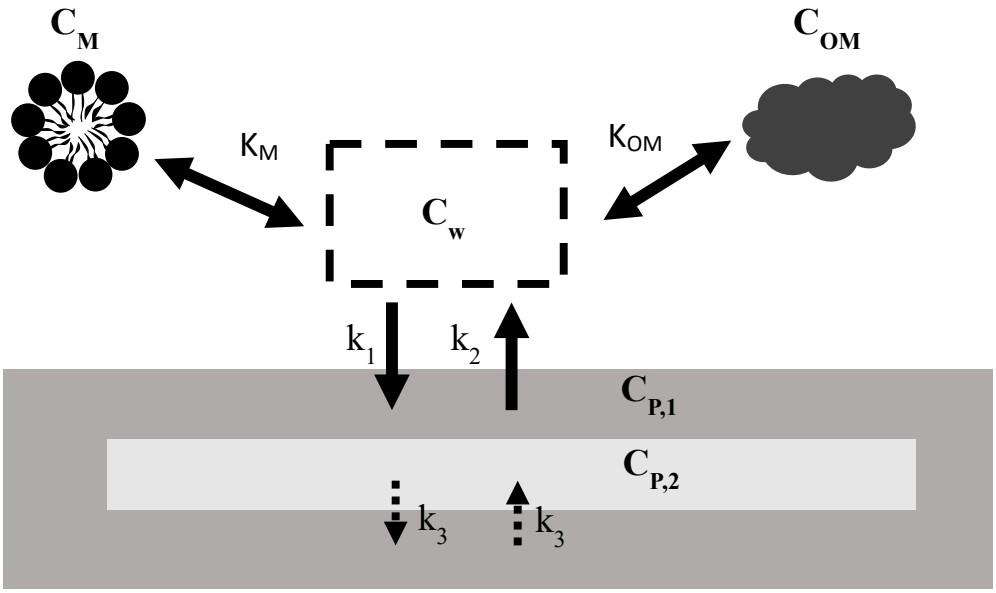

Figure S2.1. Schematic diagram of two-compartment plastic with a fast ($C_{P,1}$) and slow ($C_{P,2}$) reservoir and chemical interactions between plastic, water, micelles and food in the simulated gut fluid experiments

Model equations

Table S2.2. Equations to quantify the sorption of PCBs to organic matter and micelles with equilibrium partition coefficients and the percentage bioavailable to the organism when contaminated plastic is ingested by a clean organism and the percentage remaining (that is available to the organism) when clean plastic is present in a contaminated gut.

Description	Equation
Equilibrium partition ratio between PCB concentration in organic matter (µg/kg) and water (µg/L).	(1) $C_{OM}^{*} = K_{OM} C_W$
Equilibrium partition ratio between PCB concentration in micelles (µg/kg) and water (µg/L).	(2) $C_{M}^{*} = K_{M} C_W$
Relationship between K_{OM} and K_{OW}[a].	(3) $logK_{OM} = 0.82 \times logK_{OW} + 0.14$
Relationship between K_M and K_{OW}[b].	(4) $logK_{M} = 0.76 \times logK_{OW} + 0.88$
PCB concentration in water calculated from system characteristics. Mass concentrations of organic matter and micelles are in kg/L.	(5) $C_W = \frac{C_{total} - [P]\{f_1 C_1 + (1-f_1) C_2\}}{K_M[M] + K_{OM}[OM] + 1}$
Percentage bioavailable.	(6) $\%Bioavailable = (1 - \frac{C_P^*(t)}{C_P^*(t=0h)}) \times 100$
Percentage remaining in the gut.	(7) $\%\ \text{Remaining} = (1 - \frac{C_P^*[P]}{C_{OM}^*(t=0h) \times [OM]}) \times 100$

[a] from Schwarzenbach et al., 2005[55]
[b]from Schacht et al., 2016[73]

Chemical kinetics on plastic in Scenario 1

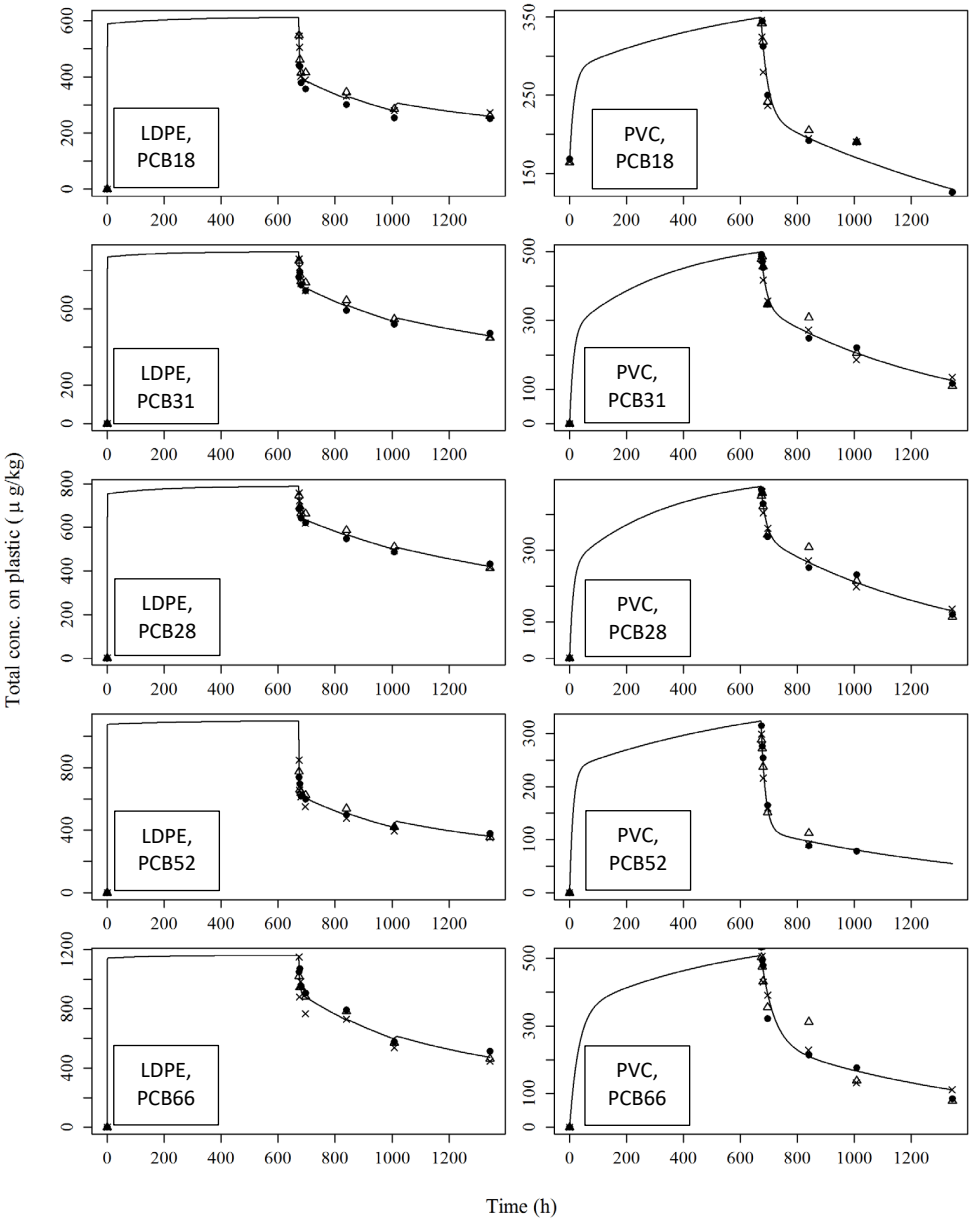

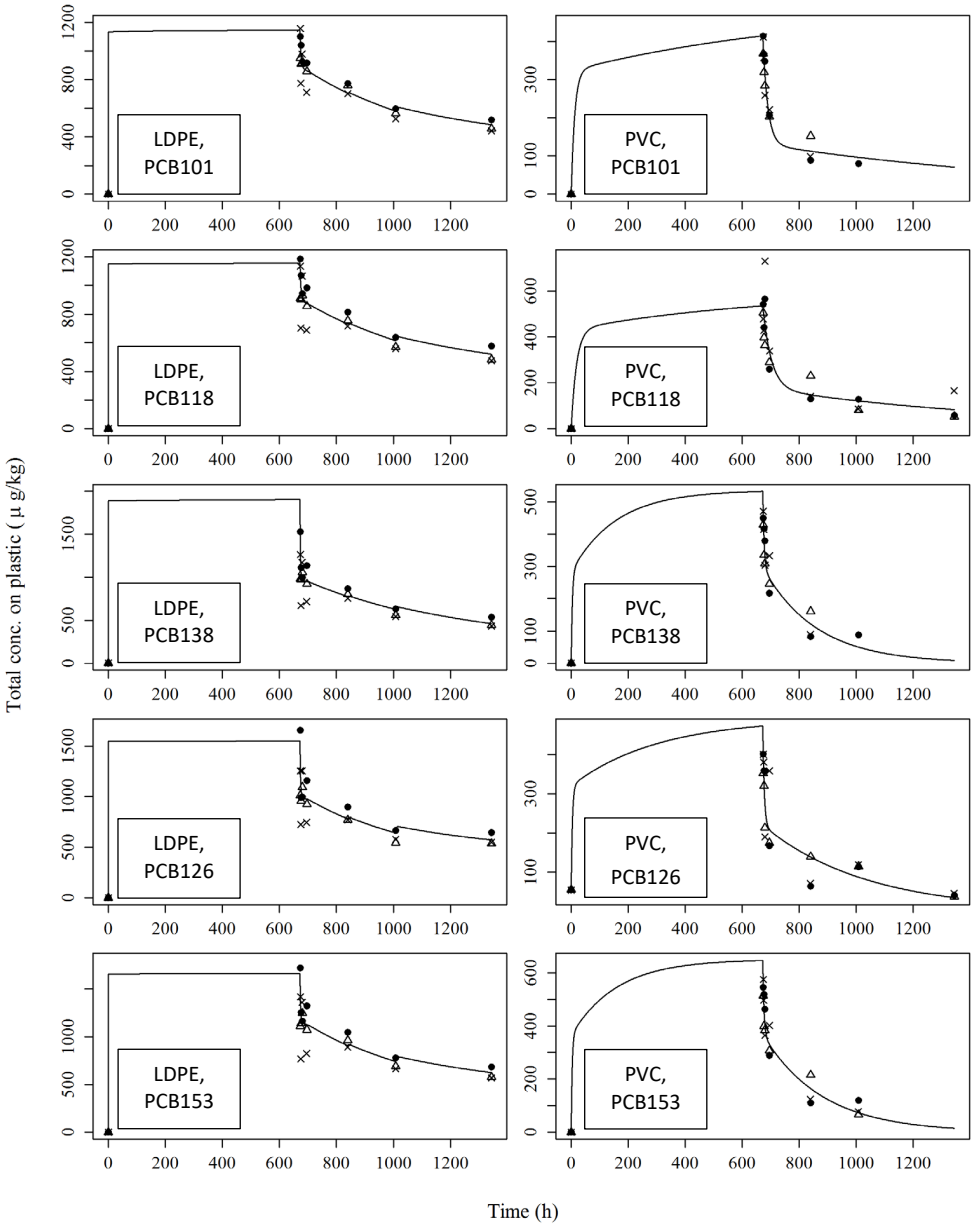
LDPE, PCB101
PVC, PCB101
LDPE, PCB118
PVC, PCB118
LDPE, PCB138
PVC, PCB138
LDPE, PCB126
PVC, PCB126
LDPE, PCB153
PVC, PCB153
Total conc. on plastic (µ g/kg)
Time (h)

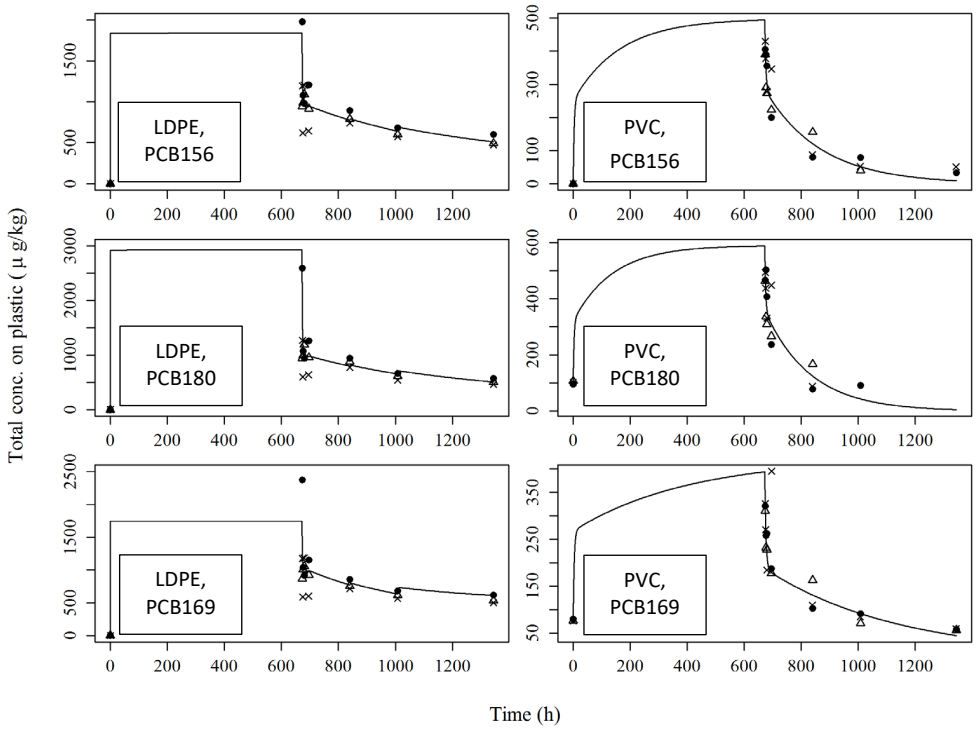

Figure S2.2. Total concentration on plastic strips (µg/kg) measured over time in Scenario 1 (Left panel-LDPE; Right panel-PVC). Plastic strips were preloaded with spiked PCBs in MQ-water from t=0 to 672 h and subsequently exposed to gut fluid conditions from t=672 to 1344 h, which triggered rapid desorption. Each symbol represents a replicate system. Line represents modeled expected values over time.

Table S2.3. Kinetic rate constants and fast reservoir fraction of LDPE in Scenario 1 with standard errors (SE) obtained from parameter estimation using the Levenberg-Marquardt algorithm (minpack.lm). (* p<0.05; ** p<0.01; *** p<0.001)

PCB	Log K_{OW}	k_1 (h^{-1})	SE	k_2 (h^{-1})	SE	k_3 (10^{-2} h^{-1})	SE	f_1	SE	K_P (L/kg)	Log K_P
18	5.24	4.21***	0.65	0.274***	0.067	0.156***	0.038	0.347***	0.032	9.77E+03	3.99
31	5.67	5.85**	1.99	0.233***	0.015	0.116***	0.025	0.190***	0.021	2.91E+04	4.46
28	5.67	4.17***	0.91	0.237***	0.059	0.091***	0.013	0.166***	0.016	2.33E+04	4.37
52	5.84	13.47***	0.97	0.496***	0.037	0.161***	0.018	0.412***	0.026	1.45E+04	4.16
66	6.2	11.04***	0.03	0.237*	0.102	0.151***	0.030	0.223***	0.053	4.61E+04	4.66
77	6.36	12.23**	3.84	0.207	0.126	0.168***	0.025	0.226*	0.097	5.77E+04	4.76
101	6.38	24.29**	6.92	0.295***	0.037	0.164***	0.022	0.228*	0.092	7.95E+04	4.90
118	6.74	46.29*	16.39	0.290	0.143	0.146**	0.040	0.225**	0.060	1.56E+05	5.19
138	6.83	42.43	116.50	0.670***	0.136	0.156	0.133	0.440**	0.136	3.17E+04	4.50
126	6.89	108.50	212.90	0.484	0.850	0.192	0.104	0.352***	0.070	1.40E+05	5.15
153	6.92	106.10**	27.93	0.524	0.359	0.179	0.089	0.300***	0.016	1.49E+05	5.17
156	7.18	111.60***	16.78	0.605***	0.083	0.155*	0.071	0.434***	0.078	9.36E+04	4.97
180	7.36	94.96	80.10	0.669	0.799	0.157**	0.048	0.599***	0.075	5.22E+04	4.72
169	7.42	402.80	250.30	0.640	0.382	0.220	0.184	0.423*	0.193	3.28E+05	5.52

Table S2.4. Kinetic rate constants and fast reservoir fraction of PVC in Scenario 1 with standard errors (SE) obtained from parameter estimation using the Levenberg-Marquardt algorithm (minpack.lm). (* p<0.05; ** p<0.01; *** p<0.001)

PCB	Log K_{OW}	k_1 (10^{-2} h^{-1})	SE	k_2 (10^{-2} h^{-1})	SE	k_3 (10^{-2} h^{-1})	SE	f_1	SE	K_P (L/kg)	Log K_P
18	5.24	2.22***	0.37	4.17***	0.29	0.084***	0.016	0.296***	0.021	3.80E+02	2.58
31	5.67	2.47***	0.38	5.10***	0.64	0.154***	0.016	0.291***	0.028	3.51E+02	2.55
28	5.67	2.87***	0.23	5.34***	0.48	0.146***	0.016	0.263***	0.018	4.33E+02	2.64
52	5.84	1.82***	0.20	6.39***	0.44	0.115**	0.037	0.513***	0.030	1.18E+02	2.07
66	6.2	1.03***	0.30	2.13***	0.55	0.130**	0.034	0.448***	0.058	2.28E+02	2.36
77	6.36	2.07	1.49	6.51	5.56	0.251***	0.051	0.298**	0.091	2.25E+02	2.35
101	6.38	2.40**	0.65	5.64**	1.53	0.094	0.101	0.529**	0.143	1.70E+02	2.23
118	6.74	2.13	1.29	3.21	1.79	0.117	0.146	0.574***	0.123	2.45E+02	2.39
138	6.83	3.92	2.81	20.53	10.95	0.546***	0.130	0.465***	0.066	8.69E+01	1.94
126	6.89	4.79	4.40	18.77	12.10	0.280*	0.100	0.520***	0.082	1.04E+02	2.02
153	6.92	6.67	4.96	21.71	11.09	0.491***	0.089	0.448***	0.063	1.45E+02	2.16
156	7.18	4.28	4.09	24.99	16.34	0.520***	0.109	0.439***	0.083	8.24E+01	1.92
180	7.36	3.27	5.09	30.23	31.14	0.642**	0.192	0.409**	0.133	5.59E+01	1.75
169	7.42	3.89	1.87	23.78**	7.66	0.216***	0.035	0.485***	0.043	7.15E+01	1.85

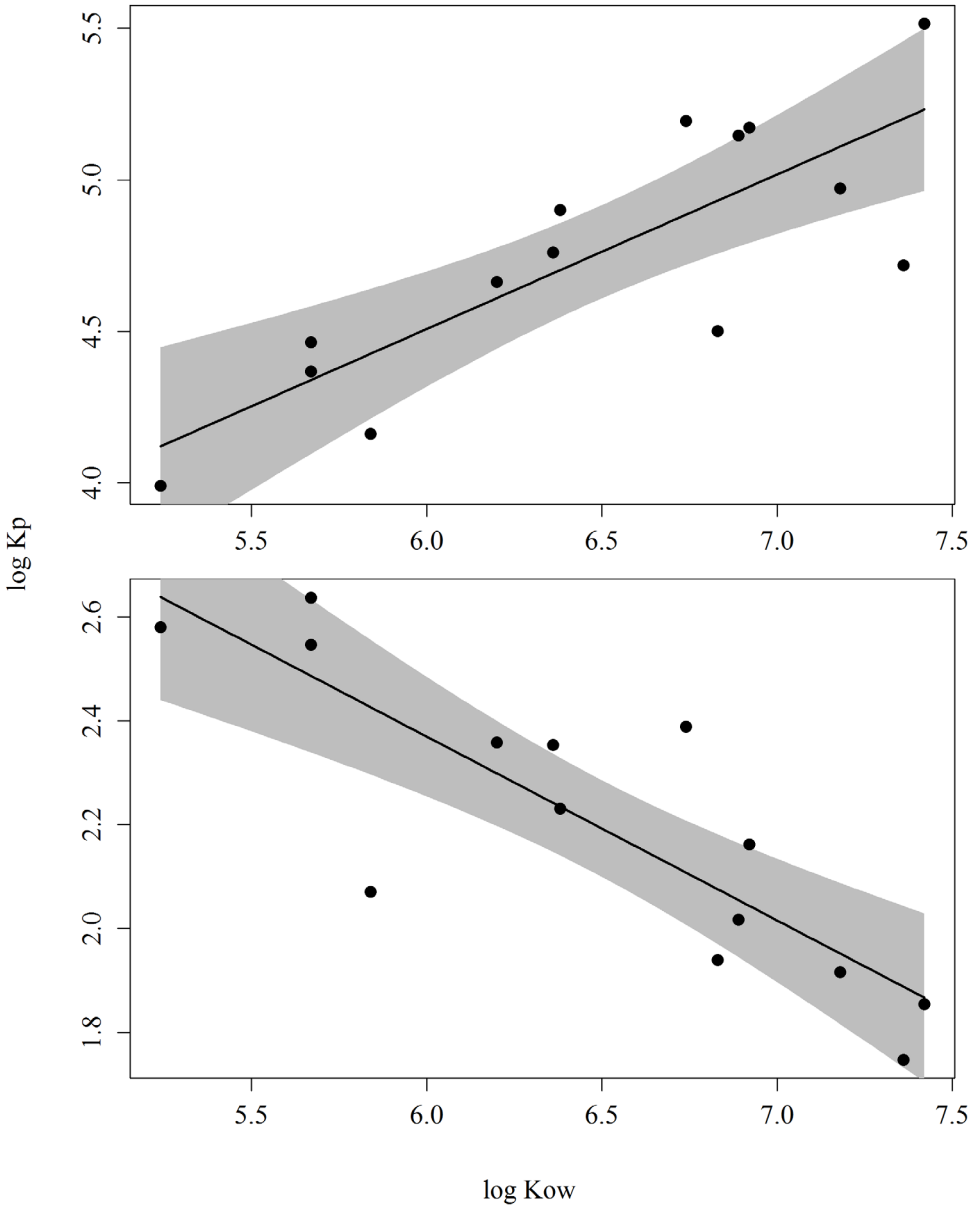

Figure S2.3. Log K_{OW} vs log K_P relationships for LDPE (above) and PVC (below). Shaded regions represent 95% confidence interval of the linear relationships.

Chemical kinetics on LDPE in Scenario 2

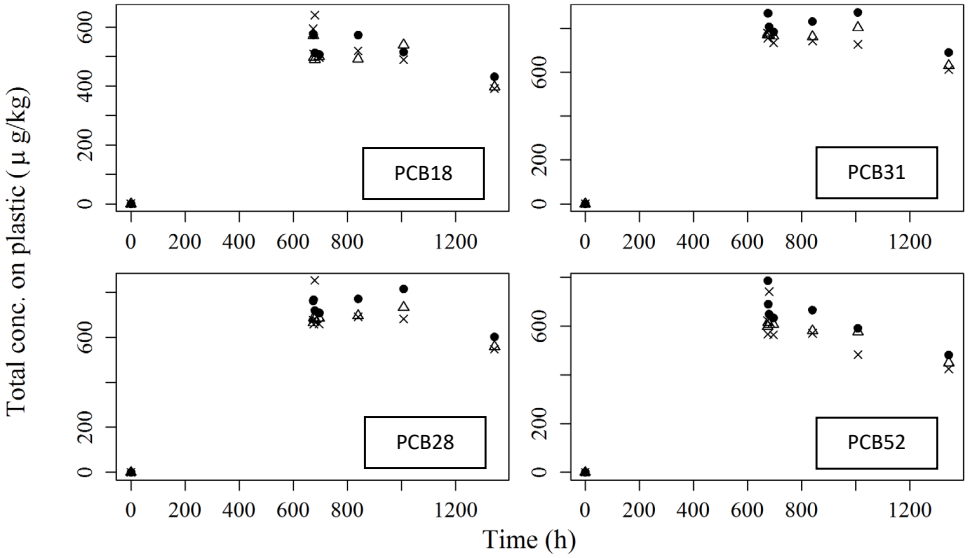

Figure S2.4. Total concentration on LDPE (µg/kg) over time in Scenario 2 for PCBs that have significant differences (see Figure S5) in concentrations between timepoints.

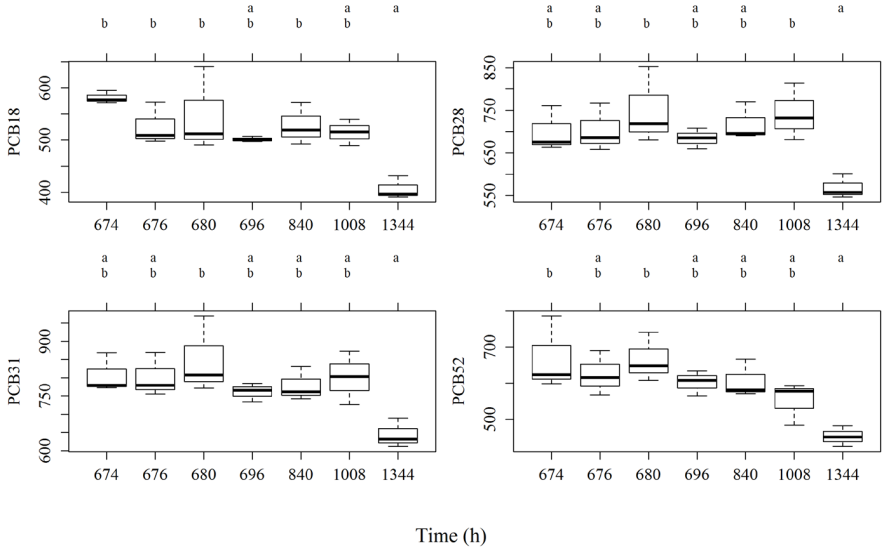

Figure S2.5. Box plots representing total concentration on LDPE (µg/kg) over time in Scenario 2. The line that divides the box into 2 parts represents the median of the data, the end of the box shows the upper and lower quartiles, and the extreme lines shows the highest and lowest value excluding outliers. Same letters above the boxes indicate that the differences between timepoints were not statistically significant.

Chemical kinetics on PVC in Scenario 2

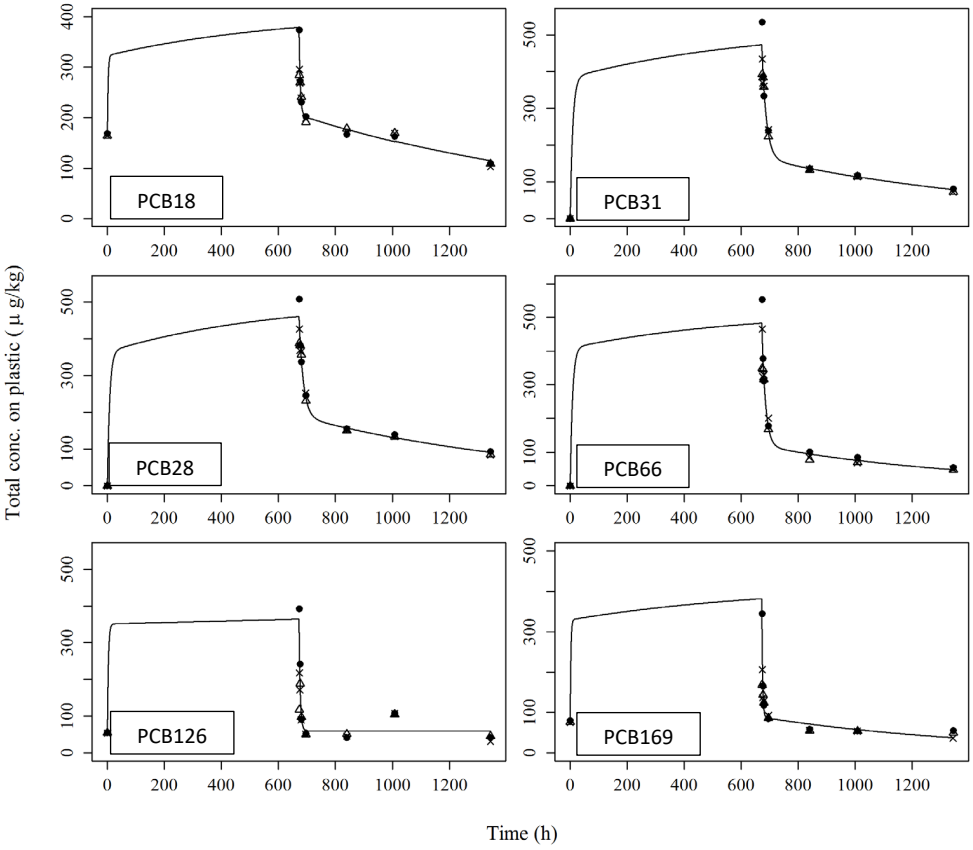

Figure S2.6. Total concentration on plastic strips (µg/kg) measured over time in Scenario 2 for PVC. Plastic strips were exposed to gut fluid conditions from t=672 to 1344 h. Each symbol represents a replicate system. Line represents modeled expected values over time.

Table S2.5. Kinetic rate constants and fast reservoir fraction of PVC in Scenario 2 with standard errors (SE) obtained from parameter estimation using the Levenberg-Marquardt algorithm (minpack.lm). (* p<0.05; ** p<0.01; *** p<0.001)

PCB	Log K_{OW}	k_1 (10^{-2} h^{-1})	SE	k_2 (10^{-2} h^{-1})	SE	k_3 (10^{-2} h^{-1})	SE	f_1	SE
18	5.24	17.62	9.72	22.33**	6.45	0.092***	0.016	0.375***	0.038
31	5.67	4.99***	0.92	6.17***	0.93	0.116*	0.045	0.541***	0.038
28	5.67	5.98***	1.09	6.44***	0.82	0.115**	0.031	0.479***	0.028
66	6.2	4.47*	1.78	7.62*	2.69	0.141	0.097	0.677***	0.059
77	6.36	3.80***	0.99	5.67***	1.07	0.017***	0.001	0.382***	0.074
126	6.89	6.23	4.88	23.08*	10.72	0.002	0.105	0.210	4.697
169	7.42	7.81	5.96	34.33*	14.14	0.128	0.074	0.689***	0.074

Chemical kinetics on plastic in Scenario 3

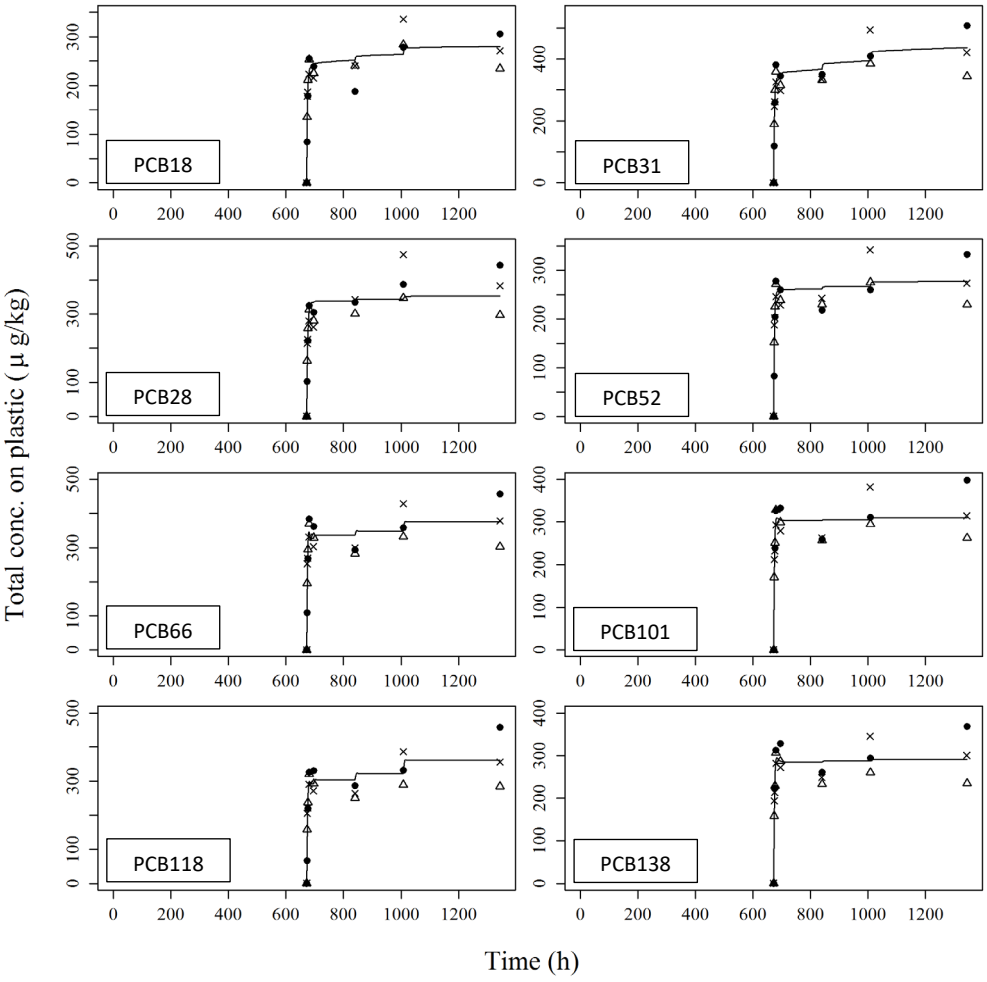

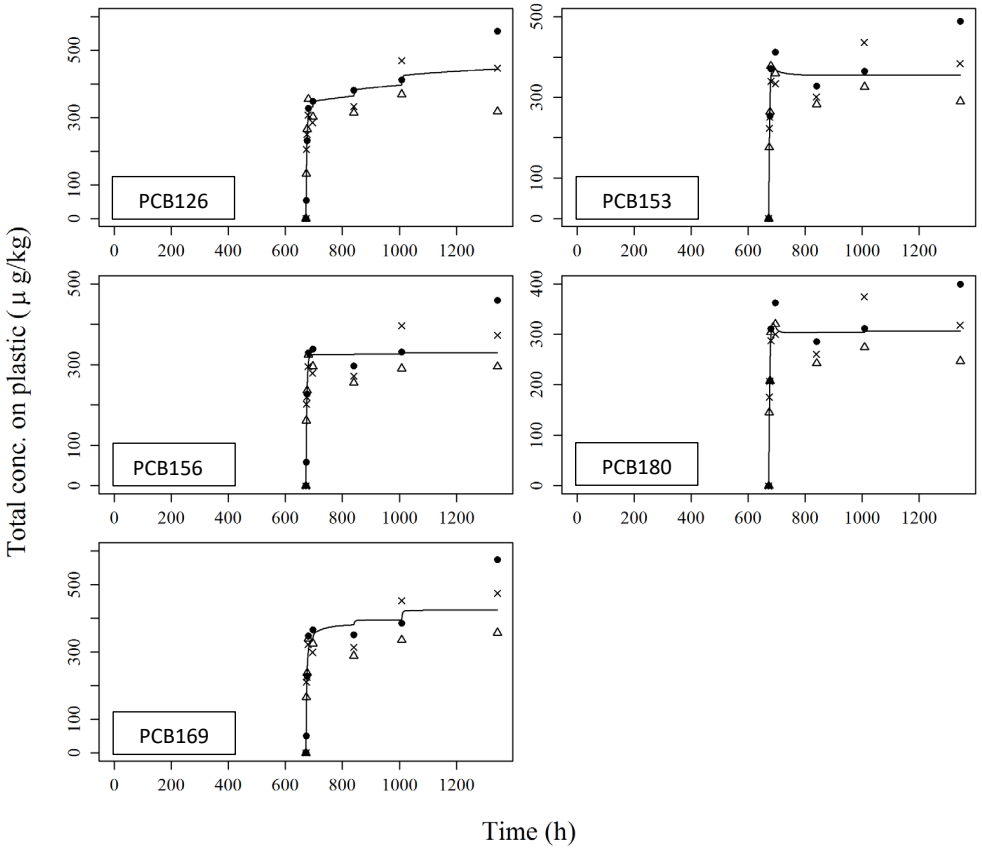

Figure S2.7. Total concentration on plastic strips (µg/kg) measured over time in Scenario 3 for LDPE. Plastic strips were exposed to contaminated gut fluid conditions from t=672 to 1344 h, after which rapid uptake of PCBs by microplastic occurred. Each symbol represents a replicate system. Line represents modeled expected values over time.

Table S2.6. Kinetic rate constants and fast reservoir fraction of LDPE in Scenario 3 with standard errors (SE) obtained from Levenberg-Marquardt algorithm (minpack.lm).). (* p<0.05; ** p<0.01; *** p<0.001)

PCB	Log K_{OW}	C_{OM} (µg/kg)	SE	k_1 (h^{-1})	SE	k_2 (h^{-1})	SE	k_3 ($10^{-2}h^{-1}$)	SE	f_1	SE	K_P (L/kg)	Log K_P
18	5.24	77.72 ***	2.46	367.20 ***	77.52	0.052	0.045	0.232	0.791	0.416	0.361	3.74E+06	6.57
31	5.67	114.10 ***	0.16	785.30 ***	172.80	0.073	0.055	0.046	0.782	0.185	2.388	1.27E+07	7.10
28	5.67	99.97 ***	8.58	580.60 ***	127.20	0.010	0.037	0.103 ***	0.000	0.658	18.920	1.95E+07	7.29
52	5.84	80.98 ***	2.61	1066	862.00	0.020 ***	0.000	0.010 ***	0.000	0.162 ***	0.000	7.39E+07	7.87
66	6.2	108.20 ***	3.71	1268	7181.00	0.206	1.165	8.624	22.720	0.115	1.229	1.17E+07	7.07
77	6.36	122.10 ***	4.34	1657	5205.00	0.121 ***	0.002	10.720	41.930	0.168	0.658	1.79E+07	7.25
101	6.38	95.30 ***	3.06	2836 ***	405.10	0.072	0.817	1.204	14.090	0.099	1.582	8.82E+07	7.95
118	6.74	96.84 ***	3.93	2579	2322.66	0.245	574.919	12.260	28766.5 10	0.124	289.869	1.88E+07	7.27
138	6.83	89.16 ***	2.68	5922 **	1524.00	0.046	0.064	1.925 ***	0.007	0.154	0.179	1.83E+08	8.26
126	6.89	109.20 ***	4.89	5512 **	1622.00	0.067	0.067	0.009	0.008	0.035	0.061	5.14E+08	8.71
153	6.92	108.80 ***	3.85	6316 ***	1610.00	0.003	0.075	0.173	3.576	0.062	0.866	7.44E+09	9.87
156	7.18	96.24 ***	3.76	9599 **	2498.00	0.050	0.691	0.325	2.346	0.061	1.108	6.99E+08	8.84
180	7.36	91.43 ***	3.02	11860 ***	1299.00	0.030 ***	0.000	0.622 ***	0.147	0.077 ***	0.003	1.14E+09	9.06
169	7.42	109.50 ***	4.51	14170 ***	3051.00	0.080 ***	0.003	0.832	1.955	0.346 ***	0.002	1.13E+08	8.05

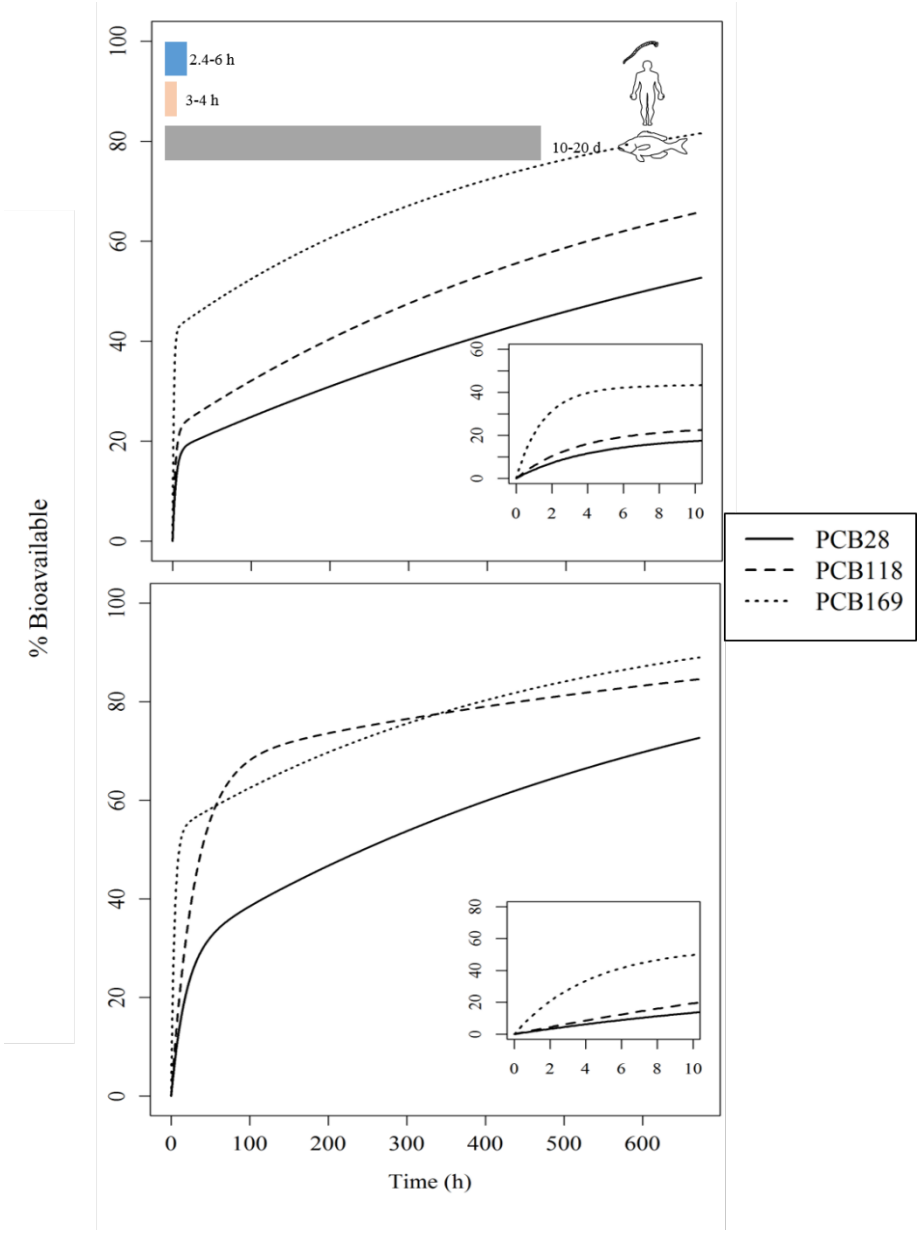

Figure S2.8. Percentage chemical bioavailability from LDPE (top) and PVC (bottom) for PCB 28, 118 and 169 over time when contaminated plastics are ingested by clean biota. Curves are compared with gut retention times of lugworm (2.4 – 6 h), human (3 – 4 h) and cod (10 – 20 h) via coloured bands. Inset plots show percentage bioavailable in the gut up till 10 h.

Chapter 3

How digestive processes can affect the bioavailability of PCBs associated with microplastics. A modelling study supported by empirical data

Nur Hazimah Mohamed Nor, Zhiyue Niu, Marie Hennebelle, Albert A. Koelmans

This chapter was submitted to *Environmental Science and Technology*.

Abstract

The bioavailability of plastic-associated chemicals represents a significant knowledge gap in understanding the human health effects of microplastic. However, the dynamics and bioavailability of plastic-associated chemicals during food digestion is unknown. We assessed if food digestion affects chemical exchange kinetics on microplastics, using an in vitro gut fluid digestive model mimicking the human upper intestinal tract. Chemical exchange kinetics of microplastics were measured for 10 polychlorinated biphenyls (PCBs) under high and low digestion kinetics of olive oil lipids representative of food. The partition coefficients of micelles and oil were determined to evaluate the relative contribution of each gut compartment to sorb PCBs. A new biphasic and reversible chemical exchange model, which included the digestion process, fitted well to empirical data. Under chemical equilibrium conditions in the upper gastrointestinal tract, microplastics can sorb chemicals from contaminated olive oil during digestion reducing chemical bioavailability, resulting in 75% higher concentrations in plastic. However, lipid digestion kinetics is rate-limiting and has little influence in the dynamics and bioavailability of plastic-associated chemicals in the scenario studied. Our chemical exchange kinetic parameter estimates for microplastics under simulated gut conditions with lipid digestion allow us to study important exposure scenarios and human health implications when dietary microplastic concentrations increase.

3.1. Introduction

The microplastic vector effect has been widely discussed in literature and is still one of the major concerns of microplastic pollution.[60] When ingested, microplastics have the potential to act as vectors and transfer chemicals to organisms under certain conditions.[18] These plastic particles contain a mixture of chemicals, which may either be intentionally or unintentionally added. During the manufacturing process, monomers, plasticizers, and additives are usually added to plastics to achieve the appropriate structure for the designated application.[2,116] In addition, during the manufacturing process or product conversion, other unintentionally added chemicals may also sorb onto the material.[117] Another possible source of chemicals in plastics is from ambient water via absorption when the plastics are released into the environment indiscriminately.[118,119]

All biota, including humans, are exposed to microplastics (< 5mm).[2] For animals, plastic consumption can happen when the plastic particles are mistaken for food due to their appearance, or by accidental ingestion due to their feeding method (e.g., filter and deposit feeding), or from the predation of plastic-contaminated organisms.[2] For humans, microplastics may accidentally be consumed from food and beverages contaminated with microplastics. They may also be inhaled from air due to their prevalence in the environment. Human interaction with microplastics is inevitable as we depend on plastic materials in almost every part of our lives (e.g., clothes, food packaging, furniture). Over an average human lifetime of 70 years, it is estimated that an adult can be exposed up to 20 million particles (1–5000 µm), which is equivalent to 12 mg.[120] These estimations were based on nine intake media that were known to have microplastics and comprise 20% of the human diet. Microplastics ingested by humans either come from abrasion and wear-and-tear of plastic products used in our daily lives to process, transport and store food and beverages, or from bioaccumulation in the food chain (e.g., seafood).[121]

As a carrier for a mixture of chemicals, these plastic particles may release chemicals in the organisms' digestive tracts when ingested, potentially increasing exposure and risks.[18,43] An established approach to investigate the chemical vector effect of microplastics when ingested is by performing in vitro gut fluid experiments. This type of experiment has been widely used to investigate chemical bioavailability from indigestible particles such as sediment, asphalt and soot in human and animal digestive tracts.[122–127] Such studies have been increasingly favored to understand the microplastic vector effect in seabirds, aquatic organisms and invertebrates for a variety of chemicals.[128–136] Bioaccessibilities of both organic compounds and heavy metals have also been investigated in different types of in vitro setups mimicking the human digestive tract.[137–139] However, due to the nature of the experiments, these studies can only elucidate the key physicochemical properties of the physiological fluids

and polymers that may have affected the chemical bioaccessibility from microplastics in each compartment of the digestive tract.

Besides measuring the chemical bioaccessibility, in vitro studies are also useful to estimate chemical exchange kinetics.[53,135,136] Using chemical kinetic rate constants and other sorption parameters, the chemical behavior has been simulated for different gut retention times to estimate the chemical bioaccessibilities from ingested plastic in different species.[136] Yet, although the aforementioned study had included food when investigating the chemical exchange inn microplastics, the food component was an inert pool.[136] In reality, this is not the case since food is digested and it is uncertain if the digestion dynamics will affect the chemical exchange kinetics in microplastics. It has also been demonstrated that ingestion of plastic can either increase or decrease the chemical bioaccumulation in organisms depending on whether the ingested plastic releases or uptakes chemicals to/from the surrounding gut components.[136] This depends on the chemical fugacity gradients between plastic and gut components (i.e., micelles and food). During food digestion, the chemical gradients between different gut components will change, but it is unknown to what extent. We hypothesize that as food is digested, the contaminants associated with food will be released, and microplastics may act as a sink for the released chemicals, potentially attenuating chemical bioaccumulation in the biota. To evaluate if microplastics act as a major sink for the chemicals, the chemical behaviour needs to be assessed across all gut components as food is digested. This includes quantifying the sorptive capacities of the other gut components such as food and micelles, which are either produced in the gut or formed from the breakdown of food.

Therefore, in the present study, an environmentally realistic scenario was mimicked whereby an organism ingests contaminated microplastics and contaminated food, followed by food digestion. The aim was to quantify the kinetic rates of chemical transfer from microplastics and elucidate the influence of food digestion dynamics on overall chemical bioavailability under simulated gut fluid conditions. To this end, batch setups of simulated gut fluids mimicking the human gastrointestinal (GI) tract conditions containing olive oil as food lipids[140] and low density polyethylene (LDPE) strips representing ingested microplastic particles were pre-equilibrated with a range of polychlorinated biphenyls (PCBs) to achieve realistic gut chemical conditions. LDPE was chosen here as it is one of the highly produced and used polymer types[141], and is thus a good proxy for microplastics in general. PCBs were used as model hydrophobic organic compounds (HOCs) as they are commonly found in environmental plastics[20,142,143] and in food[144,145], and can represent the general chemical behavior of HOCs. The chemical dynamics in the LDPE were then examined upon lipid digestion as initiated by the addition of lipase, under high and low enzyme kinetics,

respectively. Polyoxymethylene (POM) passive samplers were used to determine the aquatic phase measurements without separating the gut fluid components.[57,81,146] A dynamic multicompartment model[136] was redesigned to include the lipid digestion process. The enzyme kinetic parameters were then explored to elucidate how they affect the chemical exchange kinetics of the PCBs to and from LDPE. Finally, the chemical kinetic parameters during food digestion are discussed in the context of chemical bioavailability and rigorous risk assessments of plastic-associated chemicals for humans[120] and other physiologically similar biota.

3.2. Materials and methods

3.2.1. Materials

All chemicals used were of analytical grade or higher purity and solvents were HPLC grade. Twelve PCB congeners (IUPAC no. 18, 28, 52, 77, 101, 118, 138, 153, 156, 169, 180 and 209) with log octanol-water partition coefficients (K_{OW}) ranging from 5.24 to 8.18[114] were prepared in individual stock solutions in either acetone or isooctane at ~20 to 100 mg/L. The concentrations of each PCB congener in the spike mixture and final experimental setup are provided in the Supporting Information (SI). LDPE strips of thickness 30 µm were cut from zipper bags found in the supermarket, which were also used in our previous experiment.[136] They were cut to a final size of 5.1 × 5.1 cm. As the thickness and thus the intrapolymer diffusion path length of the strip was 30 µm, this represents the intrapolymer diffusion path length of 30 µm spherical or irregularly shaped environmentally relevant microplastics. POM strips of thickness 76 µm were obtained from CS Hyde Co. (Lake Villa, IL) and cut to strips with a size of 3.2 × 3.2 cm to be used as passive samplers to assess the aqueous phase concentrations.[146,147] Both LDPE and POM strips were cleaned in methanol (MeOH) for 24 h under constant shaking on a horizontal shaker at 150 rpm, then shaken with milli-Q water for another 24 h to remove any residual MeOH and air-died before use. Olive oil was purchased from the supermarket (Extra virgin, Carbonell, Spain). Reagents used for preparing the simulated digestive fluids include sodium taurocholate (NaTC) (97%, Alfa Aesar), bovine serum albumin (BSA) (fraction V, ≥96%, Sigma-Aldrich), sodium chloride (Merck Milllipore) and sodium azide (99%, Sigma Aldrich). Lipase FE-01 was obtained from ASA Specialenzyme GmbH, Germany.

3.2.2. Experimental design

Simulated gut fluid digestion assay. The experiment was carried out sequentially in two phases, whereby the systems containing the LDPE and olive oil in simulated gut fluid were first equilibrated for 28 days with PCBs followed by addition of lipase (time= 0 h), which initiated lipid digestion. Three treatments were set up to simulate high (lipase in its original

form) and low (heat inactivated lipase) enzyme reactions, and a control treatment to account for any background PCBs from gut fluid constituents (heat inactivated lipase with no PCBs spike). The high and low enzyme treatments are used to compare between high and low metabolic digestive systems, respectively, since all humans have different metabolic rates.

All experiments were performed in 100 mL transparent glass bottles with glass stoppers in quadruplicates. The simulated gut fluid mixture was prepared to achieve final (i.e., second phase) concentrations of 10 mM of NaTC and 5 g/L of BSA, constituted in 150 mM sodium chloride solution.[61,148] 7 g of olive oil, 10 LDPE strips and a POM passive sampler were added to each bottle filled with 69.85 mL of gut fluid. To limit biodegradation of the olive oil, sodium azide was added to a final concentration of 25 mg/L. Final pH of the mixture was 6.08. Each bottle from the high and low enzyme treatments was spiked with 100 µL of PCB stock mixture (SI Table S3.1) and shaken on a horizontal shaker at 150 rpm at 37°C for 28 days to allow the chemicals to partition to the different components in the gut fluid mixture. This is to mimic an environmentally relevant scenario of chemical intake by humans via both food and microplastic ingestion. It also mimics an already contaminated human gut due to chemical bioaccumulation in the body over the years. Final PCB concentrations in each system ranged from 30 to 124 µg/L (Table S3.1) to ensure that equilibrium concentrations in plastic and food after 28 days were environmentally realistic.[149]

After 28 days, the POM passive sampler and one LDPE strip were collected from each bottle using metal forceps. Since partition coefficients for POM passive samplers are accurately known[57,81,146], it is used to determine the PCB concentrations in the aqueous phase. In addition, 200 µL of the gut fluid mixture was sampled for lipid analysis. For the high enzyme treatment, 10 mL of lipase was added to the bottles in its original form based on the enzyme activity concentration from Minekus et al., 2014[150]. On the other hand, for the low enzyme treatment, 10 mL of lipase was heat inactivated in a 14 mL glass centrifuge tube by heating it to 100°C in a water bath for 10 minutes. The heat inactivated enzyme was then added to the bottles. This was similarly done for the control set-ups. The final food (olive oil and LDPE) to gut fluid ratio was 1:10 (v/v)[148,150] in the systems, with a 1:10 (v/v) ratio for plastic to olive oil. This ratio was chosen to represent digestive systems with a higher lipid content than the amount of ingested plastic. The contents of the bottles were mixed by swirling with hands for 5 minutes before removing one LDPE strip. Subsequently, the gut fluid kinetics experiment was carried out over 72 h with continuous shaking on a horizontal platform shaker incubator at 150 rpm at 37°C. The experiment was performed for a longer time scale than realistic digestion times. This causes higher chemical concentration gradients, which implies chemical transfer kinetic rates can be assessed more accurately. Furthermore, this way we also consider possible scenarios whereby particles are retained in the gut longer than

food. Although there is a lack of empirical evidence on the gut retention times for microplastics in humans, other studies have shown that particle retention time in animals' guts, such as fish and lobsters, differ from food.[151–153] One LDPE strip was removed after 2, 4, 6, 8, 10, 24, 48 and 72 h of exposure to lipase, then cleaned with lint-free tissue before storing in acetone-cleaned aluminum foils at –20 °C until chemical extraction. Two hundred microlitres of liquid emulsion was collected at 2, 4, 6, 10, 72 h of exposure to lipase and immediately transferred into a glass centrifuge tube filled with 2 mL of ternary solvent prepared with dichloromethane, methanol and MQ-water in a ratio of 1:2:0.8 (v/v/v) for solvent lipid extraction. Chemical analysis of the plastic strips was carried out based on a previously published method.[136] The methods for lipid extraction and analysis are provided in SI. The rates of hydrolysis in the high and low enzyme treatments were also measured by pH to calculate the amount of liberated free fatty acids (FFA) by lipase.[154,155]

Partition coefficient of micelles and olive oil. In addition to the main experiment design, two separate experiments were designed to determine the partition coefficients of micelles and olive oil across the range of K_{OW} under varying amounts of micelles and olive oil. Liberated free fatty acids from olive oil can form micelles due to their amphiphilic structure. Therefore, for the micelles experiment, mixed micellar solution was made with NaTC and additional oleic acid to obtain final micelle-forming surfactant concentrations of 5.7, 6.9, 11.6 and 64.5 g/L in 8 mL of gut fluid mixture in glass centrifuge tubes containing one POM strip each. For the olive oil experiment, three levels of olive oil concentrations: 1.3, 6.3, 12.6 g/L in 8 mL of gut fluid mixture were prepared in glass centrifuge tubes also containing one POM strip each. Each system was spiked with 10 µL of the PCB stock mix and shaken at 250 rpm at 37°C for 28 days and all experiments were run in quadruplicates. After 28 days, the POM strip was removed from each tube and analyzed for PCBs. The PCB concentrations were then used to calculate the aqueous phase concentrations in the system to estimate the partition coefficients of micelles and lipids using chemical partitioning theories (see SI for detailed calculation).[57,81,146,147,156]

3.2.3. Model design, description and implementation

The partitioning of the PCBs in the first 28 days is described with a chemical mass balance equation whereby the initial spiked PCBs, C_{total} (µg/L) is equal to the sum of the concentrations residing in water (C_w), micelles ($C_{micelle}$), oil (C_{oil}) and plastic (C_{POM} and C_{LDPE}), all in µg/L:

$$C_{total} = C_w + C_{micelle} + C_{oil} + C_{POM} + C_{LDPE} \quad (3.1)$$

Based on partitioning principles, C_W can be determined from the measured ${C_{POM}}^*$ (µg/kg) and K_{POM}[57,146,147]:

$$C_W = \frac{C_{POM}^*}{K_{POM}} \quad (3.2)$$

Where K_{POM} (L/kg) is obtained from the relationship with K_{OW}.[146]

It has been demonstrated that 76 µm POM samplers approach equilibrium within 14 days at room temperature.[146] Due to the much higher intraparticle diffusivities in both micelles[72] and oil[157] as compared to the condensed crystalline POM matrix, and the higher temperature, we can safely assume that the concentrations in micelle and oil also reached equilibrium after 28 days. The concentrations in micelle and oil, $C_{micelle}^*$ (µg/kg) and C_{oil}^*(µg/kg), can then be calculated with $K_{micelle}$ (L/kg) and K_{oil} (L/kg) established from the micelle and oil side experiments, respectively (equations provided in SI) with C_W derived from eq. 3.2:

$$C_{micelle/oil}^* = K_{micelle/oil} \times C_W \quad (3.3)$$

In the second phase of the experimental setup, the previously described biphasic kinetic model simulating the exchange of chemicals between plastics, water, micelles and food components[136] was further developed to include the digestion process. During the hydrolysis of the olive oil triglycerides, FFAs are liberated, which were quantified from the change in pH over time (Figure 3.2). For each FFA liberated, one proton (H^+) is released.[154,155] FFA concentrations display an exponential behavior over time with a limit at infinity (Figure 3.2). Therefore, the molar concentration of liberated FFA, $[FFA]$ (µM) over time (h), is fitted with a first-order kinetic rate model[158,159]:

$$\frac{d[FFA]}{dt} = -k_{FFA} \cdot ([FFA] - [FFA_{max}]) \quad (3.4)$$

where k_{FFA} is the first order rate constant (h^{-1}) and $[FFA_{max}]$ (µM) is the maximum concentration of FFA that can be liberated. FFA molecules have a tendency to form micelles due to their amphiphilic structure[160] and this thus increases the micellar compartment of the system. The total mixed micelles (kg/L) as a result of the aggregated FFA and NaTC over time is:

$$M_{mixed}(t) = M_{micelle} + [FFA](t) \times MW_{FFA} \times 10^{-9} \quad (3.5)$$

where MW_{FFA} (g/mol) is the average molecular weight of the FFA based on the fatty acid composition measured (Table S3.3). On the other hand, while FFA is being liberated, the concentration of oil (triglycerides), M_{oil} (kg/L) decreases over time. This was calculated as:

$$M_{oil}(t) = M_{oil(t=0)} - \frac{[FFA](t)}{3} \times MW_{oil} \times 10^{-9} \quad (3.6)$$

where MW_{oil} (g/mol) is the molecular weight of olive oil triglycerides which was calculated from the MW_{FFA} (see eq. S3.12 in SI). The molar concentration of oil triglycerides is

equivalent to the one third of the molar concentration of FFA since a triglyceride (lipid) is made up of three fatty acids.

Following our previous study, for all systems, the boundary condition for C_W in the second phase of the experiment was calculated by assuming a fast equilibrium redistribution to the mixed micelles, oil and water with much slower exchange in microplastic and thus, microplastic-water chemical exchange being the overall rate-determining process.[136] The PCB concentration in plastic ($C_P{}^*$) was modeled by fitting the equations (2) and (3) from Mohamed Nor and Koelmans (2019) (SI eq. S3.8 and 3.9) with the additional aforementioned digestion kinetics, that is, eq. 3.4–3.6. Due to the short timescale of the present experiment (72 h), slow intrapolymer diffusion has little influence, given that the kinetic rate constant, k_3 (h^{-1}) had a half-life of 13 to 32 days based on the previous study.[136] Therefore, only k_1 and k_2 were fitted using the minpack.lm[74] package and deSolve[75] in R. The parameters f_1 and k_3 were fixed according to obtained values from the aforementioned study since the same LDPE strip was used for both experiments. The fast compartment fraction, f_1 and the intrapolymer diffusion rate constant, k_3 were both fixed based on the established relationship with K_{OW}.[136] The boundary conditions for the PCB concentrations in LDPE was based on the concentration measured at t=0 h whereby the slow and fast compartments were assumed to be in equilibrium. The removal of LDPE strips at each time point affects the solid to liquid ratio, which was accounted for in the modeling. However, the extraction of the emulsion was not accounted for, since the total amount extracted only comprised ~1% of the total volume of the system.

3.2.4. Statistical analysis

The Shapiro-Wilk test was used to check for normality and Levene's test for homogeneity of variance before carrying out one-way ANOVA to compare between the low and high enzyme treatment group and across different oil concentration levels in the side experiment. Tukey's multiple comparison test was performed when there was significant difference between treatments. Kruskal-Wallis was used as a non-parametric test for the micelle side experiment since the data did not follow a normal distribution. Pairwise comparisons using Wilcoxon rank sum test was performed when there was significant difference among treatments.

3.3. Results and discussion

3.3.1. Sorptive capacities of olive oil triglycerides and micelles

Due to the dynamic nature of the human digestive system, the concentrations of lipids and micelles change over time as lipids break down. Since the FFA molecules produced during the hydrolysis process would form micelles in the gut fluid,[161,162] the effect of increasing concentration of micelle-forming surfactants (NaTC and FFA) on the micelle-water distribution coefficients of the combined mixture of micelles was investigated. The lowest micelle concentration (5.7 g/L) was the baseline of the gut fluid system whereby only NaTC formed micelles. Oleic acid was added into the other three treatments to achieve the respective micelle-forming surfactant concentrations. This mimics the dynamic behavior of the main experiment in which more fatty acids were produced over time as lipid digestion occurred. The highest micelle concentration had significantly higher sorptive capacity than the two lower micelle concentrations (5.7 g/L and 6.9 g/L) (p<0.05; Wilcoxon rank sum test) (Figure 3.1A). The differences were generally less than 1 order of magnitude and were highest for the very hydrophobic PCB 209 (log K_{OW} = 8.18). Since the variability of the log $K_{micelle}$ was less than 1 log unit, an average linear relationship between log $K_{micelle}$ and log K_{OW} across all mixed micelle concentrations was determined ($logK_{micelle} = 0.99\ (\pm 0.03) \times logK_{OW} + 0.61\ (\pm 0.22)$; $r^2 = 0.86$). Our linear regression was significantly different from the relationship established by Schacht et al., 2016[73], as shown by the solid green line in Figure 3.1A. This implies that the mixture of micelle-forming surfactants from NaTC and FFA and even the NaTC alone behave differently from sodium dodecyl sulphate (NaDS) which was used in the aforementioned study. Due to its aggregation properties and physical characteristics, NaTC form smaller aggregates and can solubilize chemical molecules from the aqueous phase more easily than NaDS.[163]

The effect of oil concentrations on the oil-water distribution coefficients across the range of PCBs in the present study was also investigated (Figure 3.1B). The lowest oil concentration level (1.3 g/L) was significantly different from the highest oil concentration level (12.6 g/L) (p=0.03; Tukey's test) which is attributed to one of the replicates having slightly higher oil-water distribution coefficients than the others, possibly due to experimental artefacts. The limited differences in the sorptive capacities for all the olive oil concentrations suggest that the olive oil sorbent phase did not reach its maximum capacity even at the lowest oil concentration. For all three olive oil concentration levels, log K_{oil} increased linearly with log K_{OW} ($logK_{oil} = 0.85\ (\pm 0.04) \times logK_{OW} + 2.21\ (\pm 0.24)$; $r^2 = 0.84$) and the K_{oil} values were significantly higher than K_{OW} values by an average factor of 16 (Figure 3.1B). The results

shown corroborated an earlier study on sorption of PCBs to gas oil and crude oil, which found K_{oil} values 7 times higher than K_{OW} values.[157]

The mixed micelles have lower partition distribution coefficients than olive oil. Furthermore, the micelles compartment only took up ~6% of the gut fluid system and were 15 times lower than olive oil in terms of mass concentration. Yet, the micelle-water distribution coefficients are higher than the LDPE-water distribution coefficients which are determined from the transfer rate kinetics in this study (SI Table S3.4 and Figure S3.4). Therefore, the micelle compartment has a higher sorption capacity than LDPE, but lower than the olive oil (K_{oil}>$K_{micelle}$>K_{LDPE}).

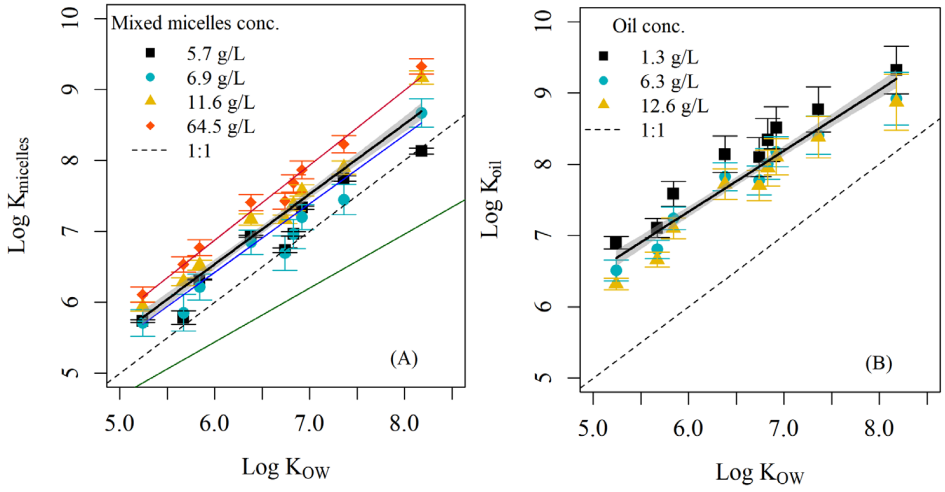

Figure 3.1. (A) Log micelle-water distribution coefficients ($K_{micelle}$) vs log K_{OW} for 4 concentration levels of micelle-forming surfactant concentrations (NaTC and FFA). Red line is the linear regression fitted for the highest concentration (64.5 g/L), blue line is the linear regression fitted for the other concentration levels (5.7, 6.9, 11.6 g/L) and black line is the linear regression fitted for all concentrations with the 95% confidence interval indicated by the grey band. Regression equations are reported in SI Table S3.2. Solid green line is the linear relationship obtained by Schacht et al., 2016.[73] **(B)** Log oil-water distribution coefficients (K_{oil}) vs log K_{OW} for 3 oil concentrations (1.3, 6.3, 12.6 g/L). Solid black line is the linear regression fitted for all concentrations with 95% confidence interval.

3.3.2. Microplastic traps PCBs released from food digestion

Lipid digestion was demonstrated by the increase in hydrogen protons liberated over time with the release of FFA (Figure 3.2). Measurement of FFA released based on pH[154] was deemed to provide an adequate representation of the lipid digestion process as this method is direct and not influenced by the possibility of continued hydrolysis after the emulsion is

extracted. Based on Tan et al., 2020[140], lipid digestion occurs rapidly during the first 2 h of the digestion process. Therefore, analysis of lipid digestion via lipid extraction is less accurate when measuring the enzyme reaction kinetics over time. Nevertheless, the triglycerides concentration measured via lipid extraction and gas-chromatography analysis showed a general decreasing trend over time (SI Figure S3.2) though the trends were indistinguishable for the high enzyme treatment and the denatured enzyme treatments (i.e., low enzyme and control). This supports our earlier suggestion that hydrolysis may have continued to happen after the emulsion samples were extracted since the lipase was still present in the emulsion.

The release of FFA in the high enzyme treatment differed significantly from the low enzyme treatment (Figure 3.2). Both demonstrated an exponential behavior approaching a limit within the 72 h experimental time period. The liberated protons over time were fitted with eq. 3.4 and the first order rate constants, k_{FFA}, and maximum FFA limit, $[FFA_{max}]$, are shown in Table 3.1.

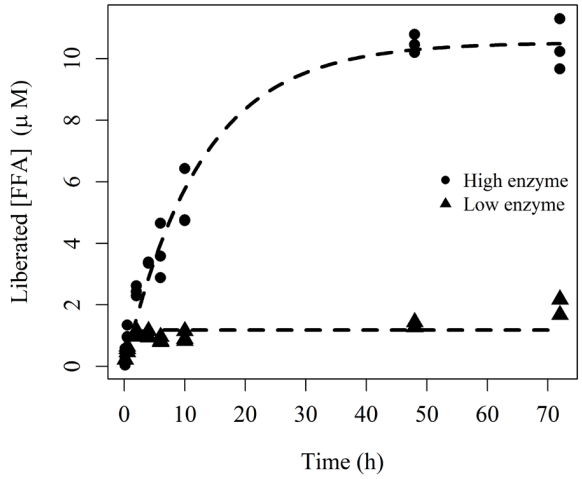

Figure 3.2. FFA concentration (μM) liberated with time (h) for high and low enzyme treatment based on pH change during lipid digestion.

Table 3.1. Parameter estimates for high and low enzymatic activity based on pH measurements over time. Standard errors are in parentheses.

	[FFA$_{max}$] (μM)	**k_{FFA} (h^{-1})**
High enzyme	10.53 (0.32)***	0.079 (0.007)***
Low enzyme	1.18 (0.09)***	1.22 (0.52)*

***significant at p<0.001; **significant at p<0.01; *significant at p<0.05

In the first 2 h of the digestion process, the initial rates of FFA released were not distinguishable between the high and low enzyme treatments. However, both showed a rapid increase, which agrees with an earlier study.[140] The first order rate constant in the low enzyme treatment is about 15 times higher than the rate constant fitted for the high enzyme treatment, despite the lower amount of enzymes due to the denaturing process. This is contrary to the generally conformed theory that rate of enzyme kinetics would increase with increasing enzyme concentration. We speculate that the fitted rate constant for the low enzymatic activity does not well represent the actual enzyme kinetics due to the lack of data within the first 2 h of the reaction. This is also further supported by the less statistically significant k_{FFA} for the low enzyme activity (p=0.029). As for the $[FFA_{max}]$ parameter, it was 9 times higher for the high enzyme treatment than for the low enzyme treatment. This significant difference implies that 9 times more FFAs were liberated for the high enzyme treatment. It is also important to note that the lipid digestion process may be affected by the concentration of microplastics in the gut fluid. A recent study observed that lipid digestion decreased with increasing polystyrene microplastic concentration as the particles hetero-aggregated with lipid droplets and also act as a sorbent for lipase, altering its secondary structure.[140] Therefore, the enzyme digestion parameters fitted here only apply to the digestive conditions of the present study.

The hydrolysis of olive oil triglycerides leads to two major implications for the human digestive system. Firstly, during the hydrolysis process, sorbed PCBs in the 'food' olive oil are released into the aqueous phase to repartition in the other gut compartments. Secondly, the FFA molecules produced from the hydrolysis process would form micelles in the gut fluid and thus, increase the total micelles concentration for solubilization of PCBs.[161,162] We observed an increase in the PCB concentrations in LDPE over time during the lipid digestion process (Figure 3.3 and SI Figure S3.3). This indicates that PCBs sorbed in our food proxy, that is, the olive oil triglycerides fraction, were released during lipid digestion and repartitioned in the gut fluid system, partially sorbing onto the LDPE strips. In other words, this demonstrates microplastic particles can sorb chemicals from contaminated food during digestion. Here, the percentage increase in the PCBs bounded to the LDPE was not significantly different between the high and low enzyme treatments within 72h. This is because LDPE represented less than 10% of the gut fluid components in terms of mass concentration, whereas olive oil made up 80% of the system. Furthermore, as discussed earlier, the LDPE in this study has a lower sorptive capacity than micelles and olive oil. As the oil breaks down and releases the sorbed contaminants, the micelles are competing with LDPE for the uptake of PCBs. Hence, we observed only a small difference in the amount of PCBs taken up by the polymer between the high and low enzyme treatments.

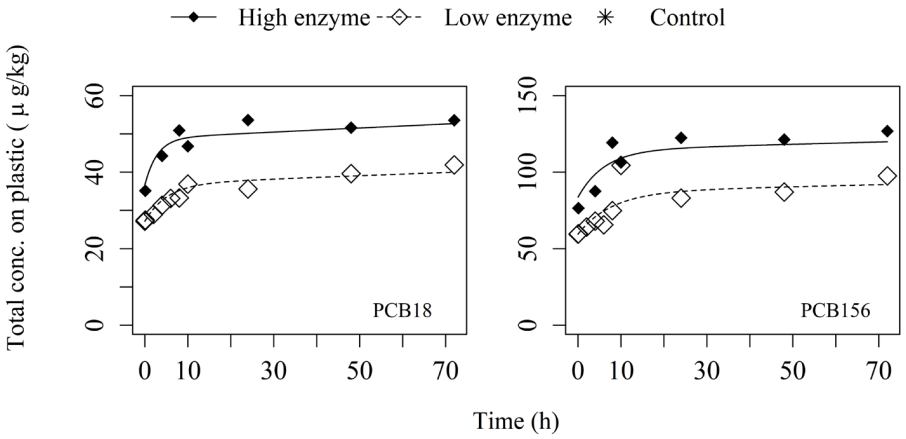

Figure 3.3. Total PCB concentrations in the plastic compartment (µg/kg) over time (h) for high and low enzyme treatment and control (no PCBs spiked) of one replicate system. PCB concentrations were below detection limit in the control systems. Solid lines represent the fitted models for the high enzyme treatment whereas the dashed lines represent the fitted models for the low enzyme treatment.

3.3.3. PCBs transfer kinetics during hydrolysis of triglycerides

We investigated a realistic human digestive tract scenario in which a human has bioaccumulated contaminants from other uptake routes (ingestion, inhalation and dermal uptake) and, ingests food and plastic which are contaminated. This was mimicked by pre-equilibrating the contaminants in the gut fluid before the system is exposed to enzymes that can alter the composition of the gut fluid. Lipase is then added to break down the olive oil triglycerides, which would release the lipid-bound PCBs into the gut fluids. We hypothesized that these released PCBs would repartition into the other gut compartments, including LDPE, thereby increasing the PCBs associated with LDPE. The chemical transfer rate kinetics in the LDPE may be affected by the enzyme digestion process, depending on which process is rate-limiting (plastic sorption vs enzyme kinetics).

As motivated above, the experiment was performed for a longer period than a standard upper gastrointestinal tract retention time. The PCB concentrations increased rapidly for the first 10 h and then approached a pseudo-equilibrium state within 72 h. Previously, we observed biphasic chemical transfer kinetics during a 28 days exposure period.[136] However, in the present study, this biphasic behavior was not apparent due to the shorter time scale (Figure 3.3). Therefore, only the fast sorption and desorption kinetic rate constants of the biphasic reversible model (see section 3.2.3, and SI for more details) were fitted to the high

and low enzyme treatments (Table S3.4). For the control treatment, only PCB 52 and PCB 101 showed a slight increase in concentration in the LDPE over time. The levels of contamination were close to the minimum detection limit and similar to the extraction method blank. Therefore, this contamination was not accounted for in the respective high and low enzyme treatments as the level of contamination was low and the data still fitted well with the model and initial boundary conditions set by the measured PCB concentrations in the POM strip ($C_{POM}{}^{*}$).

The fast sorption rate constants (k_1) were statistically significant for all PCBs in both enzyme treatments except PCB 209 (Table S3.4). They ranged from 236 to 1.37 × 10^7 h^{-1} and 138 to 3.77 × 10^4 h^{-1} for high and low enzyme treatments respectively. The fitted k_1 values for some congeners here were about 2 to 8 times higher than those from a similar chemical exchange kinetics experiment involving microplastic and food but without food digestion kinetics, in which LDPE strips from the same source were used.[136] The differences between this study and the aforementioned study were higher for the high enzyme treatment than the low enzyme treatment, since k_1 values were generally higher in the high enzyme treatment. The olive oil triglycerides may be behaving similarly to the organic matter in the aforementioned study, which facilitates chemical sorption onto the LDPE.[88,89,164,165] Furthermore, the presence of NaTC in the gut fluid also act as an oil dispersant which facilitates formation of oil-surfactant aggregates. These dispersed aggregates can promote the uptake of oil-associated contaminants.[166] However, the variability of k_1 values did not differ significantly between the treatments (p=0.50 ; one-way ANOVA). This may be due to the small difference in the bulk oil compartment between the two treatments, even after digestion. The log k_1 values were positively correlated with log K_{OW} in both high ($logk_1 = 1.40\ (\pm 0.18) \times \log K_{OW} - 5.17\ (\pm 1.18), r^2 = 0.87, n = 10$) and low ($\log k_1 = 1.21\ (\pm 0.08) \times \log K_{OW} - 4.28\ (\pm 0.51), r^2 = 0.96; n = 10$) enzyme treatments (Figure 3.4). The positive correlations are in agreement with the earlier study in the presence of organic matter.[136] The k_1 rate constants estimated here were lower in the less hydrophobic PCBs, but as hydrophobicity increased, the estimates were higher than the aforementioned study. This implies that contaminant transport to the polymer is highly dependent on facilitated transport and may differ depending on the substrates available in the gut fluid. Although the theory of facilitated adsorption for oil and organic matter is well-established in the field of environmental pollution, little is known about the effects of vegetable oil or other food matrices in the co-transport of contaminants on indigestible materials such as plastic particles in the human gut fluid.

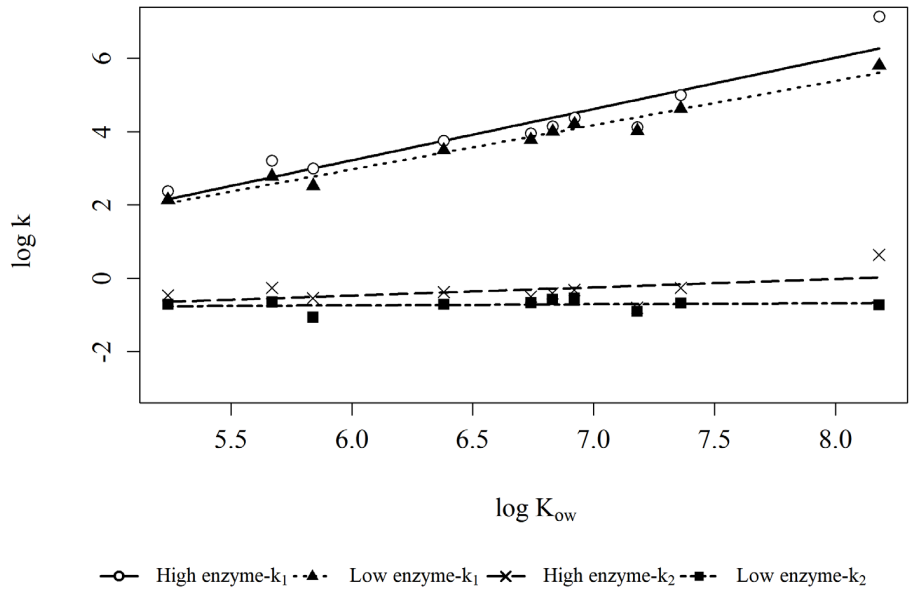

Figure 3.4. Log values of kinetic parameters (k_1 and k_2) vs log K_{OW} for low and high enzyme treatments.

The reverse transfer kinetic (desorption) was also included in our model since chemical transfer occurs in both directions simultaneously as demonstrated earlier.[136] The desorption rate constants (k_2) of the fast fraction were statistically significant for all PCBs in both treatments except PCB 209 in the high treatment (SI Table S3.4). In the high enzyme treatment, k_2 ranged from 0.283 to 4.36 h^{-1}, translating to desorption half-lives of 0.16 to 2.45 h. On the other hand, fitted k_2 values in the low enzyme treatment were significantly lower (p=0.0068; one-way ANOVA), ranging from 0.087 to 0.289 h^{-1}, translating to desorption half-lives of 2.40 to 7.97 h. Furthermore, they were in the similar range with the estimated k_2 values from our aforementioned study which investigated chemical kinetics on plastic with an inert food component.[136] The difference observed between the high and low enzyme kinetics implies that for desorption, the lipid digestion process has a more significant role. We speculate that this may be a result of the formation of more FFA molecules in the high enzyme treatment which may be driving the desorption process, as the PCB release is likely controlled by the aqueous boundary layer resistance.[167] Unlike the sorption rate constants (k_1), the desorption rate constants (k_2) for the high and low treatments had weak positive correlations with hydrophobicity, suggesting that the desorption process was not influenced by the bulk size or hydrophobicity of the PCB congeners.

LDPE distribution coefficients (K_P) were derived from the fitted $k_1$and k_2 estimates (Figure S3.4). The log K_P positively correlated with log K_{OW} ($logK_P = 1.04\ (\pm 0.03) \times logK_{OW} + 0.05\ (\pm 0.23), r^2 = 0.98, n = 20$) corroborating previous studies.[56,79,136,168] However, the relationship observed here indicates that the K_P values were almost equivalent to K_{OW} and generally higher than previously established K_P values for LDPE. As discussed previously, the oil may have sorbed onto the plastic surface and promoted the uptake of PCBs, evidenced by the high sorption rate constants.

3.3.4. Percentage reduction in chemical bioavailability

The chemical concentrations bound to LDPE after the pre-equilibration period and before the lipid digestion process was initiated, comprised 0.2 to 4% of the total concentrations in the system. These percentages depended on the hydrophobicity of the compound, with more hydrophobic compounds having higher percentages. This was largely due to the higher slope coefficient of the log K_P– log K_{OW} regression for LDPE than NaTC, implying a larger increase in sorptive capacity as log K_{OW} increases for LDPE. Hence, more hydrophobic PCBs tended to have a higher affinity to LDPE than micelles.

After the lipid digestion was initiated for 72 h, LDPE took up part of the PCBs released from the digested olive oil triglycerides, resulting in up to 75% increase in PCB concentrations in the LDPE (Figure 3.3 and SI Figure S3.3). This implies MP particles leaving the body would have substantially higher chemical concentrations than when entering the body, which may seem counterintuitive yet logical based on the processes at play. This increase, however, still only implies a decrease in chemical bioavailability by about 0.11 to 0.87% (SI Figure S3.5) of the total chemical amount present in the gut. We also observed a noticeable increase in the percentage reduction in the chemical bioavailability for more hydrophobic compounds (SI Figure S3.5). The reduction in chemical bioavailability is limited by the digestion rate kinetics which is slower than the uptake kinetics (k_1). Furthermore, LDPE is competing with micelles which have 10 times stronger binding affinity than LDPE. Although the percentage reduction in chemical bioavailability demonstrated in the present study is low, the amount of chemical uptake is also driven by the chemical fugacity of the LDPE prior to the digestion process. Our earlier study simulating gut fluid conditions with clean plastic and contaminated organic matter as food, demonstrated that it is possible for MPs to clean the gut up to almost 90% without digestion.[136]

Additionally, despite the difference in the exchange kinetics, the overall change in chemical bioavailability did not differ significantly between the high and low enzyme treatments. This implies that the digestion dynamics will not result in significant differences in the chemical bioavailability when the plastic to food ratio in the gut is similar to the present study and also

equally contaminated. Therefore, here we show that a contaminated LDPE is still capable of further taking up part of the released PCBs from food during digestion but with little effect from the digestion dynamics. Furthermore, the speculated facilitated transport attributed to the surrounding oil enhances the sorptive capacity of LDPE, potentially making it a relevant chemical "cleaning" agent for ingested contaminated food.

3.4. General discussion

We provided an in vitro experimental design and a chemical kinetic model to elucidate the chemical dynamics on microplastics under realistic simulated gut conditions inclusive of digestion dynamics. The improved gut model presented here allows for the accurate parameterization of kinetic parameters to describe the chemical transfer with microplastics and digestion dynamics. These are urgently needed since concerns with respect to health effects of microplastics are high. Most importantly, our kinetic parameters can be used to model the chemical behavior in other gut scenarios (e.g., different chemical concentrations or gut transit times) and extrapolate the results for exposure and risk assessments of plastic-associated chemicals.[27,120] Mechanistically, we found that the biphasic and reversible chemical exchange model fitted well to empirical data, describing the digestion process, changes in the different gut compartments and chemical exchange on LDPE. We also demonstrated that for short gut transit times (< 72 h), the biphasic sorption is not visible in the chemical dynamics, and the fast chemical uptake into the outer reservoir of the LDPE becomes more relevant.

Under similar gut conditions as in the present study, we conclude that the food digestion dynamics have a small influence on the chemical exchange kinetics on microplastics (Figure 3.3). Uptake kinetics (k_1) were not significantly affected while the desorption kinetics (k_2) for the high enzyme treatment was 10 times higher than the low enzyme treatment. We speculate that chemical exchange on the LDPE may be facilitated by other molecules present in the gut fluid such as the food digestion product (in this case, FFA). On the other hand, other food types and enzymes such as protein and pepsin may instead inhibit the facilitated transport of chemicals into the LDPE as they may compete for adsorption sites (Liu et al., 2020).

Here, we demonstrated that LDPE can reduce the chemical bioavailability as it takes up the contaminants released from food during the digestion process, although it is equally contaminated (Figure S3.5). The amount of chemical bioavailability is however limited by the digestion kinetics which have a half-life that is 200 times longer than the uptake kinetics. A reduction in chemical bioavailability due to the chemical uptake by microplastics is still considered counterintuitive by many, yet, is in fact what thermodynamics predicts and has

been shown now by several studies that chemical bioavailability can decrease depending on the conditions.[136,170,171] Although the sorptive capacity of LDPE was lower than micelles, LDPE was still a significant sink for the released PCBs from the digested olive oil triglycerides since the mass concentration of LDPE was two times higher than micelles in the scenario studied. Also, this substantially increases the chemical concentration on LDPE that are egested. This suggests that if there is a higher load of LDPE, there would be an even greater reduction in the amount of bioavailable chemicals once the plastic is egested.

As microplastic levels are expected to rise due to the increasing use of plastic in our daily lives and its omnipresence in the environment, microplastic exposures in biota would also increase. The calibrated model presented here allowed us to understand the chemical vector effect in the gut when lipid digestion is taking place. Our present study has specifically addressed lipids from olive oil as a proxy for food, at a certain concentration. More studies are warranted for other food types and also at varying ratios of microplastic to food concentrations since it has been shown that microplastic can also inhibit digestion.[140] This would then allow us to better understand the effects of microplastic under realistic gut conditions in terms of the chemical vector effect and digestion dynamics.

Acknowledgements

We would like to thank the Aquatic Ecology and Water Quality Group of Wageningen University and Research, Yayasan Mendaki (Singapore) for the Ridzwan Dzafir Distinction Award and the PMBM Scholarship Fund Board (Singapore) for co-funding. We also thank Peter de Gijsel from the Laboratory of Food Chemistry of Wageningen University and Research for providing support and advise on the project.

Supporting Information for Chapter 3

Table S3.1. Details of PCB congeners and concentrations in spike stock mixture and experiment set-up

Congener	Chlorine	Molecular formula	Molecular weight (g/mol)	Planarity	Log K_{OW}[1]	Spike mixture concentration (mg/L)	Concentration in main experimental setup (µg/L)
PCB 18	Tri	$C_{12}H_7Cl_3$	257.5	Non-planar	5.24	23.2	29.57
PCB 28	Tri	$C_{12}H_7Cl_3$	257.5	Non-planar	5.67	42.0	53.57
PCB 52	Tetra	$C_{12}H_6Cl_4$	292	Non-planar	5.84	73.1	93.25
PCB 77[a]	Tetra	$C_{12}H_6Cl_4$	292	Planar	6.36	23.9	30.46
PCB 101	Penta	$C_{12}H_5Cl_5$	326.4	Non-planar	6.38	97.2	123.99
PCB 118	Penta	$C_{12}H_5Cl_5$	326.4	Non-planar	6.74	36.0	45.95
PCB 138	Hexa	$C_{12}H_4Cl_6$	360.9	Non-planar	6.83	54.0	68.90
PCB 153	Hexa	$C_{12}H_4Cl_6$	360.9	Non-planar	6.92	74.6	95.17
PCB 156	Hexa	$C_{12}H_4Cl_6$	360.9	Non-planar	7.18	34.5	43.96
PCB 169[a]	Hexa	$C_{12}H_4Cl_6$	360.9	Planar	7.42	39.2	50.06
PCB 180	Hepta	$C_{12}H_3Cl_7$	395.3	Non-planar	7.36	81.1	103.49
PCB 209	Deca	$C_{12}Cl_{10}$	498.6	Non-planar	8.18	58.3	74.43

[1] Hawker and Connell, 1988[114]

[a] PCB 77 and 169 had high relative standard deviations (> 15%) for the response factors of replicate measurements of the calibration standards. Therefore, they were omitted from further analysis.

Lipid extraction and separation

The method for lipid extraction was adapted from Paik et al., 2009.[172] Two hundred µL of sample lipid emulsion was vortexed with 2 mL ternary solvent (DCM:MeOH:H_2O=1:2:0.8; v/v/v) briefly. Additional dichloromethane (DCM) and MQ-water were added to the extracts to adjust the ratio of DCM:MeOH:H_2O to 1:1:0.9 (v/v/v). The extracts were then separated by centrifugation at 2500 ×g for 15 mins. The upper layer was pipetted out and the remaining DCM layer was dried over anhydrous Na_2SO_4 and then evaporated to dryness with a gentle stream of nitrogen. The extracts were then diluted in 12 mL hexane and then stored in -80°C until further extraction was carried out.

Lipid extracts were thawed to room temperature and concentrated to 1 mL with a speed vacuum for 15 mins. The triglycerides and free fatty acids were separated based on an adapted method from Richardson et al., 2017.[173] Briefly, 1 mL of cold distilled water was added to the concentrated lipid extracts (1 mL) and vortexed. Then 1 mL of 0.4 M NaOH in MeOH was added and vortexed for 10s. This would allow the NaOH to react with the free fatty acids to form salts. Three mL of hexane were added immediately after vortexing to separate esterified fatty acids then vortexed again. The emulsion was then left to separate for 3 min before the hexane upper phase (contains esterified triglycerides) is transferred into a clean centrifuge glass tube and dried under a gentle stream of nitrogen to 20 µL. The esterified triglycerides were then derivatized to obtain fatty acid methylated esters (FAMEs).[173] Briefly, 20 µL of esterified triglycerides extract was mixed with 400 µL toluene, 3 mL MeOH and 600 µL of 8% HCl solution in methanol and incubated for 1.5h at 90°C. Samples were cooled down for 10 min before adding 1 mL of hexane and 1 mL of water. After phase separation, 600 µL of the hexane upper layer containing FAMEs was used for further analysis. A double internal standard spike was applied during the esterification process. Firstly, 1.6 mg of methyl pentadecanoate (C15:0) was added before the samples were heated at 90 °C. Then, 1.6 mg of methyl tridecanoate (C13:0) was added during the hexane extraction step. FAMEs were quantified by GC-FID using a Nukol column.[174,175] The GC was calibrated using TraceCERT FAME standards purchased from Supelco.

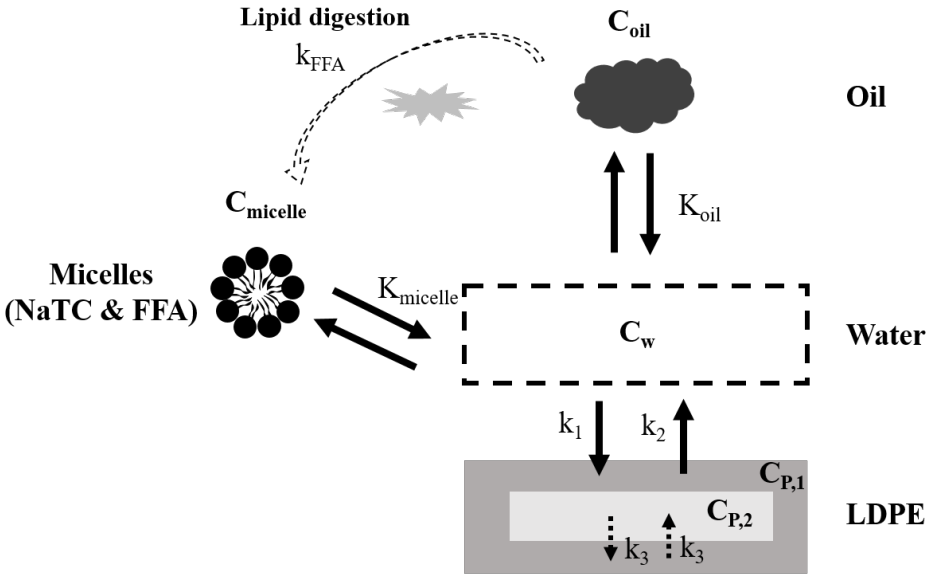

Figure S3.1. Schematic diagram of two-compartment low density polyethylene (LDPE) with a fast ($C_{P,1}$) and slow ($C_{P,2}$) reservoir and chemical interactions between LDP, water, oil and micelles (formed from sodium taurocholate (NaTC) and free fatty acids (FFA)) in the simulated gut fluid digestion assay.

Determination of distribution coefficients $K_{micelle}$ and K_{oil}

Based on chemical mass balance:

$$C_{tot} = C_{POM} + C_W + C_{micelle} \quad \text{(S3.1)}$$

where C_{tot} is the total PCB cocentration in the system, C_{POM} is the chemical concentration on the POM passive sampler, C_W is the chemical concentration in the water phase and $C_{micelle}$ is the chemical concentration in the micelle compartment. All concentrations are in µg/L.

The partition equilibrium constant K_{POM} is:

$$K_{POM} = \frac{C_{POM}{}^*}{C_W} \quad \text{(S3.2)}$$

where $C_{POM}{}^*$ is the PCB concentration in POM in µg/kg and K_{POM} is in L/kg.

$$C_{POM} = C_{POM}{}^* \cdot [POM] \quad \text{(S3.3)}$$

where [POM] is the mass concentration of POM in the system in kg/L.

Similarly, $C_{micelle}$ is:

$$C_{micelle} = C_{micelle}{}^*[micelle] = K_{micelle} \cdot C_W \cdot [micelle] \quad \text{(S3.4)}$$

Where [micelle] is the mass concentration of micelle in the system in kg/L, $C_{micelle}{}^*$(µg/kg) is the PCB concentration in the micelles, $K_{micelle}$ (L/kg) is the partition coefficint of micelle with water.

Therefore, substituting eq. (S3.3) and (S3.4) into (S3.1):

$$C_{tot} = K_{POM} \cdot C_W \cdot [POM] + C_W + K_{micelle} \cdot C_W \cdot [micelle] \quad \text{(S3.5)}$$

Rearranging and substituting $C_W = \frac{C_{POM}{}^*}{K_{POM}}$,

$$K_{micelle} = \frac{K_{POM}C_{tot} - C_{POM}{}^*(K_{POM}[POM]+1)}{C_{POM}{}^*[micelle]} \quad \text{(S3.6)}$$

Similarly,

$$K_{oil} = \frac{K_{POM}C_{tot} - C_{POM}{}^*(K_{POM}[POM]+1)}{C_{POM}{}^*[micelle]} \quad \text{(S3.7)}$$

Biphasic sorption on microplastic model (based on Chapter 2)

The exchange of chemicals between the fast and slow reservoir of the plastic is modelled as:

$$\frac{dC_1{}^*}{dt} = \frac{k_1}{f_1[P]} C_W - k_2 C_1{}^* - k_3 C_1{}^* + k_3 C_2{}^* \quad \text{(S3.8)}$$

$$\frac{dC_2{}^*}{dt} = k_3 C_1{}^* - k_3 C_2{}^* \quad \text{(S3.9)}$$

where $C_1{}^*$ and $C_2{}^*$ are concentrations of contaminants in the fast and slow reservoirs of the polymer (μg/kg) respectively, f_1 is the fast reservoir fraction of the total bound mass of chemical (dimensionless), k_1 is the sorption rate constant (d^{-1}), k_2 is the desorption rate constant (d^{-1}) and k_3 is the intra-polymer rate constant (d^{-1}), [P] is the plastic mass concentration (kg/L).

Auxiliary equations

Relationship between log K_{POM} and log K_{OW}[146]:

$$\log K_{POM} = 0.791 \cdot \log K_{OW} + 1.018 \quad \text{(S3.10)}$$

Percentage reduction in chemical bioavailability:

$$\%\ reduction\ in\ chemical\ bioavailability\ (t) =$$

$$\frac{(C_{tot}(0) - C_P{}^*(0)\cdot[P]) - (C_{tot}(t) - C_P{}^*(t)\cdot[P])}{(C_{tot}(0) - C_P{}^*(0)\cdot[P])} \times 100 \quad \text{(S3.11)}$$

Where $C_{tot}(0)$ and $C_{tot}(t)$ is the total concentration in the system (μg/L) at time 0h or t, $C_P{}^*(0)$ and $C_P^*(t)$ is the PCB concentration in LDPE (μg/kg) at time 0h or t, and [P] is the LDPE mass concentration in the system (kg/L).

Molecular weight of olive oil:

$$MW_{oil} = 3 \times Av.MW_{FFA} + 38.049 \quad \text{(S3.12)}$$

Where 38.049 g/mol is the the weight of the glycerol backbone and the average MW_{FFA} is 279.33 g/mol based on the percentage of fatty acids shown in Table S2.

Partition coeffcient of LDPE with water[136]:

$$K_P = \frac{k_1}{k_2 f_1 [P]} \quad \text{(S3.13)}$$

For units, please refer to previous section.

Table S3.2. Linear regressions between log $K_{micelle}$ and logK_{OW} for different concentrations of micelles

Experiment	Treatment	Regression	R^2
Micelle	5.7, 6.9, 11.6 mg/L	$logK_{micelle} = 0.97 \cdot logK_{OW} + 0.63$	0.89
Micelle	64.5 mg/L	$logK_{micelle} = 1.06 \cdot logK_{OW} + 0.54$	0.97
Micelle	All levels	$logK_{micelle} = 0.99 \cdot logK_{OW} + 0.61$	0.86
Micelle	Only NaTC (5.7 mg/L)	$logK_{micelle} = 0.88 \cdot logK_{OW} + 1.09$	0.94

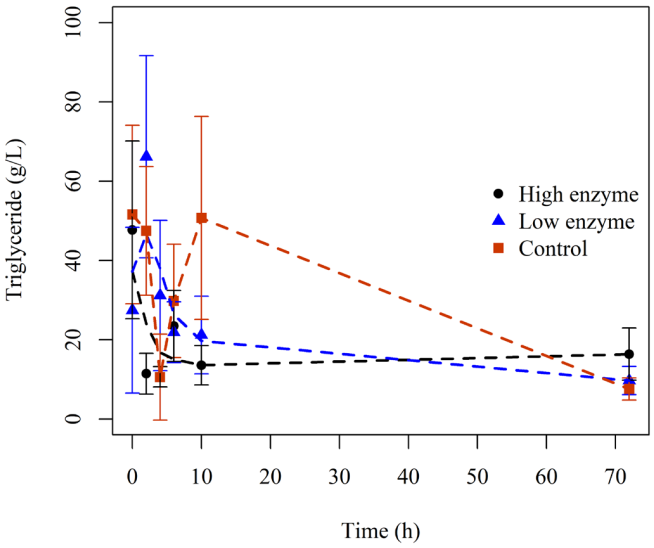

Figure S3.2. Concentration of triglycerides in the emulsion over time in each setup (high enzyme, low enzyme and control).

Table S3.3. Average percentages of major fatty acids found in olive oil across samples.

Fatty acid	Average % of fatty acid
C14:0	0.03
C16:0	11.58
C18:0	2.68
C18:1	76.81
C18:2	7.69
C18:3	0.36
C20:0	0.65
C22:0	0.11
C22:1	0.02
C24:0	0.07

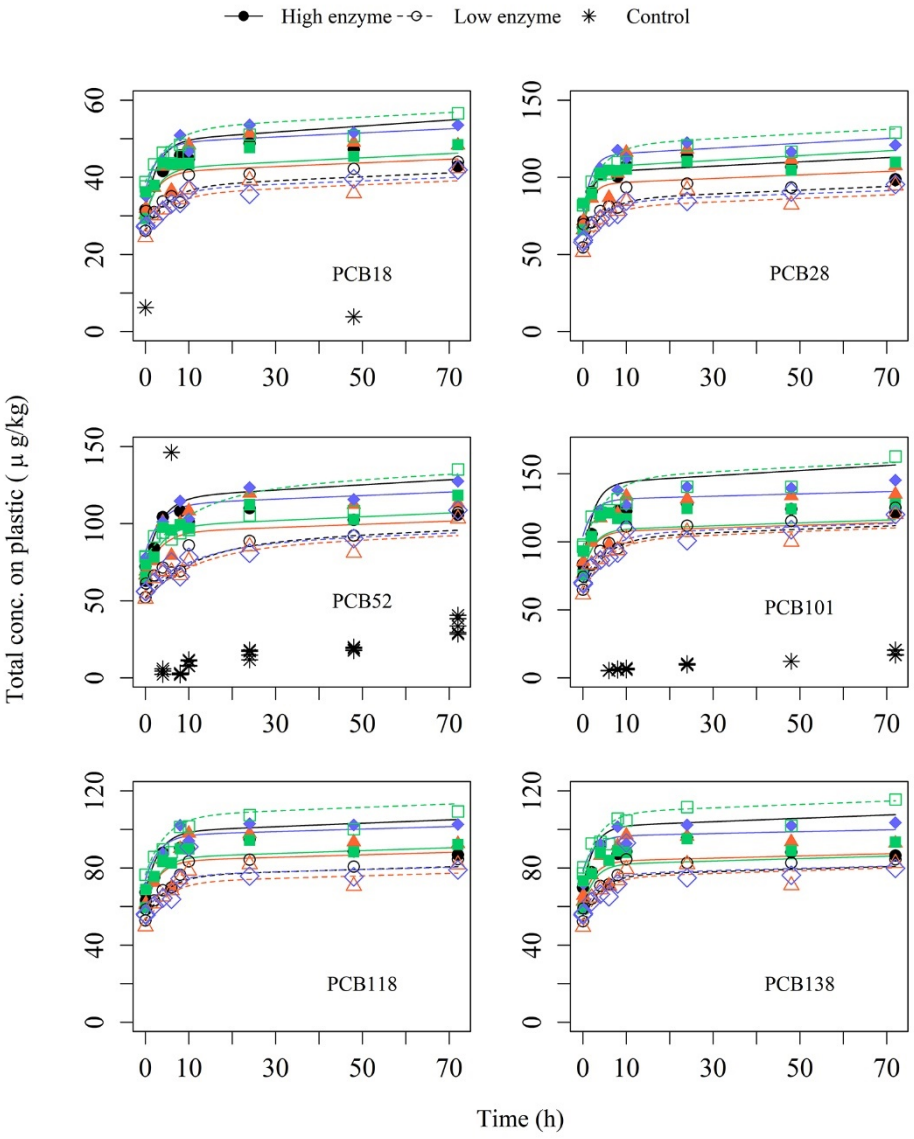

Figure S3.3. Total PCB concentrations in the LDPE compartment (µg/kg) over time (h) for high and low enzyme treatment and control (no PCBs spiked) of one replicate system. Solid lines represent the fitted models for the high enzyme treatment whereas the dashed lines represent the fitted models for the low enzyme treatment. Each colour represents a different replicate system.

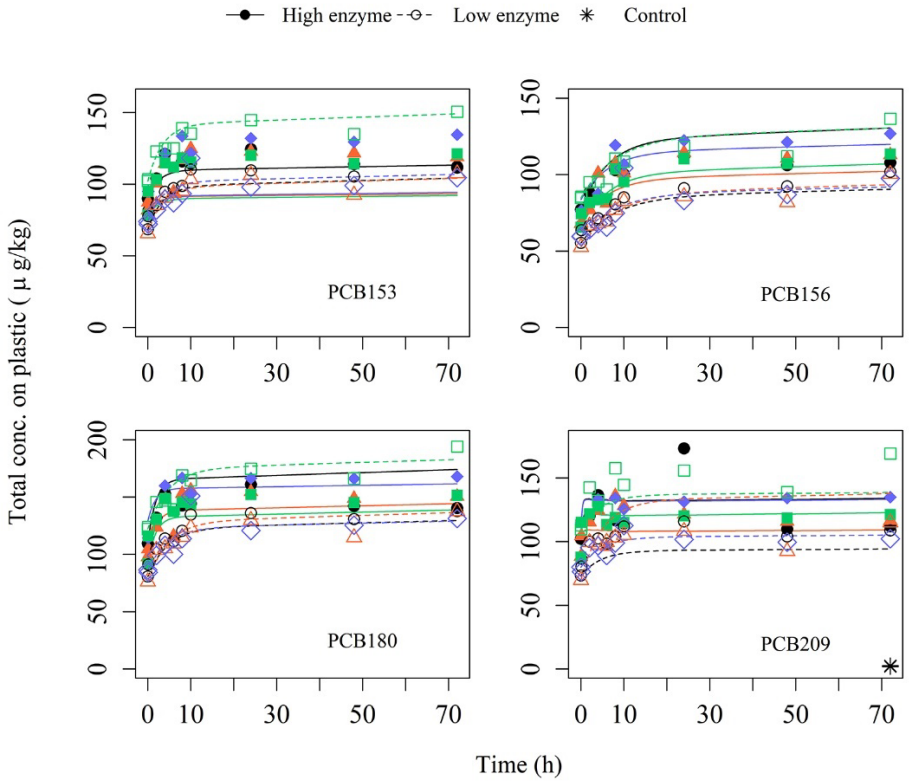

Figure S3.3. *(Continued)*

Table S3.4. Kinetic rate constants of LDPE for high and low enzyme treatment with standard errors (SE). (***significant at p<0.001; **significant at p<0.01; *significant at p<0.05)

Enzyme treatment	PCB	Log K_{OW}	k_1 (h^{-1})	SE	k_2 (h^{-1})	SE	K_P (L/kg)	log K_P
High	18	5.24	2.36E+02**	7.36E+01	0.345**	0.116	3.28E+05	5.52
High	28	5.67	1.61E+03**	4.50E+02	0.554**	0.163	1.21E+06	6.08
High	52	5.84	9.79E+02**	2.85E+02	0.283**	0.090	1.37E+06	6.14
High	101	6.38	5.59E+03*	2.39E+03	0.418*	0.190	4.44E+06	6.65
High	118	6.74	9.01E+03**	2.58E+03	0.322**	0.099	8.28E+06	6.92
High	138	6.83	1.40E+04*	5.88E+03	0.390*	0.173	1.03E+07	7.01
High	153	6.92	2.42E+04*	1.09E+04	0.477*	0.224	1.42E+07	7.15
High	156	7.18	1.33E+04***	3.38E+03	0.159**	0.045	2.15E+07	7.33
High	180	7.36	9.87E+04*	4.37E+04	0.550*	0.254	4.35E+07	7.64
High	209	8.18	1.37E+07	1.35E+07	4.355	4.316	5.85E+08	8.77
Low	18	5.24	1.38E+02***	2.09E+01	0.193***	0.033	3.42E+05	5.53
Low	28	5.67	6.04E+02***	8.40E+01	0.229***	0.036	1.10E+06	6.04
Low	52	5.84	3.33E+02***	5.43E+01	0.087***	0.017	1.51E+06	6.18
Low	101	6.38	3.13E+03***	4.15E+02	0.197***	0.030	5.28E+06	6.72
Low	118	6.74	5.92E+03***	1.08E+03	0.218***	0.044	8.04E+06	6.91
Low	138	6.83	1.00E+04***	1.77E+03	0.262***	0.051	1.10E+07	7.04
Low	153	6.92	1.58E+04***	2.81E+03	0.289***	0.056	1.53E+07	7.18
Low	156	7.18	1.03E+04***	1.75E+03	0.124***	0.024	2.13E+07	7.33
Low	180	7.36	4.22E+04***	7.04E+03	0.210***	0.039	4.87E+07	7.69
Low	209	8.18	6.32E+05**	2.14E+05	0.191*	0.071	6.16E+08	8.79

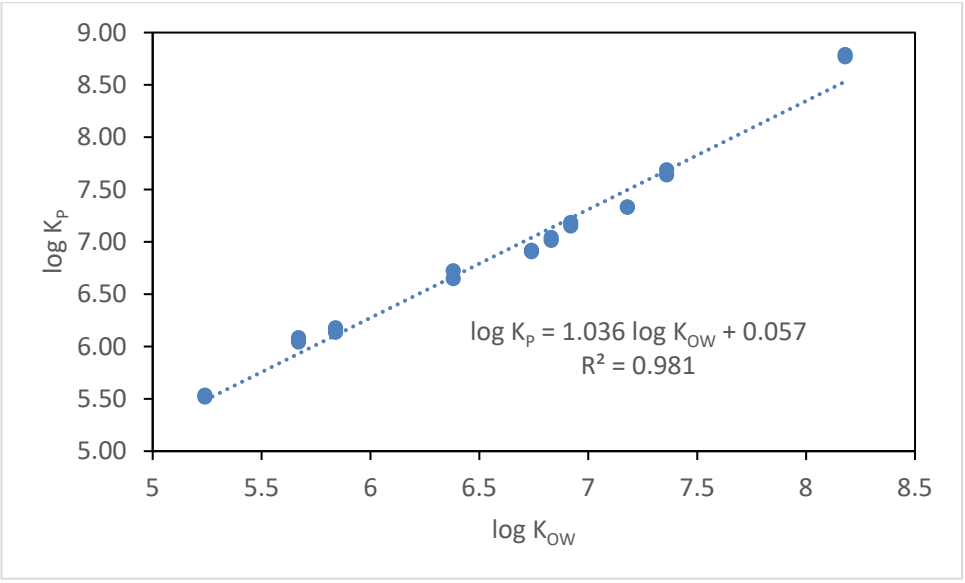

Figure S3.4. Relationship between log K_P of LDPE and log K_{OW} based on k_1 and k_2 estimates.

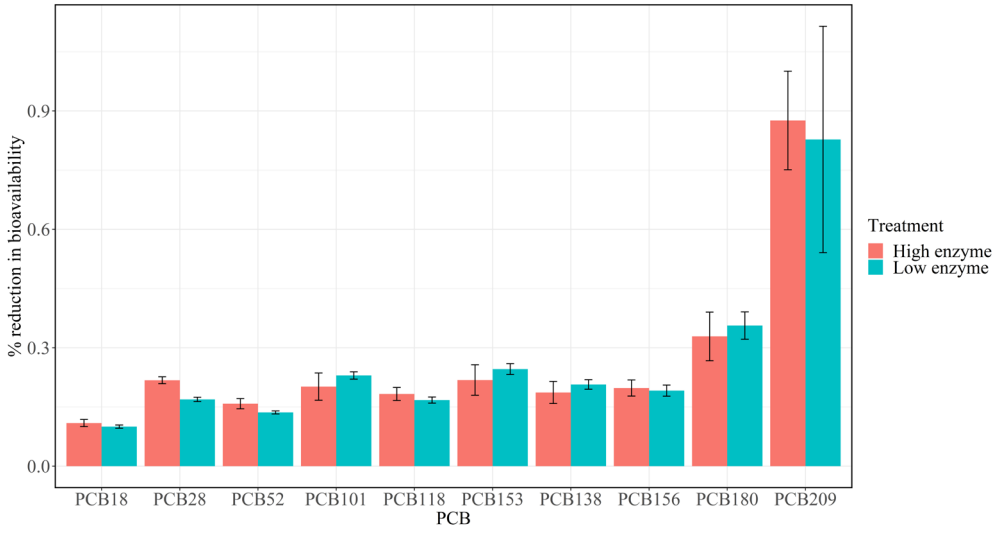

Figure S3.5. Percentage reduction in bioavailability of each PCB congener in high and low enzyme treatments respectively.

Chapter 4

Lifetime accumulation of microplastic in children and adults

Nur Hazimah Mohamed Nor, Merel Kooi, Noël Diepens, Albert A. Koelmans

This chapter is published as: Mohamed Nor, N.H., Kooi, M., Diepens, N.J. and Koelmans, A.A., 2021. Lifetime Accumulation of Microplastic in Children and Adults. *Environmental Science & Technology*, 55(8), pp.5084-5096.

Abstract

Human exposure to microplastic is recognized as a global problem, but the uncertainty, variability and lifetime accumulation is unresolved. We provide a probabilistic lifetime exposure model for children and adults, which accounts for intake via eight food types and inhalation, intestinal absorption, biliary excretion and plastic-associated chemical exposure via a physiologically based pharmacokinetic submodel. The model probabilistically simulates microplastic concentrations in the gut, body tissue, and stool, the latter allowing validation against empirical data. Rescaling methods were used to ensure comparability between microplastic abundance data. Microplastic (1–5000 μm) median intake rates are 553 particles/capita/day (184 ng/capita/day) and 883 particles/capita/day (583 ng/capita/day) for children and adults, respectively. This intake can irreversibly accumulate to 8.32×10^3 (90% CI, 7.08×10^2–1.91×10^6) particles/capita or 6.4 (90% CI, 0.1–2.31×10^3) ng/capita for children until age 18, and up to 5.01×10^4 (90% CI, 5.25×10^3–9.33×10^6) particles/capita or 40.7 (90% CI, 0.8–9.85×10^3) ng/capita for adults until age 70 in the body tissue for 1–10 μm particles. Simulated microplastic concentrations in stool agree with empirical data. Chemical absorption from food and ingested microplastic of the nine intake media based on biphasic, reversible, and size-specific sorption kinetics, reveals that the contribution of microplastics to total chemical intake is small. The as-yet-unknown contributions of other food types are discussed in light of future research needs.

4.1. Introduction

Humans are exposed to microplastics (MPs) everyday.[14,15] These small particles (1–5000 µm) are omnipresent in our food, including water and beverages, and air.[3,176–179] The first evidence of MP in human stools proves that these particles are indeed ingested and can pass through the gastrointestinal (GI) tract.[13] This has raised concerns about the actual exposure and impact on human health.[3] While it is widely accepted that humans are exposed to MPs, the magnitude, uncertainty, and variability of MP exposure concentrations and intake rates globally remain unknown. These uncertainties have resulted in many controversies regarding the potential risks that MPs may pose to human health.[180,181]

To date, only two studies have performed human exposure assessments for MP by estimating total intake from different intake media, deterministically.[14,15] A major limitation in the aforementioned studies is that there are discrepancies in the databases used, due to the differences in MP definitions and analytical techniques. Zhang et al.[15] acknowledged these discrepancies and thus made a conscientious effort to use more comparable data. However, such methods would fail to estimate MPs from other size ranges, inaccurately representing the full MP continuum (1–5000 µm).[4,182] Furthermore, single exposure estimates based on average exposure rates may not well represent the distribution of global MP intake rates.

Besides exposure, the fate and transport of ingested MPs in the human body, which include intestinal absorption and biliary excretion, have not been addressed in earlier studies and remained largely unknown.[180] Accumulation of MPs in the body tissues could cause physical stress and damage, inflammation, oxidative stress, and immune responses.[17] To date, effect studies examining MPs on human cells found little evidence of impact on cell viability.[183–186] However, it is uncertain if the range of exposure concentrations used in such studies is truly representative of the MP accumulated in body tissues.

Another speculated hazard from exposure to MPs is chemical toxicity. Plastics contain a huge variety of added and non-intentionally added chemicals.[187] Furthermore, MPs found in food types such as seafood and salt may have adsorbed chemicals from the environment it originated from.[26] The importance of MPs to influence chemical exposure in humans has been highly debated.[177,180] Past studies have only considered 100% leaching of the chemicals from the particles.[3,176,188] Although legitimate as a worst case scenario, this is not realistic since only a part of the chemicals in the particles is bioavailable due to kinetic constraints and limited gut residence time. The body also accumulates these chemical compounds through other routes of exposure, such as direct ingestion of food and inhalation.[189] Some of these compounds would cause risk if total concentrations are higher than their threshold effect concentrations, whereas carcinogenic compounds do not have a dose threshold level.[33] To

evaluate the actual risk and relative importance of MP as a chemical carrier, the actual MP intake amount from known food types and fraction of chemical leached as well as its associated uncertainties need to be quantified for the full MP continuum and chemicals residing in the particles.

The aims of the present study are to estimate the MP exposure in children and adults via eight food types and inhalation, and to assess the chemical contribution of MPs in relation to total chemical intake. Furthermore, we aim to compare the variability of MP abundance in the known eight food types and air. To this end, a probabilistic lifetime MP exposure model for children and adults is developed that accounts for the full variability of MP across different known intake media and global intake rates. The accumulation of MP in the body tissue and the amount egested in the stool are also determined and quantified in terms of particle number and mass distributions. To understand the potential risk of MP due to plastic-associated chemicals, the transfer of a relevant suite of chemicals from ingested MPs was simulated via kinetic modelling under realistic conditions whereby a human is also exposed to chemicals from dietary intake. Four representative chemicals that are commonly detected in plastic[190,191] were investigated: (1) benzo(a)pyrene (BaP), (2) di(2-ethylhexyl)-phthalate (DEHP), (3) 3,3',4,4',5-pentachlorobiphenyl (PCB126), and (4) lead. These chemicals were selected as they are widely known as main environmental pollutants due to the high carcinogenic potencies of the organic compounds,[192–194] while lead toxicity can lead to blood disorders and damage to the nervous system.[195]

4.2. Materials and methods

The probabilistic exposure assessment toolkit, Human Exposure Assessment for Small mIcroplastics (HEASI), comprises of two separate components (Figure 4.1): (A) The “Plastic Model”, which calculates MP abundance in gut, tissue, and stool with kinetic mass balance equations describing transport processes in the GI tract; and (B) the “Chemical Model” which uses the calculated MP intake from (A) to quantify chemical transfer from MP to the human body under realistic feeding conditions. Below, we provide the main features and equations of the assessment. A full description and list of fitted distribution parameters are provided in the Supporting Information (SI). Compiled databases from literature (Data S1–S6) are accessible in the following data depository: https://github.com/nhazimah/heasi. Because microplastic is a diverse material and input data show considerable uncertainty, the assessment was done probabilistically via Monte Carlo (MC) simulations, with n=10,000 iterations for each of the calculation steps. Ranges presented subsequently relate to the 90% confidence interval.

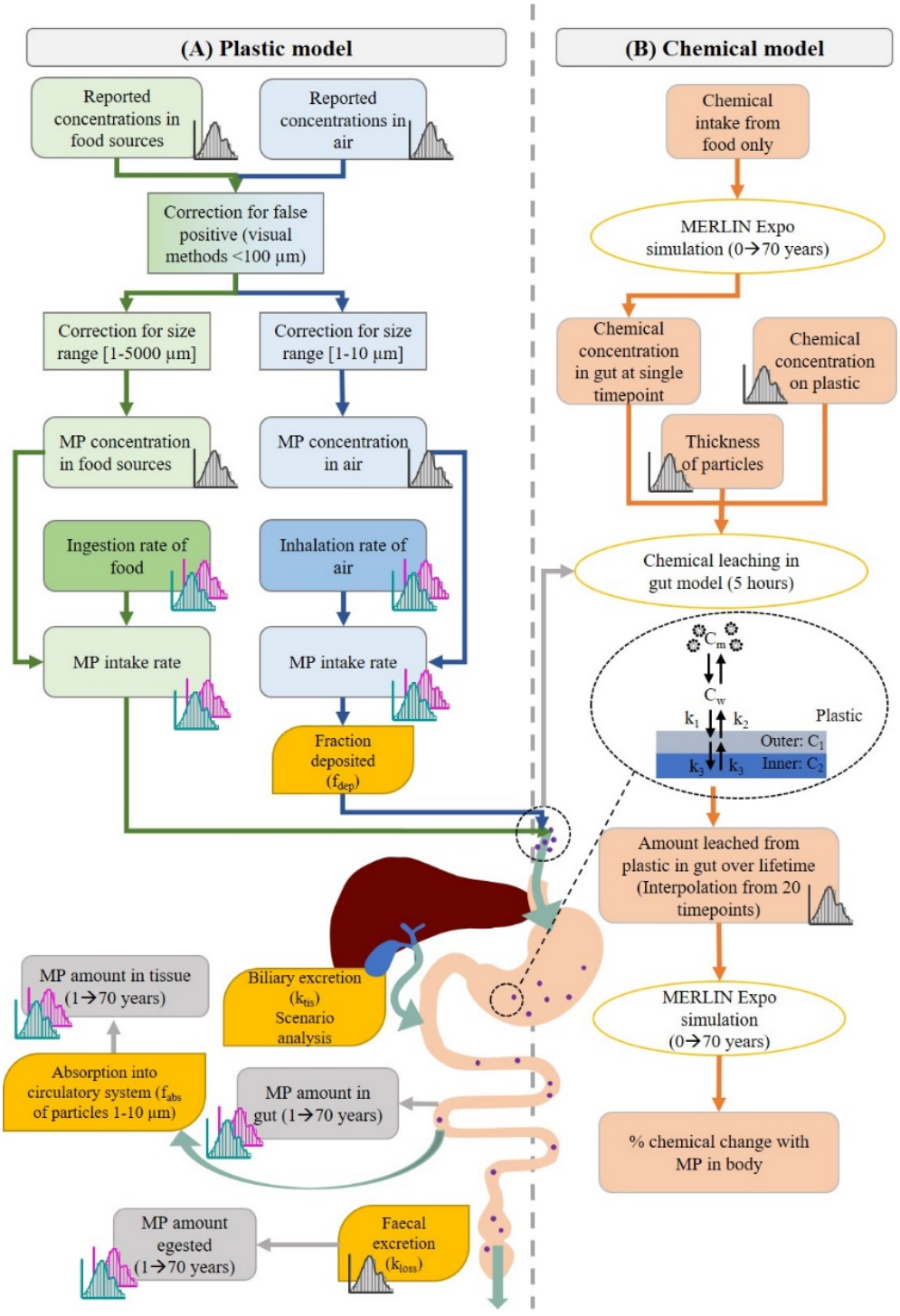
(A) Plastic model
Reported concentrations in food sources
Reported concentrations in air
Correction for false positive (visual methods <100 µm)
Correction for size range [1-5000 µm]
Correction for size range [1-10 µm]
MP concentration in food sources
MP concentration in air
Ingestion rate of food
Inhalation rate of air
MP intake rate
MP intake rate
Fraction deposited (f_{dep})
(B) Chemical model
Chemical intake from food only
MERLIN Expo simulation (0→70 years)
Chemical concentration in gut at single timepoint
Chemical concentration on plastic
Thickness of particles
Chemical leaching in gut model (5 hours)
C_m
C_w
k_1
k_2
Plastic
Outer: C_1
k_3
k_3
Inner: C_2
Amount leached from plastic in gut over lifetime (Interpolation from 20 timepoints)
MERLIN Expo simulation (0→70 years)
% chemical change with MP in body
MP amount in tissue (1→70 years)
Biliary excretion (k_{tis}) Scenario analysis
Absorption into circulatory system (f_{abs} of particles 1-10 µm)
MP amount in gut (1→70 years)
MP amount egested (1→70 years)
Faecal excretion (k_{loss})

Figure 4.1. Schematic overview of workflow for **(A)** the plastic model and **(B)** chemical model. **(A)** Green boxes and arrows indicate MP from food; blue boxes and arrows indicate MP from air. Yellow boxes represent the parameter inputs. Grey boxes and arrows represent the outputs: the MP amount accumulated in gut and tissue and amount egested. **(B)** Total MP intake calculated from the plastic model (shown at the inlet of stomach) was used to calculate total chemical leached from MP in the chemical model. C_m is the chemical concentration in gut fluid micelles, C_W is the chemical concentration in water in the gut, C_1 and C_2 are the chemical concentrations in the outer and inner phases of MP, respectively; k_1 and k_2 are the sorption and desorption rate constants, respectively; k_3 is the intrapolymer rate constant. Orange boxes represent the inputs for the chemical model and orange-outlined ovals represent the models used to calculate the chemical distributions and leaching from MP. Histogram symbols represent inputs with distributions. Green histogram: child (1–18 years); pink histogram: adults (19–70 years).

4.2.1. Plastic model

The lifetime exposure to MPs for humans is modeled as a mass balance of intake (i.e., dietary and inhalation) and loss processes in the human body (via the GI tract).[32,87] The amount of MP in the GI tract per person, C_{MP} (particles/capita), per day is calculated as

MP in GI tract (t) = (A) intake from food types + (B) intake from air + (C) transfer of accumulated MP in the body back to the GI tract – (D) loss from egestion.

In a mathematical form with terms A, B, C and D in the same order

$$\frac{dC_{MP}}{dt} = \left(1-f_{abs} \cdot f_{a,n}\right)\sum_{i=1}^{n}(Ir_i \cdot C_i) + (1 - f_{abs})\left(f_{dep} \cdot InR \cdot C_a\right) + k_{tis} \cdot C_{tis} - k_{loss} \cdot C_{MP} \quad (4.1)$$

The amount of MPs accumulated in the whole body tissue can then be calculated as

$$\frac{dC_{tis}}{dt} = f_{abs} \cdot f_{a,n}\sum_{i=1}^{n}(Ir_i \cdot C_i) + f_{abs} \cdot (f_{dep} \cdot InR \cdot C_a) - k_{tis} \cdot C_{tis} \quad (4.2)$$

For intake from food (eq 4.1, term A), index *i* refers to the *n* food types assessed in the present study (here, *n*=8, i.e., fish, mollusc, crustacean, tap water, bottled water, salt, beer and milk), C_i is the MP concentration per media in terms of number concentrations (particles/g) and Ir_i is the associated daily ingestion rate (g/capita/day). We also accounted for intestinal absorption (f_{abs}) as phagocytosis, endocytosis and persorption have been identified as mechanisms explaining uptake of particles <10 µm.[17,180,196–199] The fraction of particles that is taken up by the human GI tract is relatively unexplored. Most literature sources claim that intestinal absorption is low, reaching up to 0.3% for particles with sizes up to ~2 to 3 µm based on rodent and ex vivo models.[183,200–202] Here, we assumed a fraction of particles, f_{abs} of 0.3% of all 1–10 µm particles, is absorbed in the intestines. This is a conservative average estimate based on the range of absorbed fractions (0.2–0.45%) measured in vitro using human colon tissue.[203] The number of particles in the 1–10 µm size range is based on the fraction, $f_{a,n}$, of the total number of ingested particles, complying to the 1–5000 µm power-

law size distribution, which is explained in the next section (eq 4.4). This bioavailable fraction of particles is represented as an uptake process in the first term of eq 4.2.

MP intake from the air compartment (eq 4.1, term B) is calculated with MP concentration (1–10 μm) in air, C_a (particles/m^3) and the inhalation rate, InR (m^3/capita/day). A fraction of inhaled particles is assumed to be deposited in the nasopharyngeal cavity (f_{dep}) and then swallowed in the GI tract. This fraction is assumed as a constant of 0.83.[204] Swallowed particles from the air intake are also subjected to intestinal absorption (second term in eq 4.2) and hence, f_{abs} is also included in this term.

Removal of MP from the tissue, C_{tis} (particles/capita), is modeled as biliary excretion through the GI tract (term C in eq 4.1 and the third term in eq 4.2). Because the biliary excretion rate constant, k_{tis} (day^{-1}), is unknown for humans and microplastics, this was addressed using a scenario-based approach to describe zero, minimum, median and maximum biliary excretion kinetic rate values based on three rat and mouse studies on nanoparticles (<1 μm[205]) (SI Table S4.1).[206–208] Therefore, we assumed that the transfer rate of this pathway is similar for both MPs and nanoparticles, which are able to access organs and penetrate cell membranes.

Loss via egestion (eq 4.1, term D) is modeled with a loss rate constant based on stool frequencies,[209–214] k_{loss} (day^{-1}), assuming that MP particles are not trapped in the GI tract.[13] The amount of MP egested per stool mass per capita, C_{stool} (particles/g stool/capita), can be further calculated based on the gut steady state concentrations ($C_{MP,SS}$) and stool mass excreted per capita per day, M_{stool} (g stool) (eqs S4.1 and S4.2).[214–218]

Plastic model inputs and parameterization. A literature review was performed to identify studies that reported plastic concentrations in media relevant for human intake. Search strings included were: *microplastic, plastic, fish, seafood, salt, human, air, food*. Searches were performed until March 2020 using search engines Scopus and Google Scholar, and only studies reporting original concentration data were reviewed. Targeted searching was also conducted for databases or reviews published by nongovernmental organizations and governmental agencies. A total of 134 studies was identified reporting MP concentrations in nine media: (1) fish, (2) mollusc, (3) crustacean, (4) tap water, (5) bottled water, (6) beer, (7) milk, (8) salt, and (9) air (Data S1). For each source, a set of criteria and assumptions was made to ensure the quality and utility of data for subsequent model analysis (see SI).

Food consumption data were collected from FOSCOLLAB,[219] a database collated by the World Health Organization (WHO) and Food and Agricultural Organization (FAO) on chronic individual food consumption in different countries for different age classes (https://apps.who.int/foscollab). The list of search terms is provided in the SI (Table S4.2). Total mean ingestion rates were used to represent the whole population (i.e., including non-

consumers of the food) and the data were recategorized into two age groups: children (1–18 years) and adult (19–70 years). Inhalation rates were based on two studies[220,221] and redefined according to the aforementioned age groups (SI Table S4.3).

As most studies on MP occurrence in media associated with human intake are still limited to pioneering research, some of the methodologies that have been implemented thus far are not yet fully adequate.[11] To account for these inadequacies, we have applied a series of calculations to allow for better comparability among data with varying qualities, hence improving data utility. The model parameterization comprises the following three corrections (Figure 4.1A), which are explained hereafter and in full detail in the SI.

Correction 1: False positives. Out of the 871 datasets acquired for the exposure assessment, 203 datasets did not conduct further spectroscopic identification to confirm if the particles are indeed polymer-based.[7,11] Among these 203 datasets, 35% of them reported that their size detection limit was below 100 µm. As these studies may have overestimated the MP concentrations, we applied a correction factor to account for potential false positives. False positive rates for MP visual identification have been reported by Lenz et al.,[222] and the success rates for <50 and 50–100 µm are 63 and 67% respectively. Therefore, we assumed 65% (i.e., median success rates of <50 and 50–100 µm) of the particles had been correctly identified as MPs when the lower size limit detected by the study was below 100 µm. For particles above 100 µm, it is assumed that one can correctly identify MP through the particle texture and shapes.

Correction 2: Realignment of the size range. To allow for comparison of MP concentration data from studies targeting different size ranges, we used the size realignment method of Koelmans et al.[4] supported by studies[6,223] that have shown that fragmented plastic particles in the environment generally conform to a power-law size distribution. To realign the MP concentrations from different size ranges, particle size distributions (PSDs) for the different media in the present study are required. We assumed the PSDs for food to be different from that for air. The detailed approach for extracting this information is explained in the SI. We fitted the PSDs for 29 datasets from our literature review with the power-law function (SI Figure S4.1 and Table S4.4) according to Koelmans et al.[4] (see SI).

Using the obtained power-law exponent, α, the MP concentrations found within any size range can then be translated into the expected MP concentrations for the default size range by using a correction factor (CF_{scale}), which scales the integral of eq S4.3 for the measured (M) size range against the default (D) range:[4]

$$CF_{scale} = \frac{\int_{x_{0M}}^{x_{1M}} Cx^{-\alpha}}{\int_{x_{0D}}^{x_{1D}} Cx^{-\alpha}} = \frac{{x_{1M}}^{1-\alpha} - {x_{0M}}^{1-\alpha}}{{x_{1D}}^{1-\alpha} - {x_{0D}}^{1-\alpha}} \quad (4.3)$$

For the food types, we adjusted the measured MP concentrations to a default MP size range of 1–5000 µm.[4] For air, the datasets were adjusted to a default range of 1–10 µm because it has been demonstrated that only particles in this size range are filtered in the nose and may be swallowed via the nasopharyngeal pathway.[180,204] Based on the available PSDs from the aforementioned 29 datasets, two power-law exponents were defined, one for food (α_{food}) and one for air (α_{air}). The extrapolation of the MP concentrations to the default size range was carried out using eq 4.3 with α values selected from the probability density functions (PDFs) defined for α_{food} or α_{air}, via MC simulation in R.[76] Convergence of the PDFs for the realigned MP concentrations was obtained with 1000 iterations.

The parameter $f_{a,n}$can be calculated following the same principle as in eq 4.3, as a ratio of the integral between the interval 1–10 µm to the integral between the interval 1–5000 µm:

$$f_{a,n} = \frac{\int_1^{10} Cx^{-\alpha_{food}}}{\int_1^{5000} Cx^{-\alpha_{food}}} = \frac{10^{1-\alpha_{food}} - 1^{1-\alpha_{food}}}{5000^{1-\alpha_{food}} - 1^{1-\alpha_{food}}} \quad (4.4)$$

Correction 3: Translation of gut to muscle MP concentration in fish. The MP concentrations in the GI tract or stomach of fish, which were often reported in studies, were used to estimate the MP concentrations in the edible muscle tissue of the fish. Most studies investigating MP occurrence in fish were conducted to understand if plastic was ingested by the species. The direct application of these MP concentrations is not useful for human dietary intake in our exposure assessment as only a small fraction of the world population eats the fish stomach. Therefore, to estimate the MP concentration in the muscle tissue, we calculated the ratio between the plastic concentrations in the muscle and gut of the fish (CF_{mg}) based on empirical data for seven fish species.[224,225] The derivation of CF_{mg} and its distribution is detailed in the SI (Table S4.5).

Distributions were fitted to the MP concentrations in different intake media and physiological data with packages from R.[226–229] Datasets with zero observations were omitted for the distribution fitting; however, the probability of zero observations was accounted for by assigning a fraction of the generated random values from the MC simulations to zero observation. Table S4.6 provides an overview of the inputs used for the MP exposure model and the most appropriate distribution functions selected based on goodness-of-fit analyses (see SI for details and Data S2). Some distributions were represented as triangular distributions when few data were available.

Plastic model simulations and validation. The MP amount per capita (C_{MP}) was calculated numerically with the deSolve package[75] in R. We modelled two age group scenarios: a child scenario where exposure starts at 1 year and continues up to 18 years, and an adult scenario

where exposure continues from 18 years and goes on to the age of 70 years (UN average global life expectancy in 2019).

Number concentrations and mass concentrations are both relevant metrics for exposure and toxicological assessments. The plastic model was first applied to number concentrations of MP particles. Then, particle numbers were converted to mass concentrations based on size, shape, and density distributions of the particles (see SI). These properties were defined from the literature survey in the present study (Data S3 and S4). PDFs were fitted to the data for each property, and the mass per particle was calculated for food and air, respectively (SI Figure S4.2 and Table S4.7).

The amount of MP egested per stool mass was used as an endpoint to validate against empirical data for the MP amount in stool.[13]

4.2.2. Chemical model

The chemical transfer from MP under realistic feeding conditions is assessed via a two-step approach using two sub-models (Figure 4.1B). First, we used an established physiologically-based pharmacokinetic (PBPK) model in MERLIN Expo V3.0 (Man model),[230] which predicts the distribution of chemicals in the human body. A full description of the chemical intake data and literature used to obtain PBPK parameters are provided in the SI.

The second step consists of two separate approaches to predict the amount of hydrophobic organic chemicals (HOCs) and lead leached from MPs in the gut. For HOCs, the chemical exchange is quantified based on kinetic parameters and the concentration gradient between MPs and gut, using a previously published biphasic kinetic model for organic chemicals sorbed on MPs.[136] The chemical exchange in the fast and slow sorbing compartments is modeled as:

$$\frac{dC_1}{dt} = \frac{k_1}{f_1 \cdot (Intake \cdot m_i / V_{gut})} \cdot C_w - (k_2 + k_3) \cdot C_1 + k_3 C_2 \quad (4.5)$$

$$\frac{dC_2}{dt} = k_3 C_1 - k_3 C_2 \quad (4.6)$$

where C_1 and C_2 are chemical concentrations in the fast and slow reservoirs of the MP (µg/kg); k_1 is the fast sorption rate constant (d^{-1}), k_2 is the desorption rate constant (d^{-1}), and k_3 is the intrapolymer rate constant (d^{-1}); and f_1 is the fast reservoir fraction (dimensionless). The rate constants for desorption into gut fluids were quantified in earlier research[136] and were rescaled to account for the diversity of particle sizes based on Fick's law of diffusion (see SI). *Intake* is the number of MP taken in per media category per capita (particles/capita), V_{gut} is the volume of the gut, which we assumed to be 0.6 L[61] (note that this choice is arbitrary because the total amount of chemical leached (µg) is used in subsequent calculations), C_w is

the chemical concentration in the water of the gut calculated based on the concentration in the gut lipids (C_{gut}) simulated from the aforementioned PBPK model at a specific age assuming the fraction of lipids in gut ($f_{lip.gut}$) is 0.05:[231]

$$C_w = \frac{C_{gut}}{f_{lip.gut}} / K_{ow} \quad (4.7)$$

with Log K_{ow} = 6.13 (BaP), 7.6 (DEHP), and 6.89 (PCB126).[114,232,233] At the time of intake (t=0), the chemical concentrations in the plastic compartments C_1 and C_2 are assumed to be in equilibrium ($C_1 = C_2$) and the concentration values are based on chemical concentrations in MPs found in intake media, which is discussed in the next section.

As for lead, empirical data was used based on Godoy et al.[137] (i.e., 23.2% leaching during the intestinal absorption phase) to estimate the contribution of lead intake from MP to total dietary lead exposure using the PBPK model.

Chemical model inputs. For the chemical model, four representative chemicals were investigated: (1) BaP, (2) DEHP, (3) PCB126, and (4) lead. Literature survey on concentrations of these chemicals in organisms from the pelagic or littoral zone and atmospheric particulate matter chemical concentrations was performed (Data S5). These concentrations were used as proxies for plastic found in seafood and air, respectively. Additionally, the literature was reviewed for chemical concentrations on plastic from food packaging or manufacturing processes, which were used as proxy for the beverages in the present study. Further explanation for using these proxies is provided in the SI.

Simulation of chemical distributions in the human body. The distribution of chemicals in the tissues and organs of the human body was simulated with the Man model in MERLIN-Expo V3.0 from 0 to 70 years. Daily chemical intake of the four representative chemicals was based on selected literature: BaP,[234,235] DEHP,[236–238] PCB126,[144] and lead[239] (Data S6). For PCB126 and lead, intake through inhalation was not considered as atmospheric concentrations are negligible compared to intake through food.[240,241]

Chemical leaching from plastic in gut. We parameterized the chemical exchange of HOCs in the present study for the case of low density polyethylene (LDPE) as it is a common polymer type[11] and has the best available information thus far.[136] The amount of chemical leached from LDPE in the gut was calculated using the MC approach and the aforementioned biphasic reversible (de-) sorption model. First, we generated 10,000 particles (*i*) with different sizes for MP in food and air, respectively, based on the aforementioned power-law exponents (i.e., α_{food} and α_{air}). The mass per particle (m_i) was calculated for each ith particle using the density range of LDPE (Data S4) and shape distributions (see SI).

The MP intake amount calculated with the plastic model for the different media was redefined into four categories: (1) pelagic zone (fish and salt), (2) littoral zone (mollusc and crustacean), (3) packaging or manufacturing (tap water, bottled water, beer and milk), and (4) atmosphere. Finally, the chemical concentrations on MP for each category were also simulated probabilistically (Table S4.8).

The chemical concentrations in the fast (C_1) and slow (C_2) reservoirs of the ith particle for each media category were then solved numerically for a duration of 5 h per iteration (i.e., the average transit time through the stomach and small intestine[150]). Boundary conditions at gut transit time zero were the initial chemical concentrations in MP and the background chemical concentration in the gut from food only, as obtained from the MERLIN-Expo Man model. Calculations were performed in R using the deSolve package[75] and iterated 10,000 times for each individual particle size. The amount of chemicals (µg) released from MPs of each media category after the gut transit time was then calculated based on the plastic intake mass of that media (i.e., $Intake \times m_i$). The entire model simulation was then repeated for selected timepoints (n = 20) between 1 and 70 years of age having different chemical concentrations in the gut, based on the Man model simulation. The 50th and 97.5th percentiles of the distributions of total chemical leached from all MP intake media for these 20 timepoints were then interpolated with a cubic spline function to estimate the chemical intake from MPs in all years. Subsequently, we resimulated the chemical biodistribution using the Man model with the added intake of chemical exposure via MPs and calculated the percentage change of chemical concentrations in the adipose tissue (HOCs) and in blood (lead). A positive change reflects an increased chemical concentration in the tissue due to chemical desorption from ingested MPs, whereas a negative change reflects a reduced concentration due to absorption of chemical from the GI tract by ingested MPs.[25,32,45,136]

4.3. Results and discussion

4.3.1. Distributions of MP occurrence in food and air

The power-law exponent for food (α_{food}) was defined as a truncated normal distribution with a mean of 1.60 ± 0.51 (n=13) (Table S4.4), and for air (α_{air}), it was defined as a triangular distribution with minimum of 1.89, maximum of 2.24 and mode of 2.06 following two air studies.[242,243] Based on the fitted mean PSD for food, 75.3% of the full MP continuum (1–5000 µm) consists of small particles (1–10 µm), in terms of number concentrations. For air, these particles account for 91.4% and thus represent a significant proportion of the full MP size range. However, only 22.7% of the datasets used in the present study were able to account for these particles. Rescaling the MP concentrations to the full MP size continuum was thus necessary to not underestimate the concentrations.[4] Furthermore, in doing so, we accounted

for the smallest particles that are more relevant for accumulation in the body and potential toxicity.[17,180] The estimated power-law exponent for food in the present study is in excellent agreement with the exponents reported previously for PSDs of MPs in marine and freshwater environments.[6] Other studies have also reported power-law exponents between 1.2 and 2.93 for plastic fragmentation through impaction[244] or natural processes in the ocean.[223] The variations in the exponents may be a result of other processes at play, such as size selective emissions.

MP occurrence in eight food types and air were compiled as data were available in sufficient detail and quality for these intake media at the point of our analysis. The concentrations in food were rescaled to the full MP continuum and corrected for potential false positives accordingly (Figure 4.2A, SI Figure S4.3). We found that among seafood, molluscs had the highest MP concentration distribution with 50th and 95th percentiles of 8.07 particles/g TWW and 428.4 particles/g TWW, respectively (SI Table S4.6). These percentiles are about four times higher than the concentrations found for crustaceans and up to 40 times higher than fish. Furthermore, fish had a higher non-occurrence than the other seafood types. This may be partly attributed to the feeding ecology of the organisms and distribution of MPs in different environmental compartments. Molluscs and crustaceans are mainly filter feeders and feed on suspended materials, which may increase the likelihood of MP ingestion.[245] Moreover, molluscs are usually located at the bottom of the water bodies within the sediments, where there may be a high abundance of MPs deposited.[246]

Remarkably, the distributions of MP concentrations in the liquids analyzed in the present study have a similar order of magnitude, with 50th percentiles ranging from 125 to 337 particles/L (SI Table S4.6). Nevertheless, bottled water has 2.5 times higher median concentrations than the other packaged beverages (i.e., beer and milk). This suggests that the MPs mainly come from the polymer packaging material,[247] since beer and milk are packaged in glass, aluminum cans,[107,108] or tetrapak cartons.[248]

Salt has a wide distribution of MP concentrations based on 162 datasets from 65 locations, ranging across more than three orders of magnitude. The 50th and 95th percentiles are 1.29×10^3 and 1.19×10^5 particles/kg respectively (Table S4.6). Zhang et al.[15] recently reviewed the MP abundances in table salt globally and found that the abundances varied widely, with the highest concentration at 2.0×10^4 particles/kg. However, the authors acknowledged that the reviewed datasets could not be compared with each other due to differences in analytical methods used. Therefore, the present study has addressed this non-alignment of datasets using a novel approach so that they represent the full MP continuum and can be better compared.

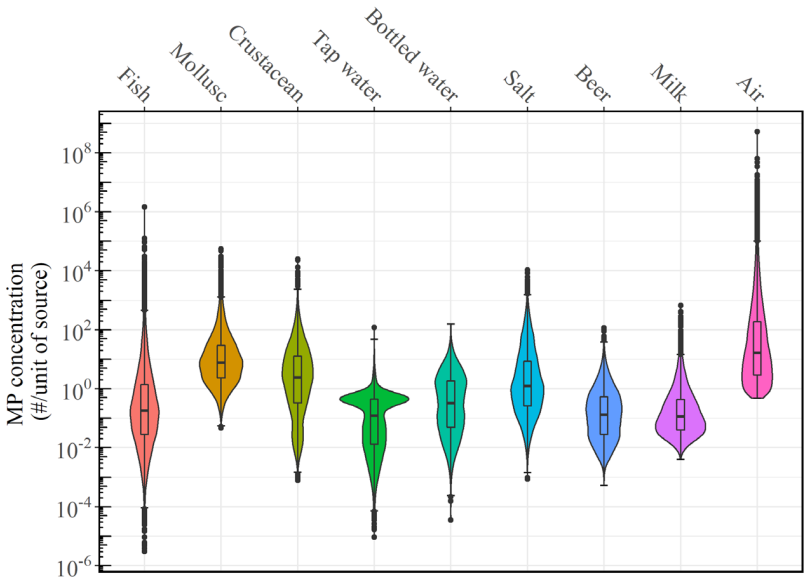

Figure 4.2. Violin plots of MP concentration in food (1–5000 µm) and air (1–10 µm). Concentrations are presented as per gram of body wet weight (BWW) for fish and crustacean, per gram of tissue wet weight (TWW) for mollusc, per litre for all liquids, per gram for salt, per m^3 for air. The box plot is showing the median (middle line), interquartile range (box length). Note that data are only realistic within the 95 % confidence interval (horizontal line on the whiskers of boxplot).

The concentration of inhalable MPs (1–10 µm) in air is 36.3 particles/m^3 and 19,000 particles/m^3 at the 50th and 95th percentiles, respectively. Standards for particulate matter smaller than 10 µm (PM_{10}) exist and according to the WHO, the annual mean of PM_{10} in ambient outdoor air should be below 20 µg/m^3.[249] For comparison, we converted the MP particle number concentrations to mass concentrations based on the mass per particle PDF for air and found that the 95th percentile of the distribution is about 0.011 µg/m^3. Based on the WHO's air quality database from 2018, the average global PM_{10} level is 72 µg/m^3 and the lowest level by region is in the high-income countries in Europe with a concentration of 22 µg/m^3.[250] Therefore, the MP concentration in the air has a negligible contribution to the PM_{10} levels, even at the 95th percentile.

4.3.2. Lifetime exposure to microplastic

Number of MP intake per capita. We estimated the global MP intake per capita per day from each of the nine media probabilistically (Figure 4.3). The medians of the total MP number intake rates found in this study are 553 (52.5–1.37×10^5) particles/capita/day for children, and 883 (86.4–1.68×10^5) particles/capita/day for adults, and the distributions were highly right

skewed. Mean exposure amounts for the American population estimated by Cox et al.[14] fall in the lower 10th percentile of the ranges estimated in the present study. This is because the aforementioned study did not rescale particle number concentrations to the full MP size continuum. This is corroborated by our earlier finding that small particles (1–10 µm) make up about 75 to 90% of the overall particle distribution and neglecting them results in a huge underestimation. Furthermore, single point estimates of consumption rates for the American population may not be representative of the global consumption rate distribution. In a later review by Zhang et al.[15], MP intake ranges in salt, drinking water, and inhalation were estimated. The median and maximum values of the range reported for salt and air are close to the upper 90th percentile range of MP intake in our study. However, the range reported for drinking water was lower than the 50th percentile of our distribution range for tap water. Although previous studies have estimated MP intakes within the 95% confidence interval of our distribution, their single point estimates and ranges did not account for the full variability of MP from different known intake media and the global consumption rates, which is done here for the first time.

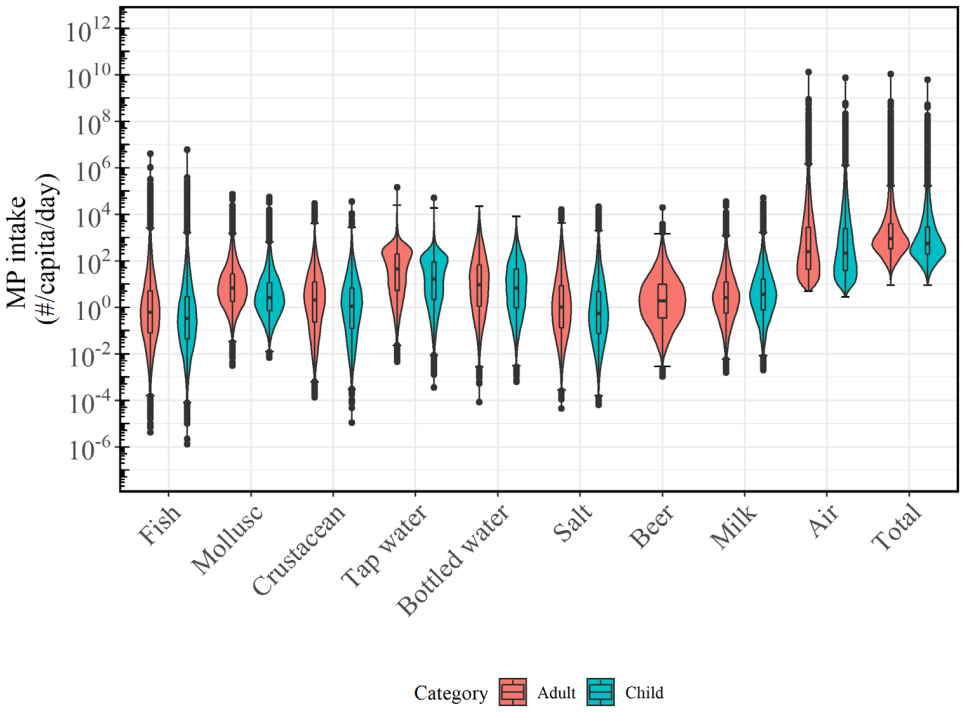

Figure 4.3. Violin plots of MP number intakes (particles/capita/day) and total MP number intake from food and air for adult and child. The box plot is showing the median (middle line), interquartile range (box length). Note that data are only realistic within the 95 % confidence interval (horizontal line on the whiskers of boxplot).

Mass of MP intake per capita. Several past studies and reviews have converted particle number concentrations using conversion factors with a constant mass per particle factor[3,188,202,247] to evaluate the chemical risks of MP. Particle mass was calculated simplistically assuming spherical particles with a specific density and diameter. However, these estimations do not account for the full MP continuum, which comprises different particle sizes, shapes, and densities.[4,6] The single estimates used so far in simple risk assessment calculations ranged from 0.007 to 4 μg/particle.[3,188,202] These estimates are above the 85th percentile of the mass distributions reported in the present study (SI Figures S4.2G and S4.2H). Our estimates show that the mean values are 5.65×10^{-6} and 3.97×10^{-7} μg/particle for food and air, respectively. This shows that previous studies have overestimated the MP exposure and potential risks.

Among the nine media, the highest median contribution of MP intake rate in terms of mass is from air, at 1.07×10^{-7} mg/capita/day. Despite the smaller size (1–10 μm), the intake rates and MP abundance in air are much higher than other media (Figure 4.4). At the 95th percentile, MP mass intake distribution from bottled water is the highest among all media, with intake rates of 1.96×10^{-2} mg/capita/day. Some countries are still very reliant on bottled water as their main source of drinking water since their piped water supplies may be contaminated and unsafe for consumption. Therefore, this source is an important route for MP exposure in these countries. The lowest median intake rate is from fish (3.7×10^{-10} mg/capita/day). As mentioned earlier, this can be explained by the highest non-occurrence for fish and from the fact that the median number concentration of MP in fish muscle is only 0.18 particles/g BWW. This suggests that its relevance for MP intake is low relative to other known media.

The total daily median MP mass intakes from the nine media for children and adults are 1.84×10^{-4} (1.28×10^{-7}–7.5) and 5.83×10^{-4} (3.28×10^{-7}–17) mg/capita/day, respectively. A recent report by the World Wildlife Fund (WWF) claimed that humans consume up to 5 g of plastic (one credit card) every week (~700 mg/capita/day) from a subset of our intake media (Figure 4.4).[251] Their estimation is above the 99th percentile of our distribution and hence, does not represent the intake of an average person. Other types of nano- and microparticles are also widely present in our diet, such as titanium dioxide and silicates. It is estimated that the dietary intake of these particles is about 40 mg/capita/day in the U.K.[252] Comparing our findings with the intake of other particles, MP mass intake rates are insignificant, as they make up for only 0.001% of these particles. However, this comparison does not imply that the toxicological profiles of these particles are similar.

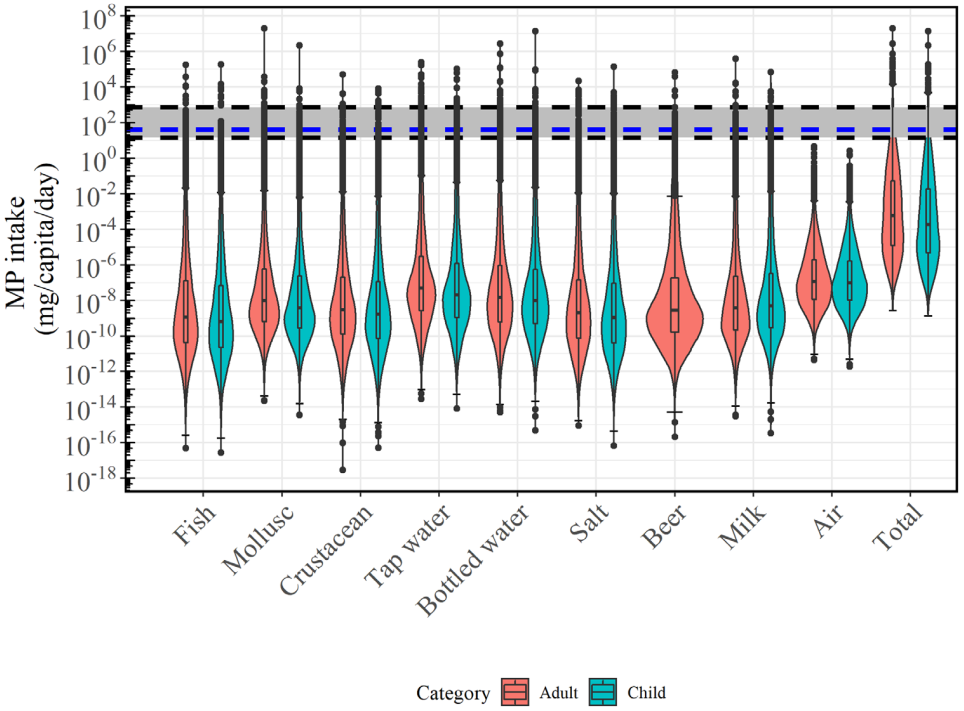

Figure 4.4. Violin plots of MP mass intakes (mg/capita/day), and the total MP mass intake from food and air for adult and child. Black dashed lines and shaded grey region (14–714 mg/capita/day) indicates the range of mass intake estimation by WWF[251] and blue dashed line (40 mg/capita/day) indicates the mass intake of inorganic particles.[252] The box plot is showing the median (middle line), interquartile range (box length). Note that data are only realistic within the 95 % confidence interval (horizontal line on the whiskers of boxplot).

Distribution of MP in the gut and tissue. MP accumulation in the gut, tissue and stool was simulated over the average human lifetime (70 years) using the MP kinetic model under four scenarios (Figure 4.5). Previous studies have revealed that microsized particles between 1 and 20 µm can be absorbed by the body through oral ingestion.[17,180,183,196–199,253] Given this range of values, we assumed that MPs smaller than 10 µm (i.e., midpoint of the range) are absorbed and distributed in the body then returned to the GI tract via biliary excretion, parameterized with a biliary excretion rate constant. Note that the cutoff at 10 µm to some extent is arbitrary, as the model output obtained for a cutoff at 10 µm can be easily converted to any other cutoff value using eq 4.4. For the biliary excretion rate constant, four scenarios were used: no biliary excretion (k_{tis} = 0 day^{-1}), minimum (k_{tis} = 0.067 day^{-1}), median (k_{tis} = 0.61 d^{-1}), and maximum (k_{tis} = 8.30 d^{-1}) (SI Table S4.1). We observe that the MP steady-state abundance in the GI tract (i.e., at the end of the simulation for each age group) is not sensitive to this parameter (p>0.05; Kruskal-Wallis), whereas the accumulation of MP (1–10 µm) in the

tissue is significantly affected (p<0.05; Kruskal-Wallis) (Figures 4.5A and 4.5B). This difference is due to the small contribution of accumulated particles in the tissues ($f_{abs} \cdot f_{a,n}$ and $f_{abs} \cdot f_{dep}$ ≈ 20% of total ingested MPs), which are excreted via the biliary pathway, to the number of particles already in the gut. In the worst case scenario where accumulated particles remain in the body throughout the lifetime (i.e., zero biliary excretion), the median concentration in the tissue is 5.01×10^4 (5.25×10^3 – 9.33×10^6) particles/capita or 0.041 (8.15×10^{-4} – 9.85) µg/capita at the end of 70 years (SI Table S4.9 and S4.10). The parameterization of this pathway is thus necessary to determine the extent of the MP exposure in the tissues and could be relevant for future effect studies. Note that biodistribution of the MPs among different organs of the body was not explicitly modeled, so this concentration relates to the whole body. In reality, the particles will accumulate in certain tissues and organs, potentially reaching much higher concentrations, locally.[253–255]

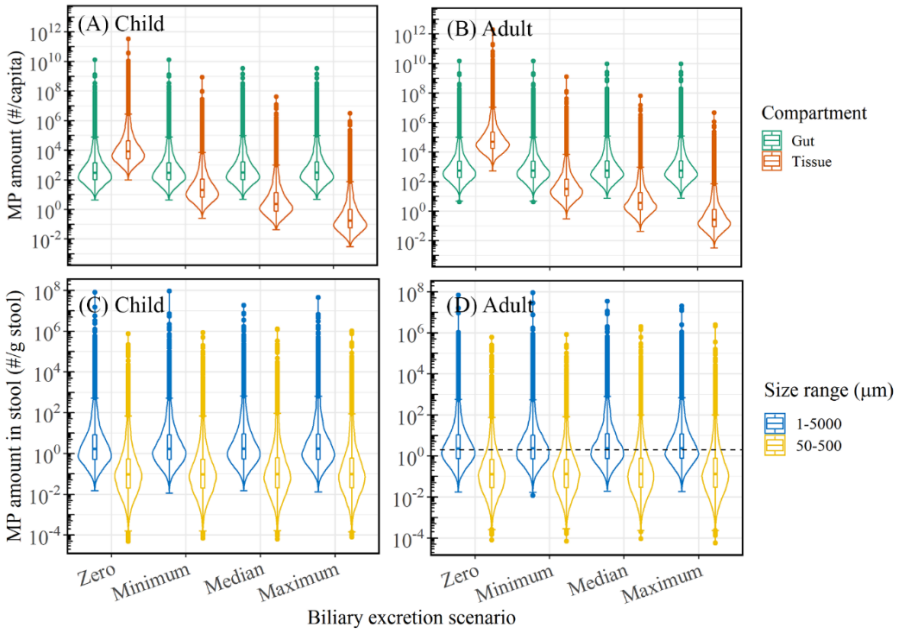

Figure 4.5. Distribution of MP amounts in the gut and tissue compartment at the end of the simulation for **(A)** child (1-18 years) and **(B)** adult (1-70 years). Scenarios: no biliary excretion (k_{tis} = 0 d^{-1}); minimum (k_{tis} = 0.067 d^{-1}), median (k_{tis} = 0.61 d^{-1}); maximum (k_{tis} = 8.30 d^{-1}). Distribution of the amount egested in stools at the end of the simulation for **(C)** child and **(D)** adult. Blue violin plots represent the full MP continuum and yellow violin plots are scaled to the size range 50-500 µm to compare with MP concentrations in stool from Schwabl et al.[13] (black dashed line). Note that data are only realistic within the 95% confidence interval (horizontal line on the whiskers of boxplot).

The MP abundances in the gut and tissue compartments were two to six times higher in adults than in children. Steady-state abundance was reached after ~40 days for each age group since the minimum biliary excretion rate (which is the rate-limiting process) is equivalent to a maximum half-life of 10 days. Therefore, even if a person lives beyond 70 years (i.e., past the model simulation time period), the abundance will not increase in both compartments, unless particles trapped in the body do not get eliminated as in the case for no biliary excretion. The median steady-state MP abundances in the gut are about 300 and 500 particles/capita for children and adults, respectively, which translate to mass abundances ranging from 7.98×10^{-4} to 1.59×10^{-3} µg/capita (SI Tables S4.9 and S4.10). We then estimated the MP abundance in stool based on gut steady-state abundances (Figures 4.5C,D). This endpoint was chosen as it is comparable to the only MP occurrence study in humans to date.[13] The median MP level (50–500 µm) found in stools of adults aged between 33 and 65 years in the aforementioned study is 2 particles/g stool.[13] This lies within the 80th percentile of our distribution for particles within the same size range. Comparing the median levels, our model estimates about 7% of the MP abundance found in the stool samples. This suggests that MP intake exposure may be higher than the intake amounts we estimate here based on known media. This is reasonable since the food types considered in the present study compose of 20% of the global average diet.[256]

4.3.3. Weight of evidence for the role of MP as chemical vectors

The chemical contribution from MP to total chemical intake was evaluated by probabilistically accounting for the full variability of ingested MP and chemical concentrations on the MP particles. Chemical leaching from MP was modeled assuming biphasic reversibility, where the direction of transfer is determined by the concentration gradients between MP and gut tissue, with kinetics determined by particle and chemical properties. In contrast, previous reports by the European Food Safety Authority (EFSA)[202] and WHO[3] were based on conservative calculations with highest chemical concentration detected in beached pellets and single MP intake measurements based on molluscs.[103] The estimation was based on an average particle diameter and density and thus, not accounting for possibly slower kinetics from much larger particles.

With our integrated and more realistic chemical modeling approach, we demonstrate that at the 50th percentile of the chemical concentrations leached, the change in the tissue concentrations for the four chemicals is negligible (Figure 4.6 and SI Figure S4.5). This also confirms our model assumption that chemical leaching from MP would not substantially affect the background chemical concentration in the gut originating from food. In the more extreme cases (i.e., at the 97.5th percentile of concentration leached from MPs), BaP showed the highest percentage change in the adipose tissue concentrations with a maximum of

17.4% increase (Figure 4.6A). PCB126 recorded the highest contribution from MP exposure to dietary intake (~0.12% at the 97.5th percentile) among the analyzed chemicals (Data S6). However, it only resulted in a small change of 2% in the adipose tissues with additional exposure via MP. These results illustrate that the proportion of chemical exposure from MP intake to total dietary intake, which has usually been used to evaluate the role of the vector effect,[3,188,202] is insufficient to inform us about the eventual chemical change in the body, due to the differences in biodistribution processes for different chemicals.

The percentage change of tissue concentrations appears to be erratic over the lifetime (Figure 4.6). Due to the processes simulated in the Man model, the chemicals in the body do not steadily increase over time (Figure 4.6). When there are higher concentrations in the adipose tissue, the gradient for transfer from the ingested MPs to the tissue is reduced and vice versa. Therefore, maxima in the adipose concentrations caused by dietary intake (lower panel A, yellow band), coincide with minima of the leaching rate of chemical from MPs (see the inset in Figure 4.6A). Interestingly, when the chemical leaching rate from MPs is at a minimum turning point, the additional chemical exposure via MPs results in a decrease in tissue concentrations (i.e., negative percentage change) compared to the zero plastic scenario (upper panel A, yellow band). Conversely, the additional chemical exposure from MPs results in an increase in tissue concentrations when the initial adipose concentrations are at a minimum (Figure 4.6B).

We simulated the percentage change of lead in blood assuming a constant percentage leaching from MPs over the lifetime, as the aforementioned biphasic kinetic model is not applicable for metals due to differences in chemical behaviour.[137] In addition, unlike the other compounds, lead is usually measured in the blood for human exposure. The percentage contribution of lead from MP exposure to dietary intake is three to five orders of magnitude lower than the aforementioned organic compounds, at the 97.5th percentile. This resulted in a decreasing percentage change in the blood over time due to the increased proportion of the chemical body burden originating from dietary and inhalation intake (Figure S4.5). Before the age of 10 years, the percentage increase is greater than 5% and can reach up to almost 20%. Lead is used widely in plastic as a stabilizer and also as a component of paint.[257] It has also been detected in plastic pellets and fragments in the marine environment.[258–261] Because the contribution of MP in lead intake is not negligible, more studies are warranted to understand the transfer kinetics of lead in plastic under realistic gut conditions.

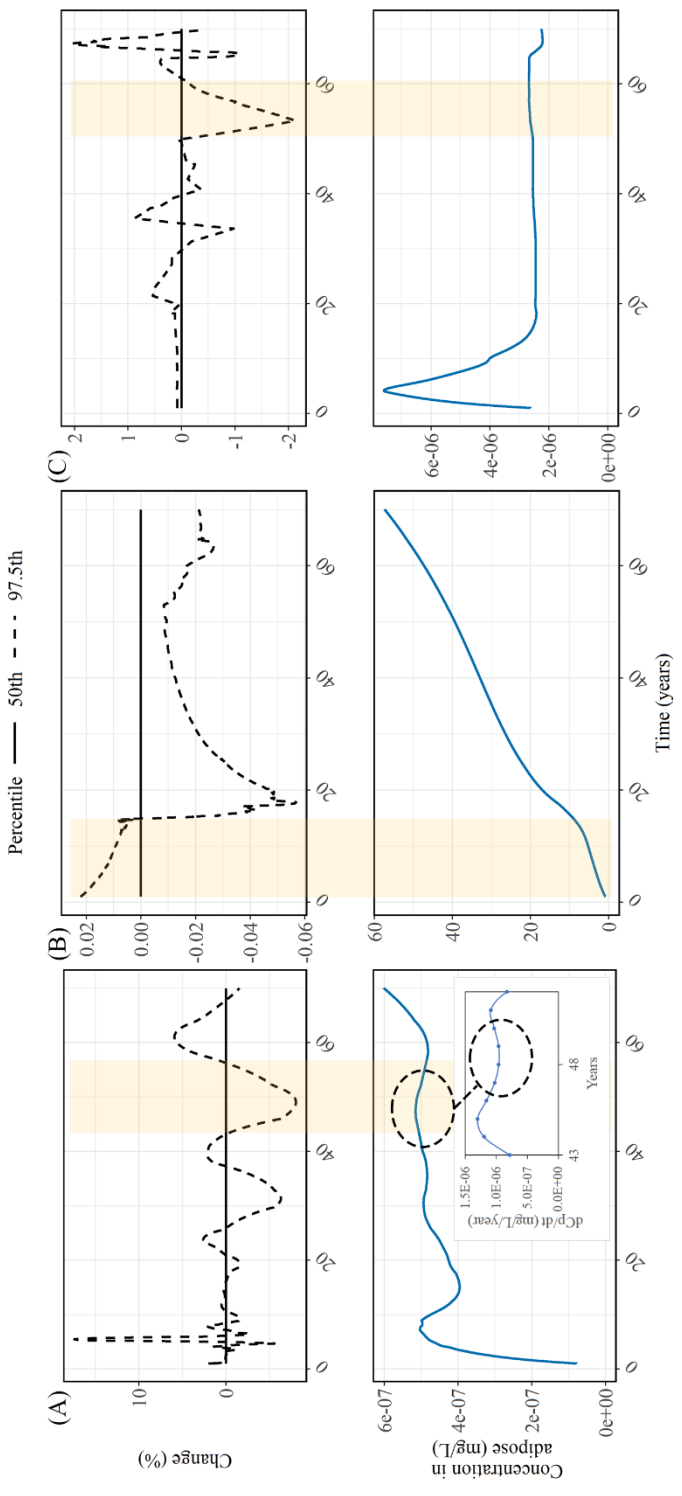

Figure 4.6. Percentage change of chemicals in adipose tissues as a result of additional chemical exposure via MPs (top panel) and the initial adipose tissue concentrations from dietary intake of compounds (bottom panel). **(A)** BaP; **(B)** DEHP; **(C)** PCB126. The yellow highlighted parts show how the percentage change varies depending on the change in adipose tissue concentrations. Inset in panel A, shows the rate of change of chemical leaching from MPs for ages between 43 and 52 years, to demonstrate that the maxima adipose tissue concentrations coincide with the minima of the leaching rate of chemicals from MPs.

4.4. Outlook and general implications

An MP human exposure assessment toolkit (HEASI) is presented, which applies innovative concepts and tools accounting for the uncertainty and variability of MPs. Previous human exposure assessments[14,15] have neglected the complexity of MP mixtures and did not take into account the discrepancies in the size ranges and methodologies of the studies used in the assessments. The HEASI toolkit also includes novel methods of translating MP number concentrations to mass concentrations using probabilistic calculations for the full MP continuum. We performed the assessment based on nine intake media that were available during the predefined period of our literature review. We found that the total MP intake rates from these nine media are negligible when compared to inorganic particles in terms of mass. Of the ingested MPs, the smaller-sized fraction (1–10 μm) may be absorbed in the intestinal region and become trapped in the human body throughout the lifetime. In the case when there is limited biliary excretion, the trapped particles would reach higher mass concentrations in the whole body tissue than in the gut despite the small particle sizes. Our methodology also allows us to estimate the MP abundance in stools, an endpoint that can be used for future calibration of the model.

Previous risk assessments that evaluate the role of MPs as chemical vectors in humans have so far assumed worst case scenarios in their calculations, with 100% instantaneous leaching of chemicals.[3,188,202] In the present study, we performed a probabilistic assessment to evaluate the actual chemical exposure via MPs in relation to dietary and inhalation intake of compounds using the simulated MP intake rates and also accounting for the full variability of the MP continuum. Our methodology also includes quantifying the actual percentage change in the body tissue concentrations with the added chemicals from MP intake. We conclude that the contribution of the MPs to chemical intake is small to negligible for the four representative chemicals investigated in this study and yet still not substantial for BaP (∼17%) and lead (∼20%) at the 97.5th percentile of the amount of chemicals leached.

As the biodistribution of MPs is still unknown to date, simulated concentrations of 1–10 μm MP in tissue relate to the whole body. However, if these MPs do get trapped, they may accumulate in specific tissues. In the research field of engineered nanoparticles, studies have identified the liver and spleen as main target organs for silver nanoparticles.[262,263] Assuming that MPs behave similarly and accumulate mainly in the liver, we estimate that local concentration could reach up to ∼0.025 μg/L at the end of a human lifetime if there is no biliary excretion. Since there is no data on MP occurrence in human tissue specimens to date, our model can provide the best estimate of local tissue concentrations, which can be useful for future human effect studies.

At present, due to the paucity of data in other foods, our estimates of the MP intake rates account for approximately 20% by mass of the total food consumed daily on average (i.e., across different food cluster diets).[256] As publications in the field of MPs increase exponentially, a few new studies reported MP occurrence in fruits and vegetables,[264] and packaged meat[265] after our analysis date. However, these are only single datasets for each food category and thus do not fulfil our criteria for the present assessment. Between these food categories, the estimated daily intakes of particles from fruits and vegetables were higher, averaging at 1.50×10^{7} particles/capita/day (in adults with average body weight of 70 kg) with median sizes of about 2 μm.[264] Based on our particle mass distribution in food, the mass of these small-sized particles would be less than 1×10^{-7} μg/particle. It is plausible that if these food categories are considered, our model would predict much higher MP mass concentrations accumulated in the body than our earlier predictions. However, even if this would increase up to 7 orders of magnitude, this is still only 0.004% of the mass of inorganic particles ingested per day.[252]

Acknowledgment

We would like to thank Yayasan Mendaki (Singapore) for the Ridzwan Dzafir Distinction Award, the PMBM Scholarship Fund Board (Singapore) and the Aquatic Ecology and Water Quality group of Wageningen University and Research for co-funding this project.

Supporting Information for Chapter 4

Materials and methods

In this section, we provide further information on the plastic model (SM4.1) and the chemical model (SM4.2). Section SM4.1 comprises seven subsections: auxiliary model equations (SM4.1.1), data collection on MP concentrations in media relevant to human intake (SM4.1.2), data collection for physiological characteristics (SM4.1.3), realignment of size ranges of plastic concentrations (SM4.1.4), translation of gut to muscle MP concentration in fish (SM4.1.5), goodness-of-fit tests for selection of PDFs (SM4.1.6), conversion of MP particle number to mass concentrations (SM4.1.7). Section SM4.2 comprises three subsections: physiologically based pharmacokinetic (PBPK) modelling with MERLIN Expo 3.0 (SM4.2.1), detailed description of the chemical leaching model (SM4.2.2) and chemical concentrations in plastic (SM4.2.3)

SM4.1. Plastic Model

SM4.1.1. Auxiliary model equations

The steady-state solution to eq (4.1) from the main text, results in the steady-state MP amount per capita:

$$C_{MP,SS} = \frac{(1-f_{abs}\cdot f_{a,n})\sum_{i=1}^{8}(Ir_i\cdot C_i)+(1-f_{abs})\cdot(f_{dep}\cdot InR\cdot C_a)+k_{tis}\cdot C_{tis}}{k_{loss}} \quad \text{(S4.1)}$$

The MP amount egested per gram of stool per capita can be calculated based on the gut steady-state concentrations:

$$C_{stool} = \frac{k_{loss}\cdot C_{MP,SS}}{M_{stool}} \quad \text{(S4.2)}$$

SM4.1.2. Data collection on MP concentrations in media relevant to human intake

For all studies, information such as the type of analytical method used, size range of the particles identified, the percentage of positive occurrence, particle size distribution, particle shape and polymer type was collected.

If a food category is to be included in the assessment, there should at least be more than three datasets available. Each study should at least have substantial evidence that the particles are indeed MP. Secondly, consumption pattern data for the food type should be available and its relative contribution to the overall human diet of the general world population should be substantial enough (i.e., consumed in some regions). Some studies, however, do not meet these criteria for data quality and availability. For example, there is a lack of evidence for MP presence in honey as Mühlschlegel et al.[109] managed to positively

identify only one particle as PET despite their initial findings of 8 to 108 #/kg of honey through visual identification. Other food types such as seaweed nori,[266] dried fish,[267] and chicken gizzards[268] have been investigated for MP presence. However, these food types are not major components of the global human diet and their consumption pattern data are also not widely available. Additionally, in the case of chicken gizzards, the data quality is poor due to lack of spectroscopic identification.[7] Furthermore, based on a simple estimation, the contribution of the MPs from these food types is insignificant even on the local level. For example, the highest possible daily intake of MP from seaweed nori, which had the highest MP concentration among the food types above (max: 3000 #/kg DW), is estimated at 30 #/capita/day if it is calculated according to the average annual consumption per capita in Japan (4 kg/capita/yr).[269] This only represents ~3% and ~0.018% of the 50th and 95th percentiles of the total MP intake from other known media (Figure 4.3).

Criteria for each media. Seafood species were selected based on the "use and trade" information reported in the IUCN (https://www.iucnredlist.org) or "human uses" information from Fishbase. The species has to be at least used for local or national human consumption, or is commercially produced to ensure its relevance for the world population. To ensure that the reported MP concentrations in the studies are at least statistically representative of the sampled species, we set a minimum number of individuals per study sample (n=5). This criterium applied to fish, molluscs, and crustaceans. One could argue that n=5 may not be representative of the species especially if there was zero occurrence of plastic in the samples. However, since we considered each food type as one category, the uncertainties from a single dataset (one species) have already been accounted for by the uncertainty of the entire dataset for that category.

As for drinking water, the data quality of the studies has recently been assessed in a review by Koelmans et al.[11] Most of the studies associated to drinking water were evaluated to be above average with respect to the quality of sampling methodology and data reporting. Therefore, the reviewed drinking water studies (i.e., tap and bottled water) were included in our literature review. In addition, three more recent studies[270–272] were included after evaluating their sampling methodology and data reporting with the same criteria table from Koelmans et al.[11] The datasets from Kutralam-Muniasamy et al.[248] for MP occurrence in eight brands of milk were also evaluated against the same set of criteria as drinking water. Two studies had investigated 'potential' plastic particles in beer from North America and Europe.[107,108] Both did not implement any spectroscopic methods to confirm the identity of the particles found and may even include particles of glass material. However, since beer is widely consumed, we considered the reported concentrations from these studies noting that

this is a conservative estimate for MP concentrations in beer and the outcome is not very sensitive to this assumption.

There was a limited number of studies for MP occurrence in salt and air. Therefore, we did not set any criteria for the number of replicates per sample size so that we could include as many datasets as possible. Increasing the number of datasets would improve the distribution of the MP concentrations in these media and otherwise, the uncertainty would have been accounted for in the probabilistic assessment. The selection of studies for MP intake from air was targeted on suspended atmospheric MP. Fallout or deposition studies were not considered as the size for these particulates is generally in the larger end of the range and they have a lower likelihood to be inhaled.[273]

Conversion of MP concentration per individual to per body wet weight. Plastic concentrations in fish and crustaceans were often reported on an individual basis. To allow for comparison of data from different species, the reported individual concentrations were converted to particle number per body wet weight (particles/g BWW). The weight of the sample is used for conversion if available. For studies where the weight of the samples was not reported and the length of the organisms was reported instead, the BWW was estimated from the linear correlations between log-transformed length and weight published in Fishbase[274] for that particular species. If both weight and length of the samples were not reported, the average length at first maturity (L_m) obtained from Fishbase was used to estimate the BWW. This assumption is justifiable as most studies sampled adult fish and would otherwise mention that they sampled juvenile fish. In the case of juveniles, a median size of juveniles of the species from literature is used. Detailed calculations for these MP concentration conversions are available upon request.

Determination of size ranges for each study. Microplastics have been widely defined as polymer particles of less than 5 mm. However, many studies also considered mesoplastics which are larger than 5 mm. While the upper size limits have been inconsistent for all the literature reviewed, the lower size limits of the studies have also depended largely on the analytical techniques used. To allow for comparison between studies, the size ranges for each study needs to be defined. Most studies clearly defined the size ranges of the particles which they aimed to identify or reported the size detection limits of their methodology or size range of particles which they actually found. One of these categories of information, when available, was used to set the size range for the study. However, some studies did not report any of the above in which case we assumed that the size range complied with the generally accepted definition of “microplastics” as particles less than 5 mm[2,4,182] and the minimum size limit is dependent on the methodology (i.e., sieves/filter used during sample processing, microscope magnification, and sorting). For studies that carried out visual sorting under a

stereomicroscope, we used their reported maximum magnification to compare against other studies with similar magnification and reported a minimum size limit. If the magnification was also not reported, we based the minimum limit as the scale bars length on the microscope images. If the study did not have any of the above, the minimum limit was set as 300 µm which was recommended by Mintenig et al.[275] as the minimum size feasible for manual sorting with forceps and 100 µm if manual sorting was not carried out but the sample was only observed and counted under a stereomicroscope, based on Lenz et al.[222]

SM4.1.3. Data collection for physiological characteristics

Food consumption data. To perform our MP human dietary exposure assessment, we used the food consumption data from FOSCOLLAB which is based on household surveys collated by the Food and Agriculture Organization (FAO) and World Health Organization (WHO). Some of the surveys from this database only represented a small number of consumers. Therefore, a criterium for sample size (n>5) was set for the dataset to be deemed as acceptable.

Separate statistics were available for different age groups for: all, infants and toddlers, children and adolescents, adults and elderly. As the evaluation of the MP exposure assessment in this study is over a lifetime, we classified the data into two age groups: children (1-18 years) and adult (19-70 years).

Inhalation data. The probability density functions (PDFs) defined for each age class as reported in Allan and Richardson[221] were used. The data from the categories: toddlers, children and teenagers were combined for the 'child' group, whereas the adult and senior categories were combined for the 'adult' group. The infant category was not considered in the child category as the food database in this study does not apply to infants. Subsequently, we defined the possible minimum and maximum inhalation rates of each age group and these values were either based on Stifelman[220] or on the 2.5 and 97.5 percentiles of the distributions defined by Allan and Richardson[221] (Table S4.3). The resulting distributions were then fitted either with normal or lognormal distributions as these are commonly used for air inhalation rates in probabilistic human health risk assessments.[276]

SM4.1.4. Realignment of size ranges of plastic concentrations

From our literature review, we collected 29 datasets with particle size distributions (PSDs) from 18 studies that met our minimum criterium of ≥ 5 size class bins for meaningful data fitting. When the PSDs were presented in histograms or bar graph formats, the data was extracted with WebPlotDigitizer (https://automeris.io/WebPlotDigitizer/). Size ranges >5 mm were also considered here to account for concentrations that included larger sized particles.

According to the law of fragmentation, we would expect a decreasing trend in particle abundance with increase in particle size. However, not all of the datasets assumed this trend. We speculate that this may be either due to poor recovery of smaller particles or analytical bias during visual inspection. Therefore, to avoid underestimation of particle abundances in the lower size range, we followed a similar approach as Kooi and Koelmans[6] for determining the size limits of the particle size distributions:

All observations with 0 abundance were excluded since it may be just an artefact of a small sample size.

The minimum size limit corresponded to the maximum relative abundance, following the same justification as Kooi and Koelmans.[6]

The maximum size limit for which the dataset is valid is determined by the size before which 0 abundances is observed.

The relative abundances for each size bin were then recalculated according to the newly defined size limits for that study based on the above criteria. For datasets which had more than 5 size class bins, the following power-law function was fitted to the PSDs (Figure S4.1):

$$y = Cx^{-\alpha} \qquad \text{for } x \in [x_0, x_1] \tag{S4.3}$$

where x is the particle size (µm), y is the relative abundance for each size, α is the power-law exponent and C is defined as a parameter depending on the limits of the distribution (min: x_0; max: x_1) and the power-law exponent:

$$C = \frac{1-\alpha}{x_1^{1-\alpha} - x_0^{1-\alpha}} \qquad \text{for } x \in [x_0, x_1]. \tag{S4.4}$$

Studies which demonstrated negative regressions for log y vs log x, weak regressions based on the adjusted R^2 (<0.6) and alpha values that were less than 1, were omitted. Secondary MPs are speculated to form as a result of fragmentation of larger particles. To conform to this theory, alpha values should be greater than 1 to explain that after fragmentation of a particle, it forms more than 1 particle.[223] The fitted parameters and regression statistics of 15 datasets from 12 studies are shown in Table S4.4.

SM4.1.5. Translation of gut to muscle MP concentrations in fish

It has been demonstrated that small MPs may likely be absorbed from the gut.[202] This absorption process may occur through several processes and may be unique for different species. To date, MP concentrations in the muscle and gut compartments of fish per unit body wet weight are available for seven fish species (Table S4.5).[224,225]

The muscle to gut concentration ratio ranges from 0.27 to 3.53. While Abbasi et al.[224] had ratios greater than 1 for 3 out of 4 species (i.e., indicating that there is higher MP concentrations in the muscle tissue than gut), the calculated ratios from Barboza et al.[225] were less than 1. This suggests that for some species, MPs are not easily absorbed and do not accumulate in the muscle tissue. Therefore, to account for these variations and physiological differences of other fish species, we captured the variability by implementing a normal distribution for the muscle (m) to gut (g) ratio (CF_{mg}) with mean of 1.28 ± 1.13 and the assumed MP concentrations in the muscle tissue are calculated as:

$$C_{PL}\left(\frac{\#MP}{gBWW} in\ muscle\ tissue\right) = CF_{mg} \cdot C_{PL}(\frac{\#MP}{gBWW} in\ stomach/gut) \quad \text{(S4.5)}$$

SM4.1.6. Goodness-of-fit analysis

To select the best probability density function (PDF) for the MP exposure from food and air, and the ingestion rates, the Kolmogorov-Smirnov test (KS-test) and Akaike's Information Criterion (AIC) were used simultaneously. The KS-test is generally used to check if a sample comes from a population with a specified distribution (null hypothesis). The null hypothesis is rejected if the *p*-value is less than the significance level (p<0.05).

The AIC is another statistical test which provides an index to compare between different fitted models. It considers the log-likelihood of the model fit (based on the standard maximum likelihood method) and the number of model parameters, penalizing when the model is overparameterized. The AIC score is calculated according to the formula:

$$AIC = -2 \cdot \log likelihood + k \cdot n_{par} \quad \text{(S4.6)}$$

where n_{par} represents the number of parameters in the fitted model and k=2 (scale parameter of the model) for the usual AIC.

The KS-test was performed for the distribution functions when fitted to the observed values and the *D* values and *p*-values are summarized in the data depository: Data S2. Several density functions were fitted to each dataset and the AIC values are compared between models to derive the optimal density function that fits the observations.

Selection of the best distribution function to describe the observations was based on a standard procedure. Firstly, models which showed insignificant *p*-values (p>0.05), were selected as this imply that the observations are similar to the specified distribution. The *D* test statistic was then used to narrow down the selection of the best function to describe the distribution. This was also done simultaneously with the evaluation of the AIC values to avoid complex distribution functions.

For the selection of the distribution function to describe MP concentrations in the media, the *p*-values could not be considered as the data was produced after an MC simulation which adjusted for the size realignment and was hence very large (n>50,000). It is well-discussed in literature that very large samples would produce statistically significant lack of fit as the KS-test is sensitive to detecting small deviations.[277,278] However, this does not imply that the specified distribution and the observations do not come from the same distribution. Therefore, to evaluate which model describes the dataset, the model with the lowest value of the *D* test statistic followed by the lowest AIC value, was selected. During the selection process, simple models were preferred over complex ones such as the bimodal distributions. Test statistics for MP concentration in air were omitted here as there were too little data to verify goodness of fit of the specified distribution.

SM4.1.7. Conversion of MP particle numbers to mass concentrations

To convert the calculated particle numbers of MP to mass, we first collected data on extrinsic properties of the particles such as size, shape and density. The approach for PSD was discussed in the earlier section SM4.1.4, where we defined two power-law exponents α_{food} and α_{air}. As for shape, we identified 49 studies containing 104 datasets for food and 3 studies for air that reported particle shape distributions. The collated dataset can be found in the data depository (Data S3). Five shape categories are defined for this study: (1) fragment, (2) filament/fibre, (3) spherules/pellets, (4) film/sheet, and (5) foam. When a study reports other shape categories or paint chips, we omitted them and recalculated the proportions. The overall average proportions of each shape category ($f_{shape,all}$) for all datasets were then determined by adding all the fractions from each dataset, *i* ($f_{shape,i}$) and dividing by the number of datasets for that category (*n*).

$$f_{shape,all} = \frac{\sum_{i=1}^{n} f_{shape,i}}{n} \quad \text{(S4.7)}$$

Distributions of the width:length (W:L) and height:length (H:L) were then determined following the method by Kooi and Koelmans,[6] where the lower and upper limits for width and height of each shape category were defined and triangular distributions were assumed. A Monte Carlo (MC) simulation of 1,000,000 iterations was performed to determine the overall respective distributions for food and air, and bimodal distribution functions were fitted using the 'mixtools' package[229] in R (Figure S4.2).

To obtain the polymer density distribution of the MPs found in the food and air, we collated 30 studies (i.e., 27 studies for food and 3 studies for air) which reported polymer types through spectroscopic identification (Data S4). We omitted polymer types that were not reported by more than two studies and natural polymers such as rayon and cellulose. In total,

there were 15 polymer types for food and 5 polymer types for air. The lower and upper limits of the densities for these polymer types[279–282] were defined with some assumptions:

- For polyacrylate we included: poly(2-cyanoenthyl acrylate), poly(acrylic acid), poly(butyl acrylate), poly(methyl acrylate). The -methacrylates were not included.[280]
- We applied the density range of polyamide (PA) to Nylon 6.
- Polystyrene acrylonitrile methyl methacrylate (Poly(styrene-co-methyl methacrylate) was assumed to have the same density as styrene methyl methacrylate, with a density ranging from 1.050 to 1.130.[282]
- For PE:PP co-polymer, only 1 density was found,[281] but since this polymer accounted for less than 0.1% of the total, this was deemed as acceptable.
- Density of PU obtained from *Prospector*.[283]

Similarly, the overall proportions of each polymer type were calculated for each media. Triangular distributions were assumed for each polymer type and MC simulation of 1,000,000 iterations was performed to determine the overall density distributions for food and air respectively, and fitted with 4-modal distributions with the 'mixtools' package in R.[229] The parameters of the fitted distribution functions for the shape characteristics and densities of MP in food and air are shown in Table S4.7.

The PDFs of the above MP characteristics were then simulated 10,000 times. The volume per MP particle was calculated assuming an ellipsoid shape (i.e., best 'one shape fits all' approximation for MP particles)[4]:

$$V_{el} = \frac{\pi}{6} \cdot (L) \cdot (W) \cdot (H) \quad \text{(S4.8)}$$

where L was estimated from the PSD, and W and H were estimated from the W:L and H:L ratio distributions respectively. The mass per MP particle was then calculated by multiplying the volume with the density values generated from the MC simulation. The distributions of the log-transformed mass per particle for food and air were fitted with mixture models using the 'mixtools' package in R (Figure S4.2 and Table S4.7) and evaluated with Kolmogorov-Smirnov tests (p=0.82 for food and p=0.83 for air).

The MP mass distributions in the gut were then calculated after the numerical solution of eq 4.1 with a two-step approach. Since the mass per particle distributions differ for food and air, we needed to distinguish how many particles came from each media. First, we simulated the MP number concentrations from dietary intake only. The MP number concentrations (food) were then converted to mass concentrations by multiplying with the mass per particle (food).

The same procedure was performed for intake through air only. The mass concentrations were then added up to provide the total MP mass. The MP mass distributions in the gut for child and adult for each scenario of biliary excretion rates are shown in Table S4.10.

SM4.2. Chemical Model

SM4.2.1. PBPK model with MERLIN Expo 3.0

Chemical intake data. There are no chemical intake data for 3,3',4,4',5-pentachlorobiphenyl (PCB126), lead, di(2-ethylhexyl)phthalate (DEHP) and benzo(a)pyrene (BaP) on a world population level. Therefore, we had to use data for specific regions or countries, assuming relevance on a global level. We acquired intake data from Llobet et al.[144] for PCB126 which represents the intake from foods in Catalonia Spain. The study reported that PCB126 contributed 50.56% to total toxic equivalent (TEQ) intake. We calculated the actual daily intake of PCB126 by multiplying the estimated WHO-TEQ intake per day with the fraction contributed by PCB126 and then divided by the WHO toxicity equivalent factor (TEF) for PCB126 (TEF=0.1). We did not distinguish between genders in the present study. Therefore, we also averaged over the genders for each age group.

Lead intake data of the Italian population was used in our PBPK simulation.[239] Since the data was reported as per kilogram body weight, we used polynomial least squares regression as described by Buonanno et al.[284] to estimate the average body weight of the Italian population and subsequently calculated the daily intake per person (averaged over the genders).

For DEHP, we used the dietary intake in the German population[236] and inhalation exposure was estimated from indoor[237] and outdoor[238] air concentrations by assuming time spent indoors:outdoors is 50:50. The body weights for children and adult of the German population[285,286] were obtained to convert the chemical intake per unit body weight to per capita.

Finally, the dietary and inhalation exposure of BaP[234,235] were based on data for the Korean population. As for the average body weight, no literature was available for the Korean population. Therefore, we had to estimate using the polynomial regression of body weight vs age which was reported for Chinese individuals.[287]

PBPK parameters. The PBPK parameters used for lead and PCB126 were already pre-set in MERLIN Expo.[230] We used the PBPK parameters as reported by Chiang et al.[288] for BaP and Gentry et al.[289] for DEHP. Except for DEHP, we simulated the ingestion of chemicals as a direct input in the liver. This is because the absorption rate constants of DEHP in the stomach lumen and gut lumen were defined.

SM4.2.2. Description of chemical leaching model

Calculation of parameters for biphasic transfer kinetic model. Ad- and desorption to microplastic can be adequately described using a two compartment model with separate compartments and kinetic parameters for slow and fast desorption[136] (eq. 4.5 and 4.6 in the main text). Based on Mohamed Nor and Koelmans,[136] the fast-desorption compartment of a thin film of MP with a thickness (t) of 30 µm comprised 32% of the total sorption reservoir (sum of slow and fast sorption compartments) across 14 PCBs (log K_{OW} ranging from 5.24 to 7.42). For such a film, the minimum diffusion path length of the fast-sorbing fraction (d_f) can be estimated as:

$$d_f = 0.32 \times 30 = 9.6\ \mu m \quad \text{(S4.9)}$$

Consequently, if the minimum dimension of the particle (d_{min}) is <9.6 µm, only fast sorption kinetics occur for that particle. However, if the minimum dimension exceeds 9.6 µm, the effective radius of the fast fraction (r_f) was set at a constant value of 4.8 µm and the slow-sorbing fraction is calculated as:

$$r_s = \frac{d_{min}}{2} - 4.8 \quad \text{(S4.10)}$$

The slow sorption kinetic rate constant, k_3 for the particle was then rescaled based on this effective radius of the slow-sorbing compartment (r_s) according to Fick's law of diffusion, using the average k_3 values from Mohamed Nor and Koelmans[136]:

$$k_3 = \frac{k_{3,lit} \times {r_{s,lit}}^2}{{r_s}^2} \quad \text{(S4.11)}$$

where $k_{3,lit}$ is 0.002 day^{-1} and $r_{s,lit}$ is 10.2 µm (t/2 –r_f).

The fast sorption kinetic rate constant, k_1 was based on the relationship with log K_{OW}[136]:

$$log k_1 = 0.86 \times log K_{OW} - 4.08 \quad \text{(S4.12)}$$

The desorption kinetic rate constant, k_2 was then estimated from the steady-state solution[136]:

$$k_2 = \frac{k_1}{K_P f_1 [P]} \quad \text{(S4.13)}$$

where K_p was estimated based on the relationship[136]:

$$\log K_P = 0.51 \times \log K_{OW} + 1.45 \quad \text{(S4.14)}$$

and f_1 can be estimated as:

$$f_1 = \begin{cases} r_f / (\frac{d_{min}}{2}), & d_{min} > 9.6\ \mu m \\ 1, & d_{min} \leq 9.6\ \mu m \end{cases} \quad \text{(S4.15)}$$

SM4.2.3. Chemical concentrations in plastic

Based on thermodynamic principles, chemical concentrations of the plastic ingested by seafood were assumed to be equivalent to the concentrations in their lipids. To some extent, this approach represents a worst case scenario because in reality, plastic has a somewhat lower fugacity than biota lipids.[26,45] Chemical concentration data in lipids of fish and molluscs/crustaceans were thus used as proxy concentrations in plastic. We categorized the seafood into two categories; organisms found in the pelagic zone (fish) and organisms found in the littoral zone (mollusc and crustaceans). In addition, since salt mainly comes from the sea, we assumed the concentrations for the pelagic zone also apply to MP in salt.

For the MPs found in air, we acquired concentration data on particulate matter (i.e., total suspended particulates, $PM_{2.5}$, PM_{10}) to use as proxies for the chemical concentrations on plastic. This is a fair representation as suspended MPs are part of particulate matter and equilibration between the various components of airborne particulate matter can be assumed.

Finally, as for the MPs in drinking water, beer and milk, we assumed that the chemical concentrations in the MPs are equivalent to that in the plastic packaging. This is partly because MP found in these media can be attributed to the packaging and also the manufacturing process.[107,248] While some chemicals are added as additives such as DEHP, plastic packaging can also contain residues from substances used during the manufacturing process (non-intentionally added substances). Therefore, it is not surprising that plastic packaging may contain traces of PCBs, PAHs and heavy metals such as lead.[187] An exception is for higher molecular weight PAHs such as BaP, which has not yet been detected in polymer packaging. Li et al.[290] suggested that this may be due to the more complex reaction pathway for such PAHs. Therefore, for BaP, we assumed that the concentration is negligible in the MPs from packaging.

The collected data used for this part of the study and other additional notes on assumptions are accessible in the data depository (Data S5). Fitted or assumed distribution functions for the chemical concentrations are also shown in Table S4.8.

Supplementary text

Comparison of particle characteristics between food and air

The mass per particle distribution in food is significantly different from that found in air (p<0.01; Kruskal-Wallis). MP particles found in air had a narrower mass distribution varying across 5 orders of magnitude while in food, the mass per particle ranged across more than 10 orders of magnitude. Our results also show that the shape distributions (defined by the height:length and width:length ratios; Figures S4.2A-D) differ for food and air. In the atmosphere, the particles mainly consisted of fibre, fragment and bead shapes which may be a result of textiles or wear-and-tear and UV-degradation of plastic products,[291] whereas for food, there was more variation in the particle shapes, including sheet and foam. Unlike the particles found in food which had 15 different polymer types, there were only 5 polymer types found in atmospheric suspension which are commonly used for textiles (Figures S4.2E and S4.2F). This verifies that the source of MP in the air is mainly textile-based.

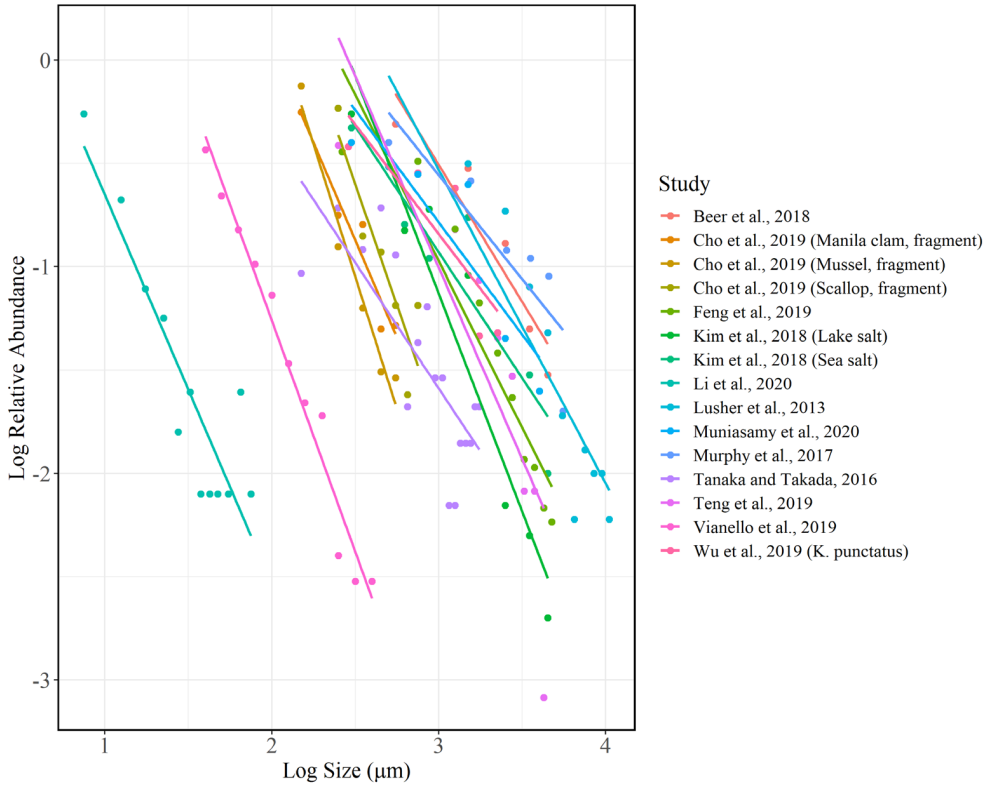

Figure S4.1. Relative abundance of microplastics vs particle sizes. The fitted trend lines $log(y) = -\alpha \cdot log(x) + C$ for each dataset are displayed.

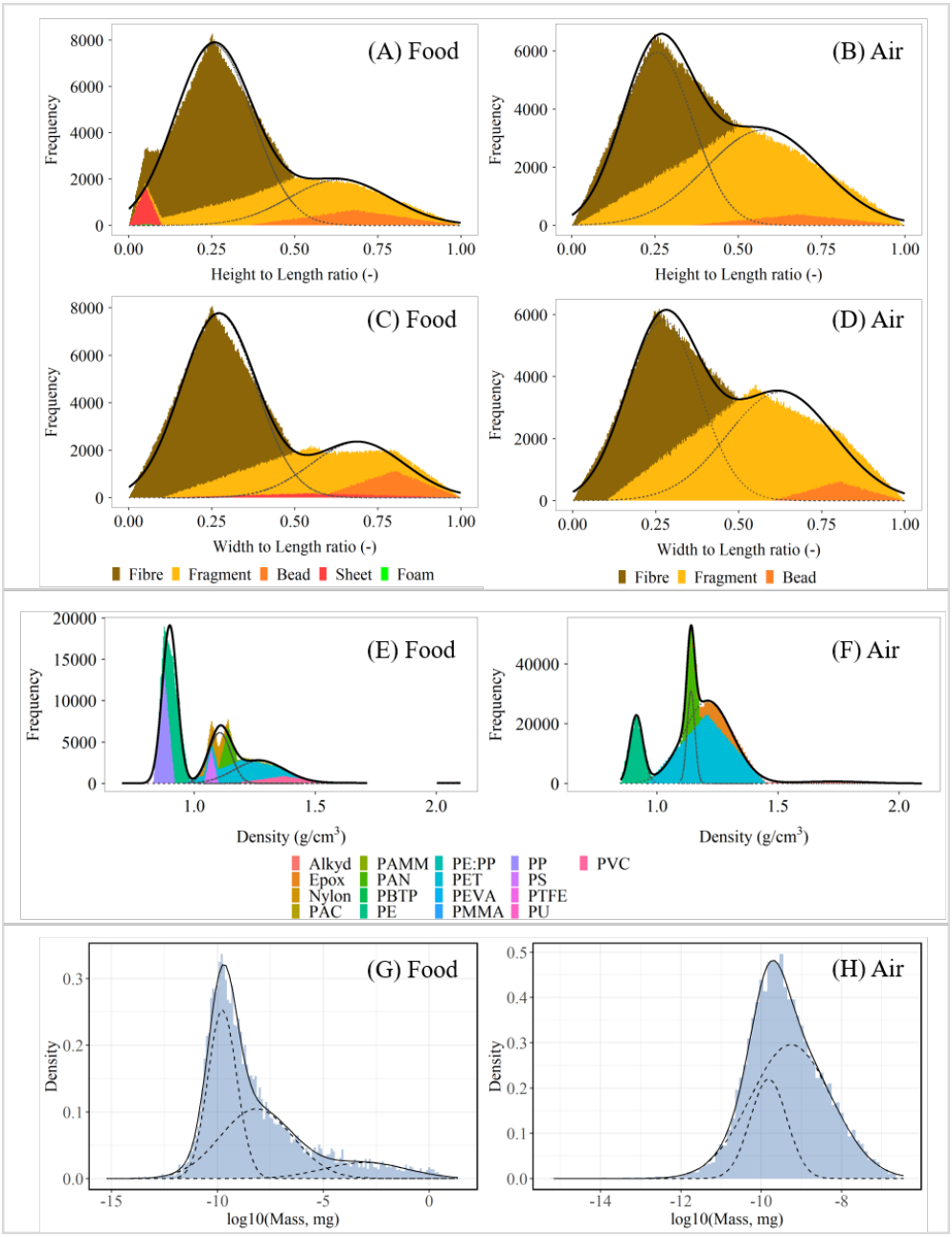

Figure S4.2. Distributions of particle characteristics from MC simulations (1,000,000 iterations). **(A)** and **(B)** Width to length ratios for food and air. **(C)** and **(D)** Height to length ratios for food and air. **(E)** and **(F)** Density for particles in food and air. **(G)** and **(H)** Mass per particle distributions for food (1-5000 µm) and air (1-10 µm).

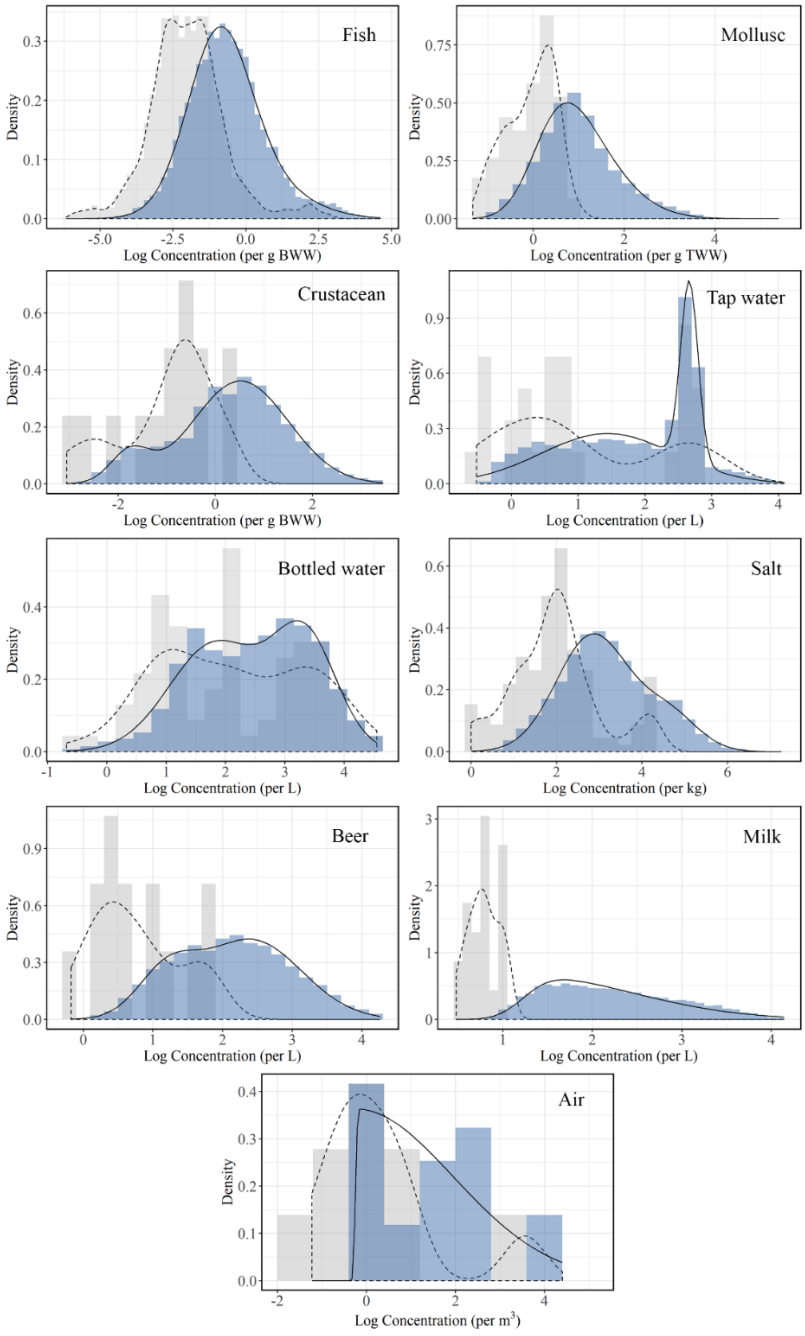

Figure S4.3. MP exposure number concentrations (logarithmic) in different media and fitted distributions (solid lines). Blue barfills are based on size realigned data (1-5000 µm for food and 1-10 µm for air). Grey barfills are based on the non-size realigned data with the density curve (dotted lines).

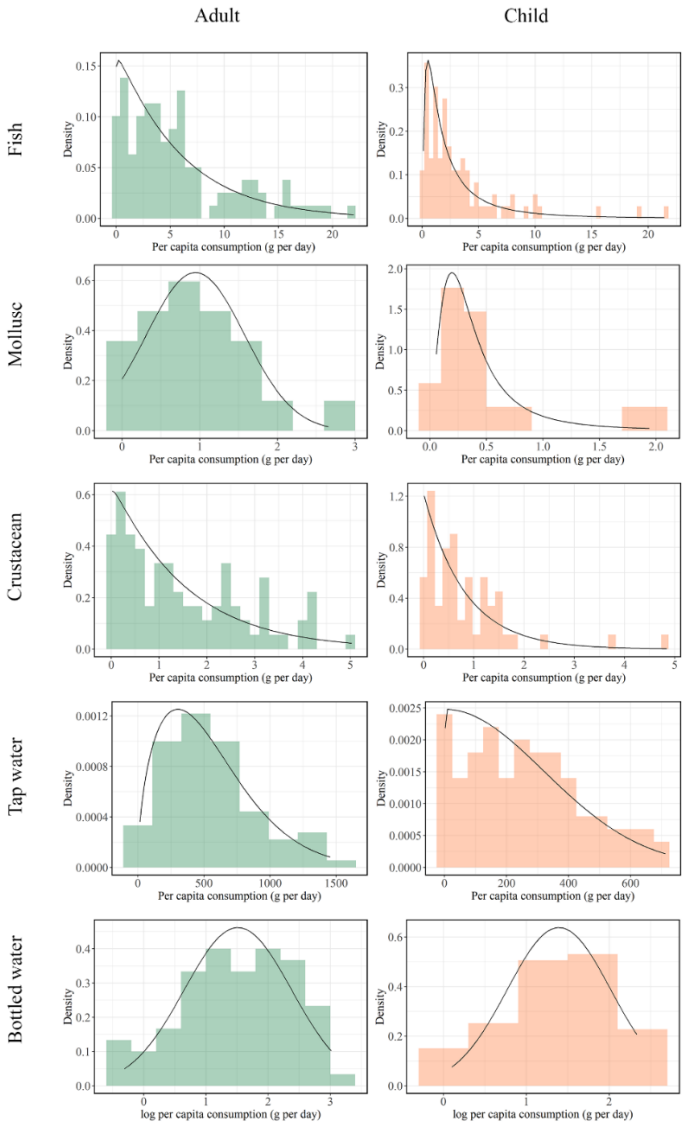

Figure S4.4. Ingestion rates of food and inhalation rates for adult (green) and child (orange). Ingestion rates for bottled water are on the logarithmic scale. Ingestion rates for beer only applies to adult (blue). The solid lines are the fitted distributions.

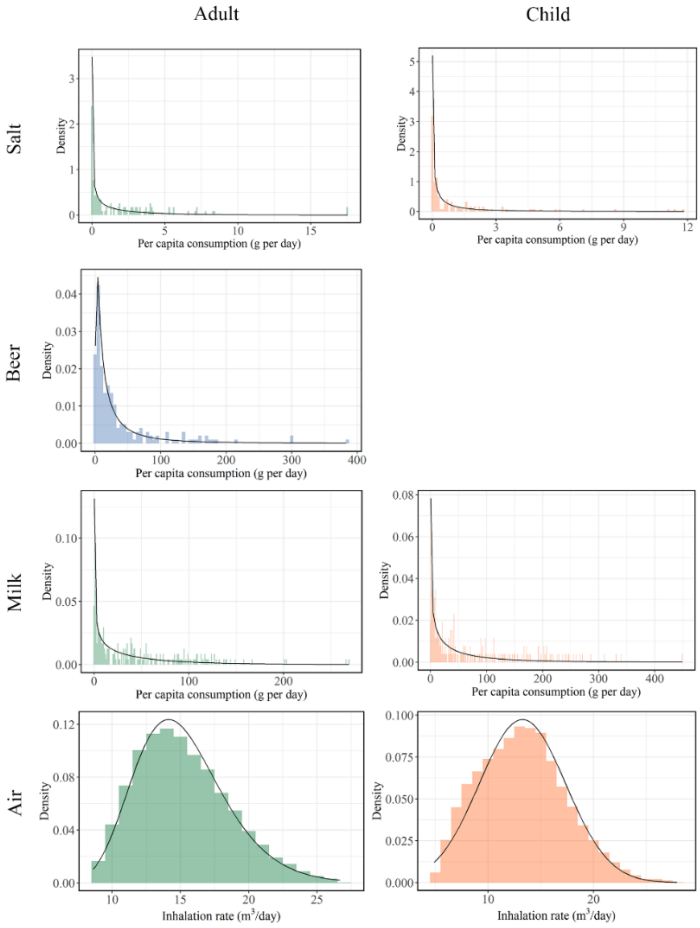

Figure S4.4. (*continued*)

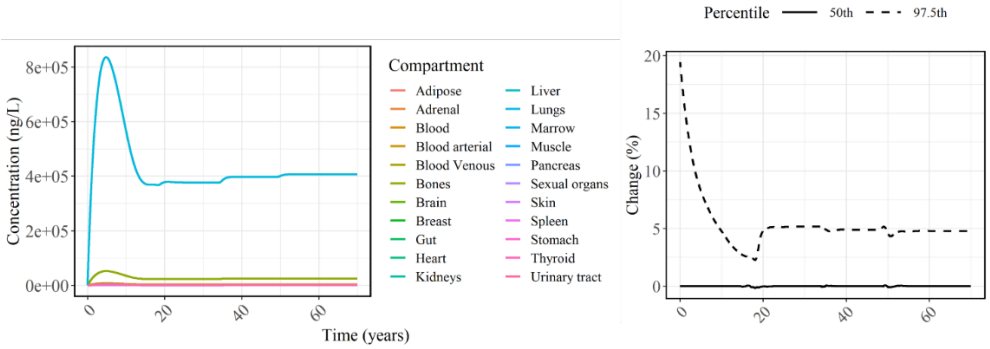

Figure S4.5. Chemical bioaccumulation of lead in different organs from dietary intake and inhalation in humans over 70 years with PBPK modelling in MERLIN Expo V3.0 (left). Percentage change of lead in adipose tissues as a result of additional chemical exposure via MP (right).

Table S4.1. Biliary excretion rates (k_{tis}) for human. The rate constants for rat and mouse from Ogawara et al.[206] and Li et al.[208] were rescaled for human with a correction factor of 2.5 which is based on the ratio from the biliary excretion rates of rat:human from Bachler et al.[207]

Material	Size (nm)	Route of exposure	Organism	k_{tis} (min^{-1})	Reference
Polystyrene	50	Intravenous	Rat	8.301	Ogawara et al. [206]
Polystyrene	500	Intravenous	Rat	8.001	Ogawara et al. [206]
Silver NP	15-150	Dermal, oral, inhalation	Human	5.098	Bachler et al. [207]
Poly(lactic-co-glycolic) acid	133.5	Intravenous	Mouse	0.0672	Li et al. [208]
Poly(lactic-co-glycolic) acid	114.8	Intravenous	Mouse	0.672	Li et al. [208]
Poly(lactic-co-glycolic) acid	97.4	Intravenous	Mouse	0.144	Li et al. [208]
Poly(lactic-co-glycolic) acid	79	Intravenous	Mouse	0.557	Li et al. [208]
Poly(lactic-co-glycolic) acid	67	Intravenous	Mouse	0.614	Li et al. [208]
Poly(lactic-co-glycolic) acid	57.5	Intravenous	Mouse	0.394	Li et al. [208]
			No excretion	0	day^{-1}
			Minimum	0.0672	day^{-1}
			Median	0.614	day^{-1}
			Maximum	8.30	day^{-1}

Table S4.2. Search terms/strings for each food type in FOSCOLLAB.

Food type	Search Strings
Fish	Fish (meat); Freshwater fish; Marine fish; Miscellaneous (misc.) coastal marine fishes; Misc. demersal marine fishes; Misc. freshwater fishes; Misc. pelagic marine fishes
Mollusc	Molluscs; Freshwater molluscs; Misc. marine molluscs
Crustacean	Crustaceans; Freshwater shrimps or prawns; Shrimps and prawns; Shrimps; common, White shrimp; Freshwater crayfishes
Tap Water	Tap water; Filtered tap water
Bottled Water	Bottled drinking water; Bottled water; Carbonated bottled drinking water; Flavoured bottled water; Fortified bottled water; Still bottled drinking water
Salt	Salt; Salt, flavoured; Salt, iodised; Salt, iodised and fluoridated; Salt, low Sodium; Sea salt
Beer	Beer; Beer and beer-like beverage; Ale beer; Lager beer; Beer, strong; Beer, regular; Beer, light; Beer, alcohol-free; Pale ale beer; Dark ale beer; Stout beer; Wheat beer; Beer-like beverages; Low malt beers
Milk	Milk; cow milk; cow milk, natural high fat; cow milk, semi skimmed (half fat); cow milk, skimmed (low fat); cow milk, whole

Table S4.3. Minimum and maximum inhalation rates defined for this study based on Allan and Richardson[221] and Stifelman.[220]

Age category	Min inhalation rate (m^3/day)	Max inhalation rate (m^3/day)
Toddlers (7 months–4 years)	4.9	16.1
Children (5 – 11 years)	8.8	23.3
Teenagers (12 – 19 years)	9.5	27.9
Adults (20 – 59 years)	9.7	26.7
Seniors (>60 years)	8.6	24.1

Table S4.4. Coefficients of fitted linear regressions of log (relative abundance) against log (size). *C* is the intercept and α is the slope of the regression. SE is the standard error of the parameters and model.

Study	*C*	SE	α	SE	R^2	Adj. R^2	SE
Food compartment							
Beer et al., 2018	3.47	0.91	1.33	0.28	0.89	0.85	0.2
Cho et al., 2019 (Manila clam fragment)	3.85	0.74	1.89	0.29	0.93	0.91	0.13
Cho et al., 2019 (Mussel fragment)	5.36	0.69	2.56	0.27	0.97	0.96	0.12
Cho et al., 2019 (Scallop fragment)	5.25	1.53	2.34	0.57	0.81	0.76	0.23
Feng et al., 2019	3.86	0.69	1.61	0.21	0.88	0.87	0.25
Kim et al., 2018 (Lake salt)	5.19	0.89	2.11	0.28	0.92	0.9	0.3
Kim et al., 2018 (Sea salt)	2.72	0.68	1.22	0.22	0.86	0.84	0.23
Lusher et al., 2013	4.02	0.85	1.52	0.23	0.82	0.8	0.3
Muniasamy et al., 2020	2.48	0.97	1.09	0.31	0.8	0.74	0.27
Murphy et al., 2017	2.47	1.00	1.01	0.29	0.74	0.68	0.25
Tanaka and Takada, 2016	2.06	0.69	1.22	0.24	0.63	0.61	0.29
Teng et al., 2019	4.55	1.41	1.85	0.43	0.72	0.68	0.49
Wu et al., 2019 (*K. punctatus*)	2.34	1.16	1.06	0.38	0.72	0.62	0.27
Air compartment							
Li et al., 2020 (Air)	1.24	0.42	1.89	0.28	0.82	0.8	0.28
Vianello et al., 2019 (Air)	3.22	0.27	2.24	0.13	0.97	0.97	0.13

Table S4.5. MP concentrations in muscle and gut per g BWW (body wet weight) and the ratio between muscle and gut concentrations (CF_{mg}). Data adapted from Abbasi et al.[224] and Barboza et al.[225]

Species	*N*	Total weight of *N* species (g)	MP conc in muscle (#/g BWW)	MP conc in gut (#/g BWW)	Ratio (muscle:gut)	Reference
Sillago sihama	17	972.4	0.055	0.015	3.533	Abbasi et al., 2018
Platycephalus indicus	12	441.6	0.109	0.057	1.921	Abbasi et al., 2018
Saurida tumbil	4	144.4	0.083	0.069	1.200	Abbasi et al., 2018
Cynoglossus abbreviatus	11	833.8	0.031	0.037	0.838	Abbasi et al., 2018
Dicentrarchus labrax	50	17150	0.001	0.004	0.269	Barboza et al., 2020
Trachurus trachurus	50	11400	0.003	0.004	0.673	Barboza et al., 2020
Scomber colias	50	17200	0.002	0.003	0.508	Barboza et al., 2020
				Average (±SD)	1.28 (±1.13)	
				Minimum	0.27	
				Maximum	3.53	

Table S4.6. Probability density functions for exposure parameters used to perform probabilistic exposure assessment to MPs through dietary and inhalation intake

Parameter	Variable	Distribution	Units	Parameters	Percentile[#]
Exposure media (logarithmic concentrations)					
Fish	Cf	Bimodal[§]	#/g BWW	μ1 = -0.94 σ1 = 1.06 λ1 = 0.71 μ2 = 0.09 σ2 = 1.69 λ2 = 0.29	50th = -0.73 95th = 1.79
Mollusc	Cm	Skew-t^	#/g TWW	x_i = 0.12 ω = 1.19 α = 2.03	50th = 0.91 95th = 2.63
Crustacean	Ccr	Bimodal[§]	#/g BWW	μ1 = -1.76 σ1 = 0.40 λ1 = 0.11 μ2 = 0.52 σ2 = 0.99 λ2 = 0.89	50th = 0.38 95th = 2.11
Tap water	Ctw	Bimodal[§]	#/L	μ1 = 1.44 σ1 = 0.99 λ1 = 0.68 μ2 = 2.66 σ2 = 0.13 λ2 = 0.32	50th = 2.10 95th = 3.02
Bottled water	Cbw	Bimodal[§]	#/L	μ1 = 1.83 σ1 = 0.78 λ1 = 0.59 μ2 = 3.34 σ2 = 0.53 λ2 = 0.41	50th = 2.53 95th = 3.97
Salt	Cs	Bimodal[§]	#/kg	μ1 = 2.84 σ1 = 0.85 λ1 = 0.80 μ2 = 4.62 σ2 = 0.68 λ2 = 0.20	50th = 3.11 95th = 5.08

Table S4.6. (*continued*)

Parameter	Variable	Distribution	Units	Parameters	Percentile[#]
Beer	Cb	Bimodal[§]	#/L	μ1=1.19 σ1=0.42 λ1=0.23 μ2=2.41 σ2=0.73 λ2=0.77	50th = 2.12 95th = 3.55
Milk	Cmk	Skew-normal[^]	#/L	x_i =1.23 ω = 1.22 α = 5.06	50th = 2.12 95th = 3.51
Air	Ca	Skew-normal[^]	#/m^3	x_i = -0.25 ω = 2.20 α = 67.8	50th = 1.56 95th = 4.28
Physiological data					
Ingestion rate, fish, adult	Irfadult	Weibull[*]	g/capita/day	k = 1.02 λ = 5.89	50th = 4.33 95th = 16.41
Ingestion rate, fish, child	Irfchild	Lognormal	g/capita/day	meanlog = 0.61 sdlog = 1.15	50th = 2.08 95th = 9.94
Ingestion rate, mollusc, adult	Irmadult	Normal	g/capita/day	μ = 0.945 σ = 0.632	50th = 0.86 95th = 1.85
Ingestion rate, mollusc, child	Irmchild	Log-log[‡]	g/capita/day	β = 2.014 α = 0.333	50th = 0.31 95th = 1.76
Ingestion rate, crustacean, adult	Ircadult	Weibull[*]	g/capita/day	k = 1.02 λ = 1.52	50th = 1.16 95th = 4.13
Ingestion rate, crustacean, child	Ircchild	Exponential[†]	g/capita/day	λ = 1.22	50th = 0.58 95th = 1.85
Ingestion rate, tapwater, adult	Irtwadult	Weibull[*]	g/capita/day	k = 1.54 λ = 598.8	50th = 502.1 95th = 1255.2
Ingestion rate, tapwater, child	Irtwchild	Skew-normal[^]	g/capita/day	x_i = 0.104 ω = 321.5 α = 183.4	50th = 241.5 95th = 619.7
Ingestion rate, botwater, adult (logarithmic)	Irbwadult	Normal	g/capita/day	μ =1.51 σ = 0.864	50th = 1.57 95th = 2.64

Table S4.6. (*continued*)

Parameter	Variable	Distribution	Units	Parameters	Percentile[#]
Ingestion rate, botwater, child (logarithmic)	Irbwchild	Normal	g/capita/day	μ = 1.39 σ = 0.626	50th = 1.41 95th = 2.28
Ingestion rate, salt, adult	Irsadult	Gamma[#]	g/capita/day	k = 0.429 θ = 0.217	50th = 0.57 95th = 7.25
Ingestion rate, salt, child	Irschild	Weibull[*]	g/capita/day	k = 0.526 λ = 0.660	50th = 0.24 95th = 5.69
Ingestion rate, beer	Irb	Lognormal	g/capita/day	meanlog = 2.71 sdlog = 1.49	50th = 16.6 95th = 161.7
Ingestion rate, milk, adult	Irmkadult	Gamma[#]	g/capita/day	k = 0.605 θ = 0.014	50th = 26.5 95th = 129.6
Ingestion rate, milk, child	Irmkchild	Weibull[*]	g/capita/day	k = 0.688 λ = 51.2	50th = 27.9 95th = 236.4
Inhalation rate, adult	InRadult	Lognormal	m^3/capita/day	meanlog = 2.70 sdlog = 0.22	50th = 14.8 95th = 21.6
Inhalation rate, child	InRchild	Normal	m^3/capita/day	μ = 13.23 σ = 4.07	50th = 13.1 95th = 20.4
Stool frequency, adult	$k_{loss,\ adult}$	Triangular	day^{-1}	min = 0.4 max = 3	
Stool frequency, child	$k_{loss,\ child}$	Triangular	day^{-1}	min = 0.8 max = 3	
Stool mass, adult	$M_{stool,\ adult}$	Triangular	g/capita/day	min = 51 max = 796	
Stool mass, child	$M_{stool,\ child}$	Triangular	g/capita/day	min = 51 max = 699	

[§]μ is the mean, σ is the standard deviation and λ is the probability of the bimodal distribution functions
[^]x_i is the location parameter, ω is the scale parameter, α is the shape parameter for skew-normal, skew-*t* and skew-cauchy distribution.
[*]*k* is the shape parameter and λ is the scale parameter for a Weibull distribution.
[#]*k* is the shape parameter and θ is the rate parameter for a gamma distribution.
[†]λ is the rate constant for an exponential distribution.
[‡]β is the shape parameter and α is the scale parameter for a log-logistic distribution.
BWW: Body wet weight
TWW: Tissue wet weight

Table S4.7. Parameters of fitted distributions for shape, density and mass of MP particles for number to mass concentrations conversion.

Media	Property	Fitted distribution	Probability	μ	σ
Food	Height:Length	Bimodal	0.749	0.255	0.116
			0.251	0.632	0.153
Food	Width:Length	Bimodal	0.728	0.271	0.113
			0.272	0.690	0.140
Air	Height:Length	Bimodal	0.528	0.256	0.107
			0.472	0.577	0.173
	Width:Length	Bimodal	0.533	0.272	0.110
			0.467	0.626	0.161
Food	Density	4-modal	0.031	1.687	0.564
			0.234	1.105	0.045
			0.237	1.268	0.104
			0.498	0.898	0.031
Air	Density	4-modal	0.024	1.726	0.144
			0.124	1.140	0.016
			0.151	0.915	0.027
			0.700	1.209	0.101
Food	Mass	3-modal	0.45	-8.17	1.71
			0.43	-9.77	0.68
			0.12	-3.04	1.96
Air	Mass	Bimodal	0.75	-9.26	1.01
			0.25	-9.82	0.45

Table S4.8. Probability density functions for chemical concentrations on plastic of each media category. Goodness-of-fit analysis was not carried out for these datasets due to low sample size. Distributions with the best fit were evaluated visually.

Chemical	Media category	Distribution	Units	Parameters
PCB126	Pelagic	Exponential†	ng/g lipid	λ=0.225
	Littoral	Exponential†	ng/g lipid	λ=17.48
	Packaging	Triangle	µg/kg	min=0 max=7.9
	Air	Log-logistic‡	pg/m^3	β=1.12 α=0.155
Lead	Pelagic	Lognormal	mg/kg ww	meanlog=-2.17 sdlog=2.12
	Littoral	Lognormal	mg/kg ww	meanlog=-1.78 sdlog=1.32
	Packaging	Lognormal	mg/kg	meanlog=4.00 sdlog=4.00
	Air	Lognormal	ng/m^3	meanlog=4.22 sdlog=1.88
DEHP	Pelagic	Lognormal	ng/g lipid	meanlog=8.83 sdlog=1.60
	Littoral	Triangle	ng/g lipid	min=0 max=5284
	Packaging	Log-logistic‡	µg/kg	β=0.59 α=89261.05
	Air	Log-logistic‡	pg/m^3	β=1.42 α=35594.55
BaP	Pelagic	Lognormal	ng/g lipid	meanlog=6.09 sdlog=3.55
	Littoral	Exponential	ng/g lipid†	λ=0.023
	Air	Log-logistic‡	pg/m^3	β=1.55 α=146.09

†λ is the rate constant for an exponential distribution.
‡β is the shape parameter and α is the scale parameter for a log-logistic distribution.

Table S4.9. Percentiles of MP number concentration in gut, tissue and stools for each scenario of biliary excretion. Scenarios: no biliary excretion (k_{tis} = 0 d^{-1}); minimum (k_{tis} = 0.067 d^{-1}), median (k_{tis} = 0.61 d^{-1}); maximum (k_{tis} = 8.30 d^{-1}).

Age category	Percentile (%)	Zero	Minimum	Median	Maximum
Concentration in gut (log #/capita); p<0.05 between children & adults (Kruskal-Wallis)					
Child	2.50	1.27	1.27	1.29	1.29
	5	1.42	1.43	1.44	1.44
	25	2.00	2.00	2.02	2.02
	50	2.48	2.48	2.50	2.50
	75	3.16	3.16	3.21	3.21
	95	4.77	4.78	4.93	4.93
	97.5	5.45	5.46	5.55	5.55
Adult	2.50	1.53	1.54	1.56	1.56
	5	1.70	1.70	1.71	1.71
	25	2.28	2.28	2.29	2.29
	50	2.74	2.74	2.74	2.74
	75	3.38	3.38	3.41	3.41
	95	4.93	4.93	5.05	5.05
	97.5	5.55	5.55	5.69	5.69
Concentration in tissue (log #/capita); p<0.05 between children & adults (Kruskal-Wallis)					
Child	2.50	2.72	0.12	-0.83	-1.96
	5	2.85	0.26	-0.68	-1.81
	25	3.42	0.83	-0.11	-1.24
	50	3.92	1.32	0.37	-0.76
	75	4.64	2.04	1.14	0.00
	95	6.28	3.68	2.86	1.73
	97.5	6.92	4.33	3.49	2.36
Adult	2.50	3.56	0.33	-0.63	-1.76
	5	3.72	0.48	-0.46	-1.59
	25	4.25	1.05	0.09	-1.04
	50	4.70	1.51	0.55	-0.58
	75	5.37	2.17	1.25	0.12
	95	6.97	3.75	2.92	1.79
	97.5	7.61	4.41	3.57	2.44

Table S4.9. *(continued)*

Age category	Percentile (%)	Zero	Minimum	Median	Maximum
Concentration in stool (#/g stool/capita); $p<0.05$ between children & adults (Kruskal-Wallis)					
Child	2.50	0.084	0.083	0.084	0.087
	5	0.124	0.124	0.128	0.127
	25	0.510	0.513	0.530	0.517
	50	1.657	1.634	1.715	1.731
	75	8.188	8.197	9.166	8.935
	95	328.56	343.5	479.4	482.0
	97.5	1578.3	1599.1	1935.6	2032.7
Adult	2.50	0.12	0.12	0.12	0.12
	5	0.17	0.18	0.18	0.18
	25	0.74	0.73	0.75	0.77
	50	2.31	2.36	2.38	2.39
	75	10.5	10.4	12.2	11.6
	95	372.1	363.0	490.7	487.2
	97.5	1617.3	1627.1	2140.2	2138.4

Table S4.10. Percentiles of MP mass concentration in gut and tissue for each scenario of biliary excretion. Scenarios: no biliary excretion (k_{tis} = 0 d^{-1}); minimum (k_{tis} = 0.067 d^{-1}), median (k_{tis} = 0.61 d^{-1}); maximum (k_{tis} = 8.30 d^{-1}).

Age category	Percentile (%)	Zero	Minimum	Median	Maximum
Concentration in gut (mg MP/capita); p<0.05 between children & adults (Kruskal-Wallis)					
Child	2.50	3.14E-09	3.13E-09	3.13E-09	3.13E-09
	5	6.38E-09	6.15E-09	6.44E-09	6.25E-09
	25	7.05E-08	7.31E-08	7.24E-08	7.11E-08
	50	8.05E-07	7.98E-07	8.77E-07	8.52E-07
	75	2.69E-05	2.72E-05	2.58E-05	2.88E-05
	95	3.12E-01	1.96E-01	1.86E-01	2.18E-01
	97.5	4.67	2.68	3.26	2.97
Adult	2.50	5.32E-09	5.67E-09	5.38E-09	5.25E-09
	5	9.76E-09	1.07E-08	1.11E-08	1.04E-08
	25	1.28E-07	1.26E-07	1.33E-07	1.34E-07
	50	1.42E-06	1.41E-06	1.55E-06	1.59E-06
	75	5.01E-05	4.64E-05	5.97E-05	4.89E-05
	95	5.79E-01	3.45E-01	4.62E-01	5.88E-01
	97.5	7.29	5.17	8.21	7.21
Concentration in tissue (mg MP/capita); p<0.05 between children & adults (Kruskal-Wallis)					
Child	2.50	6.21E-08	1.72E-10	1.85E-11	1.33E-12
	5	1.17E-07	3.07E-10	3.47E-11	2.65E-12
	25	9.99E-07	2.82E-09	3.15E-10	2.24E-11
	50	6.36E-06	1.73E-08	1.95E-09	1.43E-10
	75	5.05E-05	1.38E-07	1.55E-08	1.17E-09
	95	2.31E-03	5.55E-06	7.02E-07	5.41E-08
	97.5	8.87E-03	2.15E-05	3.70E-06	2.48E-07
Adult	2.50	4.47E-07	2.61E-10	2.69E-11	2.24E-12
	5	8.15E-07	4.66E-10	5.23E-11	4.16E-12
	25	7.08E-06	4.26E-09	4.71E-10	3.70E-11
	50	4.07E-05	2.53E-08	2.89E-09	2.22E-10
	75	2.82E-04	1.95E-07	2.32E-08	1.76E-09
	95	9.85E-03	6.22E-06	9.00E-07	6.89E-08
	97.5	4.81E-02	2.61E-05	3.62E-06	2.85E-07

Chapter 5

Synthesis

5.1. Objectives and main findings of the thesis

The main objective of this thesis was to improve our knowledge on the level of microplastic exposure to humans worldwide and the role of microplastic as a vector for chemical bioaccumulation. This objective has been divided into six sub-objectives that are formulated as:

- Objective 1: To investigate the chemical dynamics of hydrophobic organic chemicals (HOCs) with microplastics of different polymer matrix structure (glassy/rubbery) under simulated gut fluid conditions. **(Chapter 2)**
- Objective 2: To compare the sorption affinities of the HOCs with microplastics and other gut components such as micelles and food lipids to fully understand the chemical dynamics in the gut. **(Chapter 3)**
- Objective 3: To investigate the influence of food digestion on the chemical transfer kinetics in microplastics and thus overall chemical bioavailability to biota. **(Chapter 3)**
- Objective 4: To collate published data on prevalence of microplastics in intake media relevant for humans, and to analyse their distributions. **(Chapter 4)**
- Objective 5: To quantify the lifetime exposure of humans to microplastics from presently known sources of microplastics by age group (adult vs children). **(Chapter 4)**
- Objective 6: To assess the extent of microplastics contribution to overall chemical bioaccumulation in humans. **(Chapter 4)**

These objectives have been addressed in three scientific studies, presented in Chapters 2 to 4. First, the chemical dynamics of HOCs between microplastics and gut components was found to be biphasic and reversible in an in vitro gut fluid experiment **(Chapter 2)**. This was demonstrated in three exposure scenarios, which were relevant for microplastic-associated chemicals in biota. This finding led to the development and parameterization of a chemical exchange model, which became the basis of this thesis as it was used in the following chapters. Using the model, scenario studies could be performed to evaluate when microplastics act as a “carrier” or “cleaner” for a biota when ingested.

Following the establishment of an experimental method (in vitro gut fluid setup) and chemical exchange models to investigate the chemical dynamics of HOCs on microplastics in

the gut, a second study was performed wherein another aspect of environmental realism was added by mimicking a human gut with food digestion **(Chapter 3)**. In this chapter, it was demonstrated that microplastics can potentially trap HOCs from contaminated food as the food is digested. Since the microplastics absorb HOCs from the gut environment, this reduces the chemical bioavailability once they are egested. However, the role of this mechanism on total chemical exposure may remain limited. Furthermore, digestion rate kinetics was rate-limiting and did not influence the chemical transfer kinetics in the microplastics.

A major part of this thesis investigated the lifetime human exposure to microplastics and its associated chemicals. It included the first quantitative probabilistic exposure assessment and also a chemical model toolset to evaluate the role of microplastics as vectors for chemical bioaccumulation in humans. This thesis is the first to collate all microplastic studies relevant to human intake and provide novel methods to account for the non-alignment of methods and reporting units of microplastics studies. It also provided a distribution model that describes pathways for ingested and inhaled microplastics as it passes through the human gut. Based on 20% of the average human diet (presently known sources of microplastic), microplastics mass intakes are low relative to other types of anthropogenic inorganic particles. In the chemical model toolset, the previously established biphasic and reversible chemical model for microplastics **(Chapter 2)** was implemented in conjunction with a physiologically based pharmacokinetic model (PBPK) model to probabilistically evaluate the extent of the chemical contribution from microplastics under realistic feeding conditions. This thesis concluded that at presently known levels of microplastic intake, the contribution of microplastics to total chemical intake in humans is small to negligible.

In this synthesis chapter, a reflection on the application of in vitro gut fluid studies to investigate the microplastic vector effect (the chosen experimental method used for this thesis) is presented. Then, the weight of evidence for the microplastic vector effect is evaluated based on similar in vitro gut fluid studies. This includes some recommendations for future studies to be relevant in natural conditions. In the following subsection, different models that have been used to describe the chemical dynamics on microplastics in the gut, are discussed. Finally, an outlook on further model development for microplastic exposure in humans and applications in risk assessments is then discussed.

5.2. Reflections on in vitro gut fluid studies

In vitro gut fluid studies mimic gut conditions of organisms with surfactants which is the main component responsible for chemical solubilization. These surfactants aggregate to form micelles when it is above the critical micelle concentration,[62] which solubilizes HOCs which are sorbed in the intake media, for example food and microplastics. Some studies include

other non-micellar components such as proteins and lipids in the setups. An example of an in vitro gut fluid study is shown in Figure 5.1.

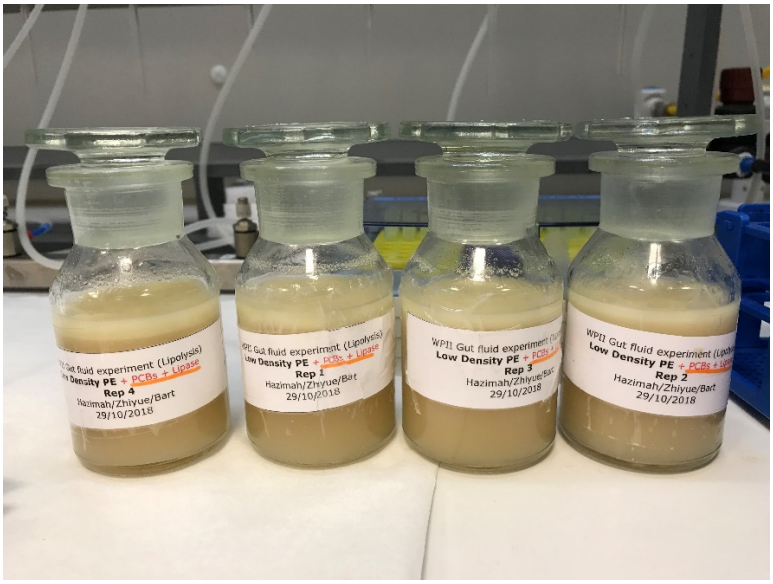

Figure 5.1. In vitro gut fluid setup using surfactants, proteins and the enzyme lipase from Chapter 3.

In vitro gut fluid studies are regarded as a more accurate method to investigate the detailed chemical exchange kinetics under different possible exposure scenarios when the microplastic particles pass through the gut. The level of control and accuracy of in vitro gut fluid studies are higher than whole organism studies since each individual has different digestive environments and health state. Most in vitro gut fluid studies investigating the microplastic vector effect measure the amount or percentage of chemicals solubilized in the gut fluid. This only reflects the chemical released or bioavailable from the microplastics in the scenario studied. Furthermore, it does not reflect the realistic natural conditions whereby other gut components may also be contaminated.

However, this thesis unraveled a more accurate way to understand the chemical vector effect of microplastics in the gut environment by measuring the chemical kinetic parameters in the microplastics itself and pairing it with an appropriate chemical dynamics model. Such an approach allows for the simulation of all possible scenarios and extrapolation to the actual environment.

5.3. Quality criteria and weight of evidence for chemical vector effect

Chemical transfer kinetics between plastic particles and gut fluids have been investigated in many in vitro studies, including those from this thesis (e.g., Teuten *et al.* (2007); Bakir, Rowland and Thompson (2014); Beckingham and Ghosh (2017); Lee et al. (2019); Martin and Turner (2019); Mohamed Nor and Koelmans (2019)). Besides the typical quality assurance (QA) criteria that apply to any study that needs the analysis of chemical concentrations on plastic, there are several criteria that need to be fulfilled in order to make a study relevant with respect to risks caused by the microplastic vector effect.

Chemical desorption kinetics in artificial gut fluids have been assessed in order to show the microplastic vector effect. Such studies should either use long term adsorption prior to desorption in order to not overestimate the desorption rates, or the level of non-equilibrium should be accounted for in the desorption kinetic parameter estimation.[136] The sorption process is a dynamic reversible process that needs to be accounted for in the experimental setups and data analysis. Kinetic modelling to acquire the rate constants may need to take mechanistic principles such as, intra-polymer diffusive mass transfer and/or bimodal behavior into account.[66,131,292,293] Kinetic parameters should be provided with significance levels and/or error estimates, preferably using multiple time points in the desorption curve and multiple replicates allowing for a rigorous estimation of parameter values.[136] Furthermore, besides exchange fluxes between microplastic and gut fluid, the fluxes from food should be assessed to assure that kinetic data is in the context of all relevant processes that govern the uptake and elimination of the chemicals of interest. Models have been developed that allow for such a context dependent evaluation using the kinetic parameters obtained from in vitro desorption studies.[25,26] Studies that account for all the aforementioned aspects would be most relevant for assessing the relevance of the microplastic vector effect in the context of chemical risks assessment.

Twenty in vitro studies reported on the chemical release kinetics from microplastic in the context of the chemical vector effect (Table 5.1). In general, most in vitro studies only reported the amount bioavailable or leached from plastic after exposure in the simulated gut fluid. These bioaccessibility percentages that are generally reported, are not relevant in nature as they also depend on external factors such as fugacities in other compartments, which would be different in nature. Exchange fluxes with other components in the gut, like food organic matter or micelles, are also usually neglected. Generally, analysis of experiment results with models that describe the experimental data are lacking. This limits the applicability of the findings as they cannot be extrapolated to the actual gut environment. All

studies except two **(Chapter 2 and 3)** had used a clean gut system, which is unrealistic. This may result in an overestimation of the amount leached from plastic. Only few studies relate experimental observations with the chemical and sorbent characteristics. Most studies did not provide error estimates or significance levels for their parameter estimations. Due to these limitations, 17 out of 20 studies were evaluated as inconclusive. The first study which provided conclusive evidence, demonstrated that the occurrence of a vector effect was context-dependent **(Chapter 2)**.[136] We showed that the boundary conditions (i.e., where either the microplastic or the food was initially contaminated, or both) determined whether transfer occurred and in which direction. Later on, Liu et al., 2020[169] also concluded that microplastic-associated pharmaceuticals posed low risks as the daily chemical intake from microplastics was significantly lower than the acceptable risk level. In **Chapter 3**, it was also shown that microplastics may not enhance the bioaccumulation of microplastic-associated chemicals in the human upper intestinal tract during food digestion. Microplastics instead reduce bioavailability of chemicals as food breaks down and releases chemicals in the gut fluid.

5.4. Sorption models to evaluate the chemical vector effect

Many models exist to describe sorption kinetics of chemicals to soils, sediments and other natural organic matter. Some of these models have been applied to analyze the sorption kinetics of microplastic-associated chemicals in the in vitro gut fluid studies reviewed in the previous section (Section 5.3). Models range from simple first order-rate kinetics to more complex diffusion models.[66,293] As the saying goes, "Models are lies, but they make us tell the truth", some of these sorption models lack the complexities, which are present in reality but may still be good enough to provide a useful approximation to reality. A model should be as simple as possible and not overparameterized. Overparameterization of a model would yield less meaningful and significant parameters. There are two common approaches in fitting models to the chemical dynamic data from in vitro studies. The first approach is by fitting a sorption kinetic model to the chemical concentration in the microplastic over time. The other approach is to fit a model to describe the chemical concentration in the gut fluid over time. Both would explain the mechanisms in the microplastic; the former approach being more direct, while the latter approach is indirect. An overview of the sorption kinetic models which have been applied so far in in vitro gut fluid studies to evaluate the chemical vector effect of microplastics is provided here (Table 5.2).

Table 5.1. Overview of laboratory in vitro studies supporting the role of microplastic (MP) ingestion by organisms on bioaccumulation of plastic associated chemicals. General approach, type of evidence, and environmental realism are summarized.

Study	Demonstrated	Inconclusive	Not supported	Comments
Teuten et al., 2007[52]		X		Compared desorption rates of sorbed phenanthrene from plastic and sediment in seawater and sodium taurocholate that simulated the gut fluid of *Arenicola marina*. Model analysis was limited to pseudo first order rate analysis to determine initial desorption. Considered theoretical calculations using equilibrium partitioning method with different compartments to understand their respective relative contributions. This analysis overestimated the amount bioaccessible to benthic organisms as the environment was more dynamic and it also neglected other pathways.
Bakir et al., 2014[53]		X		Investigated the desorption rates of chemicals from PVC and PE under simulated gut conditions. Model analysis was limited as only first order rate kinetics was considered, neglecting backward sorption and bimodal behaviour. Chemicals were sorbed for a short time but non-equilibrium desorption kinetics were not considered. Assessment with maximum concentration gradient is not relevant in nature. Other pathways in the gut were neglected.
Turner and Lau, 2016[294]		X		Evaluated bioaccessibility of elements indicative of halogenated flame retardants in a simulated digestion fluid of seabirds. Model analysis was limited and obtained rate constants using a diffusion-controlled and parabolic model. Assessment with maximum concentration gradient is not relevant in nature. Evaluation of the results in the context of the actual environment was based on total percentage leached from plastic which may be less relevant as the gut of the seabirds are already contaminated from other sources.

Beckingham and Ghosh, 2017[54]		X		Compared gut fluid solubilization between polypropylene and other natural and anthropogenic organic particles. Model limited and data was analyzed assuming equilibrium was reached for all congeners in system after 4h. Maximum concentration gradient between contaminated particles and gut fluid is not environmentally relevant.
Massos and Turner, 2017[260]		X		Evaluated bioaccessibility of Cd, Pb and Br from beached microplastics in a physiologically-based extraction test. Considered only percentage bioaccessible (over total available in the plastic) that does not reflect what happens in nature as the results are only applicable for the case when the organism do not have any accumulated elements. Compared bioaccessibility of the elements from plastic against dietary concentrations and did not consider that the bioaccessible percentages may change in the presence of food.
Turner, 2018[133]		X		Evaluated bioaccessibility of hazardous elements in simulated digestion fluid of northern fulmar. Model analysis was limited and did not consider accounting for individual exchange fluxes as it uses the pseudo first order diffusion model. Did not consider the scenario in which the elements have bioaccumulated in the fulmar. Maximum concentration gradients and evaluation of bioaccessibility percentage based on maximum leached (equilibrium concentrations) as in the experiment, are not relevant in nature.
Lee et al., 2019[131]		X		Evaluated relevance of ingested microplastics to overall transfer of chemicals into fish using simulated intestinal fluid and model analysis. Model analysis did not include error estimates and did not reflect experimental results as it was not calibrated. Did not evaluate the results in the context of the actual environment.
Coffin et al., 2019[128]		X		Evaluated leaching of plastic-additives from commonly ingested plastic items in gut mimic models for fish and seabirds. Used virgin plastic items, maximizing the concentration gradient between plastic and gut fluid, which is not relevant in nature. Single timepoint statistical analysis of the concentration leaching out from plastic and its effects on estrogenicity only

				reflects the vector effect under such experimental conditions and did not evaluate results in the context of other relevant processes.
Guo et al., 2019[129]		X		Investigated leaching of flame retardants from acrylonitrile-butadiene-styrene (ABS) in simulated avian digestive systems and the effect of co-ingesting sediment. Did not consider further evaluation of results with models or calculations with chemical characteristics (K_{OW}). Results indicated chemicals transferred from plastic to sediment. However, study did not consider sorption capacities of the components in the system and its exchange fluxes.
Martin and Turner, 2019[132]		X		Evaluated the mobilization of cadmium under simulated digestive conditions over 6h. Model was limited and did not consider the other phases and exchange fluxes. Applicability of the rate constants obtained by fitting a second order diffusion model to the experimental data was not discussed. Evaluation of environmental implication is not relevant in nature as there is no clean sediment in nature. Sediment used in experiment was collected from a protected and unpolluted location which is not representative of other areas.
Mohamed Nor and Koelmans, 2019[a,136]			X	Evaluated chemicals exchange of PCBs in gut fluid mimic systems considering different scenarios representing different fugacity levels between plastic and organism. Considered all exchange fluxes in the system and bimodal behaviour in model analysis, showing error estimates for parameters. Considered exchange fluxes with other components in the gut such as food. Discussed bioavailability from ingested plastic to organisms under different scenarios.
Heinrich and Braunbeck, 2020[130]		X		Studied the effect of PE MP addition to RTL-W1 cells dosed with 7-ethoxyresorufin-O-deethylase (EROD) inducers by addition. The addition of MP reduced EROD activity. The authors concluded that the presence of MP can reduce the amount of bioavailable pollutants *in situ* ('cleaning' effect), but that it remains unclear to what extent this mechanism occurs under natural conditions.

Godoy et al., 2020[137]		X		Investigated the percentage bioaccessibility and bioavailability of Cr and Pb from polyethylene and polypropylene MPs in the presence of skimmed milk by using a dynamic in vitro simulator of the human gastrointestinal tract. Results are only applicable for the scenario studied and may not reflect reality whereby the gut has accumulated metals from other pathways. Considered the presence of food but metal concentrations in the milk were not analysed.
Liao and Yang, 2020[139]		X		Estimated the oral bioaccessibilities of sorbed Cr on MPs in a whole human simulated digestive system for five polymer types after each digestive phase. An extreme case scenario with maximum concentration gradient was simulated with MPs which were pre-exposed to the maximum contaminant level for total Cr in drinking water. Exchange fluxes from food and the gut itself were not considered. Evaluation of results in the context of human health risk assessment may not be relevant since it is based on total percentage released from MPs in an empty and uncontaminated gut.
Liu et al., 2020a[169]			X	Assessed the desorption mechanisms of atorvastatin and amlodipine from pristine and aged polystyrene MPs under simulated gastric and intestinal conditions of marine organisms at two temperatures to mimic cold- and warm-blooded organisms. Desorption kinetics fitted with first-order two-compartment kinetic model, with error estimates. Estimated bioaccessibilities in different gut compartments under different gut conditions. Compared daily chemical intake from MPs with acceptable risk levels and concluded that MP-associated pharmaceuticals posed low risks.
Liu et al., 2020b[138]		X		Assessed bioaccessibilities of pyrene and 4-nonylphenol for 18 MPs of different polymer types and degrees of aging with an in vitro human digestive model. A neural network and sensitivity analysis was performed to determine the contribution of each MP property to the chemical bioaccessibility. Analysed reversibility of the sorption process by calculating the hysteresis index. Maximum concentrations gradients in the gut were considered which is not realistic in nature.

Shan et al., 2020[135]		X		Investigated the sorption and desorption behaviours of crude oil on PE MPs in simulated fish intestinal tract. Determined the rate limiting steps and mechanisms of oil sorption on PE MPs by fitting sorption kinetics data with three nonlinear sorption models and sorption isotherms with three isotherm models. Did not consider other chemical uptake pathways and maximum concentration gradients were not environmentally realistic.
Wu et al., 2020[295]		X		Evaluated desorption kinetics of BPA from PVC MPs in simulated intestinal fluids. A first order model with three stages of desorption was fitted to describe the desorption kinetics of BPA from PVC MPs. Analysed reversibility of the sorption process by calculating the hysteresis index. Bioaccessibilities were reported but do not reflect environmental realism since the study assumed that the gut environment is clean and there are no other intake media for BPA.
Fan et al., 2021[296]		X		Assessed the adsorption/desorption behaviours of tetracycline and ciprofloxacin by pristine and aged polylactic acid and polyvinyl chloride in simulated intestinal fluid. Analysis of data was limited to amount desorbed and percentage desorption rate, which are not relevant in nature. Did not consider further evaluation of results with models and other chemical pathways in the intestine.
Mohamed Nor et al., 2021[b]			X	Evaluated the effects of food digestion on chemical exchange kinetics of PCBs on microplastics with an in vitro model of the human upper intestinal tract. Both food and MPs were contaminated in the system, emulating an environmentally realistic scenario. A multi-compartment model describing the food digestion kinetic and sorption process in MPs was developed to analyse the transfer kinetics of chemicals.

[a] Study written as Chapter 2 in this thesis.
[b] Study written as Chapter 3 in this thesis.

Table 5.2. Sorption kinetic models used in in vitro gut fluid studies.

Sorption kinetic models	Mathematical equation	References
Pseudo first-order rate[a]	$ln\frac{q_t}{q_e} = -kt$	52,53,135
Pseudo second-order[b]	$\frac{t}{q_t} = \frac{1}{k_2 {q_e}^2} + \frac{t}{q_e}$	135
Intraparticle diffusion[c]	$q_t = K_{ip} t^{1/2} + C$	135
First-order two-compartment irreversible desorption[d]	$\frac{q_t}{q_0} = F_{fast} \cdot e^{-k_{fast} t} + F_{slow} \cdot e^{-k_{slow} t}$	169
First order two-compartment reversible sorption[e]	$\frac{d{C_1}^*}{dt} = \frac{k_1}{f_1[P]} C_W - k_2 {C_1}^* - k_3 {C_1}^* + k_3 {C_2}^*$ $\frac{d{C_2}^*}{dt} = k_3 {C_1}^* - k_3 {C_2}^*$	136

q_t is the amount of chemical sorbed at time t. q_e is the amount of chemical sorbed at equilibrium. q_e is the amount of chemical sorbed at time 0h.

[a] k is the first order rate constant.

[b] k_2 is the second order rate constant.

[c] K_{ip} is the internal diffusion rate constant. C is a constant related to liquid film thickness and boundary layer.

[d] F_{fast} and F_{slow} are the fractions of chemicals in the fast and slow desorption compartments. k_{fast} and k_{slow} are the rate constants in the fast and slow desorption compartments.

[e] Refer to Chapter 2 for the explanation of the parameters.

The pseudo first-order kinetic model principally describes a second-order reaction that is approximated to be first order due to the large excess of one of the components involved. In the case for the occurrence of microplastics in the simulated gut fluid, the microplastic sorbent is in large excess and therefore its sorption domains do not change as sorption proceeds. All of the studies which have applied the pseudo first-order kinetic model to their chemical dynamic data, simulated the scenario whereby contaminated microplastics reside in a clean gut environment.[52,53,135] Due to the maximum concentration gradient, the studies assumed that the chemical transfer only occurred in one direction; from polymer to gut fluid. In reality, sorption of most hydrophobic organic chemicals are reversible because it is mainly driven by the transfer across the aqueous boundary layer and intrapolymer diffusion; both processes are dynamic and reversible.[29] Therefore, these studies have neglected the reversibility of the sorption process and may be underestimating the transfer kinetic parameters. Similarly, the pseudo second-order sorption can either describe the transfer of the chemical molecule across the aqueous boundary layer or the intraparticle diffusion of the molecule through the pores of the polymer.[297] It also neglects the reversibility of the sorption process of the chemical molecules in the polymer. On the other hand, the intraparticle

diffusion model quantifies an additional parameter, which is the thickness/radius of the film/sphere particle.

The last two models in Table 5.2 both describe that sorption occurs in two phases in the sorbent: a fast and a slow compartment. Both studies that had applied the biphasic models observed a rapid sorption process followed by a slow sorption process in the chemical dynamics of the microplastics.[136,169] In the first-order two compartment model used by Liu et al., 2020,[169] only a unidirectional transfer was described and hence, neglecting the reversibility of the sorption process. On the other hand, the other first-order two compartment model that this thesis has presented in **Chapter 2**,[136] accounts for an apparent biphasic sorption behavior in the experimental data and reversibility. Furthermore, it can be implemented in the context of any system since the model is parameterized by also considering the other components in the simulated gut fluid system if their kinetic parameters or distribution coefficients are known. An example of how this can be performed is demonstrated in **Chapter 3**, where the model was used in conjunction with a food digestion kinetic model. The applicability of the biphasic reversible model was also demonstrated in **Chapter 4** to simulate the scenario of microplastic-associated chemicals as it passes through the human gut which is also "contaminated" due to chemical bioaccumulation from other pathways. Since the model contains both the sorption and desorption kinetic parameters, the net transfer of chemicals in any scenario can be predicted given the concentrations in each compartment of the gut. Therefore, as demonstrated by the results of the chemical model in **Chapter 4**, the microplastic chemical vector effect can either be positive (increasing chemical bioavailability) or negative (decreasing chemical bioavailability).

The selection of an appropriate model should be based on good fits with the experimental data and not be too simple or complex so that they are much easier to apply in larger modelling frameworks. Although simple models are preferred by many authors, it should be noted that the models should still have good fits with their experimental data.[53] This is to ensure that they actually prove their accuracy and reliability for understanding the sorption kinetics.

5.5. Conclusion and outlook on further model development for risk assessment frameworks

This thesis has developed two biphasic reversible models for microplastic-associated chemicals, which fitted well to the empirical observations for a range of PCBs in low density polyethylene (LDPE) and polyvinyl chloride (PVC) from two in vitro gut fluid studies. Many studies investigating sorption kinetics for microplastic-associated chemicals fitted their data with models that do not describe the sorption behavior well. One example that was discussed

in **Chapter 2** is that from Bakir et al., 2014.[53] An irreversible, desorption-only one compartment first order rate kinetics model was fitted to the experimental data, which, on the contrary, suggested a biphasic sorption behavior. Furthermore, the study had neglected reversibility in the sorption of chemicals on microplastic. Reversibility of the sorption process has been confirmed in two chapters from this thesis **(Chapters 2 and 3)**. The sorption parameter, k_1, was statistically significant for most of the datasets. Therefore, including this rate parameter did not result in overparameterization of the model and is actually crucial.

Additionally, the models have considered contaminated food as one of the compartments in the in vitro gut fluid experiments; a pathway that has been largely neglected by other in vitro gut fluid studies on microplastic-associated chemicals. To date, the percentage of chemical bioavailable from microplastics predicted by many studies may not be relevant in nature as these studies have only considered one chemical uptake pathway (via microplastics) and maximum chemical gradient in the gut fluid (Table 5.2). This thesis has addressed this concern by performing scenario studies and including other chemical intake pathways in all of its main chapters **(Chapters 2 to 4)**. Findings also show that the sorption kinetics may be dependent on the facilitated transfer by other components in the gut such as organic matter **(Chapter 2)** and food lipids **(Chapter 3)** across the aqueous boundary layer surrounding the microplastic. These components may reduce the thickness of the aqueous boundary layer and hence increase the sorption rate kinetics.

Static in vitro gut fluid experimental setups were preferred and implemented in **Chapters 2 and 3**, where the focus had been mainly on the upper intestinal tract since micelles formed in this section is the main compartment responsible for the solubilization of chemicals. Food digestion kinetics had also been included in **Chapter 3**, which showed that microplastics can take up more chemicals and reduce chemical bioavailability during food digestion. In **Chapter 4**, intestinal uptake of the chemicals into the human body was also accounted for via PBPK modeling in MERLIN Expo V4.0.

Overall, evidence from this thesis indicates that the microplastic vector effect may have a small to negligible contribution to total chemical intake in humans, based on presently known microplastic intakes **(Chapter 4)**. However, current microplastic occurrence data only comprise 20% of an average human diet. Furthermore, to date, data on the mixture of chemicals and actual concentrations in plastic or microplastics present in intake media are unknown. The vector effect may be relevant when chemical concentrations occurring in the microplastic are higher than other intake media (absorption from food or air) or when there is more knowledge on the microplastic concentrations from the other as yet unknown 80% of the diet. Nevertheless, the presented models in **Chapter 4** still represent an adequate toolset to address new scenarios and other chemicals.

In the earlier microplastic exposure studies in humans, Cox et al., 2019[14] and Zhang et al., 2020[15] have provided single exposure estimates compiled from different intake media based on average values. These studies also did not consider data incomparability and the full microplastic continuum. The above limitations result in less accurate representations of the actual microplastic exposure to humans globally. **Chapter 4** takes these factors into consideration by providing a probabilistic microplastic exposure assessment for children and adults, which accounts for the full microplastic continuum (1–5000 µm) across different intake media and the variabilities in intake rates globally.

This thesis had also probabilistically estimated the amount of microplastic accumulated in the body and amount egested in **Chapter 4** through a simple gut passage and absorption model based on the best available information to date. However, there are still some uncertainties in the plastic model parameters such as the size fraction of the particle that can translocate across the intestinal membrane, and the percentage that is actually being absorbed. These uncertainties are due to the lack of experimental data available for the translocation of microplastic particles with different shapes and sizes across the intestinal wall. Furthermore, in the aforementioned study, we had assumed the body as a homogenous component. This is because the transport of microplastic particles in the body and the distribution among organs are still unknown to this date. Therefore, further studies on the translocation of microplastics across membranes and distribution among organs are warranted. This can lead to improved parameterization of future models, which also need to be validated with more experimental data such as from post-mortem studies.

The lifetime human exposure model for microplastics presented in **Chapter 4** estimates microplastic exposure, accumulation over a lifetime, and the chemical vector effect due to microplastic intake. Such a model can be used in the future to further develop risk assessment frameworks, which can provide advice to expert panels on whether microplastic exposures surpass toxicity thresholds in humans (particle and chemical toxicity) and which microplastic sources need to be addressed to reduce exposure levels. In this thesis, we had used the biphasic reversible model **(Chapter 2)** in the chemical model as a separate component. In reality, the chemical dynamics occur concurrently and future work should integrate the biphasic reversible chemical exchange model for microplastics in a PBPK model to obtain a more accurate estimate of the amount of chemicals accumulated from all intake pathways.

References

(1) Thompson, R. C.; Olsen, Y.; Mitchell, R. P.; Davis, A.; Rowland, S. J.; John, A. W. G.; McGonigle, D.; Russell, A. E. Lost at Sea: Where Is All the Plastic? *Science (80-.).* **2004**, *304* (5672), 838.

(2) SAPEA. A Scientific Perspective on Microplastics in Nature and Society | SAPEA. *Evid. Rev. Rep.* **2019**. https://doi.org/10.26356/microplastics.

(3) World Health Organization. Microplastics in Drinking-Water. **2019**. https://doi.org/ISBN: 978-92-4-151619-8.

(4) Koelmans, A. A.; Redondo-Hasselerharm, P. E.; Mohamed Nor, N. H.; Kooi, M. Solving the Non-Alignment of Methods and Approaches Used in Microplastic Research to Consistently Characterize Risk. *Environ. Sci. Technol.* **2020**, *54* (19), 12307–12315. https://doi.org/https://doi.org/10.1021/acs.est.0c02982.

(5) Zhang, K.; Hamidian, A. H.; Tubić, A.; Zhang, Y.; Fang, J. K. H.; Wu, C.; Lam, P. K. S. Understanding Plastic Degradation and Microplastic Formation in the Environment: A Review. *Environ. Pollut.* **2021**, *274*, 116554. https://doi.org/https://doi.org/10.1016/j.envpol.2021.116554.

(6) Kooi, M.; Koelmans, A. A. Simplifying Microplastic via Continuous Probability Distributions for Size, Shape,and Density. *Environ. Sci. Technol. Lett.* **2019**. https://doi.org/10.1021/acs.estlett.9b00379.

(7) Hermsen, E.; Mintenig, S.; Besseling, E.; Koelmans, A. A. Quality Criteria for the Analysis of Microplastic in Biota Samples. Critical Review. *Environ. Sci. Technol.* **2018**. https://doi.org/10.1021/acs.est.8b01611.

(8) Lambert, S.; Wagner, M. Microplastics Are Contaminants of Emerging Concern in Freshwater Environments: An Overview. In *Handbook of Environmental Chemistry*; 2018; Vol. 58, pp 1–23. https://doi.org/10.1007/978-3-319-61615-5_1.

(9) de Souza Machado, A. A.; Kloas, W.; Zarfl, C.; Hempel, S.; Rillig, M. C. Microplastics as an Emerging Threat to Terrestrial Ecosystems. *Glob. Chang. Biol.* **2018**, *24* (4). https://doi.org/10.1111/gcb.14020.

(10) Smith, M.; Love, D. C.; Rochman, C. M.; Neff, R. A. Microplastics in Seafood and the Implications for Human Health. **2018**, 375–386.

(11) Koelmans, A. A.; Mohamed Nor, N. H.; Hermsen, E.; Kooi, M.; Mintenig, S. M.; De France, J. Microplastics in Freshwaters and Drinking Water: Critical Review and Assessment of Data Quality. *Water Res.* **2019**, *155*. https://doi.org/10.1016/j.watres.2019.02.054.

(12) Gasperi, J.; Wright, S. L.; Dris, R.; Collard, F.; Mandin, C.; Guerrouache, M.; Langlois, V.; Kelly, F. J.; Tassin, B. Microplastics in Air: Are We Breathing It In? *Curr. Opin. Environ. Sci. Heal.* **2018**. https://doi.org/10.1016/j.coesh.2017.10.002.

(13) Schwabl, P.; Koppel, S.; Konigshofer, P.; Bucsics, T.; Trauner, M.; Reiberger, T.; Liebmann, B. Detection of Various Microplastics in Human Stool: A Prospective Case Series. *Ann. Intern. Med.* **2019**. https://doi.org/10.7326/M19-0618.

(14) Cox, K. D.; Covernton, G. A.; Davies, H. L.; Dower, J. F.; Juanes, F.; Dudas, S. E. Human Consumption of Microplastics. *Environ. Sci. Technol.* **2019**, *53* (12), 7068–7074. https://doi.org/10.1021/acs.est.9b01517.

(15) Zhang, Q.; Xu, E. G.; Li, J.; Chen, Q.; Ma, L.; Zeng, E. Y.; Shi, H. A Review of Microplastics in Table Salt, Drinking Water, and Air: Direct Human Exposure. *Environ. Sci. Technol.* **2020**. https://doi.org/10.1021/acs.est.9b04535.

(16) de Ruijter, V. N.; Redondo-Hasselerharm, P. E.; Gouin, T.; Koelmans, A. A. Quality Criteria for Microplastic Effect Studies in the Context of Risk Assessment: A Critical Review. *Environ. Sci. Technol.* **2020**, *54* (19), 11692–11705. https://doi.org/10.1021/acs.est.0c03057.

(17) Van Raamsdonk, L. W. D.; Van Der Zande, M.; Koelmans, A. A.; Hoogenboom, P. L. A.; Peters, R. J. B.; Groot, M. J.; Peijnenburg, M. A. C.; Weesepoel, Y. J. A. Current Insights into Monitoring, Bioaccumulation, and Potential Health Effects of Microplastics Present in the Food Chain. *Foods* **2020**. https://doi.org/10.3390/foods9010072.

(18) Koelmans, A. A.; Diepens, N. J.; Mohamed Nor, N. H. Weight of Evidence for the Microplastic Vector Effect in the Context of Chemical Risk Assessment. In *Microplastic in the Environment Pattern and Process*; Bank, M. S., Ed.; Nature Publishing Group, Springer Open Press, 2021; p 400.

(19) Hermabessiere, L.; Dehaut, A.; Paul-Pont, I.; Lacroix, C.; Jezequel, R.; Soudant, P.; Duflos, G. Occurrence and Effects of Plastic Additives on Marine Environments and Organisms: A Review. *Chemosphere* **2017**, *182*, 781–793. https://doi.org/https://doi.org/10.1016/j.chemosphere.2017.05.096.

(20) Frias, J. P. G. L.; Sobral, P.; Ferreira, A. M. Organic Pollutants in Microplastics from Two Beaches of the Portuguese Coast. *Mar. Pollut. Bull.* **2010**. https://doi.org/10.1016/j.marpolbul.2010.07.030.

(21) Shi, J.; Sanganyado, E.; Wang, L.; Li, P.; Li, X.; Liu, W. Organic Pollutants in Sedimentary Microplastics from Eastern Guangdong: Spatial Distribution and Source Identification. *Ecotoxicol. Environ. Saf.* **2020**, *193*, 110356. https://doi.org/https://doi.org/10.1016/j.ecoenv.2020.110356.

(22) Rios Mendoza, L. M.; Jones, P. R. Characterisation of Microplastics and Toxic Chemicals Extracted from Microplastic Samples from the North Pacific Gyre. *Environ. Chem.* **2015**, *12* (5), 611–617.

(23) Lo, H.-S.; Wong, C.-Y.; Tam, N. F.-Y.; Cheung, S.-G. Spatial Distribution and Source Identification of Hydrophobic Organic Compounds (HOCs) on Sedimentary Microplastic in Hong Kong. *Chemosphere* **2019**, *219*, 418–426. https://doi.org/https://doi.org/10.1016/j.chemosphere.2018.12.032.

(24) Mato, Y.; Isobe, T.; Takada, H.; Kanehiro, H.; Ohtake, C.; Kaminuma, T. Plastic Resin Pellets as a Transport Medium for Toxic Chemicals in the Marine Environment. *Environ. Sci. Technol.* **2001**, *35* (2), 318–324. https://doi.org/10.1021/es0010498.

(25) Koelmans, A. A.; Besseling, E.; Wegner, A.; Foekema, E. M. Plastic as a Carrier of POPs to Aquatic Organisms: A Model Analysis. *Environ. Sci. Technol.* **2013**, *47* (14), 7812–7820. https://doi.org/10.1021/es401169n.

(26) Koelmans, A. A.; Bakir, A.; Burton, G. A.; Janssen, C. R. Microplastic as a Vector for Chemicals in the Aquatic Environment: Critical Review and Model-Supported Reinterpretation of Empirical Studies. *Environ. Sci. Technol.* **2016**, *50* (7), 3315–3326. https://doi.org/10.1021/acs.est.5b06069.

(27) Bakir, A.; O'Connor, I. A.; Rowland, S. J.; Hendriks, A. J.; Thompson, R. C. Relative Importance of Microplastics as a Pathway for the Transfer of Hydrophobic Organic Chemicals to Marine Life. *Environ. Pollut.* **2016**, *219*, 56–65.

(28) Liu, P.; Zhan, X.; Wu, X.; Li, J.; Wang, H.; Gao, S. Effect of Weathering on Environmental Behavior of Microplastics: Properties, Sorption and Potential Risks. *Chemosphere* **2020**, *242*, 125193. https://doi.org/https://doi.org/10.1016/j.chemosphere.2019.125193.

(29) Endo, S.; Koelmans, A. A. Sorption of Hydrophobic Organic Compounds to Plastics in the Marine Environment: Equilibrium. In *Handbook of Environmental Chemistry*;

2019. https://doi.org/10.1007/698_2016_11.

(30) Hartmann, N. B.; Rist, S.; Bodin, J.; Jensen, L. H. S.; Schmidt, S. N.; Mayer, P.; Meibom, A.; Baun, A. Microplastics as Vectors for Environmental Contaminants: Exploring Sorption, Desorption, and Transfer to Biota. *Integr. Environ. Assess. Manag.* **2017**. https://doi.org/10.1002/ieam.1904.

(31) Dong, M.; Zhang, Q.; Xing, X.; Chen, W.; She, Z.; Luo, Z. Raman Spectra and Surface Changes of Microplastics Weathered under Natural Environments. *Sci. Total Environ.* **2020**, *739*, 139990. https://doi.org/https://doi.org/10.1016/j.scitotenv.2020.139990.

(32) Diepens, N. J.; Koelmans, A. A. Accumulation of Plastic Debris and Associated Contaminants in Aquatic Food Webs. *Environ. Sci. Technol.* **2018**, *52* (15), 8510–8520. https://doi.org/10.1021/acs.est.8b02515.

(33) Koelmans, A. A.; Besseling, E.; Foekema, E.; Kooi, M.; Mintenig, S.; Ossendorp, B. C.; Redondo-Hasselerharm, P. E.; Verschoor, A.; Van Wezel, A. P.; Scheffer, M. Risks of Plastic Debris: Unravelling Fact, Opinion, Perception, and Belief. *Environ. Sci. Technol.* **2017**. https://doi.org/10.1021/acs.est.7b02219.

(34) Van, A.; Rochman, C. M.; Flores, E. M.; Hill, K. L.; Vargas, E.; Vargas, S. A.; Hoh, E. Persistent Organic Pollutants in Plastic Marine Debris Found on Beaches in San Diego, California. *Chemosphere* **2012**, *86* (3), 258–263. https://doi.org/10.1016/j.chemosphere.2011.09.039.

(35) Zhang, W.; Ma, X.; Zhang, Z.; Wang, Y.; Wang, J. J.; Wang, J. J.; Ma, D. Persistent Organic Pollutants Carried on Plastic Resin Pellets from Two Beaches in China. *Mar. Pollut. Bull.* **2015**, *99* (1–2), 28–34. https://doi.org/10.1016/j.marpolbul.2015.08.002.

(36) Antunes, J. C.; Frias, J. G. L.; Micaelo, A. C.; Sobral, P. Resin Pellets from Beaches of the Portuguese Coast and Adsorbed Persistent Organic Pollutants. *Estuar. Coast. Shelf Sci.* **2013**, *130*, 62–69. https://doi.org/10.1016/j.ecss.2013.06.016.

(37) Rios, L. M.; Moore, C.; Jones, P. R. Persistent Organic Pollutants Carried by Synthetic Polymers in the Ocean Environment. *Mar. Pollut. Bull.* **2007**, *54* (8), 1230–1237. https://doi.org/10.1016/j.marpolbul.2007.03.022.

(38) Teuten, E. L.; Saquing, J. M.; Knappe, D. R. U.; Barlaz, M. A.; Jonsson, S.; Björn, A.; Rowland, S. J.; Thompson, R. C.; Galloway, T. S.; Yamashita, R.; Ochi, D.; Watanuki, Y.; Moore, C.; Viet, P. H.; Tana, T. S.; Prudente, M.; Boonyatumanond, R.; Zakaria, M. P.; Akkhavong, K.; Ogata, Y.; Hirai, H.; Iwasa, S.; Mizukawa, K.; Hagino, Y.; Imamura, A.; Saha, M.; Takada, H. Transport and Release of Chemicals from Plastics to the Environment and to Wildlife. *Philos. Trans. R. Soc. B Biol. Sci.* **2009**, *364* (1526), 2027–2045. https://doi.org/10.1098/rstb.2008.0284.

(39) Tanaka, K.; Takada, H.; Yamashita, R.; Mizukawa, K.; Fukuwaka, M.; Watanuki, Y. Accumulation of Plastic-Derived Chemicals in Tissues of Seabirds Ingesting Marine Plastics. *Mar. Pollut. Bull.* **2013**, *69* (1–2), 219–222.

(40) Yamashita, R.; Takada, H.; Fukuwaka, M.; Watanuki, Y. Physical and Chemical Effects of Ingested Plastic Debris on Short-Tailed Shearwaters, Puffinus Tenuirostris, in the North Pacific Ocean. *Mar. Pollut. Bull.* **2011**, *62* (12), 2845–2849.

(41) Ryan, P. G.; Connell, A. D.; Gardner, B. D. Plastic Ingestion and PCBs in Seabirds: Is There a Relationship? *Mar. Pollut. Bull.* **1988**, *19* (4), 174–176.

(42) Rochman, C. M. The Complex Mixture, Fate and Toxicity of Chemicals Associated with Plastic Debris in the Marine Environment. In *Marine Anthropogenic Litter*; 2015; pp 117–140. https://doi.org/10.1007/978-3-319-16510-3_5.

(43) Ziccardi, L. M.; Edgington, A.; Hentz, K.; Kulacki, K. J.; Kane Driscoll, S.

Microplastics as Vectors for Bioaccumulation of Hydrophobic Organic Chemicals in the Marine Environment: A State-of-the-Science Review. *Environ. Toxicol. Chem.* **2016**, *35* (7), 1667–1676. https://doi.org/10.1002/etc.3461.

(44) Lohmann, R. Microplastics Are Not Important for the Cycling and Bioaccumulation of Organic Pollutants in the Oceans—but Should Microplastics Be Considered POPs Themselves? *Integr. Environ. Assess. Manag.* **2017**, *13* (3), 460–465. https://doi.org/10.1002/ieam.1914.

(45) Gouin, T.; Roche, N.; Lohmann, R.; Hodges, G. A Thermodynamic Approach for Assessing the Environmental Exposure of Chemicals Absorbed to Microplastic. *Environ. Sci. Technol.* **2011**, *45* (4), 1466–1472.

(46) Koelmans, A. A.; Besseling, E.; Wegner, A.; Foekema, E. M. Erratum: Plastic as a Carrier of POPs to Aquatic Organisms: A Model Analysis (Environmental Science and Technology (2013) 47 (7812-7820) DOI: 10.1021/Es401169n). *Environmental Science and Technology*. 2013. https://doi.org/10.1021/es403018h.

(47) Koelmans, A. A. Modeling the Role of Microplastics in Bioaccumulation of Organic Chemicals to Marine Aquatic Organisms. A Critical Review. In *Marine Anthropogenic Litter*; 2015; pp 309–324. https://doi.org/10.1007/978-3-319-16510-3_11.

(48) Besseling, E.; Wegner, A.; Foekema, E. M.; Van Den Heuvel-Greve, M. J.; Koelmans, A. A. Effects of Microplastic on Fitness and PCB Bioaccumulation by the Lugworm Arenicola Marina (L.). *Environ. Sci. Technol.* **2012**, *47* (1), 593–600.

(49) Rochman, C. M.; Hoh, E.; Kurobe, T.; Teh, S. J. Ingested Plastic Transfers Hazardous Chemicals to Fish and Induces Hepatic Stress. *Sci. Rep.* **2013**, *3*, 3263. https://doi.org/10.1038/srep03263.

(50) Browne, M. A.; Niven, S. J.; Galloway, T. S.; Rowland, S. J.; Thompson, R. C. Microplastic Moves Pollutants and Additives to Worms, Reducing Functions Linked to Health and Biodiversity. *Curr. Biol.* **2013**, *23* (23), 2388–2392.

(51) Devriese, L. I.; De Witte, B.; Vethaak, A. D.; Hostens, K.; Leslie, H. A. Bioaccumulation of PCBs from Microplastics in Norway Lobster (Nephrops Norvegicus): An Experimental Study. *Chemosphere* **2017**, *186*, 10–16.

(52) Teuten, E. L.; Rowland, S. J.; Galloway, T. S.; Thompson, R. C. Potential for Plastics to Transport Hydrophobic Contaminants. *Environ. Sci. Technol.* **2007**, *41* (22), 7759–7764.

(53) Bakir, A.; Rowland, S. J.; Thompson, R. C. Enhanced Desorption of Persistent Organic Pollutants from Microplastics under Simulated Physiological Conditions. *Environ. Pollut.* **2014**, *185*, 16–23.

(54) Beckingham, B.; Ghosh, U. Differential Bioavailability of Polychlorinated Biphenyls Associated with Environmental Particles: Microplastic in Comparison to Wood, Coal and Biochar. *Environ. Pollut.* **2017**, *220*, 150–158.

(55) Schwarzenbach, R. P.; Gschwend, P. M.; Imboden, D. M. Sorption I: General Introduction and Sorption Processes Involving Organic Matter. *Environ. Org. Chem.* **2005**, 275–330.

(56) Lohmann, R. Critical Review of Low-Density Polyethylene's Partitioning and Diffusion Coefficients for Trace Organic Contaminants and Implications for Its Use as a Passive Sampler. *Environ. Sci. Technol.* **2011**, *46* (2), 606–618.

(57) Jonker, M. T. O.; Koelmans, A. A. Polyoxymethylene Solid Phase Extraction as a Partitioning Method for Hydrophobic Organic Chemicals in Sediment and Soot. *Environ. Sci. Technol.* **2001**, *35* (18), 3742–3748. https://doi.org/10.1021/es0100470.

(58) Perkel, R.; Ullman, R. The Adsorption of Polydimethylsiloxanes from Solution. *J.*

Polym. Sci. **1961**, *54* (159), 127–148.

(59) Koelmans, A. A.; Besseling, E.; Foekema, E. M. Leaching of Plastic Additives to Marine Organisms. *Environ. Pollut.* **2014**, *187*, 49–54.

(60) GESAMP. Sources, Fate and Effects of Microplastics in the Marine Environment: A Global Assessment". *Reports Stud. GESAMP* **2015**. https://doi.org/10.13140/RG.2.1.3803.7925.

(61) Marques, M. R. C.; Loebenberg, R.; Almukainzi, M. Simulated Biological Fluids with Possible Application in Dissolution Testing. *Dissolution Technol.* **2011**, *18* (3), 15–28. https://doi.org/10.14227/DT180311P15.

(62) Voparil, I. M.; Mayer, L. M. Commercially Available Chemicals That Mimic a Deposit Feeder's (Arenicola Marina) Digestive Solubilization of Lipids. *Environ. Sci. Technol.* **2004**, *38* (16), 4334–4339.

(63) Dulfer, W. J.; Groten, J. P.; Govers, H. A. Effect of Fatty Acids and the Aqueous Diffusion Barrier on the Uptake and Transport of Polychlorinated Biphenyls in Caco-2 Cells. *J. Lipid Res.* **1996**, *37* (5), 950–961.

(64) Schwarzenbach, R. P.; Gschwend, P. M.; Imboden, D. M. *Environmental Organic Chemistry*; John Wiley & Sons, 2002. https://doi.org/10.1002/0471649643.

(65) Massoudieh, A.; Ju, D.; Young, T. M.; Ginn, T. R. Approximation of a Radial Diffusion Model with a Multiple-Rate Model for Hetero-Disperse Particle Mixtures. *J. Contam. Hydrol.* **2008**, *97* (1–2), 55–66. https://doi.org/10.1016/j.jconhyd.2007.12.004.

(66) Seidensticker, S.; Zarfl, C.; Cirpka, O. A.; Fellenberg, G.; Grathwohl, P. Shift in Mass Transfer of Wastewater Contaminants from Microplastics in the Presence of Dissolved Substances. *Environ. Sci. Technol.* **2017**, *51* (21), 12254–12263. https://doi.org/10.1021/acs.est.7b02664.

(67) ten Hulscher, T. E. M.; Vrind, B. A.; van den Heuvel, H.; van der Velde, L. E.; van Noort, P. C. M.; Beurskens, J. E. M.; Govers, H. A. J. Triphasic Desorption of Highly Resistant Chlorobenzenes, Polychlorinated Biphenyls, and Polycyclic Aromatic Hydrocarbons in Field Contaminated Sediment. *Environ. Sci. Technol.* **1999**, *33* (1), 126–132. https://doi.org/10.1021/es980091o.

(68) Chai, Y.; Kochetkov, A.; Reible, D. D. Modeling Biphasic Sorption and Desorption of Hydrophobic Organic Contaminants in Sediments. *Environ. Toxicol. Chem.* **2006**, *25* (12), 3133–3140. https://doi.org/10.1897/05-704R.1.

(69) Wu, S. C.; Gschwend, P. M. Sorption Kinetics of Hydrophobic Organic Compounds to Natural Sediments and Soils. *Environ. Sci. Technol.* **1986**, *20* (7), 717–725. https://doi.org/10.1021/es00149a011.

(70) Koelmans, A. A.; De Lange, H. J.; Lijklema, L. Desorption of Chlorobenzenes from Natural Suspended Solids and Sediments. *Water Sci. Technol.* **1993**, 171–180.

(71) Jeyachandran, Y. L.; Mielczarski, E.; Rai, B.; Mielczarski, J. A. Quantitative and Qualitative Evaluation of Adsorption/Desorption of Bovine Serum Albumin on Hydrophilic and Hydrophobic Surfaces. *Langmuir* **2009**, *25* (19), 11614–11620. https://doi.org/10.1021/la901453a.

(72) D'Archivio, A. A.; Galantini, L.; Tettamanti, E. Study on Intermicellar Interactions and Micellar Size in Aqueous Solutions of Sodium Taurocholate by Measurements of Collective Diffusion and Self-Diffusion Coefficients. *J. Phys. Chem. B* **2000**, *104* (39), 9255–9259. https://doi.org/10.1021/jp000070s.

(73) Schacht, V. J.; Grant, S. C.; Escher, B. I.; Hawker, D. W.; Gaus, C. Solubility Enhancement of Dioxins and PCBs by Surfactant Monomers and Micelles Quantified with Polymer Depletion Techniques. *Chemosphere* **2016**, *152*, 99–106.

https://doi.org/10.1016/j.chemosphere.2016.02.122.

(74) Elzhov, T. V.; Spiess, A.-N.; Bolker, B.; Mullen, K. M. Minpack.Lm: R Interface to the Levenberg-Marquardt Nonlinear Least-Squares Algorithm Found in MINPACK, Plus Support for Bounds. R package. 2016.

(75) Soetaert, K.; Petzoldt, T.; Setzer, R. W. Solving Differential Equations in R : Package DeSolve. *J. Stat. Softw.* **2010**, *33*. https://doi.org/10.18637/jss.v033.i09.

(76) R Core Team. R: A Language and Environment for Statistical Computing. R Foundation for Statistical Computing. Vienna, Austria 2019.

(77) Fox, J.; Weisberg, S. An R Companion to Applied Regression. https://doi.org/10.1177/0049124105277200.

(78) Hothorn, T.; Bretz, F.; Westfall, P. Simultaneous Inference in General Parametric Models. *Biometrical J.* **2008**, *50* (3), 346–363.

(79) Adams, R. G.; Lohmann, R.; Fernandez, L. A.; MacFarlane, J. K.; Gschwend, P. M. Polyethylene Devices: Passive Samplers for Measuring Dissolved Hydrophobic Organic Compounds in Aquatic Environments. *Environ. Sci. Technol.* **2007**, *41* (4), 1317–1323.

(80) Weber, W. J.; LeBoeuf, E. J.; Young, T. M.; Huang, W. Contaminant Interactions with Geosorbent Organic Matter: Insights Drawn from Polymer Sciences. *Water Res.* **2001**, *35* (4), 853–868. https://doi.org/10.1016/S0043-1354(00)00339-0.

(81) Velzeboer, I.; Kwadijk, C. J. A. F.; Koelmans, A. A. Strong Sorption of PCBs to Nanoplastics, Microplastics, Carbon Nanotubes, and Fullerenes. *Environ. Sci. Technol.* **2014**, *48* (9), 4869–4876. https://doi.org/10.1021/es405721v.

(82) Brandrup, J.; Immergut, E.; Grulke, E. A. Polymer Handbook. *John Wiley Sons, Inc* **1990**, *7*. https://doi.org/10.1016/0168-3659(90)90108-6.

(83) Pascall, M. A.; Zabik, M. E.; Zabik, M. J.; Hernandez, R. J. Uptake of Polychlorinated Biphenyls (PCBs) from an Aqueous Medium by Polyethylene, Polyvinyl Chloride, and Polystyrene Films. *J. Agric. Food Chem.* **2005**, *53* (1), 164–169.

(84) Rochman, C. M.; Hoh, E.; Hentschel, B. T.; Kaye, S. Long-Term Field Measurement of Sorption of Organic Contaminants to Five Types of Plastic Pellets: Implications for Plastic Marine Debris. *Environ. Sci. Technol.* **2013**, *47* (3), 1646–1654.

(85) Endo, S.; Takizawa, R.; Okuda, K.; Takada, H.; Chiba, K.; Kanehiro, H.; Ogi, H.; Yamashita, R.; Date, T. Concentration of Polychlorinated Biphenyls (PCBs) in Beached Resin Pellets: Variability among Individual Particles and Regional Differences. *Mar. Pollut. Bull.* **2005**, *50* (10), 1103–1114. https://doi.org/10.1016/j.marpolbul.2005.04.030.

(86) Mato, Y.; Takada, H.; Zakaria, M. P. Toxic Chemicals Contained in Plastic Resin Pellets in the Marine Environment - Spatial Difference in Pollutant Concentrations and the Effects of Resin Type. *Kankyo Kagakukaishi* **2002**. https://doi.org/10.11353/sesj1988.15.415.

(87) Herzke, D.; Anker-Nilssen, T.; Nøst, T. H.; Götsch, A.; Christensen-Dalsgaard, S.; Langset, M.; Fangel, K.; Koelmans, A. A. Negligible Impact of Ingested Microplastics on Tissue Concentrations of Persistent Organic Pollutants in Northern Fulmars off Coastal Norway. *Environ. Sci. Technol.* **2016**, *50* (4), 1924–1933. https://doi.org/10.1021/acs.est.5b04663.

(88) Kupryianchyk, D.; Noori, A.; Rakowska, M. I.; Grotenhuis, J. T. C.; Koelmans, A. A. Bioturbation and Dissolved Organic Matter Enhance Contaminant Fluxes from Sediment Treated with Powdered and Granular Activated Carbon. *Environ. Sci. Technol.* **2013**, *47* (10), 5092–5100. https://doi.org/10.1021/es3040297.

(89) Johnson, W. P.; Amy, G. L. Facilitated Transport and Enhanced Desorption of Polycyclic Aromatic Hydrocarbons by Natural Organic Matter in Aquifer Sediments. *Environ. Sci. Technol.* **1995**, *29* (3), 807–817. https://doi.org/10.1021/es00003a032.

(90) Kan, A. T.; Tomson, M. B. Ground Water Transport of Hydrophobic Organic Compounds in the Presence of Dissolved Organic Matter. *Environ. Toxicol. Chem.* **1990**, *9* (3), 253–263. https://doi.org/10.1002/etc.5620090302.

(91) Rummel, C. D.; Adolfsson-Erici, M.; Jahnke, A.; MacLeod, M. No Measurable "Cleaning" of Polychlorinated Biphenyls from Rainbow Trout in a 9 Week Depuration Study with Dietary Exposure to 40% Polyethylene Microspheres. *Environ. Sci. Process. Impacts* **2016**, *18* (7), 788–795.

(92) Wardrop, P.; Shimeta, J.; Nugegoda, D.; Morrison, P. D.; Miranda, A.; Tang, M.; Clarke, B. O. Chemical Pollutants Sorbed to Ingested Microbeads from Personal Care Products Accumulate in Fish. *Environ. Sci. Technol.* **2016**, *50* (7), 4037–4044. https://doi.org/10.1021/acs.est.5b06280.

(93) Foekema, E. M.; Gruijter, C. De; Mergia, M. T.; Franeker, J. A. Van; Murk, A. J.; Koelmans, A. A. Plastic in North Sea Fish. *Environ. Sci. Technol.* **2013**, *47* (15), 8818–8824.

(94) Denuncio, P.; Bastida, R.; Dassis, M.; Giardino, G.; Gerpe, M.; Rodríguez, D. Plastic Ingestion in Franciscana Dolphins, Pontoporia Blainvillei (Gervais and d'Orbigny, 1844), from Argentina. *Mar. Pollut. Bull.* **2011**, *62* (8), 1836–1841. https://doi.org/10.1016/j.marpolbul.2011.05.003.

(95) Lazar, B.; Gračan, R. Ingestion of Marine Debris by Loggerhead Sea Turtles, Caretta Caretta, in the Adriatic Sea. *Mar. Pollut. Bull.* **2011**, *62* (1), 43–47. https://doi.org/10.1016/j.marpolbul.2010.09.013.

(96) Van Franeker, J. A.; Blaize, C.; Danielsen, J.; Fairclough, K.; Gollan, J.; Guse, N.; Hansen, P. L.; Heubeck, M.; Jensen, J. K.; Le Guillou, G.; Olsen, B.; Olsen, K. O.; Pedersen, J.; Stienen, E. W. M.; Turner, D. M. Monitoring Plastic Ingestion by the Northern Fulmar Fulmarus Glacialis in the North Sea. *Environ. Pollut.* **2011**, *159* (10), 2609–2615. https://doi.org/10.1016/j.envpol.2011.06.008.

(97) Murray, F.; Cowie, P. R. Plastic Contamination in the Decapod Crustacean Nephrops Norvegicus (Linnaeus, 1758). *Mar. Pollut. Bull.* **2011**, *62* (6), 1207–1217. https://doi.org/10.1016/j.marpolbul.2011.03.032.

(98) Oomen, A. G.; Sips, A. J. A. M.; Groten, J. P.; Sijm, D. T. H. M.; Tolls, J. Mobilization of PCBs and Lindane from Soil during in Vitro Digestion and Their Distribution among Bile Salt Micelles and Proteins of Human Digestive Fluid and the Soil. *Environ. Sci. Technol.* **2000**, *34* (2), 297–303. https://doi.org/10.1021/es990446j.

(99) Friedman, H. I.; Nylund, B. Intestinal Fat Digestion, Absorption, and Transport. A Review. *American Journal of Clinical Nutrition*. 1980. https://doi.org/10.1093/ajcn/33.5.1108.

(100) Van Cauwenberghe, L.; Claessens, M.; Vandegehuchte, M. B.; Janssen, C. R. Microplastics Are Taken up by Mussels (Mytilus Edulis) and Lugworms (Arenicola Marina) Living in Natural Habitats. *Environ. Pollut.* **2015**, *199*, 10–17.

(101) Van Cauwenberghe, L.; Janssen, C. R. Microplastics in Bivalves Cultured for Human Consumption. *Environ. Pollut.* **2014**, *193*, 65–70. https://doi.org/10.1016/j.envpol.2014.06.010.

(102) De Witte, B.; Devriese, L.; Bekaert, K.; Hoffman, S.; Vandermeersch, G.; Cooreman, K.; Robbens, J. Quality Assessment of the Blue Mussel (Mytilus Edulis): Comparison between Commercial and Wild Types. *Mar. Pollut. Bull.* **2014**, *85* (1),

146–155. https://doi.org/10.1016/j.marpolbul.2014.06.006.

(103) Li, J.; Qu, X.; Su, L.; Zhang, W.; Yang, D.; Kolandhasamy, P.; Li, D.; Shi, H. Microplastics in Mussels along the Coastal Waters of China. *Environ. Pollut.* **2016**, *214*, 177–184. https://doi.org/10.1016/j.envpol.2016.04.012.

(104) Li, J.; Yang, D.; Li, L.; Jabeen, K.; Shi, H. Microplastics in Commercial Bivalves from China. *Environ. Pollut.* **2015**, *207*, 190–195. https://doi.org/10.1016/j.envpol.2015.09.018.

(105) Wright, S. L.; Thompson, R. C.; Galloway, T. S. The Physical Impacts of Microplastics on Marine Organisms: A Review. *Environ. Pollut.* **2013**, *178*, 483–492.

(106) Rochman, C. M.; Tahir, A.; Williams, S. L.; Baxa, D. V; Lam, R.; Miller, J. T.; Teh, F.-C.; Werorilangi, S.; Teh, S. J. Anthropogenic Debris in Seafood: Plastic Debris and Fibers from Textiles in Fish and Bivalves Sold for Human Consumption. *Sci. Rep.* **2015**, *5*, 14340.

(107) Kosuth, M.; Mason, S. A.; Wattenberg, E. V. Anthropogenic Contamination of Tap Water, Beer, and Sea Salt. *PLoS One* **2018**, *13* (4). https://doi.org/10.1371/journal.pone.0194970.

(108) Liebezeit, G.; Liebezeit, E. Synthetic Particles as Contaminants in German Beers. *Food Addit. Contam. - Part A Chem. Anal. Control. Expo. Risk Assess.* **2014**, *31* (9), 1574–1578. https://doi.org/10.1080/19440049.2014.945099.

(109) Mühlschlegel, P.; Hauk, A.; Walter, U.; Sieber, R. Lack of Evidence for Microplastic Contamination in Honey. *Food Addit. Contam. - Part A Chem. Anal. Control. Expo. Risk Assess.* **2017**, *34* (11), 1982–1989. https://doi.org/10.1080/19440049.2017.1347281.

(110) Yang, D.; Shi, H.; Li, L.; Li, J.; Jabeen, K.; Kolandhasamy, P. Microplastic Pollution in Table Salts from China. *Environ. Sci. Technol.* **2015**, *49* (22), 13622–13627. https://doi.org/10.1021/acs.est.5b03163.

(111) Karami, A.; Golieskardi, A.; Keong Choo, C.; Larat, V.; Galloway, T. S.; Salamatinia, B. The Presence of Microplastics in Commercial Salts from Different Countries. *Sci. Rep.* **2017**, *7*, 46173. https://doi.org/10.1038/srep46173.

(112) Mason, S. A.; Welch, V.; Neratko, J. Synthetic Polymer Contamination in Bottled Water. *Front. Chem.* **2018**, *6* (407).

(113) Daugherty, A.; Mrsny, R. Transcellular Uptake Mechanisms of the Intestinal Epithelial Barrier Part One. *Pharm. Sci. Technolo. Today* **1999**, *2* (4), 144–151. https://doi.org/10.1016/S1461-5347(99)00142-X.

(114) Hawker, D. W.; Connell, D. W. Octanol-Water Partition Coefficients of Polychlorinated Biphenyl Congeners. *Environ. Sci. Technol.* **1988**, *22* (4), 382–387. https://doi.org/10.1021/es00169a004.

(115) Moermond, C. T. A.; Roessink, I.; Jonker, M. T. O.; Meijer, T.; Koelmans, A. A. Impact of Polychlorinated Biphenyl and Polycyclic Aromatic Hydrocarbon Sequestration in Sediment on Bioaccumulation in Aquatic Food Webs. *Environ. Toxicol. Chem.* **2007**, *26* (4), 607–615. https://doi.org/10.1897/06-288R.1.

(116) Thompson, R. C.; Swan, S. H.; Moore, C. J.; Vom Saal, F. S. Our Plastic Age. *Philosophical Transactions of the Royal Society B: Biological Sciences*. 2009. https://doi.org/10.1098/rstb.2009.0054.

(117) Freeman, S. Plastic Food Contact Articles—Food Chemical Safety Unwrapped. *Environ. Heal. Rev.* **2018**. https://doi.org/10.5864/d2018-028.

(118) Amelia, T. S. M.; Khalik, W. M. A. W. M.; Ong, M. C.; Shao, Y. T.; Pan, H. J.; Bhubalan, K. Marine Microplastics as Vectors of Major Ocean Pollutants and Its

Hazards to the Marine Ecosystem and Humans. *Prog. Earth Planet. Sci.* **2021**. https://doi.org/10.1186/s40645-020-00405-4.

(119) Wang, F.; Wong, C. S.; Chen, D.; Lu, X.; Wang, F.; Zeng, E. Y. Interaction of Toxic Chemicals with Microplastics: A Critical Review. *Water Res.* **2018**. https://doi.org/10.1016/j.watres.2018.04.003.

(120) Mohamed Nor, N. H.; Kooi, M.; Diepens, N. J.; Koelmans, A. A. Lifetime Accumulation of Microplastic in Children and Adults. *Environ. Sci. Technol.* **2021**. https://doi.org/10.1021/acs.est.0c07384.

(121) Domenech, J.; Marcos, R. Pathways of Human Exposure to Microplastics, and Estimation of the Total Burden. *Curr. Opin. Food Sci.* **2021**, *39*, 144–151. https://doi.org/https://doi.org/10.1016/j.cofs.2021.01.004.

(122) Hack, A.; Selenka, F. Mobilization of PAH and PCB from Contaminated Soil Using a Digestive Tract Model. *Toxicol. Lett.* **1996**. https://doi.org/10.1016/0378-4274(96)03738-1.

(123) Holman, H. Y. N.; Goth-Goldstein, R.; Aston, D.; Yun, M.; Kengsoontra, J. Evaluation of Gastrointestinal Solubilization of Petroleum Hydrocarbon Residues in Soil Using an in Vitro Physiologically Based Model. *Environ. Sci. Technol.* **2002**. https://doi.org/10.1021/es010987k.

(124) Oomen, A. G.; Hack, A.; Minekus, M.; Zeijdner, E.; Cornelis, C.; Schoeters, G.; Verstraete, W.; Van De Wiele, T.; Wragg, J.; Rompelberg, C. J. M.; Sips, A. J. A. M.; Van Wijnen, J. H. Comparison of Five in Vitro Digestion Models to Study the Bioaccessibility of Soil Contaminants. *Environ. Sci. Technol.* **2002**. https://doi.org/10.1021/es010204v.

(125) Vasiluk, L.; Pinto, L. J.; Walji, Z. A.; Wing, S. T.; Gobas, F. A. P. C.; Eickhoff, C.; Moore, M. M. Benzo[a]Pyrene Bioavailability from Pristine Soil and Contaminated Sediment Assessed Using Two in Vitro Models. *Environ. Toxicol. Chem.* **2007**. https://doi.org/10.1897/06-343R.1.

(126) Zhang, Y.; Pignatello, J. J.; Tao, S.; Xing, B. Bioaccessibility of PAHs in Fuel Soot Assessed by an in Vitro Digestive Model with Absorptive Sink: Effect of Food Ingestion. *Environ. Sci. Technol.* **2015**, *49* (24), 14641–14648.

(127) Voparil, I. M.; Mayer, L. M. Dissolution of Sedimentary Polycyclic Aromatic Hydrocarbons into the Lugworm's (Arenicola Marina) Digestive Fluids. *Environ. Sci. Technol.* **2000**. https://doi.org/10.1021/es990885i.

(128) Coffin, S.; Huang, G. Y.; Lee, I.; Schlenk, D. Fish and Seabird Gut Conditions Enhance Desorption of Estrogenic Chemicals from Commonly-Ingested Plastic Items. *Environ. Sci. Technol.* **2019**, *53* (8), 4588–4599. https://doi.org/10.1021/acs.est.8b07140.

(129) Guo, H.; Zheng, X.; Ru, S.; Luo, X.; Mai, B. The Leaching of Additive-Derived Flame Retardants (FRs) from Plastics in Avian Digestive Fluids: The Significant Risk of Highly Lipophilic FRs. *J. Environ. Sci. (China)* **2019**, *85*, 200–207. https://doi.org/10.1016/j.jes.2019.06.013.

(130) Heinrich, P.; Braunbeck, T. Microplastic Particles Reduce EROD-Induction Specifically by Highly Lipophilic Compounds in RTL-W1 Cells. *Ecotoxicol. Environ. Saf.* **2020**. https://doi.org/10.1016/j.ecoenv.2019.110041.

(131) Lee, H.; Lee, H. J.; Kwon, J. H. Estimating Microplastic-Bound Intake of Hydrophobic Organic Chemicals by Fish Using Measured Desorption Rates to Artificial Gut Fluid. *Sci. Total Environ.* **2019**, *651*, 162–170. https://doi.org/10.1016/j.scitotenv.2018.09.068.

(132) Martin, K.; Turner, A. Mobilization and Bioaccessibility of Cadmium in Coastal

Sediment Contaminated by Microplastics. *Mar. Pollut. Bull.* **2019**, *146* (July), 940–944. https://doi.org/10.1016/j.marpolbul.2019.07.046.

(133) Turner, A. Mobilisation Kinetics of Hazardous Elements in Marine Plastics Subject to an Avian Physiologically-Based Extraction Test. *Environ. Pollut.* **2018**, *236*, 1020–1026. https://doi.org/10.1016/j.envpol.2018.01.023.

(134) Coffin, S.; Lee, I.; Gan, J.; Schlenk, D. Simulated Digestion of Polystyrene Foam Enhances Desorption of Diethylhexyl Phthalate (DEHP) and In Vitro Estrogenic Activity in a Size-Dependent Manner. *Environ. Pollut.* **2019**, *246*, 452–462. https://doi.org/10.1016/j.envpol.2018.12.011.

(135) Shan, J.; Wang, J.; Zhan, J.; Liu, L.; Wu, F.; Wang, X. Sorption Behaviors of Crude Oil on Polyethylene Microplastics in Seawater and Digestive Tract under Simulated Real-World Conditions. *Chemosphere* **2020**, *257*, 127225. https://doi.org/https://doi.org/10.1016/j.chemosphere.2020.127225.

(136) Mohamed Nor, N. H.; Koelmans, A. A. Transfer of PCBs from Microplastics under Simulated Gut Fluid Conditions Is Biphasic and Reversible. *Environ. Sci. Technol.* **2019**, *53*, 1874–1883. https://doi.org/10.1021/acs.est.8b05143.

(137) Godoy, V.; Martínez-Férez, A.; Martín-Lara, M. Á.; Vellido-Pérez, J. A.; Calero, M.; Blázquez, G. Microplastics as Vectors of Chromium and Lead during Dynamic Simulation of the Human Gastrointestinal Tract. *Sustain.* **2020**. https://doi.org/10.3390/su12114792.

(138) Liu, X.; Gharasoo, M.; Shi, Y.; Sigmund, G.; Hüffer, T.; Duan, L.; Wang, Y.; Ji, R.; Hofmann, T.; Chen, W. Key Physicochemical Properties Dictating Gastrointestinal Bioaccessibility of Microplastics-Associated Organic Xenobiotics: Insights from a Deep Learning Approach. *Environ. Sci. Technol.* **2020**. https://doi.org/10.1021/acs.est.0c02838.

(139) Liao, Y.; Yang, J. Microplastic Serves as a Potential Vector for Cr in an In-Vitro Human Digestive Model. *Sci. Total Environ.* **2020**, *703*, 134805. https://doi.org/https://doi.org/10.1016/j.scitotenv.2019.134805.

(140) Tan, H.; Yue, T.; Xu, Y.; Zhao, J.; Xing, B. Microplastics Reduce Lipid Digestion in Simulated Human Gastrointestinal System. *Environ. Sci. Technol.* **2020**, *54* (19), 12285–12294. https://doi.org/10.1021/acs.est.0c02608.

(141) Andrady, A. L. Microplastics in the Marine Environment. *Mar. Pollut. Bull.* **2011**, *62* (8), 1596–1605. https://doi.org/https://doi.org/10.1016/j.marpolbul.2011.05.030.

(142) Bouhroum, R.; Boulkamh, A.; Asia, L.; Lebarillier, S.; Halle, A. Ter; Syakti, A. D.; Doumenq, P.; Malleret, L.; Wong-Wah-chung, P. Concentrations and Fingerprints of PAHs and PCBs Adsorbed onto Marine Plastic Debris from the Indonesian Cilacap Coast and the North Atlantic Gyre. *Reg. Stud. Mar. Sci.* **2019**, *29*, 100611. https://doi.org/https://doi.org/10.1016/j.rsma.2019.100611.

(143) Ogata, Y.; Takada, H.; Mizukawa, K.; Hirai, H.; Iwasa, S.; Endo, S.; Mato, Y.; Saha, M.; Okuda, K.; Nakashima, A. International Pellet Watch: Global Monitoring of Persistent Organic Pollutants (POPs) in Coastal Waters. 1. Initial Phase Data on PCBs, DDTs, and HCHs. *Mar. Pollut. Bull.* **2009**, *58* (10), 1437–1446.

(144) Llobet, J. M.; Bocio, A.; Domingo, J. L.; Teixidó, A.; Casas, C.; Müller, L. Levels of Polychlorinated Biphenyls in Foods from Catalonia, Spain: Estimated Dietary Intake. *J. Food Prot.* **2003**. https://doi.org/10.4315/0362-028X-66.3.479.

(145) Malisch, R.; Kotz, A. Dioxins and PCBs in Feed and Food — Review from European Perspective. *Sci. Total Environ.* **2014**, *491–492*, 2–10. https://doi.org/https://doi.org/10.1016/j.scitotenv.2014.03.022.

(146) Hawthorne, S. B.; Miller, D. J.; Grabanski, C. B. Measuring Low Picogram Per Liter

Concentrations of Freely Dissolved Polychlorinated Biphenyls in Sediment Pore Water Using Passive Sampling with Polyoxymethylene. *Anal. Chem.* **2009**, *81* (22), 9472–9480. https://doi.org/10.1021/ac9019413.

(147) Hawthorne, S. B.; Jonker, M. T. O.; van der Heijden, S. A.; Grabanski, C. B.; Azzolina, N. A.; Miller, D. J. Measuring Picogram per Liter Concentrations of Freely Dissolved Parent and Alkyl PAHs (PAH-34), Using Passive Sampling with Polyoxymethylene. *Anal. Chem.* **2011**, *83* (17), 6754–6761. https://doi.org/10.1021/ac201411v.

(148) Ménard, O.; Bourlieu, C.; De Oliveira, S. C.; Dellarosa, N.; Laghi, L.; Carrière, F.; Capozzi, F.; Dupont, D.; Deglaire, A. A First Step towards a Consensus Static in Vitro Model for Simulating Full-Term Infant Digestion. *Food Chem.* **2018**. https://doi.org/10.1016/j.foodchem.2017.07.145.

(149) Jiménez-Skrzypek, G.; Hernández-Sánchez, C.; Ortega-Zamora, C.; González-Sálamo, J.; González-Curbelo, M. Á.; Hernández-Borges, J. Microplastic-Adsorbed Organic Contaminants: Analytical Methods and Occurrence. *TrAC Trends Anal. Chem.* **2021**, *136*, 116186. https://doi.org/https://doi.org/10.1016/j.trac.2021.116186.

(150) Minekus, M.; Alminger, M.; Alvito, P.; Ballance, S.; Bohn, T.; Bourlieu, C.; Carrière, F.; Boutrou, R.; Corredig, M.; Dupont, D.; Dufour, C.; Egger, L.; Golding, M.; Karakaya, S.; Kirkhus, B.; Le Feunteun, S.; Lesmes, U.; MacIerzanka, A.; MacKie, A.; Marze, S.; McClements, D. J.; Ménard, O.; Recio, I.; Santos, C. N.; Singh, R. P.; Vegarud, G. E.; Wickham, M. S. J.; Weitschies, W.; Brodkorb, A. A Standardised Static in Vitro Digestion Method Suitable for Food-an International Consensus. *Food Funct.* **2014**. https://doi.org/10.1039/c3fo60702j.

(151) Grigorakis, S.; Mason, S. A.; Drouillard, K. G. Determination of the Gut Retention of Plastic Microbeads and Microfibers in Goldfish (Carassius Auratus). *Chemosphere* **2017**, *169*, 233–238. https://doi.org/https://doi.org/10.1016/j.chemosphere.2016.11.055.

(152) Roch, S.; Ros, A. F. H.; Friedrich, C.; Brinker, A. Microplastic Evacuation in Fish Is Particle Size-Dependent. *Freshw. Biol.* **2021**, *66* (5), 926–935. https://doi.org/https://doi.org/10.1111/fwb.13687.

(153) Welden, N. A. C.; Cowie, P. R. Environment and Gut Morphology Influence Microplastic Retention in Langoustine, Nephrops Norvegicus. *Environ. Pollut.* **2016**, *214*, 859–865. https://doi.org/https://doi.org/10.1016/j.envpol.2016.03.067.

(154) Meisner, H.; Tenney, K. PH as an Indicator of Free Fatty Acid Release from Adipocytes. *J. Lipid Res.* **1977**. https://doi.org/10.1016/s0022-2275(20)41596-2.

(155) Gotthilf, N. Lipase Titrimetric Assay. In *Methods of Enzymatic Analysis*; 1974. https://doi.org/10.1016/b978-0-12-091302-2.50061-x.

(156) Besseling, E.; Foekema, E. M.; van den Heuvel-Greve, M. J.; Koelmans, A. A. The Effect of Microplastic on the Uptake of Chemicals by the Lugworm *Arenicola Marina* (L.) under Environmentally Relevant Exposure Conditions. *Environ. Sci. Technol.* **2017**, *51* (15), 8795–8804. https://doi.org/10.1021/acs.est.7b02286.

(157) Jonker, M. T. O.; Barendregt, A. Oil Is a Sedimentary Supersorbent for Polychlorinated Biphenyls. *Environ. Sci. Technol.* **2006**. https://doi.org/10.1021/es0601080.

(158) de Gelder, S.; Sæle, Ø.; de Veen, B. T. H.; Vos, J.; Flik, G.; Berntssen, M. H. G.; Klaren, P. H. M. The Polycyclic Aromatic Hydrocarbons Benzo[a]Pyrene and Phenanthrene Inhibit Intestinal Lipase Activity in Rainbow Trout (Oncorhynchus Mykiss). *Comp. Biochem. Physiol. Part - C Toxicol. Pharmacol.* **2017**. https://doi.org/10.1016/j.cbpc.2017.04.008.

(159) Bello-Perez, L. A.; Agama-Acevedo, E.; Garcia-Valle, D. E.; Alvarez-Ramirez, J. A Multiscale Kinetics Model for the Analysis of Starch Amylolysis. *Int. J. Biol. Macromol.* **2019**. https://doi.org/10.1016/j.ijbiomac.2018.10.161.

(160) Zhu, T. F.; Budin, I.; Szostak, J. W. Preparation of Fatty Acid Micelles. In *Methods in Enzymology*; 2013. https://doi.org/10.1016/B978-0-12-420067-8.00022-2.

(161) Cistola, D. P.; Hamilton, J. A.; Jackson, D.; Small, D. M. Ionization and Phase Behavior of Fatty Acids in Water: Application of the Gibbs Phase Rule. *Biochemistry* **1988**, *27* (6), 1881–1888. https://doi.org/10.1021/bi00406a013.

(162) Hargreaves, W. R.; Deamer, D. W. Liposomes from Ionic, Single-Chain Amphiphiles. *Biochemistry* **1978**, *17* (18), 3759–3768. https://doi.org/10.1021/bi00611a014.

(163) Nithipatikom, K.; McGown, L. B. Fluorescence Studies of Energy Transfer in Sodium Taurocholate and Sodium Dodecyl Sulfate Micellar Solutions. *Anal. Chem.* **1989**, *61* (13), 1405–1410. https://doi.org/10.1021/ac00188a020.

(164) ter Laak, T. L.; van Eijkeren, J. C. H.; Busser, F. J. M.; van Leeuwen, H. P.; Hermens, J. L. M. Facilitated Transport of Polychlorinated Biphenyls and Polybrominated Diphenyl Ethers by Dissolved Organic Matter. *Environ. Sci. Technol.* **2009**, *43* (5), 1379–1385. https://doi.org/10.1021/es802403v.

(165) Haftka, J. J. H.; Parsons, J. R.; Govers, H. A. J.; Ortega-Calvo, J.-J. Enhanced Kinetics of Solid-Phase Microextraction and Biodegradation of Polycyclic Aromatic Hydrocarbons in the Presence of Dissolved Organic Matter. *Environ. Toxicol. Chem.* **2008**, *27* (7), 1526–1532. https://doi.org/https://doi.org/10.1897/07-544.1.

(166) Gong, Y.; Zhao, X.; O'Reilly, S. E.; Qian, T.; Zhao, D. Effects of Oil Dispersant and Oil on Sorption and Desorption of Phenanthrene with Gulf Coast Marine Sediments. *Environ. Pollut.* **2014**, *185*, 240–249. https://doi.org/https://doi.org/10.1016/j.envpol.2013.10.031.

(167) Mayer, P.; Karlson, U.; Christensen, P. S.; Johnsen, A. R.; Trapp, S. Quantifying the Effect of Medium Composition on the Diffusive Mass Transfer of Hydrophobic Organic Chemicals through Unstirred Boundary Layers. *Environ. Sci. Technol.* **2005**, *39* (16), 6123–6129. https://doi.org/10.1021/es050556s.

(168) Smedes, F.; Geertsma, R. W.; Zande, T. van der; Booij, K. Polymer−Water Partition Coefficients of Hydrophobic Compounds for Passive Sampling: Application of Cosolvent Models for Validation. *Environ. Sci. Technol.* **2009**, *43* (18), 7047–7054. https://doi.org/10.1021/es9009376.

(169) Liu, P.; Wu, X.; Liu, H.; Wang, H.; Lu, K.; Gao, S. Desorption of Pharmaceuticals from Pristine and Aged Polystyrene Microplastics under Simulated Gastrointestinal Conditions. *J. Hazard. Mater.* **2020**, *392*, 122346. https://doi.org/https://doi.org/10.1016/j.jhazmat.2020.122346.

(170) Wang, J.; Li, J.; Wang, Q.; Sun, Y. Microplastics as a Vector for HOC Bioaccumulation in Earthworm Eisenia Fetida in Soil: Importance of Chemical Diffusion and Particle Size. *Environ. Sci. Technol.* **2020**, *54* (19), 12154–12163. https://doi.org/10.1021/acs.est.0c03712.

(171) Thaysen, C.; Sorais, M.; Verreault, J.; Diamond, M. L.; Rochman, C. M. Bidirectional Transfer of Halogenated Flame Retardants between the Gastrointestinal Tract and Ingested Plastics in Urban-Adapted Ring-Billed Gulls. *Sci. Total Environ.* **2020**. https://doi.org/10.1016/j.scitotenv.2020.138887.

(172) Paik, M. J.; Kim, H.; Lee, J.; Brand, J.; Kim, K. R. Separation of Triacylglycerols and Free Fatty Acids in Microalgal Lipids by Solid-Phase Extraction for Separate Fatty Acid Profiling Analysis by Gas Chromatography. *J. Chromatogr. A* **2009**. https://doi.org/10.1016/j.chroma.2009.06.051.

(173) Richardson, C. E.; Hennebelle, M.; Otoki, Y.; Zamora, D.; Yang, J.; Hammock, B. D.; Taha, A. Y. Lipidomic Analysis of Oxidized Fatty Acids in Plant and Algae Oils. *J. Agric. Food Chem.* **2017**. https://doi.org/10.1021/acs.jafc.6b05559.

(174) Breuer, G.; Evers, W. A. C.; de Vree, J. H.; Kleinegris, D. M. M.; Martens, D. E.; Wijffels, R. H.; Lamers, P. P. Analysis of Fatty Acid Content and Composition in Microalgae. *J. Vis. Exp.* **2013**, No. 80, 50628. https://doi.org/10.3791/50628.

(175) Teuling, E.; Wierenga, P. A.; Schrama, J. W.; Gruppen, H. Comparison of Protein Extracts from Various Unicellular Green Sources. *J. Agric. Food Chem.* **2017**, *65* (36), 7989–8002. https://doi.org/10.1021/acs.jafc.7b01788.

(176) EFSA. Presence of Microplastics and Nanoplastics in Food , with Particular Focus on Seafood EFSA Panel on Contaminants in the Food Chain (CONTAM). *EFSA J.* **2016**, *14* (May). https://doi.org/10.2903/j.efsa.2016.4501.

(177) Barboza, L. G. A.; Vethaak, A. D.; Lavorante, B. R. B. O.; Lundebye, A.; Guilhermino, L. Marine Microplastic Debris : An Emerging Issue for Food Security , Food Safety and Human Health. *Mar. Pollut. Bull.* **2018**, *133* (June), 336–348. https://doi.org/10.1016/j.marpolbul.2018.05.047.

(178) Peixoto, D.; Pinheiro, C.; Amorim, J.; Oliva-teles, L.; Natividade, M. Microplastic Pollution in Commercial Salt for Human Consumption : A Review. *Estuar. Coast. Shelf Sci.* **2019**, *219* (January 2018), 161–168. https://doi.org/10.1016/j.ecss.2019.02.018.

(179) Enyoh, C. E.; Verla, A. W.; Verla, E. N.; Ibe, F. C.; Amaobi, C. E. Airborne Microplastics: A Review Study on Method for Analysis, Occurrence, Movement and Risks. *Environ. Monit. Assess.* **2019**. https://doi.org/10.1007/s10661-019-7842-0.

(180) Wright, S. L.; Kelly, F. J. Plastic and Human Health: A Micro Issue? *Environ. Sci. Technol.* **2017**, *51* (12), 6634–6647. https://doi.org/10.1021/acs.est.7b00423.

(181) Rodrigues, M. O.; Abrantes, N.; Gonçalves, F. J. M.; Nogueira, H.; Marques, J. C.; Gonçalves, A. M. M. Impacts of Plastic Products Used in Daily Life on the Environment and Human Health: What Is Known? *Environ. Toxicol. Pharmacol.* **2019**. https://doi.org/10.1016/j.etap.2019.103239.

(182) Hartmann, N. B.; Hüffer, T.; Thompson, R. C.; Hassellöv, M.; Verschoor, A.; Daugaard, A. E.; Rist, S.; Karlsson, T.; Brennholt, N.; Cole, M.; Herrling, M. P.; Hess, M. C.; Ivleva, N. P.; Lusher, A. L.; Wagner, M. Are We Speaking the Same Language? Recommendations for a Definition and Categorization Framework for Plastic Debris. *Environ. Sci. Technol.* **2019**. https://doi.org/10.1021/acs.est.8b05297.

(183) Stock, V.; Böhmert, L.; Lisicki, E.; Block, R.; Cara-Carmona, J.; Pack, L. K.; Selb, R.; Lichtenstein, D.; Voss, L.; Henderson, C. J.; Zabinsky, E.; Sieg, H.; Braeuning, A.; Lampen, A. Uptake and Effects of Orally Ingested Polystyrene Microplastic Particles in Vitro and in Vivo. *Arch. Toxicol.* **2019**. https://doi.org/10.1007/s00204-019-02478-7.

(184) Hesler, M.; Aengenheister, L.; Ellinger, B.; Drexel, R.; Straskraba, S.; Jost, C.; Wagner, S.; Meier, F.; von Briesen, H.; Büchel, C.; Wick, P.; Buerki-Thurnherr, T.; Kohl, Y. Multi-Endpoint Toxicological Assessment of Polystyrene Nano- and Microparticles in Different Biological Models in Vitro. *Toxicol. Vitr.* **2019**. https://doi.org/10.1016/j.tiv.2019.104610.

(185) Hwang, J.; Choi, D.; Han, S.; Choi, J.; Hong, J. An Assessment of the Toxicity of Polypropylene Microplastics in Human Derived Cells. *Sci. Total Environ.* **2019**. https://doi.org/10.1016/j.scitotenv.2019.05.071.

(186) Schirinzi, G. F.; Pérez-Pomeda, I.; Sanchís, J.; Rossini, C.; Farré, M.; Barceló, D. Cytotoxic Effects of Commonly Used Nanomaterials and Microplastics on Cerebral

and Epithelial Human Cells. *Environ. Res.* **2017**. https://doi.org/10.1016/j.envres.2017.08.043.

(187) Groh, K. J.; Backhaus, T.; Carney-Almroth, B.; Geueke, B.; Inostroza, P. A.; Lennquist, A.; Leslie, H. A.; Maffini, M.; Slunge, D.; Trasande, L.; Warhurst, A. M.; Muncke, J. Overview of Known Plastic Packaging-Associated Chemicals and Their Hazards. *Sci. Total Environ.* **2019**. https://doi.org/10.1016/j.scitotenv.2018.10.015.

(188) Food and Agriculture Organization of the United Nations. *Microplastics in Fisheries and Aquaculture Status of Knowledge on Their Occurrence and Implications for Aquatic Organisms and Food Safety*; 2017.

(189) Koch, H. M.; Calafat, A. M. Human Body Burdens of Chemicals Used in Plastic Manufacture. *Philos. Trans. R. Soc. B Biol. Sci.* **2009**. https://doi.org/10.1098/rstb.2008.0208.

(190) Erythropel, H. C.; Maric, M.; Nicell, J. A.; Leask, R. L.; Yargeau, V. Leaching of the Plasticizer Di(2-Ethylhexyl)Phthalate (DEHP) from Plastic Containers and the Question of Human Exposure. *Appl. Microbiol. Biotechnol.* **2014**. https://doi.org/10.1007/s00253-014-6183-8.

(191) Kim, K. C.; Park, Y. B.; Lee, M. J.; Kim, J. B.; Huh, J. W.; Kim, D. H.; Lee, J. B.; Kim, J. C. Levels of Heavy Metals in Candy Packages and Candies Likely to Be Consumed by Small Children. *Food Res. Int.* **2008**. https://doi.org/10.1016/j.foodres.2008.01.004.

(192) Hussain, K.; Hoque, R. R.; Balachandran, S.; Medhi, S.; Idris, M. G.; Rahman, M.; Hussain, F. L. Monitoring and Risk Analysis of PAHs in the Environment. In *Handbook of Environmental Materials Management*; 2019. https://doi.org/10.1007/978-3-319-73645-7_29.

(193) Eriksson, E.; Baun, A.; Scholes, L.; Ledin, A.; Ahlman, S.; Revitt, M.; Noutsopoulos, C.; Mikkelsen, P. S. Selected Stormwater Priority Pollutants - a European Perspective. *Sci. Total Environ.* **2007**. https://doi.org/10.1016/j.scitotenv.2007.05.028.

(194) Eljarrat, E.; Barceló, D. Priority Lists for Persistent Organic Pollutants and Emerging Contaminants Based on Their Relative Toxic Potency in Environmental Samples. *TrAC - Trends Anal. Chem.* **2003**. https://doi.org/10.1016/S0165-9936(03)01001-X.

(195) Wani, A. L.; Ara, A.; Usmani, J. A. Lead Toxicity: A Review. *Interdisciplinary Toxicology*. 2015. https://doi.org/10.1515/intox-2015-0009.

(196) Rieux, A. Des; Ragnarsson, E. G. E.; Gullberg, E.; Préat, V.; Schneider, Y. J.; Artursson, P. Transport of Nanoparticles across an in Vitro Model of the Human Intestinal Follicle Associated Epithelium. *Eur. J. Pharm. Sci.* **2005**, *25* (4–5), 455–465. https://doi.org/10.1016/j.ejps.2005.04.015.

(197) Mowat, A. M. I. Anatomical Basis of Tolerance and Immunity to Intestinal Antigens. *Nat. Rev. Immunol.* **2003**, *3* (4), 331–341. https://doi.org/10.1038/nri1057.

(198) Hodges, G. M.; Carr, E. A.; Hazzard, R. A.; Carr, K. E. Uptake and Translocation of Microparticles in Small Intestine - Morphology and Quantification of Particle Distribution. *Dig. Dis. Sci.* **1995**, *40* (5), 967–975. https://doi.org/10.1007/BF02064184.

(199) Jani, P. U.; McCarthy, D. E.; Florence, A. T. Nanosphere and Microsphere Uptake via Peyer's Patches: Observation of the Rate of Uptake in the Rat after a Single Oral Dose. *Int. J. Pharm.* **1992**. https://doi.org/10.1016/0378-5173(92)90202-D.

(200) Carr, K. E.; Smyth, S. H.; McCullough, M. T.; Morris, J. F.; Moyes, S. M.

Morphological Aspects of Interactions between Microparticles and Mammalian Cells: Intestinal Uptake and Onward Movement. *Prog. Histochem. Cytochem.* **2012**. https://doi.org/10.1016/j.proghi.2011.11.001.

(201) Doyle-McCullough, M.; Smyth, S. H.; Moyes, S. M.; Carr, K. E. Factors Influencing Intestinal Microparticle Uptake in Vivo. *Int. J. Pharm.* **2007**. https://doi.org/10.1016/j.ijpharm.2006.10.043.

(202) EFSA. Presence of Microplastics and Nanoplastics in Food, with Particular Focus on Seafood. *EFSA J.* **2016**, *14* (6). https://doi.org/10.2903/j.efsa.2016.4501.

(203) Schmidt, C.; Lautenschlaeger, C.; Collnot, E. M.; Schumann, M.; Bojarski, C.; Schulzke, J. D.; Lehr, C. M.; Stallmach, A. Nano- and Microscaled Particles for Drug Targeting to Inflamed Intestinal Mucosa - A First in Vivo Study in Human Patients. *J. Control. Release* **2013**. https://doi.org/10.1016/j.jconrel.2012.10.019.

(204) Fry, F. A.; Black, A. Regional Deposition and Clearance of Particles in the Human Nose. *J. Aerosol Sci.* **1973**. https://doi.org/10.1016/0021-8502(73)90063-3.

(205) Gigault, J.; Halle, A. ter; Baudrimont, M.; Pascal, P. Y.; Gauffre, F.; Phi, T. L.; El Hadri, H.; Grassl, B.; Reynaud, S. Current Opinion: What Is a Nanoplastic? *Environ. Pollut.* **2018**. https://doi.org/10.1016/j.envpol.2018.01.024.

(206) Ogawara, K. ichi; Yoshida, M.; Kubo, J. ichi; Nishikawa, M.; Takakura, Y.; Hashida, M.; Higaki, K.; Kimura, T. Mechanisms of Hepatic Disposition of Polystyrene Microspheres in Rats: Effects of Serum Depend on the Sizes of Microspheres. *J. Control. Release* **1999**, *61* (3), 241–250. https://doi.org/10.1016/S0168-3659(99)00121-2.

(207) Bachler, G.; von Goetz, N.; Hungerbühler, K. A Physiologically Based Pharmacokinetic Model for Ionic Silver and Silver Nanoparticles. *Int. J. Nanomedicine* **2013**, *8* (1), 3365–3382. https://doi.org/10.2147/IJN.S46624.

(208) Li, M.; Panagi, Z.; Avgoustakis, K.; Reineke, J. Physiologically Based Pharmacokinetic Modeling of PLGA Nanoparticles with Varied MPEG Content. *Int. J. Nanomedicine* **2012**, *7*, 1345–1356. https://doi.org/10.2147/IJN.S23758.

(209) Martelli, H.; Devroede, G.; Arhan, P.; Duguay, C.; Dornic, C.; Faverdin, C. Some Parameters of Large Bowel Motility in Normal Man. *Gastroenterology* **1978**, *75* (4), 612–618.

(210) Walter, S. A.; Kjellström, L.; Nyhlin, H.; Talley, N. J.; Agréus, L. Assessment of Normal Bowel Habits in the General Adult Population: The Popcol Study. *Scand. J. Gastroenterol.* **2010**. https://doi.org/10.3109/00365520903551332.

(211) Sujatha, B.; Velayutham, D. R.; Deivamani, N.; Bavanandam, S. Normal Bowel Pattern in Children And Dietary and Other Precipitating Factors in Functional Constipation. *J. Clin. Diagnostic Res.* **2015**. https://doi.org/10.7860/JCDR/2015/13290.6025.

(212) Weaver, L. T.; Steiner, H. The Bowel Habit of Young Children. *Arch. Dis. Child.* **1984**. https://doi.org/10.1136/adc.59.7.649.

(213) Corazziari, E.; Staiano, A.; Miele, E.; Greco, L. Bowel Frequency and Defecatory Patterns in Children: A Prospective Nationwide Survey. *Clin. Gastroenterol. Hepatol.* **2005**. https://doi.org/10.1016/S1542-3565(05)00848-7.

(214) Myo-Khin; Thein-Win-Nyunt; Kyaw-Hla, S.; Thein-Thein-Myint; Bolin, T. D. A Prospective Study on Defecation Frequency, Stool Weight, and Consistency. *Arch. Dis. Child.* **1994**. https://doi.org/10.1136/adc.71.4.311.

(215) Williams, C. L.; Bollella, M. C.; Campanaro, L.; Strobino, B. A.; Boccia, L. Plant Stanol Ester and Bran Fiber in Childhood: Effects on Lipids, Stool Weight and Stool Frequency in Preschool Children. *J. Am. Coll. Nutr.* **1999**, *18* (6), 572–581.

https://doi.org/10.1080/07315724.1999.10718891.

(216) Asl, S.; Hosseini, S. Determination of the Mean Daily Stool Weight, Frequency of Defecation and Bowel Transit Time: Assessment of 1000 Healthy Subjects. *Arch Iran. Med. www. ams. ac. ir/AIM/ …* **2000**.

(217) Rose, C.; Parker, A.; Jefferson, B.; Cartmell, E. The Characterization of Feces and Urine: A Review of the Literature to Inform Advanced Treatment Technology. *Crit. Rev. Environ. Sci. Technol.* **2015**, *45* (17), 1827–1879. https://doi.org/10.1080/10643389.2014.1000761.

(218) MacLennan, R.; Jensen, O. M.; Mosbech, J.; Vuori, H. Diet, Transit Time, Stool Weight, and Colon Cancer in Two Scandinavian Populations. *Am. J. Clin. Nutr.* **1978**, *31* (10 ,SUPPL.), 3–6. https://doi.org/10.1093/ajcn/31.10.s239.

(219) WHO. FOSCOLLAB: Global platform for food safety data and information http://www.who.int/foodsafety/foscollab_dashboards/en/.

(220) Stifelman, M. Using Doubly-Labeled Water Measurements of Human Energy Expenditure to Estimate Inhalation Rates. *Sci. Total Environ.* **2007**, *373* (2–3), 585–590. https://doi.org/10.1016/j.scitotenv.2006.11.041.

(221) Allan, M.; Richardson, G. M. Human and Ecological Risk Assessment : An International Probability Density Functions Describing 24-Hour Inhalation Rates For Use in Human Health Risk Assessments Probability Density Functions Describing 24-Hour Inhalation Rates For Use in Human Health Ri. **2010**, *7039*. https://doi.org/10.1080/10807039891284389.

(222) Lenz, R.; Enders, K.; Stedmon, C. A.; MacKenzie, D. M. A.; Nielsen, T. G. A Critical Assessment of Visual Identification of Marine Microplastic Using Raman Spectroscopy for Analysis Improvement. *Mar. Pollut. Bull.* **2015**. https://doi.org/10.1016/j.marpolbul.2015.09.026.

(223) Cózar, A.; Echevarría, F.; González-Gordillo, J. I.; Irigoien, X.; Úbeda, B.; Hernández-León, S.; Palma, Á. T.; Navarro, S.; García-de-Lomas, J.; Ruiz, A.; Fernández-de-Puelles, M. L.; Duarte, C. M. Plastic Debris in the Open Ocean. *Proc. Natl. Acad. Sci. U. S. A.* **2014**. https://doi.org/10.1073/pnas.1314705111.

(224) Abbasi, S.; Soltani, N.; Keshavarzi, B.; Moore, F.; Turner, A.; Hassanaghaei, M. Microplastics in Different Tissues of Fish and Prawn from the Musa Estuary, Persian Gulf. *Chemosphere* **2018**, *205*, 80–87. https://doi.org/10.1016/j.chemosphere.2018.04.076.

(225) Barboza, L. G. A.; Lopes, C.; Oliveira, P.; Bessa, F.; Otero, V.; Henriques, B.; Raimundo, J.; Caetano, M.; Vale, C.; Guilhermino, L. Microplastics in Wild Fish from North East Atlantic Ocean and Its Potential for Causing Neurotoxic Effects, Lipid Oxidative Damage, and Human Health Risks Associated with Ingestion Exposure. *Sci. Total Environ.* **2020**, *717*, 134625. https://doi.org/10.1016/j.scitotenv.2019.134625.

(226) Delignette-Muller, M. L.; Dutang, C. Fitdistrplus: An R Package for Fitting Distributions. *J. Stat. Softw.* **2015**, *64* (4), 1–34.

(227) Azzalini, A. The R Package "Sn": The Skew-Normal and Related Distributions Such as the Skew-t (Version 1.6-2). 2020.

(228) Dutang, C.; Goulet, V.; Pigeon, M. Actuar: An R Package for Actuarial Science. *J. Stat. Softw.* **2008**, *25* (7), 1–37.

(229) Benaglia, T.; Chauveau, D.; Hunter, D. R.; Young, D. Mixtools: An R Package for Analyzing Finite Mixture Models. *J. Stat. Softw.* **2009**, *32* (6), 1–29.

(230) Brochot, C.; Quindroit, P. Modelling the Fate of Chemicals in Humans Using a Lifetime Physiologically Based Pharmacokinetic (PBPK) Model in MERLIN-Expo. In

Handbook of Environmental Chemistry; 2018. https://doi.org/10.1007/978-3-319-59502-3_10.

(231) Saunders, D. R.; Ways, P. O.; Parmentier, C. M.; Rubin, C. E. Studies on the Lipid Composition of Human Small Bowel Mucosa. *J. Clin. Invest.* **1966**. https://doi.org/10.1172/JCI105458.

(232) de Maagd, P. G. J.; ten Hulscher, D. T. E. M.; van den heuvel, H.; Opperhuizen, A.; Sijm, D. T. H. M. Physicochemical Properties of Polycyclic Aromatic Hydrocarbons: Aqueous Solubilities, n-Octanol/Water Partition Coefficients, and Henry's Law Constants. *Environ. Toxicol. Chem.* **1998**, *17* (2), 251–257. https://doi.org/https://doi.org/10.1002/etc.5620170216.

(233) De Bruijn, J.; Busser, F.; Seinen, W.; Hermens, J. Determination of Octanol/Water Partition Coefficients for Hydrophobic Organic Chemicals with the "Slow-stirring" Method. *Environ. Toxicol. Chem.* **1989**. https://doi.org/10.1002/etc.5620080607.

(234) Lee, B. M.; Shim, G. A. Dietary Exposure Estimation of Benzo[a]Pyrene and Cancer Risk Assessment. *J. Toxicol. Environ. Heal. - Part A Curr. Issues* **2007**, No. 70, 1391–1394. https://doi.org/10.1080/15287390701434182.

(235) Hong, W. J.; Jia, H.; Ma, W. L.; Sinha, R. K.; Moon, H. B.; Nakata, H.; Minh, N. H.; Chi, K. H.; Li, W. L.; Kannan, K.; Sverko, E.; Li, Y. F. Distribution, Fate, Inhalation Exposure and Lung Cancer Risk of Atmospheric Polycyclic Aromatic Hydrocarbons in Some Asian Countries. *Environ. Sci. Technol.* **2016**. https://doi.org/10.1021/acs.est.6b01090.

(236) Heinemeyer, G.; Sommerfeld, C.; Springer, A.; Heiland, A.; Lindtner, O.; Greiner, M.; Heuer, T.; Krems, C.; Conrad, A. Estimation of Dietary Intake of Bis(2-Ethylhexyl)Phthalate (DEHP) by Consumption of Food in the German Population. *Int. J. Hyg. Environ. Health* **2013**. https://doi.org/10.1016/j.ijheh.2013.01.001.

(237) Fromme, H.; Lahrz, T.; Piloty, M.; Gebhart, H.; Oddoy, A.; Rüden, H. Occurrence of Phthalates and Musk Fragrances in Indoor Air and Dust from Apartments and Kindergartens in Berlin (Germany). *Indoor Air* **2004**. https://doi.org/10.1111/j.1600-0668.2004.00223.x.

(238) Xie, Z.; Selzer, J.; Ebinghaus, R.; Caba, A.; Ruck, W. Development and Validation of a Method for the Determination of Trace Alkylphenols and Phthalates in the Atmosphere. *Anal. Chim. Acta* **2006**. https://doi.org/10.1016/j.aca.2006.02.027.

(239) Malavolti, M.; Fairweather-Tait, S. J.; Malagoli, C.; Vescovi, L.; Vinceti, M.; Filippini, T. Lead Exposure in an Italian Population: Food Content, Dietary Intake and Risk Assessment. *Food Res. Int.* **2020**, *137*, 109370. https://doi.org/https://doi.org/10.1016/j.foodres.2020.109370.

(240) Komarnicki, G. J. K. Lead and Cadmium in Indoor Air and the Urban Environment. *Environ. Pollut.* **2005**. https://doi.org/10.1016/j.envpol.2004.12.006.

(241) Xu, Q.; Zhu, X.; Henkelmann, B.; Schramm, K. W.; Chen, J.; Ni, Y.; Wang, W.; Pfister, G.; Mu, J.; Qin, S.; Li, Y. Simultaneous Monitoring of PCB Profiles in the Urban Air of Dalian, China with Active and Passive Samplings. *J. Environ. Sci. (China)* **2013**. https://doi.org/10.1016/S1001-0742(12)60030-8.

(242) Li, Y.; Shao, L.; Wang, W.; Zhang, M.; Feng, X.; Li, W.; Zhang, D. Airborne Fiber Particles: Types, Size and Concentration Observed in Beijing. *Sci. Total Environ.* **2020**, *705*. https://doi.org/10.1016/j.scitotenv.2019.135967.

(243) Vianello, A.; Jensen, R. L.; Liu, L.; Vollertsen, J. Simulating Human Exposure to Indoor Airborne Microplastics Using a Breathing Thermal Manikin. *Sci. Rep.* **2019**, *9* (1). https://doi.org/10.1038/s41598-019-45054-w.

(244) Timár, G.; Blömer, J.; Kun, F.; Herrmann, H. J. New Universality Class for the

Fragmentation of Plastic Materials. *Phys. Rev. Lett.* **2010**, *104* (9), 095502. https://doi.org/https://doi.org/10.1103/PhysRevLett.104.095502.

(245) Setälä, O.; Norkko, J.; Lehtiniemi, M. Feeding Type Affects Microplastic Ingestion in a Coastal Invertebrate Community. *Mar. Pollut. Bull.* **2016**. https://doi.org/10.1016/j.marpolbul.2015.11.053.

(246) Wang, J.; Wang, M.; Ru, S.; Liu, X. High Levels of Microplastic Pollution in the Sediments and Benthic Organisms of the South Yellow Sea, China. *Sci. Total Environ.* **2019**, *651*, 1661–1669. https://doi.org/10.1016/j.scitotenv.2018.10.007.

(247) Welle, F.; Franz, R. Microplastic in Bottled Natural Mineral Water–Literature Review and Considerations on Exposure and Risk Assessment. *Food Addit. Contam. - Part A Chem. Anal. Control. Expo. Risk Assess.* **2018**. https://doi.org/10.1080/19440049.2018.1543957.

(248) Kutralam-Muniasamy, G.; Pérez-Guevara, F.; Elizalde-Martínez, I.; Shruti, V. C. Branded Milks – Are They Immune from Microplastics Contamination? *Sci. Total Environ.* **2020**, *714*. https://doi.org/10.1016/j.scitotenv.2020.136823.

(249) World Health Organization. *Air Quality Guidelines. Global Update 2005*; 2006. https://doi.org/10.1007/BF02986808.

(250) World Health Organisation. *WHO Global Ambient Air Quality Database (Update 2018)*; 2018.

(251) Senathirajah, K.; Attwood, S.; Bhagwat, G.; Carbery, M.; Wilson, S.; Palanisami, T. Estimation of the Mass of Microplastics Ingested – A Pivotal First Step towards Human Health Risk Assessment. *J. Hazard. Mater.* **2020**. https://doi.org/10.1016/j.jhazmat.2020.124004.

(252) Powell, J. J.; Faria, N.; Thomas-McKay, E.; Pele, L. C. Origin and Fate of Dietary Nanoparticles and Microparticles in the Gastrointestinal Tract. *J. Autoimmun.* **2010**. https://doi.org/10.1016/j.jaut.2009.11.006.

(253) Deng, Y.; Zhang, Y.; Lemos, B.; Ren, H. Tissue Accumulation of Microplastics in Mice and Biomarker Responses Suggest Widespread Health Risks of Exposure. *Sci. Rep.* **2017**. https://doi.org/10.1038/srep46687.

(254) Deng, Y.; Zhang, Y.; Qiao, R.; Bonilla, M. M.; Yang, X.; Ren, H.; Lemos, B. Evidence That Microplastics Aggravate the Toxicity of Organophosphorus Flame Retardants in Mice (Mus Musculus). *J. Hazard. Mater.* **2018**. https://doi.org/10.1016/j.jhazmat.2018.06.017.

(255) Yang, Y. F.; Chen, C. Y.; Lu, T. H.; Liao, C. M. Toxicity-Based Toxicokinetic/Toxicodynamic Assessment for Bioaccumulation of Polystyrene Microplastics in Mice. *J. Hazard. Mater.* **2019**. https://doi.org/10.1016/j.jhazmat.2018.12.048.

(256) Héraud, F.; Barraj, L. M.; Moy, G. G. GEMS/Food Consumption Cluster Diets. *Total Diet Stud.* **2013**. https://doi.org/10.1007/978-1-4419-7689-5_43.

(257) Coyle, P.; Kosnett, M. J.; Hipkins, K. Severe Lead Poisoning in the Plastics Industry: A Report of Three Cases. *Am. J. Ind. Med.* **2005**. https://doi.org/10.1002/ajim.20123.

(258) Ashton, K.; Holmes, L.; Turner, A. Association of Metals with Plastic Production Pellets in the Marine Environment. *Mar. Pollut. Bull.* **2010**. https://doi.org/10.1016/j.marpolbul.2010.07.014.

(259) Holmes, L. A.; Turner, A.; Thompson, R. C. Adsorption of Trace Metals to Plastic Resin Pellets in the Marine Environment. *Environ. Pollut.* **2012**, *160*, 42–48. https://doi.org/10.1016/j.envpol.2011.08.052.

(260) Massos, A.; Turner, A. Cadmium, Lead and Bromine in Beached Microplastics. *Environ. Pollut.* **2017**, *227*, 139–145. https://doi.org/10.1016/j.envpol.2017.04.034.

(261) Carbery, M.; MacFarlane, G. R.; O'Connor, W.; Afrose, S.; Taylor, H.; Palanisami, T. Baseline Analysis of Metal(Loid)s on Microplastics Collected from the Australian Shoreline Using Citizen Science. *Mar. Pollut. Bull.* **2020**. https://doi.org/10.1016/j.marpolbul.2020.110914.

(262) Gaillet, S.; Rouanet, J. M. Silver Nanoparticles: Their Potential Toxic Effects after Oral Exposure and Underlying Mechanisms - A Review. *Food Chem. Toxicol.* **2015**, *77*, 58–63. https://doi.org/10.1016/j.fct.2014.12.019.

(263) Jani, P.; Halbert, G. W.; Langridge, J.; Florence, A. T. Nanoparticle Uptake by the Rat Gastrointestinal Mucosa: Quantitation and Particle Size Dependency. *J. Pharm. Pharmacol.* **1990**. https://doi.org/10.1111/j.2042-7158.1990.tb07033.x.

(264) Oliveri Conti, G.; Ferrante, M.; Banni, M.; Favara, C.; Nicolosi, I.; Cristaldi, A.; Fiore, M.; Zuccarello, P. Micro- and Nano-Plastics in Edible Fruit and Vegetables. The First Diet Risks Assessment for the General Population. *Environ. Res.* **2020**. https://doi.org/10.1016/j.envres.2020.109677.

(265) Kedzierski, M.; Lechat, B.; Sire, O.; Le Maguer, G.; Le Tilly, V.; Bruzaud, S. Microplastic Contamination of Packaged Meat: Occurrence and Associated Risks. *Food Packag. Shelf Life* **2020**. https://doi.org/10.1016/j.fpsl.2020.100489.

(266) Li, Q.; Feng, Z.; Zhang, T.; Ma, C.; Shi, H. Microplastics in the Commercial Seaweed Nori. *J. Hazard. Mater.* **2020**, *388* (October 2019), 122060. https://doi.org/10.1016/j.jhazmat.2020.122060.

(267) Karami, A.; Golieskardi, A.; Ho, Y. Bin; Larat, V.; Salamatinia, B. Microplastics in Eviscerated Flesh and Excised Organs of Dried Fish. *Sci. Rep.* **2017**, *7* (1), 1–9. https://doi.org/10.1038/s41598-017-05828-6.

(268) Huerta Lwanga, E.; Mendoza Vega, J.; Ku Quej, V.; Chi, J. de los A.; Sanchez del Cid, L.; Chi, C.; Escalona Segura, G.; Gertsen, H.; Salánki, T.; van der Ploeg, M.; Koelmans, A. A.; Geissen, V. Field Evidence for Transfer of Plastic Debris along a Terrestrial Food Chain. *Sci. Rep.* **2017**, *7* (1), 1–7. https://doi.org/10.1038/s41598-017-14588-2.

(269) Ferdouse, F.; Løvstad Holdt, S.; Smith, R.; Murúa, P.; Yang, Z. The Global Status of Seaweed Production, Trade and Utilization. *FAO Globefish Res. Program.* **2018**.

(270) Winkler, A.; Santo, N.; Ortenzi, M. A.; Bolzoni, E.; Bacchetta, R.; Tremolada, P. Does Mechanical Stress Cause Microplastic Release from Plastic Water Bottles? *Water Res.* **2019**. https://doi.org/10.1016/j.watres.2019.115082.

(271) Zhang, M.; Li, J.; Ding, H.; Ding, J.; Jiang, F.; Ding, N. X.; Sun, C. Distribution Characteristics and Influencing Factors of Microplastics in Urban Tap Water and Water Sources in Qingdao, China. *Anal. Lett.* **2019**, *0* (0), 1–16. https://doi.org/10.1080/00032719.2019.1705476.

(272) Kankanige, D.; Babel, S. Smaller-Sized Micro-Plastics (MPs) Contamination in Single-Use PET-Bottled Water in Thailand. *Sci. Total Environ.* **2020**. https://doi.org/10.1016/j.scitotenv.2020.137232.

(273) Kennedy, N. J.; Hinds, W. C. Inhalability of Large Solid Particles. *J. Aerosol Sci.* **2002**. https://doi.org/10.1016/S0021-8502(01)00168-9.

(274) Froese, R.; Pauly, D. Fishbase. World Wide Web electronic publication.

(275) Mintenig, S. M.; Bäuerlein, P. S.; Koelmans, A. A.; Dekker, S. C.; Van Wezel, A. P. Closing the Gap between Small and Smaller: Towards a Framework to Analyse Nano- and Microplastics in Aqueous Environmental Samples. *Environ. Sci. Nano*

2018. https://doi.org/10.1039/c8en00186c.

(276) USEPA. *EXPOSURE FACTORS HANDBOOK : 2011 EDITION*; 2011. https://doi.org/EPA/600/R-09/052F.

(277) Johnson, R. A.; Wichern, D. W. Applied Multivariate Statistical Analysis. Prentice Hall, Englewood Cliffs, NJ. *Appl. Multivar. Stat. Anal. Prentice-Hall, Englewood Cliffs, NJ.* **1992**.

(278) Granger, C. W. J. Extracting Information from Mega-Panels and High-Frequency Data. *Stat. Neerl.* **1998**, *52* (3), 258–272.

(279) Duis, K.; Coors, A. Microplastics in the Aquatic and Terrestrial Environment: Sources (with a Specific Focus on Personal Care Products), Fate and Effects. *Environ. Sci. Eur.* **2016**. https://doi.org/10.1186/s12302-015-0069-y.

(280) Polymerdatabase.com. Average density of amorphous polymers http://polymerdatabase.com/polymer physics/Polymer Density.html (accessed Aug 5, 2020).

(281) Scientific polymer products. Density of polymers (by density) https://scientificpolymer.com/density-of-polymers-by-density/ (accessed Aug 5, 2020).

(282) Omnexus. Density of plastics: Technical properties https://omnexus.specialchem.com/polymer-properties/properties/density (accessed Aug 5, 2020).

(283) Prospector. Polyurethane (PUR) typical properties generic PUR, unspecified https://plastics.ulprospector.com/generics/45/c/t/polyurethane-pur-properties-processing (accessed Aug 5, 2020).

(284) Buonanno, G.; Giovinco, G.; Morawska, L.; Stabile, L. Lung Cancer Risk of Airborne Particles for Italian Population. *Environ. Res.* **2015**. https://doi.org/10.1016/j.envres.2015.07.019.

(285) Stolzenberg, H.; Kahl, H.; Bergmann, K. E. Körpermaße Bei Kindern Und Jugendlichen in Deutschland. *Bundesgesundheitsblatt. Gesundheitsforschung. Gesundheitsschutz* **2007**. https://doi.org/10.1007/s00103-007-0227-5.

(286) Manz, F.; Johner, S. A.; Wentz, A.; Boeing, H.; Remer, T. Water Balance throughout the Adult Life Span in a German Population. *Br. J. Nutr.* **2012**. https://doi.org/10.1017/S0007114511004776.

(287) Gao, Q.; Ben, Y.; Dong, Z.; Hu, J. Age-Dependent Human Elimination Half-Lives of Dioxin-like Polychlorinated Biphenyls Derived from Biomonitoring Data in the General Population. *Chemosphere* **2019**. https://doi.org/10.1016/j.chemosphere.2019.01.168.

(288) Chiang, K. C.; Liao, C. M. Heavy Incense Burning in Temples Promotes Exposure Risk from Airborne PMs and Carcinogenic PAHs. *Sci. Total Environ.* **2006**. https://doi.org/10.1016/j.scitotenv.2006.08.012.

(289) Gentry, P. R.; Clewell, H. J.; Clewell, R.; Campbell, J.; Van Landingham, C.; Shipp, A. M. Challenges in the Application of Quantitative Approaches in Risk Assessment: A Case Study with Di-(2-Ethylhexyl)Phthalate. *Critical Reviews in Toxicology*. 2011. https://doi.org/10.3109/10408444.2011.599366.

(290) Li, S. Q.; Ni, H. G.; Zeng, H. PAHs in Polystyrene Food Contact Materials: An Unintended Consequence. *Sci. Total Environ.* **2017**. https://doi.org/10.1016/j.scitotenv.2017.07.262.

(291) Chen, G.; Feng, Q.; Wang, J. Mini-Review of Microplastics in the Atmosphere and Their Risks to Humans. *Sci. Total Environ.* **2020**.

https://doi.org/10.1016/j.scitotenv.2019.135504.

(292) Town, R. M.; van Leeuwen, H. P.; Blust, R. Biochemodynamic Features of Metal Ions Bound by Micro- and Nano-Plastics in Aquatic Media. *Front. Chem.* **2018**. https://doi.org/10.3389/fchem.2018.00627.

(293) Seidensticker, S.; Zarfl, C.; Cirpka, O. A.; Grathwohl, P. Microplastic–Contaminant Interactions: Influence of Nonlinearity and Coupled Mass Transfer. *Environ. Toxicol. Chem.* **2019**. https://doi.org/10.1002/etc.4447.

(294) Turner, A.; Lau, K. S. Elemental Concentrations and Bioaccessibilities in Beached Plastic Foam Litter, with Particular Reference to Lead in Polyurethane. *Mar. Pollut. Bull.* **2016**, *112* (1–2), 265–270. https://doi.org/10.1016/j.marpolbul.2016.08.005.

(295) Wu, P.; Tang, Y.; Jin, H.; Song, Y.; Liu, Y.; Cai, Z. Consequential Fate of Bisphenol-Attached PVC Microplastics in Water and Simulated Intestinal Fluids. *Environ. Sci. Ecotechnology* **2020**, *2*, 100027. https://doi.org/https://doi.org/10.1016/j.ese.2020.100027.

(296) Fan, X.; Zou, Y.; Geng, N.; Liu, J.; Hou, J.; Li, D.; Yang, C.; Li, Y. Investigation on the Adsorption and Desorption Behaviors of Antibiotics by Degradable MPs with or without UV Ageing Process. *J. Hazard. Mater.* **2021**, *401*, 123363. https://doi.org/https://doi.org/10.1016/j.jhazmat.2020.123363.

(297) Plazinski, W.; Dziuba, J.; Rudzinski, W. Modeling of Sorption Kinetics: The Pseudo-Second Order Equation and the Sorbate Intraparticle Diffusivity. *Adsorption* **2013**, *19* (5), 1055–1064. https://doi.org/10.1007/s10450-013-9529-0.

Summary

Microplastics are small plastic particles (1–5000 µm), which are omnipresent in the environment and may likely be ingested by biota, especially humans. There has been an increasing concern on how much microplastics humans are actually exposed to in the world and if the levels can actually cause any effect in us. One of the potential effects of microplastics that have been identified is its ability to transport chemicals into the organism (commonly referred to as the vector effect) when the particles are ingested. Therefore, the fundamental aim of this thesis was to unravel the lifetime exposure of microplastics in humans around the world and the extent of the role of microplastics as a vector for chemical bioaccumulation in humans and other biota. To accomplish these aims, a mechanistic approach was needed that involved developing sophisticated experimental methods, mechanistic models, and modeling tools. The primary focus of this thesis was the transport of microplastics through the gastrointestinal tract and the extent of the chemical vector effect during the gut retention time.

This thesis started with understanding the chemical dynamics of microplastics in a simulated gut environment using an in vitro experimental approach. A series of experimental setups to represent three different environmentally relevant scenarios was examined. First, an organism ingests contaminated (i.e., associated with chemicals) microplastics. Second, an organism ingests contaminated microplastics and contaminated food. Third, an organism ingests clean microplastics and contaminated food. Chemical transfer was demonstrated to be biphasic and fully reversible on the microplastics, with fast exchange within hours followed by a slow transfer lasting for weeks to months. Therefore, a biphasic reversible chemical exchange model was constructed and parameterized for organic chemicals on microplastics with the in vitro experimental data. Low density polyethylene (LDPE) showed faster sorption kinetics than polyvinyl chloride (PVC). Additionally, the apparent affinity of chemicals with PVC decreases as chemical hydrophobicity increases, which is contrasting to that found for LDPE. Model parameters from this first study was also later used in a later part of this thesis to understand the chemical vector effect in humans. Overall, this study demonstrated that whether microplastics increase or decrease the chemical body burden of an organism is context dependent.

Although the first study in this thesis had provided a fundamental understanding on the chemical dynamics of microplastic-associated organic chemicals in the gut fluid systems, the food component in the experimental setup was an inert pool. In reality, food is constantly digested in the gastrointestinal tract of the biota, which would affect the chemical dynamics.

Therefore, a follow-up in vitro gut fluid study was designed to include the food digestion kinetics and further develop the earlier biphasic reversible chemical exchange model. At the same time, the chemical affinities for different gut components (olive oil lipids and micelles) were investigated to evaluate the relative chemical distribution for each component. Our findings showed that as the olive oil lipids were digested by the enzyme, lipase, food-associated chemicals were released and taken up by microplastics. This process would decrease the amount of chemicals available for uptake by the organism when the microplastics are egested. Additionally, the lipid digestion kinetics was rate-limiting and had a small influence in the overall chemicals dynamics on microplastics. Kinetic parameter estimates from the new model in this study can be used to extrapolate chemical behaviour in realistic human gut conditions to evaluate the human health implications of microplastics.

Finally, this thesis unravelled the lifetime exposure of microplastics to humans in the final main chapter in which a probabilistic lifetime exposure model toolkit was constructed for children and adults, accounting for intake via eight food types and inhalation (presently known microplastic sources at the point of the thesis). This included the accumulation of microplastics in the body via a gut distribution model which accounted for intestinal absorption, biliary and intestinal excretion. This exposure assessment stands out from previous ones as not only does it quantify the uncertainties surrounding microplastic exposure in humans, it also accounts for the non-alignment of methods used in microplastic research, the heterogeneity of microplastics and the distribution of global intake rates in the world. Therefore, the exposure estimates were reported probabilistically and presented as distributions, accounting for the aforementioned uncertainties and variabilities. The toolkit also included a chemical model, which helps us to understand the potential risk of microplastic due to microplastic-associated chemicals. The previously developed biphasic and reversible chemical exchange model was integrated in the chemical model here. The transfer of four representative chemicals, which are widely known environmental pollutants, from ingested microplastics was simulated under realistic conditions whereby the gut was also exposed to chemicals from dietary intake. Our findings suggest that the chemical contribution from ingested microplastics from the known nine intake media is small. However, our estimates in this study only account for approximately 20% by mass of the total food consumed daily on average. There is still a lack thereof data in other food types such as grains, vegetables, meats and processed food. It is plausible that when these food clusters are included in the future as more studies report microplastic occurrence, the distribution of actual microplastics exposure and intake in humans would widen. This may then result in different implications for the chemical vector effect of microplastics in humans.

This thesis was concluded with an evaluation of the weight of evidence for the microplastic chemical vector effect from in vitro gut fluid studies. Recommendations for future in vitro gut fluid studies that aim to elucidate the chemical vector effect are also included. An evaluation of the current developments on models for exposure assessments of microplastic and its associated chemicals was also discussed. In conclusion, the chemical exchange models and probabilistic microplastic human exposure toolkit developed in this thesis can be used in bigger model frameworks in the future such as for ecological and human risk assessments.

Acknowledgements

This PhD journey would not have been possible without my ever caring, kind, patient, and very supportive supervisor and promotor, Bart. I feel so lucky to be able to work with you for the past 4.5 years and to have known you for the past 5 years. I remember you telling me how you somehow felt like you had to respond to my email enquiry about a PhD position with you among the many other email requests you got daily. To me, you are the best supervisor any PhD student can get. You have been such an inspiring and creative scientist, and I am constantly amazed at how your brain works wonders. You have my utmost respect as you balance your own projects and classes while supervising your PhD students with such care and concern. Despite the tiny bumps and valleys in this PhD, you always got me out of them with your constant encouragement and long chats and chocolates. This PhD has indeed been an adventurous one for me filled with laughter and tears, and you were always there to share those moments with me.

I am also very grateful for the AEW family, special mention to Frits, Marlies, Nancy and Wendy. Of course, working with organic chemicals and microplastics entails me to use the machine that no one else knows how to operate except for dear Frits. Hence, none of my experiments would have been successful without the patient guidance and "magic fingers" of Frits. Thank you Frits for always coming to my rescue in the laboratory when I needed it and providing so much useful advise for my experiments. Also thank you Marlies, who also helped to monitor my projects in the laboratory and providing advise on how to optimize my experimental setups, and also just being there for chats in the quiet laboratory. Thank you, Wendy for organizing the laboratory so that everything is in order and always jumping to help me find experiment materials when I needed them. Nancy, you have been the sweetest "work-mama" in AEW, always taking care of my welfare and listening to my complaints about work and life. Not forgetting all the other administrative staff who left during my PhD: John and Petra, and also Dorine who joined in the last few months of my PhD.

My time in AEW and Wageningen had also been wonderful and fun because of the loveliest people I met and now missed so much. Firstly, thank you Merel for everything. You have been my constant throughout my PhD. Thank you for crying and laughing with me, making dinners for me, cheering me on, introducing the Dutch language to me, advising me on R, and all the lunches and coffee breaks. Thank you, Noël, for introducing climbing to me, a sport that kept me sane and away from the PhD stress. You have also been a constant moral supporter, close friend and mentor throughout my PhD. Also thank you Els for always pushing me to stop work and go for climbing training with you. Our weekly climbing sessions was one of the things

which I look forward to because then we would get to ride in the car and chat about life and PhD ups and downs. Thank you for always understanding my limits in climbing and just making climbing fun! I really miss climbing with you. Thank you, Paula, who was the first person to chat with me and introduced me to the group. She had convinced me to do a PhD in Wageningen and join the Bart Koelmans' group. Her constant motivation throughout my PhD and support as a friend and fellow colleague were invaluable. Finally, not forgetting the funny and tall Sanne, who always comes into the office with good cheer and dance moves. The office would have been so boring and dull without you around. I also want to thank Maira, Pablo, Vera, Anna, Markus, Lara, Zhao, Bregje, Georgiana, Miquel, Ingrid, Egbert, Jeroen and many others who have been there for me one way or another during my PhD journey.

A big thank you to my students, Zhiyue and Angelo who have helped me during my experimental work. It was really great working with you two. Thank you, Marie Hennebelle and Peter de Gijsel from the Food Chemistry laboratory for your utmost patience and guidance in one of my projects. It was really great collaborating with you two and seeing another perspective of my project.

Finally, to my family and friends (you know who you are), who had been there for me throughout my PhD journey or at one point of my PhD, thank you for believing in me that I can successfully finish my PhD one day. Thank you for your patience, unconditional love and support. Thank you for listening to me talk about my tiredness, problems with my projects and also sharing all the good times with me.

About the author

Nur Hazimah Bte Mohamed Nor was born on 20th April 1990 in Singapore. In 2009, she followed a Bachelor of Engineering programme in the National University of Singapore (NUS), majoring in Environmental Engineering. Her interest in research on water quality and environmental risk assessment began in her third year when she undertook an Undergraduate Research Opportunity Program to investigate methods to extract pharmaceuticals and personal care product compounds from environmental media. In her final year, she did her dissertation on microplastics occurrence in Singapore's coastal mangrove ecosystems, which was published in the Marine Pollution Bulletin.

In 2013, she started her career as a research engineer in in the Singapore-Delft Water Alliance in NUS. Her projects ranged from haze mitigation to monitoring micro-contaminants in Singapore's mangrove ecosystems. After one year, she started a new project on freshwater cyanobacteria in the NUS Environmental Research Institute. At the same time, she started her Masters in Engineering (M.Eng.) programme in NUS, specializing in Environmental Sciences and Engineering. Her M.Eng. dissertation focused on the influence of environmental factors on toxin production by the cyanobacteria species, Cylindrospermopsis.

After her Masters, she was still curious about the hype behind microplastics and wanted to investigate if the contaminant is a primary environmental concern. She was awarded the Ridzwan Dzafir Community Award by MENDAKI Singapore to pursue her interests in a PhD programme in Wageningen University and Research in 2017. During her PhD programme, she collaborated with the World Health Organization on a review for microplastics in water, co-authored a book section, presented her research in several international conferences and was guest speaker for an international microplastic workshop. She also supervised several dissertation students throughout her research career and PhD. In June 2021, she started a new job as a research fellow in Nanyang Technological University in Singapore.

Scientific publications

Risk assessment of microplastic particles
Koelmans, A. A., Redondo-Hasselerharm, P. E., **Mohamed Nor, N. H.**, de Ruijter, V., Mintenig, S. M., Kooi, M.
Accepted for publication in Nature Reviews Materials.

How digestive processes can affect the bioavailability of PCBs associated with microplastics. A modelling study supported by empirical data
Mohamed Nor, N.H., Niu, Z., Hennebelle, M., Koelmans, A. A.
Submitted to Environmental Science and Technology.

Lifetime accumulation of microplastic in children and adults
Mohamed Nor, N. H., Kooi, M., Diepens, N. J., Koelmans, A. A., 16 March 2021, In: Environmental Science and Technology. 55(8), p. 5084-5096

Weight of evidence for the microplastic vector effect in the context of chemical risk assessment
Koelmans, A. A., Diepens, N. J., **Mohamed Nor, N. H.**, 2021, Nature Publishing Group, Springer Open Press.

Solving the non-alignment of methods and approaches used in microplastic research in order to consistently characterize risk
Koelmans, A. A., Redondo, P. H., **Mohamed Nor, N. H.** & Kooi, M., 4 Sept 2020, In: Environmental Science and Technology.

Microplastics in freshwaters and drinking water: Critical review and assessment of data quality
Koelmans, A. A., **Mohamed Nor, N. H.,** Hermsen, E., Kooi, M., Mintenig, S. M. & De France, J., 15 May 2019, In: Water Research. 155, p. 410 – 422

Environmental factors influence cylindrospermopsin production of *Cylindrospermopsis raciborskii* (CR12)
Mohamed Nor, N. H., Te, S. H., Mowe, M. A. D. & Gin, K. Y. H., Mar – Apr 2019, In: Journal of Plankton Research. 41 (2), p. 114 – 126

Transfer of PCBs from microplastics under simulated gut fluid conditions is biphasic and reversible
Mohamed Nor, N. H. & Koelmans, A. A., 14 Jan 2019, In: Environmental Science and Technology. 53 (4), p. 1874 – 1883

Draft genome sequence of *Cylindrospermopsis* sp. Strain CR12 extracted from the minimetagenome of a nonaxenic unialgal culture from a tropical freshwater lake

Mohamed Nor, N. H., Tan, B. F., Te, S. H., Thompson, J. R. & Gin, K. Y. H., 11 Feb 2016, In: Genome Announcements. 4 (1), e01726-15

Microplastics in Singapore's coastal mangrove ecosystems

Mohamed Nor, N. H. & Obbard, J. P., 15 Feb 2014, In: Marine Pollution Bulletin. 79 (1 – 2), p. 278 – 283

Netherlands Research School for the
Socio-Economic and Natural Sciences of the Environment

D I P L O M A

for specialised PhD training

The Netherlands research school for the
Socio-Economic and Natural Sciences of the Environment
(SENSE) declares that

Nur Hazimah Bte Mohamed Nor

born on 20th April 1990 in Singapore

has successfully fulfilled all requirements of the
educational PhD programme of SENSE.

Wageningen, 2 March 2022

Chair of the SENSE board

Prof. dr. Martin Wassen

The SENSE Director

Prof. Philipp Pattberg

The SENSE Research School has been accredited by the Royal Netherlands Academy of Arts and Sciences (KNAW)

KONINKLIJKE NEDERLANDSE
AKADEMIE VAN WETENSCHAPPEN

The SENSE Research School declares that **Nur Hazimah Bte Mohamed Nor** has successfully fulfilled all requirements of the educational PhD programme of SENSE with a work load of 33.9 EC, including the following activities:

SENSE PhD Courses

- Environmental research in context (2017)
- Research in context activity: 'Communicating microplastic science through Twitter (@MicroplasticLab) and group website (microplasticlab.com)' (2021)
- Statistical Uncertainty Analysis of Dynamic Models (2017)
- Speciation and Bioavailability of Metals, Organics and Nanoparticles (2017)
- Uncertainty Propagation in Spatial Environmental Modelling (2018)
- Advanced Statistics course Design of Experiments (2018)

Other PhD and Advanced MSc Courses

- Teaching in International Classroom, Wageningen University (2019)
- Career Perspectives, Wageningen Graduate Schools (2020)

Management and Didactic Skills Training

- Supervising two MSc students with thesis entitled 'Effect of lipid digestion on chemical exchange in microplastics' (2018) and 'The sorption of PCBs to weathered microplastics present in seawater' (2020)

Oral Presentations

- *Dynamics of chemical transfer on microplastic in gut*. 6th International Marine Debris Conference 12-16 March 2018, San Diego, United States of America
- *Do chemicals transfer to or from microplastics in the gut?* Micro 2018, 19-23 November 2018, Lanzarote, Spain
- *Effect of lipid digestion on PCBs transfer from microplastics during in vitro digestion.* SETAC 2019, 26-30 May 2019, Helsinki, Finland

SENSE coordinator PhD education

Dr. ir. Peter Vermeulen

The research described in this thesis was financially supported by the Mendaki Ridzwan Dzafir Community Award Scholarship and the Aquatic Ecology and Water Quality Management Group of Wageningen University.

Financial support from Wageningen University for printing this thesis is gratefully acknowledged.

Cover design and artwork: Nur Hazimah Bte Mohamed Nor

Printed by GVO drukkers & vormgevers B.V. on FSC-certified paper